Iodine distribution in the Australian sector of the Southern Ocean and its relation to new production and water masses

by

Ana Cláudia Moreira

Ana Cláudia Brandão

B.Sc. Oceanography, UERJ, Brazil
M.Sc. Chemistry, PUC-Rio, Brazil

IASOS

Submitted in fulfilment of the requirements for the degree of

Doctor of Philosophy

University of Tasmania

November 2001

Declaration

This thesis contains no material which has been accepted for a degree or diploma by the University or any other institution, except by way of background information and duly acknowledged in the Thesis. To the best of my knowledge and belief, this thesis contains no material previously published or written by another person, except where due acknowledgement is made in the text of the Thesis.

Ana Cláudia Brandão

This thesis may be available for loan and limited copying in accordance with the *Copyright Act 1986.*

Ana Cláudia Brandão

Abstract

The distribution of iodate and iodide was studied in seawaters from the Australian sector of the Southern Ocean and Antarctic coastal waters. Most samples were collected along the WOCE repeat section SR3, from Tasmania to Antarctica, during one winter and two summer cruises. Two other transects were also sampled, the WOCE S4 (Australian sector) and the Princess Elizabeth Trough. Iodide was determined directly by matrix-elimination ion chromatography with post-column reaction detection using a new method developed for this work. The detection limit of the method was about 6 nM, with a relative standard deviation better than 4 % at 40 nM (n=5).

Iodate concentration in surface waters increased from Tasmania to Antarctica, with the most dramatic increase occurring along the Subtropical Front, which separates Subtropical from Subantarctic waters at approximately 46°S. Iodide concentration in surface waters showed the opposite trend. Iodide concentration in Antarctic surface waters during summer was below 40 nM, with the lowest measured surface concentration of 15 nM, one of the lowest ever recorded for the region. This was the first iodine study ever conducted in the Australian Sector of the Southern Ocean that included samples from Subtropical, Subantarctic and Antarctic regions.

Along the SR3 transect, iodate concentration in surface waters decreased from winter (July) to summer (January), presumably due to biological uptake. Differences in iodide concentration during the same period were not observed. Depth-integrated average iodate depletion in surface waters from winter to summer varied from

0.08 mmol m^{-2} in the Antarctic Zone north of the 64°S to 2.5 mmol m^{-2} in the Subtropical Zone. Annual differences were also noticed. As iodate showed good correlation with nitrate in surface waters, depth-integrated iodate depletion was related to carbon production and used, for the first time, to estimate seasonal primary production in different zones within the Southern Ocean. Average estimated seasonal production values estimated from iodate depletion from July to January were: 3,684 mmol C m^{-2} for the Subantarctic Zone, 696 mmol C m^{-2} for the Polar Frontal Zone, 496 mmol C m^{-2} for the Antarctic Zone north of 64°S, and 2,659 mmol C m^{-2} for the Antarctic Zone south of 64°S. These values are within ranges found in the literature.

Iodate concentration generally increased from the surface to deep waters. South of 60°S, however, a decrease in iodate concentration below 1000-m depth was also observed. This decrease is reported here for the first time and was related to the presence of Antarctic Bottom Water (AABW). Iodate concentration in AABW appeared to be significantly smaller than iodate concentration in the Circumpolar Deep Water above and it is suggested that iodate could perhaps be used as an independent tracer of AABW inside the Australian Antarctic Basin.

Acknowledgements

I first would like to thank my supervisors, in no particular order, Dr. Ed Butler, for his expertise, support, guidance and for offering me the opportunity to study here in Australia; Dr. Peter Sedwick, for his guidance, expertise and for helping me to stay focused; and Prof. Paul Haddad, for his expertise, support and the great work environment in the ACROSS group.

I also would like to thank:

CNPq (Brazil), DEETYA, Antarctic CRC and ACROSS for the financial support;

Antarctic Division for the ASAC grant, project number 748, for berth on cruises au9404 and au9501;

Dionex Corporation for providing the AS-11 analytical columns;

The Captain and crews of RSV *Aurora Australis* cruises au9407 and au9404 for all the logistical support and the great environment onboard;

Dr. Bronte Tilbrook for offering me the position on cruise au9407;

Many people at CSIRO Marine Labs, Hobart, who helped with the autoanalyser, cruise preparations, etc., especially: Kate Berry, Paul Boult, Ron Plaschke and Ros Watson;

Mark Rosenberg for his help sampling onboard the *Aurora,* and the temperature and salinity contour pictures;

Dr. Ross Edwards, who collected the samples on my behalf during cruise au9501;

Dr. Peter Fagan, for all the help during the development of the IC method and the reaction coil pictures;

Dr. Wolfgang Buchberger for the guidance during the development of the IC method and the collaboration on the article for the Journal of Chromatography;

Dr. Per Anderson and Dr. Philip Doble for their help in the lab and friendship;

Martin Lourey for his time in preparing the iodate contour pictures;

Dr. Steve Rintoul for his help with water mass distribution in the Southern Ocean and his comments on section 4.2;

Dr. Tom Trull for his comments on section 4.1;

Dr. Anna Farrenkopf for all her support, and her comments on an earlier draft of this thesis;

Dr. Ruth Eriksen, Dr. Alison Featherstone, Dr. Annie Wong and future Doctor Helmy Cook for their friendship, support and comments;

Dr. Will Howard for all the casual work;

My parents, Edy and Victor Brandão, for their love and support at all times;

And Mateus Brandão for his lovely smiles and his patience, especially in this last year, while I was very busy writing the "book".

Publication

1. **Brandão, A. C. M., Buchberger, W. W., Butler, E. C. V., Fagan, P. A., and Haddad, P. R.** (1995). Matrix-elimination ion chromatography with post-column reaction detection for the determination of iodide in saline waters. *J.Chromatogr., A* **706**, 271-275.

Table of Contents

CHAPTER 1 INTRODUCTION

This thesis has been divided in 5 Chapters. Chapter 1 is an introduction to iodine's close association with biological processes and its distribution in the oceans; Chapter 2 includes a brief review of experimental methods for iodine measurement in seawater and the methodology used in this work; Chapter 3 presents an introduction to the area studied and the distribution of iodine species in the region; Chapter 4 presents some further results using iodate concentration as a tracer of biological and physical processes in the studied region; and in Chapter 5 the conclusions are presented.

Chapter 1 has been divided in three sections. The first section briefly reviews the main species of iodine in seawater and their possible involvement in biotic and abiotic processes in the water column. The second section presents an overview of iodine distribution and speciation in different regions of the oceans. And the third section presents the aims of this dissertation.

1.1 The biophilic nature of iodine in the sea

1.1.1 The main species of dissolved iodine in seawater

The linking of iodine with the sea can be traced back to 1811, when B. Courtois discovered the element after extracting it from seaweed ash with sulfuric acid. The new element was then named by J.L.Gay Lussac in 1813, from the Greek ἰωδης, meaning violet-coloured (Greenwood and Earnshaw, 1984).

Dissolved iodine, mainly as iodate (IO_3^-) and iodide (I^-), is present in seawater as a trace element with a concentration of around 0.5 μM. Iodine is the third most common minor element in seawater after lithium (25 μM) and rubidium (1.4 μM). However, in contrast with the latter two, iodine is known as a biophilic and non-conservative element (Wong and Brewer, 1974; Elderfield and Truesdale, 1980;

Wong, 1991; Truesdale, 1994; Campos *et al.*, 1996a). A typical vertical profile of dissolved iodine in seawater resembles that of the main nutrients (phosphate and nitrate), which led to its classification as a bio-intermediate element (Figure 1.1) (Broecker and Peng, 1982; Truesdale, 1994).

Iodine is present in seawater in different oxidation states. In oxic waters, iodate has been recognised as the main species since Winkler in1916 (Johannesson, 1957) made the first direct determination of iodate in seawater. Iodate concentration in the sea varies from about 200 to 500 nM (Luther *et al.*, 1988).

The second most abundant species of iodine in seawater is iodide, which is generally most abundant in surface waters. Iodide concentration in the oceans varies from < 10 nM to 200 nM (Luther *et al.*, 1988), with surface water concentrations varying from ~ 20 nM to 200 nM (Campos *et al.*, 1996a; Campos *et al.*, 1999). According to Sillen (1961), at typical seawater conditions of pH = 8.1 and pE = 12.5, the ratio $IO3^-$ / I^- would be $10^{13.5}$. However, because iodide exists in much higher concentration than thermodynamically predicted, especially in surface waters, its presence is presumed to be a disequilibrium caused by biological activity.

In anoxic and sub-oxic conditions, iodide is the main species of iodine found in seawater (Wong and Brewer, 1977; Chapman, 1983; Wong *et al.*, 1985; Butler *et al.*, 1988; Wong, 1995; Farrenkopf *et al.*, 1997a; Rue *et al.*, 1997; Truesdale and Bailey, 2000). Iodide is also the main iodine species found in waters close to the surface of both oxic and anoxic pelagic sediments (Kennedy and Elderfield, 1987; Passier *et al.*, 1997). The flux of iodide from the sediments has been suggested as the cause of observed increase in water-column iodide concentrations close to the seafloor (Tsunogai, 1971a; Wong and Brewer, 1977; Nakayama *et al.*, 1989). Concentration of iodide in the pore waters of deep-sea sediments is of the order of ~1 to 5 μM (Kennedy and Elderfield, 1987; Passier *et al.*, 1997). In the bulk sediments, however, total iodine can vary from 19 to 139 μg/g (15 to 110 μM) (Kennedy and Elderfield, 1987). Estimates of iodine fluxes from the seafloor sediments were 0.55×10^{-8} μmol $cm^{-2}sec^{-1}$(~ 1.7×10^{-4} mol m^{-2} y^{-1}), from the average of incubation

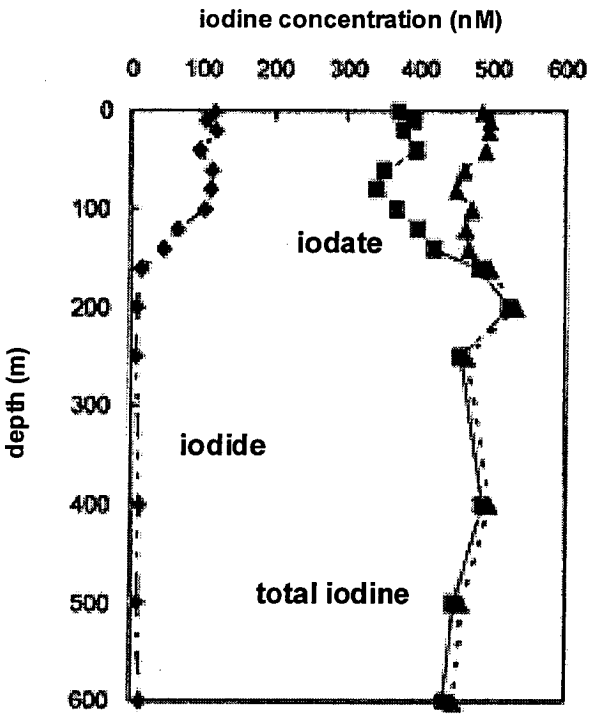

Figure 1.1 Example of iodine distribution in the oceans from Campos *et al.* (1996a) in the Bermuda time-series station in January 1994.

experiments (Kennedy and Elderfield, 1987), and 4.4 x 10^{-4} mol m^{-2} y^{-1} from iodide concentration in ocean deep waters (Tsunogai, 1971a).

The presence of non-volatile dissolved organic iodine in seawater was first detected by Truesdale (1975). He measured 2 to 40 nM of dissolved organic iodine (DOI) in inshore waters, which accounted for up to 11% of total dissolved iodine. Smith and Butler (1979) reported up to 15% of iodine as organic iodine in the Yarra River estuary. The concentration of organic iodine seems to decrease from coastal to open waters. Luther *et al.* (1991) found that organic iodine concentration in Chesapeake Bay, U.S.A., waters accounted for as much as 70% of total dissolved iodine. They believe that the organic iodine forms were probably non-volatile, residing mainly in the peptide and humic fractions. The presence of high amounts of organic iodine was associated with high primary productivity and bacterial processes. In open-ocean waters it is believed that DOI would account for 5 to10% of total dissolved iodine (Luther *et al.*, 1988; Cheng *et al.*, 1993). As the amount of organic iodine is measured by difference of total iodine, or iodate, prior and post UV oxidation, the imprecision of its values is still very high, especially in oceanic waters where the expected values would be < 40 nM. Wong and Cheng (1998) determined DOI in coastal and open waters by an "improved" oxidation procedure. In open ocean waters, DOI values were mostly < 10 nM, which was less than 5% of the total iodine. DOI values decreased from coastal to open waters and from the surface to below the euphotic zone.

The presence of volatile organic forms of iodine in the oceans has been reported by several workers (Lovelock *et al.*, 1973; Lovelock, 1975; Klick and Abrahamsson, 1992; Moore and Tokarczyk, 1992,1993; Moore and Groszko, 1999). The concentration of methyl iodide (CH_3I) in the open ocean is approximately 1ng/L (8 x 10^{-3} nM), and its presence has been associated with phytoplankton production (Klick and Abrahamsson, 1992; Tait and Moore, 1995; Moore *et al.*, 1995,1996; Manley and de la Cuesta, 1997); macroalgae production (Gschwend *et al.*, 1985; Manley and Dastoor, 1988; Manley *et al.*, 1992; Laturnus and Adams, 1998; Giese *et al.*, 1999; Laturnus, 2001); and photochemical production (Moore and Zafiriou, 1994; Happel

and Wallace, 1996). Other volatile iodated organic compounds have also been measured in seawater. Laturnus (1995) and Laturnus *et al.* (1996) measured iodo-ethane, chloro-iodomethane and di-iodomethane released by Antarctic and Arctic macroalgae cultures. Klick and Abrahamsson (1992) also measured 2-iodopropane, 1-iodopropane, 1-iodobutane and di-iodomethane in coastal and Antarctic open waters. Their results indicated that these latter compounds were produced by marine planktonic organisms and not by macroalgae. Manley (1994) also measured methyl iodide production in seawater after reacting iodide or molecular iodine with methylcobalamin (methyl vitamin B_{12}) in the laboratory; methylcobalamin is found naturally in seawater.

The interest in studying methyl iodide in the oceans comes from its probable role in tropospheric ozone destruction (Chameides and Davis, 1980). As the oceans are the prime source of this compound to the atmosphere, much attention has been paid to determining oceanic sources of methyl iodide and other volatile iodated organic compounds (Lovelock *et al.*, 1973; Lovelock, 1975; Moore and Zafiriou, 1994; Happell and Wallace, 1996; Campos *et al.*, 1996b).

Miyake and Tsunogai (1963) studied the "evaporation" of iodine from the oceans after iodide oxidation by ultra-violet radiation from sunlight (300 to 560 nm), producing molecular iodine (I_2). They believed molecular iodine exported to the atmosphere was responsible for the observed enrichment of iodine in the atmosphere, relative to the other halides. The reaction proposed was:

$$2I^- + \tfrac{1}{2} O_2 + H_2O + h\upsilon = I_2 + 2\ OH^- \qquad (1.1)$$

The hydrolysis of molecular iodine in a basic solution is very fast, implying that its lifetime in seawater is extremely short, and that, unless it is formed at a very fast rate, it will not be the major iodine species to be exported to the atmosphere from the oceans (Wong, 1980,1991). Also, the presence of dissolved organic matter and sunlight may contribute to an even shorter life for molecular iodine in natural seawater (Truesdale and Moore, 1992). Molecular iodine added to seawater reacts

very quickly with organic matter forming organo-iodine compounds and hypoiodous acid (HIO), which decomposes to form iodate and iodide or, more likely, reacts with organic matter forming iodinated organic compounds or iodide (Truesdale, 1974; Wong, 1980; Luther *et al.*, 1995). At the pH of seawater, both molecular iodine and hypoiodous acid (HIO) are unstable in relation to both iodate and iodide, which makes the oxidation of iodide to molecular iodine thermodynamically unfavorable (Wong, 1991). However, this oxidation of iodide by oxygen can be activated by sunlight (Luther *et al.*, 1995). The production of molecular iodine as a result of iodide reaction with ozone (O_3) in surface waters in the sea could also be another source of iodine to the atmosphere (Garland and Curtis, 1981; Thompson and Zafiriou, 1983; Moller *et al.*, 1996), although this reaction is only important at the surface microlayer, as ozone does not penetrate any deeper than the first micrometers of the ocean surface (Luther at al., 1995).

1.1.2 Photochemistry of iodine in seawater

The influence of direct sunlight on iodine speciation in seawater was first suggested by Miyake and Tsunogai (1963). As mentioned before, they considered iodide oxidation to molecular iodine in presence of natural solar irradiation. Other possible photochemical reactions involving iodine in seawater are:

$CH_3I + h\upsilon = CH_3^{\bullet} + I^{\bullet}$	(direct photolysis, Zafiriou *et al.*, 1984)
$I^- +$ organics $+ h\upsilon =$ HIO + oxidised organics	(Zafiriou *et al.*, 1984)
$I^- + h\upsilon = I^{\bullet} + e^-_{aq}$	(Zafiriou, 1977)
$R_{org}\,I + h\upsilon = R^{\bullet} + I^{\bullet}$	(Zafiriou, 1983)

Jickells *et al.* (1988) used photo-oxidation of iodide to iodate for total iodine analysis. They found that deep-water results were erratic and gave low recoveries of

added iodide, for samples with nitrate concentration higher than 10 μM. They suggested that nitrite produced from nitrate photo-reduction was reacting with iodate to produce iodide. The proposed reactions are below.

$$NO_3^- + h\upsilon = NO_3^-* \quad (300\ nm) \qquad (a)$$

$$NO_3^-* = NO_2^- + O \qquad (b)$$

$$NO_3^- + O = NO_2^- + O_2 \qquad (c)$$

$$IO_3^- + O = (IO_2^-) + O_2 \qquad (d)$$

$$(IO_2^-) = I^- + O_2 \qquad (e)$$

They suggested that iodate could interfere with reaction c, competing with nitrate and preferentially reacting with atomic oxygen yielding a product of uncertain composition (reaction d), which will decompose to form iodide (reaction e). They further concluded that the decrease in iodate concentration in some surface waters was unlikely to be due solely to biological activity and suggested iodate photo-reduction as a complementary source of iodide.

Luther *et al.* (1995) proposed that the photochemically mediated reaction of iodide with oxygen produces reactive iodine atoms, which can react with other iodine atoms to form molecular iodine or with other anions (Cl^-, OH^-, etc) to form radical anion species (ICl^-, IOH^-, etc). These latter species quickly reform iodide and HIO. The authors also believed that photochemical oxidation of iodide was unlikely to produce iodate as a final product, as the highest iodide concentrations in the oceans are generally found in surface waters.

Spokes and Liss (1996) measured iodide production in seawater after samples were exposed to direct sunlight. Their results showed that measured iodide photo-production was not biologically mediated, and that the presence of organic matter

was essential for it to happen. Brandão (1992), however, did not find any increase in iodide concentration in seawater samples after several hours of direct sunlight exposure. The author also estimated, based on artificial UV light irradiation of seawater, containing 4 mg L^{-1} of dissolved organic carbon, that iodide production in surface waters due to natural occurring UV irradiation would be around 6.77×10^{-2} nM I^- h^{-1} maximum and it would be restricted to the first few meters in the water column, which is very small when compared to the biological iodide production observed in culture experiments (1 nM I^- h^{-1}).

Wong and Cheng (2001) recently reported iodide production from dissolved organic iodine (DOI) in inshore waters exposed to solar irradiation. One mol of iodide was formed from one mole of DOI exposed to sunlight, and the reaction appeared to be of first order.

1.1.3 Biological cycling of iodine

Seaweeds have long been known to accumulate large amounts of iodine. Some marine macroalgae, especially brown algae (Phaeophyta), can have iodine concentrations of up to 30,000 times higher than seawater. In marine macroalgae, iodine is present mostly as iodide. The presence of an "iodide oxidase" enzyme allows iodide to be oxidised to I_2, which hydrolyses to HIO and then is absorbed into the cells, where it will be again reduced to iodide or react with organic matter forming organic iodine (Shaw, 1962). These enzymes were later identified as being a type of peroxidase enzyme that catalyse the oxidation of halide ions (Cl^-, I^-, Br^-) with peroxide, forming halogenated organic compounds. These enzymes are generally called haloperoxidases, or iodoperoxidases when catalysing the oxidation of iodide. Iodoperoxidases have been found in several species of Phaeophyta in the marine environment (Neidleman and Geigert, 1986). Culture experiments with Phaeophyta *Ectocarpus siliculosus* also showed that iodine was essential for growth and development, and that the algae used iodine as either iodide or iodate with no distinction (Woolery and Lewin, 1973).

Marine macroalgae are also well known for producing volatile iodinated compounds, such as methyl iodide. Halogens (Cl, Br and I) incorporated into organic compounds appear to enhance the biological activity of these compounds (Neidleman and Geigert, 1986), with some halogenated compounds found in macroalgae believed to have antimicrobial or antigrazing functions (Nightingale *et al.*, 1995). Low molecular halocarbons (such as methyl iodide) maybe are an intermediate product during the synthesis of more complex anti-grazing compounds, or a result of breakdown of such compounds (Hay, 1992 cited by Nightingale *et al.*, 1995). Nightingale *et al.* (1995) found that macroalgae *Ascophyllum nodosum* released more methyl iodide in the dark and under grazing pressure, which agrees with earlier findings that suggested macroalgae released iodinated compounds under stressful conditions (Gschwend *et al.*, 1985).

Marine microalgae (phytoplankton) are also able to produce volatile iodinated compounds (Tokarczyck and Moore, 1994; Tait and Moore, 1995; Moore *et al.*, 1995, 1996; Manley and de la Cuesta, 1997; Scarratt and Moore, 1996, 1998, 1999). The presence of haloperoxidases in marine diatoms has also been identified, with one *Navicula* species, found to produce iodinated compounds, showing to possess iodoperoxidase (Moore *et al.*, 1996). Extracts from marine microalgae *Porphyridium purpureum* also have shown to be able to oxidise iodide, with the enzyme partially purified from these extracts showing to be a peroxidase containing a heme component (Murphy *et al.*, 2000).

The direct uptake of either iodate or iodide in phytoplankton cultures has also been studied (Sugawara and Terada, 1967; Truesdale, 1978b; Butler *et al.*, 1981; Fuse *et al.*, 1989; Brandão *et al.*, 1994; Moisan *et al.*, 1994; Udomkit, 1994).

Sugawara and Terada (1967) found that marine diatom *Navicula sp* absorbs iodide preferably to iodate. They also found that iodate concentration would increase with algal growth, showing that there was interconversion of iodide to iodate.

Truesdale (1978b) cultured different species of marine phytoplankton and found a decrease of less than 10 μg/L in total iodine, with less than 5 μg/L of iodine being interconverted, for both iodine enriched and non-enriched media.

Butler *et al.* (1981) found a decrease in iodate concentration during diatom *Skeletonema costatum* culturing, while total iodine concentrations remained unchanged. The changes in iodine speciation occurred after six days of culturing and may be related to the release of decay products or other cell contents from senescent cells or to an increase in bacterial activity.

Fuse *et al.* (1989) cultured five species of marine phytoplankton and found iodide uptake was preferential to iodate. Iodine content in cells was as high as 2.62 mg/g dry cell for *Thalassiosira weissflogii* cultured in high iodide concentration.

Brandão *et al.* (1994) observed a diurnal cycle of iodine in phytoplankton directly taken from the sea and cultured with added nitrate, phosphate and urea. Both iodate and iodide concentrations decreased during the day at rates varying from 3.6 to 8.2 nM h^{-1}, and increased at night. These changes appeared to be related to photosynthesis and respiration. After 45 hours a net increase of 50 ± 3.5 nM of iodide was observed, probably derived from organic iodine compounds liberated by algae, as iodate concentration did not change significantly.

Moisan *et al.* (1994) found that four species of phytoplanktonic algae studied (*Thalassiosira oceanica, Skeletonema costatum, Emiliania huxleyi* and *Dunaliella tertiolecta*) were able to assimilate iodate at rates ranging from 0.003 to 0.024 nmol IO_3^- μg chlorophyll a^{-1} h^{-1} and liberate dissolved iodine probably as iodide. They also found that phytoplankton could take up as much as 3% of the ambient pool of iodate on a daily basis in the studied estuary, cycling the entire iodate pool in about one month.

Udomkit (1994) studied the uptake of iodate in six different species of marine phytoplankton: *Skeletonema costatum, Dunaliella tertiolecta, Amphidinium carterae,*

Tetraselmis levis, *Emiliania huxleyi* and *Synechoccus* sp. The author found that in both iodate enriched and non-enriched cultures all species took up iodate and produced iodide. The decrease in iodate was not always equivalent to the iodide increase, suggesting that, for some species, there was accumulation of iodine inside the cells or production of other reduced species of iodine besides iodide. The author also found a close relationship between iodate reduction and nitrate uptake in phytoplankton.

Tsunogai and Sase (1969) studied the reduction of iodate to iodide by nitrate-reducing marine bacteria. They showed that the nitrate-reductase enzyme was able to reduce iodate to iodide in seawater. Nitrate-reductase is present not only in anaerobic, but also in aerobic organisms, for nitrate assimilation. Iodate reduction was lessened by higher concentrations of nitrate (Tsunogai and Sase, 1969).

Farrenkopf *et al.* (1997b) showed that a facultative anaerobic bacteria, *Shewanella putrefaciens*, could reduce iodate to iodide in oxic waters of the Arabian Sea. The absence of sulfide and low concentrations of ammonia and nitrite (< 5 μM), led them to conclude that most iodate reduction seen in the water column of the Arabian Sea was due to bacterial activity. They also found that iodate was not being reduced directly to iodide, but there was an intermediate product, with the probable formation of either or both C-I and N-I bonds, which would, subsequently, form iodide.

A close relation between iodine speciation and bacterial density was also found in the Ace Lake, Australian Antarctic Territory (Butler *et al.*, 1988). Total iodine concentrations increasing with depth were noticed. The authors suggested that iodine was being assimilated by phytoplankton, which was then grazed by zooplankton. Iodine was then carried as sinking faecal pellets, or biodetritus, until being remineralised by heterotrophic bacteria immediately above the redox boundary or at the bottom of the lake.

Most of the biologically mediated remineralisation of iodine from organic matter appears to produce primarily iodide (Butler *et al.*, 1988; Farrenkopf *et al.*, 1997b).

However, iodide oxidation to iodate does occur, as iodide concentration decreases with depth. The chemical oxidation of iodide in seawater is not a facile process, so that the oxidation of iodide in the oceans is believed to occur mainly through biological mediation (Luther *et al.*, 1995). Tsunogai (1971a) estimated that the amount of iodide oxidised to iodate in deep ocean waters was about three times higher than that released from the bottom sediments. Gozlan and Margalith (1973, 1974) reported a iodoperoxidase-like enzyme present in marine bacteria *Pseudomonas iodooxidans.* This bacteria was able to produce molecular iodine in the presence of iodide and starch, cellulose or glycogen. Iodide oxidation to iodate also has been reported in pore waters from pelagic sediments, and was believed to be mediated by bacteria (Kennedy and Elderfield, 1987; Passier *et al.*, 1997). Campos *et al.* (1996a) found a relatively short lifetime of about 70 days for iodide in surface waters before oxidation, which was presumed to be caused by processes involving phytoplankton, maybe related to the presence of haloperoxidase enzymes.

The assimilation of iodine by phytoplankton is also suggested by studies of particulate iodine. Wong *et al.* (1976) performed the first studies on particulate iodine in the oceans, in order to better understand the recycling of iodine. Their findings showed that particulate iodine distribution was very similar to that of particulate organic carbon, phosphorus and nitrogen suggesting biological origin. The higher concentration of particulate iodine was always within the euphotic zone, and the sharp drop over the thermocline suggested a rapid recycling of particulate iodine in surface waters. Using a simple box model they estimated that only 3% of particulate iodine produced in the surface would reach the deep water, meaning that 97% (0.412 g I m^{-2} yr^{-1}) of particulate iodine was recycled within the euphotic zone. Also from the 3% (0.011 g I m^{-2} yr^{-1}) that reach deep water, only 1% would be removed to the sediments (1.6×10^{-4} g I m^{-2} yr^{-1}).

More recent work on particulate iodine in oligotrophic waters of the North Pacific has shown highly variable I/C ratios for both sediment trap and large volume filtration results (Farrenkopf, 2000). I/C ratio for filtered samples varied from 2×10^{-6} to 1.8×10^{-3}, while sediment trap I/C ratios varied from 6.6×10^{-7} to 1×10^{-4}.

Iodine fluxes calculated from sediment traps varied from 8 x 10^{-9} mol m^{-2} d^{-1} in October 1994 to 8.4 x 10^{-6} mol m^{-2} d^{-1} in March 1994. The high variability found did not agree with previous works (Elderfield and Truesdale, 1980; Wong *et al.*, 1976), but was believed to be the result of high resolution analysis, which was able to measure tens of picomolar concentrations of iodine (Farrenkopf, 2000).

The biotic and abiotic cycling of iodine in the oceans, according to above references is summarised in Figure 1.2, expanded from Figure 9 in Luther *et al.* (1995). Although the processes shown in Figure 1.2 are not quantitatively represented, one can notice the large influence of biological processes on iodine cycling in the oceans. In the photic zone, bacteria and phytoplankton are involved in iodate reduction and probably iodide oxidation. Phytoplankton are also associated with both iodate and iodide uptake, and the production of volatile organic iodine compounds. In intermediate, deep and bottom waters, only a small amount of iodine-containing organic matter is present, with iodide being released after remineralisation. The oxidation of iodide to iodate, probably through bacterial mediation, is also likely to occur in this zone. In the water column close to the bottom sediments, higher iodide concentrations are a result of diffusion from iodine-rich sediments. In the pore waters, from both oxic and anoxic sediments, iodide is released after organic matter decomposition and diffused to the water column above, being partially scavenged back into the sediments through organic matter adsorption. In oxic sediments, below the iodide-rich layer, a layer where iodide oxidation occurs is noticed, with an increase in iodate concentration probably due to bacterial activity.

1.1.4 Using iodine to estimate primary production in the ocean

Wong and Brewer (1974) made the first attempt to quantify the involvement of iodine in the uptake of nutrients from the ocean. They measured iodate in South Atlantic Waters and found that, for a station in the Argentine Basin, iodate concentrations correlated very well with those for apparent oxygen utilisation (AOU), phosphate and nitrate (+ nitrite). The molar ratios reported were AOU: nitrate: phosphate: iodate = 2440:357:22.7:1, suggesting that iodate has a nutrient-like

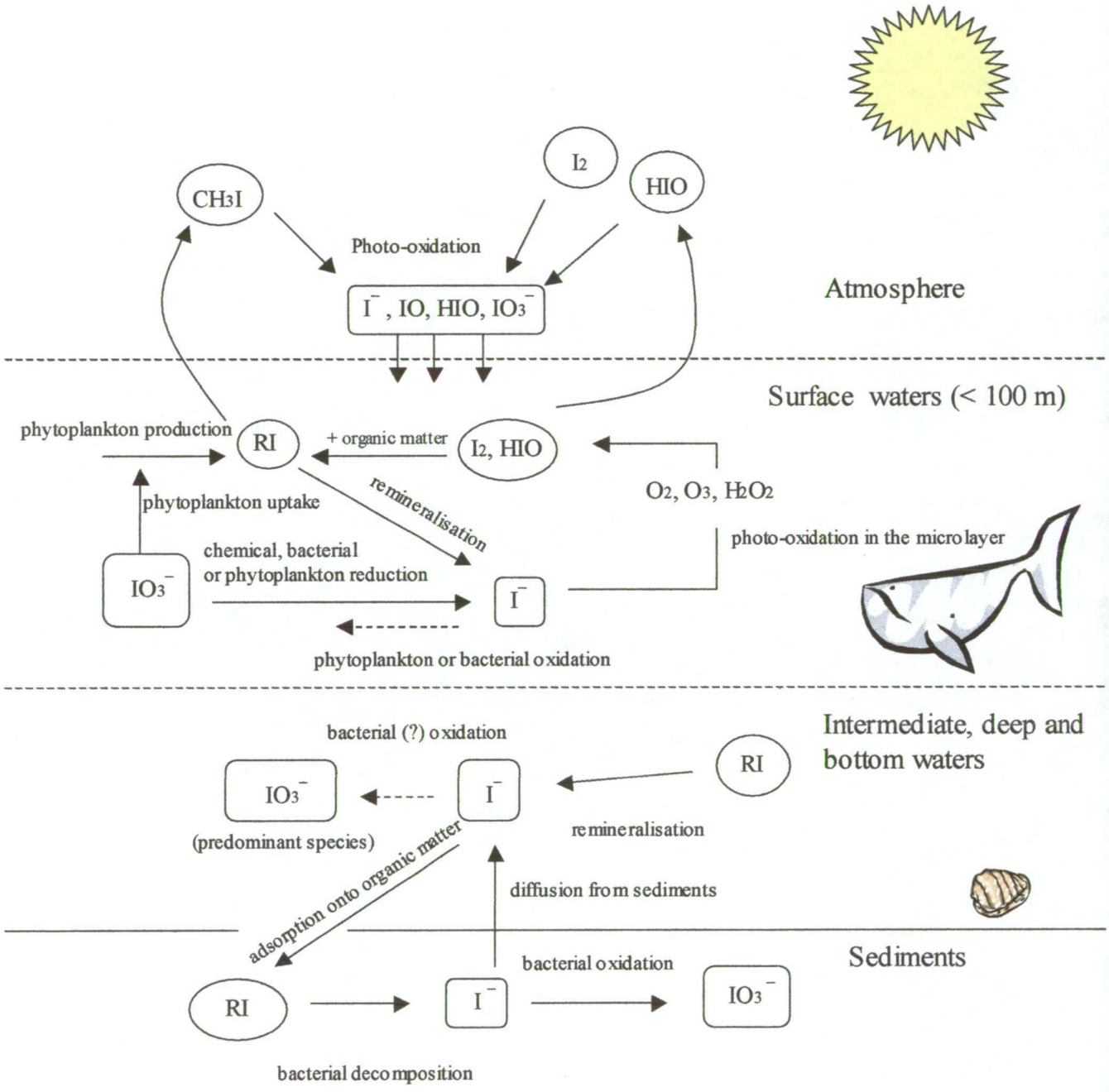

Figure 1.2- Simplified iodine cycle in the oceans, based on Figure 9 from Luther *et al.* (1995) and references in sub-sections 1.1.1, 1.1.2 and 1.1.3. "RI" represents organo-iodine compounds.

behaviour in seawater. However, their results for a tropical station in the Angola Basin showed very different patterns, with very low (0.27 μM) iodate concentrations in the surface waters and poorer correlation with nutrients.

Elderfield and Truesdale (1980) compared total iodine and iodate to phosphate using specific concentration values (i.e. concentration divided by salinity), to avoid artefacts due to dilution problems. They found a good linear correlation between total iodine and phosphate, suggesting that iodine and nutrients were involved in similar assimilation/regeneration patterns in the oceans. Their calculated I/C ratio (1.0×10^{-4}), based on a Redfield C/N ratio, agreed with the I/C ratio measured in plankton (1.4×10^{-4}). However, iodate concentrations did not correlate as well with nutrient data because of high iodate variation in the surface, probably reflecting changes in productivity or nitrate availability, or both. Pacific deep waters from Panama Basin (>1000 m depth) also showed especially high values of total iodine compared to phosphate and they were believed to be an "anomaly". These workers noticed that both iodate and total iodine were depleted in surface waters with near constant values in deep waters. The depletion in total iodine was smaller than that in iodate, suggesting iodate was being converted to more reduced species, probably iodide, in the surface waters. They noticed that most intense iodate depletion occurred in sub-tropical Pacific waters, and not in areas of higher productivity such as the Antarctic and equatorial Pacific oceans. They thus suggested that factors other than productivity were important in determining iodate to iodide interconversion, such as nitrate availability or photochemical interconversion.

The use of Redfield-type correlations between dissolved iodine and nutrients in oceanic waters was later suggested to be questionable (Truesdale, 1994). As iodine seems to be recycled in surface waters to greater extent than nutrients, phosphate and nitrate, it is not surprising to find "deep water anomalies", when comparing the two (Truesdale, 1994). The comparison of iodine and nutrient data from Atlantic stations seems to have introduced a bias towards a Redfield-type relation. As North Atlantic Deep Water ventilates through the deep Pacific and Indian oceans, a downstream increase in phosphate and nitrate can be noticed. When looking at Pacific Ocean

nutrient profiles a typical nutrient maximum can be seen, which is not followed by iodine. At a reassessment of Panama Basin station "anomaly" (Elderfield and Truesdale, 1980), total iodine results showed good linear correlation with phosphate up to the phosphate maximum (~ 700 m), but below that, as phosphate concentration decreases and iodine concentration remains constant, the linear relationship did not exist (Truesdale, 1994).

Truesdale *et al.* (2000) also found a high linear correlation between nitrate and iodate in surface waters (< 200 m) in tropical and sub-tropical Atlantic. They suggested that this iodate-nitrate relationship was due to hydrological and not chemical features, and that the iodate/nitrate ratio was not constant, but instead showed an inverse dependency on nitrate concentration at 200 m, with the iodate/nitrate ratio decreasing as nitrate concentration at 200 m increased. This suggested that the iodate and nitrate minima in stratified surface waters would occur for different reasons. While nitrate is depleted in the surface due to assimilation-regeneration processes, iodate depletion is more likely due to dissimilatory or non-assimilatory reduction, such as bacterial reduction occurring in external cell walls (Tsunogai and Sase, 1969; Campos *et al.*, 1996a; Truesdale *et al.*, 2000).

Jickells *et al.* (1988) also noticed that iodate reduction would only occur when water masses were isolated by hydrographic features, which would allow low water exchange and higher phytoplankton activity. They measured seasonal variations in iodate and total iodine concentrations in the Sargasso Sea and Bermuda inshore waters. Total iodine suffered little loss, while interconversion of iodate to a reduced species, probably iodide, was noticed to have a annual seasonal cycle. The necessity of a stable surface layer for a considerable period of time for iodate reduction to occur, plus the slow oxidation of iodide, apparently resulted in iodine and primary production cycles being out of phase. The changes in iodine speciation noticed were also larger than changes expected from I/C plankton ratio and primary production rates, suggesting that perhaps I/C ratios in phytoplankton were underestimated.

Evidence of iodate reduction to iodide due to regenerated production was found in the Mediterranean Sea (Tian *et al.*, 1996). Iodide, measured directly, showed a maximum in November (late autumn), corresponding to an iodate minimum. Total inorganic iodine (iodate + iodide) was invariant through the year. While primary productivity reached a maximum in April, with the water column warmer and high in nitrate after deep mixing in winter, iodide in the surface only started to increase in May, when nitrate was becoming undetectable from biological uptake. As nitrate levels were below detection limit from June on, primary production then was mainly due to recycled nutrients in the surface layer. This regenerated production, from recycled forms of nitrogen, such as ammonium and urea, as opposed to new production from nitrate, was linked to the increase in iodide in the surface. Based on their results they suggest that the increase in iodide (ΔI^-) in surface waters can be used to estimate *f*-ratio (new production/total production):

$$f\text{-ratio} = \Delta D / (\Delta I^- + \Delta D) \qquad (1.2)$$

where ΔD is the removal of total iodine in the surface (due to new production), estimated from the difference between surface and deep water concentrations; and ΔI^- is the iodide increase in the surface (due to regenerated production). Total production is the sum of regenerated and new production.

As iodine speciation in the oceans seems to be closely related to biological processes, the possibility of using iodine species to estimate new and total production was also suggested by G. Luther and T. Jickells, as commented by Farrenkopf (2000). As nitrate is depleted down to undetectable values in the presence of high primary production, and other forms of nitrogen easily recycled in the water column, inorganic nitrogen species cannot be used to estimate total production. The biological cycling of iodine, however, produces iodide which accumulates in the water column, as a result of its slow oxidation rates to iodate (Luther *et al.*, 1995). The use of seasonal variation in total iodine to estimate new production was suggested, as:

$$(TI)_s = (TI)_w - b\,(NP) \qquad (1.3)$$

where $(TI)_s$ and $(TI)_w$ are total iodine in the summer (*s*) and winter (*w*), NP is new primary production that occurs between *w* and s, and b is the I/C ratio of freshly sedimenting organic material.

According to Farrenkopf (2000), equation (1.3) can be simplified further if deep winter mixing reaches sufficient depth to eliminate surface depletion making:

$$(TI)_w = a\ (Sal) \qquad (1.4)$$

where Sal is the salinity of the water mass and a the TI/Sal conservative ratio noted for deeper waters (Elderfield and Truesdale, 1980). From (1.3) and (1.4), then:

$$(TI)_s = a\ (Sal) - b\ (NP) \qquad (1.5)$$

Thus, any measurement of total iodine in the summer water column might be able to provide an estimate of seasonal new production.

A simpler and more direct relation between iodide production and primary productivity, in a comparison between two time-series stations in oligotrophic waters, was later used by Campos *et al.* (1996a). Their assumption was that "iodide is only formed by reduction of iodate in association with primary production". The rate of iodide formation being:

$$\frac{dI^-}{dt} = FP \qquad (1.6)$$

where F is the ratio of iodate reduction to carbon fixation, which was taken to be equivalent to the primary production P. The authors emphasised that equation (1.6) did not imply that phytoplankton was directly responsible for iodate reduction, but only that the iodide production was related to the rate of primary production by a simple factor. Bacterial activity could also be related to the observed iodate reduction, although they believed that the role of bacteria was not so important.

Campos *et al.* (1996a) also considered that photochemical processes forming iodide were not relevant in the oceans, and that the only losses of iodide from the surface layer (< 100 m) would be due to the oxidation of iodide to iodate (dI^-_{ox}/dt) and to the mixing out of the euphotic zone (dI^-_{mix}/dt). The equation would than be:.

$$\frac{dI^-}{dt} = \frac{dI^-_{ox}}{dt} + \frac{dI^-_{mix}}{dt} = k_0 \int_0^{100} dI^- + \frac{\left(\int_0^{100} dI^- - \int_{101}^{200} dI^- \right)}{\tau} \qquad (1.7)$$

where, k_0 is the first order rate constant for iodide oxidation in the surface layer, τ is residence time of water in the upper 100 m and $\int dI^-$ the iodide concentrations integrated over the designated depth range.

Considering the oxidation as a first order reaction with constant k_0, then:

$$k_0 \int_0^{100} dI^- + \frac{\left(\int_0^{100} dI^- - \int_{101}^{201} dI^- \right)}{\tau} = FP \qquad (1.8)$$

Using two equations(for the two sites) with two unknowns (k_0 and F), and assuming that F and k_0 were the same at both sites, they found values for k_0 (iodide oxidation constant) and F (iodate reduction to carbon fixation ratio). The values found were:

$F = 6.38 \times 10^{-3}$ and $k_0 = 5.15$ year^{-1}

This value of F is higher than previously reported I/C value for phytoplankton of 1.4×10^{-4} (Elderfield and Truesdale, 1980), and even higher than I/C value estimated for particulate matter at the Bermuda station of 6×10^{-5} (Campos *et al.*, 1996a). As this F was calculated from dissolved iodide value, Campos *et al.* (1996a) suggested that iodide formation is a lot quicker than iodine assimilation by the plankton, maybe occurring externally on cell walls. This could explain iodate reduction rates being maybe 100 times higher than iodine incorporation into organic material.

The value of k_0 found would give a lifetime of iodide of 70 days, which is higher than the extremely low rate of years for chemical oxidation previously suggested by Luther *et al.* (1995). Campos *et al.* (1996a) also suggested that biological oxidation of iodide might be occurring in the studied regions, maybe due to the presence of haloperoxidase enzymes in phytoplankton.

Recently Wong (2001) proposed that the depletion of iodate in the surface water is linked to nitrate uptake. From previous work (Wong and Hung, 2001), he found evidence that iodate is taken up by phytoplankton during nitrate uptake, but most iodate taken up is exuded as iodide in surface water, while nitrate is exported to deeper waters as particulate organic carbon. He, then proposed that:

$$(IO_3^-)_r = F^*N_p = F^*(fP_p) \qquad (1.9)$$

where $(IO_3^-)_r$ is the iodate uptake and reduction to iodide, F* is the ratio of iodate uptake/reduction to nitrate uptake (N_p), f is the ratio of nitrate uptake to primary production, P_p. According to Wong (2001), nitrate uptake represents nitrate-based production or *new* production. He also considered that:

$$F^* = (IO_3^-)_r/N_p = ([IO_3^-]_d - [IO_3^-]_s)/[NO_3^-]_d \qquad (1.10)$$

where $[IO_3^-]_d$ is iodate concentration in deep water, $[IO_3^-]_s$ is iodate concentration in the surface water and $[NO_3^-]_d$ is nitrate concentration in deep water. Nitrate concentration in surface water was considered zero. The iodate depletion in surface water relative to deep water was equivalent to iodate reduced in surface water. As iodate surface depletion is about 150 nM and the world average concentration of nitrate in deep water is about 35 μM, F* is about 4×10^{-3}, where F* is also approximately equivalent to the slope of iodate plotted against nitrate.

Wong (2001) also reviewed previous works by Tian *et al.* (1996) and Campos *et al.* (1996a). The author criticised Tian *et al.*'s (1996) approach of total inorganic iodine (iodate + iodide) depletion in surface waters being proportional to "new" production

(see equation 1.2), which is nitrate uptake, saying that no data was presented to support this assumption. Wong (2001) considered that the fact that total inorganic iodine remained nearly constant while iodate and iodide varied significantly over the period of Tian *et al.* (1996) measurements (from July 1993 to June 1994) was an indication that total inorganic iodine was not proportional to nitrate uptake, namely, new primary production. Wong (2001) also considered that Tian *et al.* (1996) assumption that iodide was a product of regenerated production, based on noticed iodide production being out of phase with primary production, failed, first, to recognise that iodide and primary production are processes involving different phases and are likely to operate on different time scales, and, second, to consider that iodide production might have been small enough to only be measurable after weeks or months after phytoplankton growth started.

Wong (2001) believed that Campos *et al.* (1996a) did not have data to support their hypothesis that iodide production was proportional to primary production in their comparison between two time-series sites. Wong (2001) considered that iodide production is directly related to iodate reduction/uptake and, so, is directly related to nitrate uptake (see equation 1.9).

Wong (2001) considered that:

$$(I^-)_p = F' N_p = F' f P_p \qquad (1.11)$$

Using Campos *et al.* (1996a) data, Wong (2001) found that the life-time for iodide in the euphotic zone was likely to be larger than the 70 days previously calculated by these authors. Wong (2001) found that the life-time of iodide in surface waters was very sensitive to changes on the *f* ratios for both sites. He then estimated the life-time (t*) of iodide in surface waters using different values for F* and found that at HOT, t* would not be below 2 years, and depending on F* it could be longer than the life-time of the mixing layer of approximately 20 years, but at all times were very distant from the 70-day estimate calculated by Campos *et al.* (1996a).

Most of the studies so far discussed were made in tropical or sub-tropical oceans (Jickells *et al.*, 1988; Campos *et al.*, 1996a) or in enclosed seas (Tian *et al.*, 1996). To date, very few studies on iodine speciation have been conducted on the Southern Ocean and Antarctic coastal waters, and none of those involved the use of either of the iodine species to estimate primary production.

1.2 Distribution of iodine in the oceans

Iodine studies have covered a large extent of the world seas and oceans. The aim of this section is to briefly review some of these studies, concentrating on the differences and similarities of iodine distribution in different parts of the world's oceans: the Pacific, the Atlantic, the Indian and the Southern Oceans.

1.2.1 The Pacific Ocean

Sugawara and Terada (1957) were the first to do a study of iodine distribution covering a large area in the open ocean. Their study in the Western Pacific Ocean covered from 0° to 60°N and helped the understanding of iodine speciation in the open oceans. The values reported for total iodine, however, from 60 to 447 nM were very variable due to the analytical technique used (for more details on methods for iodine analysis in seawater see section 2.1). Barkley and Thompson (1960a) also determined total iodine in the North Pacific by two different analytical methods and found an average value of 504 nM.

Miyake and Tsunogai (1966) measured total iodine and iodide in the North Pacific and two stations on the Drake Passage using an improved Sugawara's method (Tsunogai, 1971b). They reported the first results in open ocean waters that consistently showed iodide concentration decreasing with depth and iodate concentration with the opposite trend.

Tsunogai and Henmi (1971) studied iodide and total iodine in the North and South Pacific also using an improved Sugawara's method (Tsunogai, 1971b). They reported

average iodide value at the surface of 130 nM, with the highest value in Equatorial waters. Their results along a north-south transect in the Pacific, at ~ 170°W, showed iodide concentration increasing from the tropics (10°N) to near the Equator, where a maximum value for iodide of ~ 150 nM was detected. South of the Equator, iodide concentration was around 100 nM, and another increase to ~120 nM, close to the Tropic of Capricorn (~ 23°S) was noticed. South of the Tropic, iodide concentration dropped again to < 30 nM at 40°S, probably coinciding with the Subtropical Front (STF) (Figure 1.3). South of the STF, iodide concentration decreased even more (~ 10 nM). Only two stations at 60°S and 62°S showed very high iodide values (> 170 nM), which they attributed to melting sea ice and very high biological activity in a thin surface layer (<50m). Total iodine concentrations were also very low at these stations. Total iodine values in the surface along the longitudinal transect (170°W) showed a minimum at ~ 20°S, which coincided with iodide second maximum, but were mostly around 380 nM along the entire transect (Figure 1.3). Tsunogai and Henmi's (1971) results were the first to show the variability of total iodine and iodide through different ocean zones. They also related high iodide concentrations in surface waters with high surface temperatures (> 20°C) and low nitrate concentration, which was the case observed in tropical and subtropical regions.

More recent studies of Nakayama *et al.* (1989) in the North Pacific revealed similar trends for both iodide and total-iodine in tropical and subtropical waters. Iodide concentration in surface waters was lower at high latitudes (>35°N) and between 15° and 10°N with concentrations ~ 50 nM, accounting for 12-15% of total iodine. Highest iodide concentrations (> 150 nM) were found near 25°N and at the Equator, and accounted for 30-40% of total iodine (Figure 1.3). Total iodine concentrations in surface waters did not vary as much as iodide, and were around 400 nM, increasing to ~ 480 nM in deep waters (> 1000 m). At the higher latitudes (> 40°N), the authors related iodide presence with the large amount of easily oxidisable organic matter, which could favour iodate reduction. However, in the surface waters of the subtropical zone at 30° and 24°N, very high iodide was associated with a severe deficiency of nitrate (Figure 1.3).

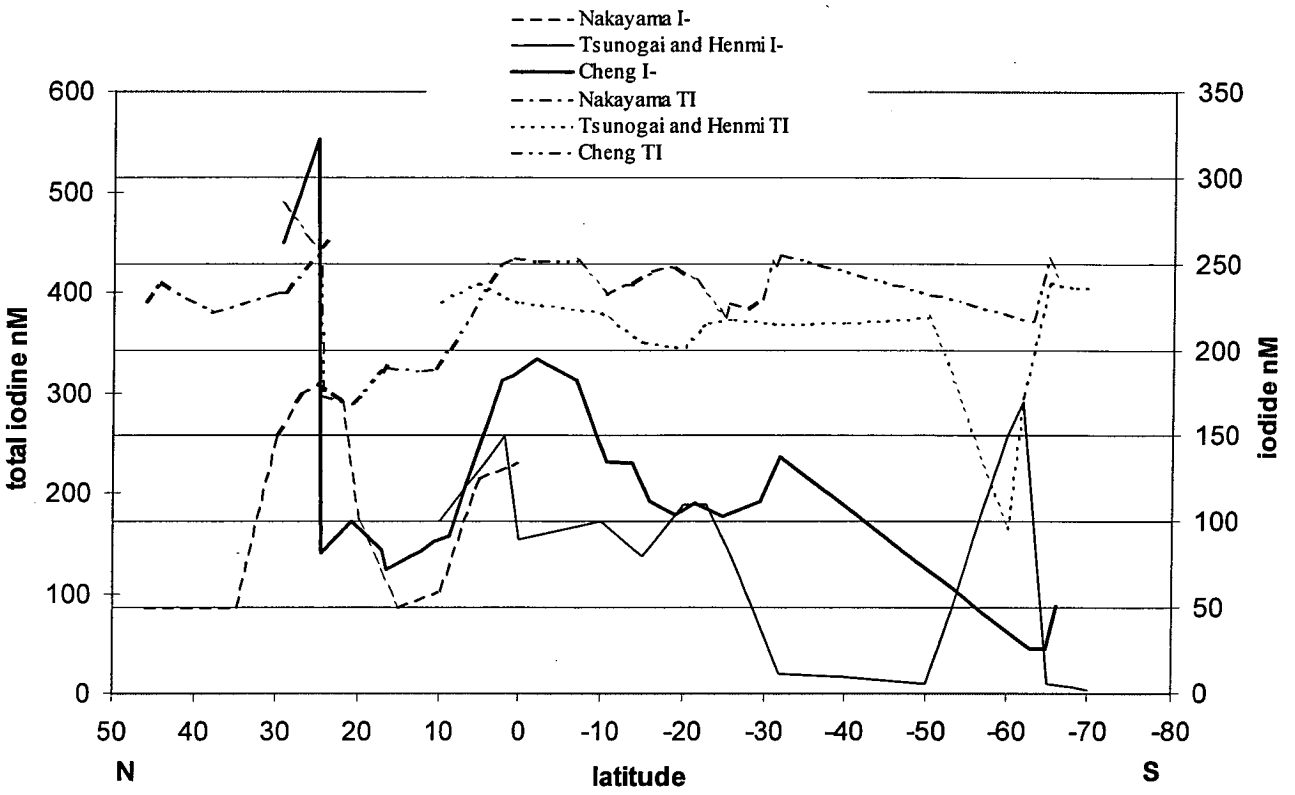

Figure 1.3 Iodide (I^-) and total iodine (TI) distribution in surface waters of the North and South Pacific according to Tsunogai and Henmi (1971), Nakayama *et al.* (1989) and Cheng *et al.* (1993).

Cheng *et al.* (1993) measured total inorganic iodine and iodate in surface waters from the North (29.5°N, 124.3°E) to the South Pacific (64.9°S, 80°W). Iodide distribution was similar to Nakayama *et al.* (1989) with a maximum at ~ 25°N, and a second maximum at the Equator (Figure 1.3). Total iodine concentrations varied greatly between the North and the South Pacific. Total iodine concentrations in the North Pacific were lower concentrations in the South Pacific. Approximate results from Tsunogai and Henmi (1971) and Nakayama *et al.* (1989) are presented beside results from Cheng *et al.* (1993) in Figure 1.3. The apparent discrepancy between Cheng *et al.* (1993) and Tsunogai and Henmi (1971) iodide distributions south of 30°S, can probably be explained by differences in longitude, with Cheng *et al.*'s iodide maximum further south, and by the lack of iodide data between 32° and 63°S.

Farrenkopf (2000) presented seasonal iodine data from the Hawaii Ocean Time-series (HOT) station ALOHA (A Long-term Oligotrophic Habitat Assessment) at ~ 23.8°N, 158°W. Iodide concentration in the surface varied from 178 nM in March up to 284 nM in October and January, with an iodide annual average of 215 ± 52 nM, from 0 to 100 m. Total iodine in the surface varied from 380 nM in January to 500 nM in June, and the author believed that station ALOHA was not characterised by a seasonal pattern of spring or fall bloom, but subject to "episodic productivity events" through the year.

1.2.2 The Atlantic Ocean

Wong and Brewer (1974) measured iodate concentration at three stations in the South Atlantic. Two stations in the Argentine Basin had similar features, such as a large depletion of iodate in the surface, a maximum at 1400 m, and a minimum between 2000 and 2800 m in the North Atlantic Deep Water (NADW). An increase in iodate, as well as nitrate and phosphate, was noticed towards the bottom, below 3500 m, and it was due to Circumpolar Deep Water (CDW) as commented later by Truesdale (1994). This increase was not seen at the third station in the Angola Basin (2°S), where iodate maximum was at 400 m. Also at the Equatorial station, iodate concentration at the surface was 274 nM, lower than iodate concentration of 400 nM

found in the surface waters of Argentine Basin. This low iodate in Equatorial surface waters was associated with higher biological activity, as seen previously in the Pacific.

Wong (1976) measured iodate in Atlantic Equatorial surface waters. High iodate concentrations from 450 to 600 nM were found at around 80 m from 33° to 10°W across the Equator. This layer of high iodate concentration, generally higher than deep waters, was associated with the high salinity-high oxygen eastward flowing core of the Equatorial Undercurrent. The iodate maximum did not correspond to nutrient or iodide maximum or minimum and was not believed to be caused by decomposition of organic matter, but possibly by advection of waters with high iodate concentration.

The first and only large-scale measurement of iodine in particulate matter was also conducted in the Atlantic (Wong *et al.*, 1976). The authors' results confirmed that iodine was enriched in particulate matter in relation to its crustal abundance, and also showed similar distribution to particulate organic carbon, phosphorus and nitrogen. The particulate iodine maximum for all stations occurred within the euphotic zone. Higher concentrations of particulate iodine were found at higher latitudes, where biological activity was highest. Most particles seemed to be transported by water masses along isopycnals, and, in stations where a weak thermocline was present, particulate iodine was transported to greater depths. Lower concentrations of particulate iodine throughout the entire water column were found at one station at 27°N in the middle of the North Atlantic gyre, where productivity is known to be low.

Elderfield and Truesdale (1980) measured iodate and total iodine in several stations in the Pacific, Atlantic and two stations in the Southern Ocean. Stations in the Panama Basin (~5°N, 80°W) showed lowest total iodine concentration in surface water (<430 nM). Lowest iodate concentration (230 nM) was found at 11.5°S, 85.9°W, in the tropical Pacific. In the North Atlantic, lowest iodate concentration in the surface (370 nM) was found at a subtropical station at ~35.9°N, 13°W, while

total iodine did not vary much. When comparing their total iodine with phosphate they found that iodine distribution fell into "envelopes" for different regions studied, with Pacific deep waters containing "anomalous high" total iodine concentrations. They also found differences in iodate between different water masses, with North Atlantic Central Water containing ~0.02 μM less iodate than North Atlantic Deep Water below. Later the apparent anomaly of Pacific deep waters was explained by differences between nutrient profiles in waters from the Pacific and Atlantic oceans (Truesdale, 1994). While iodate and total iodine profiles increased monotonically with depth in both Atlantic and Pacific Oceans, phosphate did not (Truesdale, 1994). Some phosphate profiles from the North Atlantic do not show the pronounced phosphate maxima that can be seen in some stations from the tropical and south Atlantic and also in the Pacific. These stations from the North Atlantic show a much closer correlation between total-iodine and phosphate than the stations in the Panama Basin. In stations where phosphate has a pronounced maxima, iodine-phosphate correlation was very good up to the phosphate maxima, but not below that point. The absence of such a pronounced maxima in the iodine profiles might indicate that more organic iodine is recycled in the shallower part of the profile than is the case with phosphorus and nitrogen (Truesdale, 1994), which is in agreement with previous findings for particulate iodine (Wong *et al.*, 1976).

Chapman (1983) measured iodate and total iodine in oxygen depleted waters in the Benguela Current upwelling system, along the west coast of South Africa. This system is characterised by intense upwelling that occurs mostly during the summer months due to prevalent easterly and south-easterly winds, which transport surface waters westwards allowing cold subsurface waters to surface. Total iodine concentrations generally varied from 400 to 455 nM, except at mid-water in some of the latitudinal transect lines, where high-concentrations of total iodine (> 1.2 μM) were found. Iodate concentrations varied from > 315 nM to < 175 nM, and decreased from north to south and from the surface to the bottom of the water column. Dissolved oxygen also decreased from the surface to the bottom, while iodide, calculated by difference, increased. The author believed that the increase in iodide was related to organic matter remineralisation associated with bacterial activity. High concentrations of total iodine at mid-depth were believed to be caused by

phytoplankton degradation just below the strong thermocline or from input from shelf sediments, as observed by Farrenkopf (2000) in sub-oxic waters in the Arabian Sea.

Campos *et al.* (1996) measured iodide and total iodine in the Bermuda Atlantic Time Series station (BATS) from December 1993 to July 1994. Iodide surface concentration was around half of that reported for HOT, in the Pacific (Farrenkopf, 2000). Iodide concentrations also varied less, from ~100 to 110 nM in the near surface along the year, averaging 102±16 nM for the first 100 m. Total iodine was mostly around 480–500 nM in the near surface.

Campos *et al.* (1999) measured iodide and total iodine in a longitudinal transect from the South Atlantic gyre (~30°S) to the Weddell Sea (~72°S). Iodide concentrations in surface waters dropped southwards from 100 nM in the gyre to 20 nM in the Weddell Sea. Iodide concentrations in deep waters were low between 0.5 and 2 nM. The inverse correlation of iodide with nitrate in surface waters varied for different zones of the sea. The highest I^-/N (29×10^{-3}) occurred in the South Atlantic gyre, and the lowest I^-/N (1.6×10^{-3}) south of the Subantarctic front (SAF), between 48° and 55°S. Total iodine concentrations varied little. South of the Polar Front, total iodine depletions relative to deep waters were very small (4±8 nM), differing from total iodine depletion north of the Polar Front (30±31 nM).

Truesdale *et al.* (2000) measured total iodine and iodate in surface waters (< 200 m) from the British Isles (~ 50°N) to the Falkland Isles (~ 50°S). Total iodine varied very little and were typically between 420 and 440 nM. In one of the cruise tracks, during late September-October, a slight decrease in total iodine (360 nM) was noticed at 4° to 5°N. Iodate concentrations showed much greater variation, varying from less than 300 nM just north of the Equator to greater than 420 nM south of 42°S and below ~ 100 m depth. Iodate concentrations increased sharply across the subtropical front at ~ 37°S. Iodate concentrations plotted against nitrate concentrations had correlation coefficients between 0.93 and 0.97 between 33°N and 28°S, but this correlation was a lot poorer at higher latitudes in both hemispheres,

lying between 0.08 and 0.69. Iodate concentrations also correlated poorly with primary productivity measurements. Based on their findings, the authors proposed that iodate reduction was closely associated with water column stratification, with lower iodate concentrations at the Equator, and higher iodate concentrations for latitudes higher than 30°, where the vertical mixing is more intense. Their findings also agreed with Tsunogai and Henmi's (1971) iodate distribution patterns in the Pacific.

1.2.3 The Indian Ocean

Very few studies on iodine distribution have been carried out in the Indian Ocean. Most of the data available are from the Northwest Indian Ocean, in the Arabian Sea.

Farrenkopf (2000) measured total iodine and iodide in the Arabian Sea. Most of the Arabian Sea is characterised by an oxygen minimum zone (OMZ) in the sub-surface. Most stations studied were characterised by sub-surface iodide maximum below the oxygen minimum. Maximum values for iodide were found between 500 and 950 nM within the OMZ. In the well-oxygenated surface waters, above the OMZ, iodide concentration varied from 158 to 558 nM, but integrated iodide concentrations did not vary significantly between stations. High values for total iodine were also observed (up to 800 nM) within the OMZ and suggested that there is a deep-water source of iodine probably from sediments. The high rate of reduction of iodate to iodide was believed to be mainly mediated by bacteria (Farrenkopf *et al.*, 1997a).

1.2.4 Australian and New Zealand Waters

Butler (1981) determined iodate and total inorganic iodine along the east coast of Australia, from the tropical Coral Sea to the temperate Bass Strait. Iodate concentration in the surface of tropical stations was lower than sub-tropical and temperate stations. Differences in total inorganic iodine between the regions, however, could not be noticed. Iodate concentrations in the surface of the Coral Sea varied from 276 nM to 339 nM, while total inorganic iodine was around 473 nM. In

Spring, iodate concentration in the sub-tropical surface waters of the Tasman Sea was noticeably higher than further north, varying from 315 nM to 394 nM, while inorganic iodine varied from 418 nM to 441 nM. Further south, in the Bass Strait, iodate concentration in the surface was 355 nM at 38°S and 426 nM at 41°S. At one station in the Tasman Sea, iodate and inorganic iodine concentration were also measured in Autumn and results suggested that inorganic iodine in surface waters increased from Spring to Autumn and so did iodide, calculated by difference.

Butler and Plaschke (1988) also measured iodate south of Australia in a transect along 155°E, from 44° to 57°S. Iodate concentration in the surface increased southwards. At 46°S, north of the Subantarctic Front (SAF), iodate concentration in the surface was ~ 420 nM. At 51°S, between the SAF and the Polar Front (PF) in the Subantarctic Zone (SAZ), iodate concentration ~ 445 nM. At 57°S, south of the PF, iodate concentration was ~ 455 nM.

Butler *et al.* (1992) measured iodate along the subtropical frontal zone, south of New Zealand. They found that iodate concentration increased from subtropical to subantarctic waters. They also noticed that both iodate *vs.* phosphate and iodate *vs.* nitrate plots had a break point, which coincided with samples closer to the southern limit of the subtropical frontal zone. They suggested that iodate is either assimilated or regenerated differently than nutrients in subtropical and subantarctic waters.

McTaggart (1994) measured iodate and iodide in waters from the southern and central Great Barrier Reef. In the southern Great Barrier Reef, iodide concentration decreased from 130-170 nM in the surface to less than 20 nM below 200 m. Iodate concentration varied from 280-310 nM, in the surface, to ~ 440 nM, at 500 m. In the central Great Barrier Reef, iodide concentration in the surface varied from 110 to 170 nM, while iodate concentration varied from 290 to 340 nM.

1.2.5 The Southern Ocean and Antarctic Waters

One of the first published results on iodine concentration in the Southern Ocean was from Sugawara *et al.* (1962). They measured total iodine and found concentrations of ~ 433 nM in surface waters.

As said previously in Subsection 1.2.1, Miyake and Tsunogai (1966) measured total iodine and iodide for two stations at Drake Passage. At one of the stations (58.9°S-62.7°W), iodide concentration in the surface was 185 nM and iodate was 139 nM, which might have been an analytical problem. At the other station (62.6°S-62.3°W), iodide concentration in the surface was 87 nM, and iodate concentration was 358 nM.

Tsunogai and Henmi (1971) measured iodide and total iodine from the north to the south Pacific along a transect at ~ 170°W and went as far south as 70°S. Their results for one station at 60°S were very high for iodide and low for total iodine, and it was believed to have been caused by high biological activity. Total iodine concentration was around 400 nM for surface waters in the Subantarctic and Antarctic regions. Iodide concentrations decreased from around 80 nM at 30°S to around 20 nM for latitudes greater than 40°S and are closer to values measured more recently.

Elderfield and Truesdale (1980) measured iodate and total iodine in two stations at around 57°S in the Atlantic Section of the Southern Ocean. They found iodate concentration in surface waters (440 nM) was very close to that of total iodine (450 nM). They also found that the I/C interconversion ratio in Southern Ocean was lower than in the tropical waters of the Pacific, and believed that I/C ratio variation was due to a combination of differences in both productivity and nitrate availability.

Butler (1981) measured inorganic iodine and iodate in Antarctic Coastal waters between Australian Antarctic stations of Mawson (~ 63°E) and Davis (~ 78°E). Non-normalised iodate concentrations in surface waters varied from 331 nM to 426 nM. Calculated non-normalised iodide concentrations varied from 24 nM to 47 nM.

McTaggart (1994) measured iodate in surface waters of Prydz Bay, eastern Antarctica, monthly from late winter to early summer. Although some of the results were affected by storage problems, near-surface iodate concentration dropped from ~ 450 nM in November to ~ 410 nM in December, and to less than 370 nM in January, following phytoplankton growth. The presence of high concentrations of nitrate was believed to have influenced low iodate uptake below 5-m depth.

Cheng *et al.* (1993) presented results for three stations in the Pacific and Indian sectors of the Southern Ocean. Iodide concentrations varied from 26 to 51 nM and total iodine varied from 372 to 433 nM. Organic iodine concentrations of 42 and 46 nM were also measured at two stations. Cheng *et al.* (1994) also measured total inorganic iodine and iodate in surface Antarctic waters between 60° and 90°E. Total iodine concentrations varied from 329 nM to 443 nM. Iodate concentrations varied from 303 nM to 407 nM. Dissolved organic iodine was about 10% of total iodine.

Campos *et al.* (1999) measured iodate and iodide in the Weddell and Scotia Seas. Iodide concentrations south of the Polar Front (~51°S) were below 40 nM for the first 100 m. Iodide concentration at the surface at 70°S was below 20 nM. Total inorganic iodine, iodate plus iodide, appeared to be depleted in surface waters in relation to deep waters north of the Polar Front, but not south of this Front.

Truesdale *et al.* (2000), as said in sub-section 1.2.2, measure iodate and total iodine in surface waters in the south Atlantic. The authors measured increasing iodate concentrations, from 350 to 420 nM, along the subtropical front at ~ 37°S. Few stations were measured south of 42°S, and showed iodate and total iodine concentrations higher than 420 nM in the first 100 m. Iodate and nitrate correlation was poorer in the most southern latitudes in comparison to tropical and equatorial regions, and this poorer correlation was attributed to the more intense mixing in latitudes greater than 30° at both hemispheres.

The distribution of iodine in the oceans has covered a large extent of the Pacific and Atlantic oceans, including some of their shelf seas and the Mediterranean Sea, which

were not included in this brief review. Table 1.1 summarises main surveys on iodine in the world's oceans according to different regions. It is apparent from this review and the summary in Table 1.1 that the Southern Ocean has been poorly covered so far. Some works concentrated only in latitudes higher than 60°S (Butler, 1981; McTaggart, 1994; Cheng *et al.*, 1993, 1994) or were sparsely sampled (Sugawara, 1962; Miyake and Tsunogai, 1966; Elderfield and Truesdale, 1980). Tsunogai and Henmi's (1971) transect in the South Pacific presented some extremely high iodide results for Antarctic coastal waters, which were not reported in more recent surveys. Campos *et al.* (1999) and Truesdale *et al.* (2000) studies covered the western side of the South Atlantic and concentrated in surface waters. It is apparent that iodine studies in the Australian sector of the Southern Ocean were few, covering only higher latitudes, and that there is a need for further iodine studies in the area.

Table 1.1 Summary of total iodine, iodate and iodide distribution in oxic surface and deep waters in different regions of the world's oceans according to different surveys (*results normalised to salinity of 35.0; P– Pacific Ocean; A–Atlantic Ocean; I–Indian Ocean).

Region	Approximate station positions (ocean, no. stations)	Surf. total iodine conc. range (nM)	Surf. iodate conc. range (nM)	Surf. iodide conc. range (nM)	Deep iodate (IO_3^-), iodide (I^-), and total iodine (TI) concentration range (nM)	Ref.
Tropical	11.5°S 85.9°W (P,1)	440*	230*		450* (IO_3^-), 470* (TI)	a
(20°N-20°S)	1°N–10°S, 86°W–107°W (P, 5)	440–460*	320–360*		450–460* (IO_3^-), 480* (TI)	a
	~5°N, 80°W (P, 2)	420–430*	280–300*		460–470* (IO_3^-), 480–490* (TI)	a
	2°S 4.5°W (A, 1)		274–281			c
	Various °N/S (A, 11)	360–440	<300–380			i
Subtropical	35.8°N, 13.1°W (A, 1)	440*	370*		460* (IO_3^-, TI)	a
(20° to ~42°N/S)	24°–30°N (P, 2)	400–460		100–200	480 (TI)	g
	25–26.5°N (P, 8)		250–375*	62–170*		h
	32.5°S, 36°S (A, 2)		387–403			c
	Various °N/S (A, 9)	420–440	380–420			i
	Various °S (A, 6)			60–100	0.5–2 (I^-)	j
	23.8°N, 158°W (P, 7)	380–500		178–284		k
	Bermuda Time Series (A, 8)	~500		102±16		l
Temperate	46–52.5°N (A, 19)	430–440*	370–410*		440–460* (IO_3^-), 440–450* (TI)	a
(42°N/S to SAF)	45°–50°S, 170°W (P, 5)	~380		10–50		b
	46°–57°S, 155°E (P,21)		420–460*		473–482* (IO_3^-)	m
	46°–49°S, 163°–172°E (P, 57)		390–420			n
	42.8°N, 138°E (P, 1)	380–400		100–110	~10 (I^-), 430 (TI)	g
	45°–47°N, 162°–178°E (P, 2)	390–430		~50	2.5 (I^-), ~480 (TI)	g
	45°–60°S (A, 5)			20–60	<5 (I^-)	j
	>40°N/S (A, 4)	410–430	>400			i
Southern Ocean	Drake Passage (A/P, 2)		139–358	87–185		o
	50°–60°S,170°W(P,11)	~400		<20		b
	56.8°S, 31.3°W (A, 2)	450	440		460 (IO_3^-, TI)	a
	62.9°, 64.8°, 66°S, ~80°E (I, 3)	372–433		26–51		f
	48°–70°S (A, 18)			<20	0.5–2 (I^-)	j
Antarctic Waters	63°–78°E (I, 11)		331–426	24–47		d
	Prydz Bay (I, 6)		370–450			e

References: (**a**) Elderfield and Truesdale (1980); (**b**) Tsunogai and Henmi (1971); (**c**)Wong and Brewer (1974); (**d**) Butler (1981); (**e**) McTaggart (1994); (**f**) Cheng *et al.* (1993); (**g**) Nakayama *et al.* (1989); (**h**)Wong and Hung (2001); (**i**)Truesdale *et al.* (2000); (**j**)Campos *et al.* (1999); (**k**)Farrenkopf (2000); (**l**) Campos *et al.* (1996); (**m**) Butler and Plaschke (1988); (**n**) Butler *et al.* (1992); (**o**)Miyake and Tsunogai, (1966).

1.3 Aims of the dissertation

The first aim of this thesis was to extend the knowledge of iodine distribution and speciation to the Australian sector of the Southern Ocean, a region where the few data available are restricted to coastal Antarctic waters. The first step to achieve this goal was to develop a sensitive method for direct measurement of iodide in seawater to be used onboard ship. The method for determination of iodide by matrix-elimination ion chromatography with post-column reaction detection was developed for this purpose, and is described in Chapter 2. Seawater samples were thus collected and analysed separately for iodate and iodide, and results are presented in Chapter 3. Special attention was paid to the distribution of iodate, and to a certain extent iodide also, through the different oceanic zones crossed from Tasmania to Antarctica and through different water masses, including deep and bottom waters, present in the studied region.

The second aim of this thesis was to investigate the use iodate as a tracer of biological and physical processes in the Southern Ocean, Australian sector. This second aim has been divided in the development of two hypothesis. The first hypothesis is that iodate seasonal depletion along the SR3 transect (42°–65°S, ~ 139°E) is directly proportional to seasonal new production in the region, and can be used to provide estimates of new production that are comparable to other estimates using nutrient seasonal depletion. The second hypothesis is that iodate concentration in bottom waters inside the studied region is significantly different from iodate concentration in deep waters above and can be used to trace Adélie Land Bottom Water (ALBW) freshly formed at the southern end of the SR3 transect.

Seasonal depletion of iodate as an indicator of seasonal new production

As explained previously in section 1.1, iodine is a biophilic element, with a distribution resembling that of nutrients in surface waters. Phytoplankton growth appears to affect iodine speciation in surface waters, although it is still not clear how

and why iodine is used. Iodate is believed to be reduced with nitrate, via the nitrate reductase enzyme, by phytoplankton, but while nitrate is effectively incorporated into cells and exported to deep waters as particulate nitrogen, iodate appears to be quickly released as iodide, in a non-assimilatory or dissimilatory reduction (Wong, 2001). This explains the differences in the vertical distribution of these two anions in the oceans, with nitrate being mostly remineralised below the photic zone, showing a minimum at surface and a maximum at ~ 500 m, whereas iodate is mostly recycled back to its dissolved reduced inorganic form, iodide, in the upper water columns, showing a minimum near the surface and no pronounced maximum at greater depths (Truesdale, 1994).

It has been suggested by several works that iodine's close link with biological processes would allow its use to estimate carbon uptake in the oceans (Wong and Brewer, 1974; Elderfield and Truesdale, 1980; Tian *et al.*, 1996; Campos *et al.*, 1996a; Wong, 2001; Wong and Hung, 2001). In the Southern Ocean, which is known for being a high-nutrient, low-chlorophyll (HNLC) zone, estimates of carbon uptake and export to deeper waters are of great importance, especially considering the increase of CO_2 in the atmosphere and the vast extent of this circumpolar ocean and its possible impact on past and future climate change (Priddle *et al.*, 1998a; Trull *et al.*, 2001). While direct measurements of primary production have several disadvantages, such as being a time-consuming procedure and being difficult to extrapolate to annual production values (Eppley, 1989), the use of seasonal nutrient depletion to estimate new or export production in the Southern Ocean has been used by several workers (Jennings *et al.*, 1984; Karl *et al.*, 1991; Minas and Minas, 1992; Bates *et al.*, 1998; Ishii *et al.*, 1998; Rubin *et al.*, 1998; Hoppema and Goeyens, 1999; Lourey and Trull, 2001). The depletion of nutrients in surface waters from winter to spring, summer or autumn is believed to represent the seasonal net community production, which is similar to the net seasonal new production, and, considering steady state situation, also similar to the seasonal export production, or the amount of carbon exported from the surface to the deep water (Ishii et al, 1998; Minas and Minas, 1992).

As proposed by G. Luther and T. Jickells (Farrenkopf, 2000) total iodine depletion in surface water between winter and summer is proportional to new production (equation 1.3, section 1.1.4). In this work, as iodide concentration along the SR3 transect, from Tasmania to Antarctica, between winter (July) and summer (January) appeared to be have varied little, I propose that:

$$(IO_3^-)_w - (IO_3^-)_s = a\,P_s \qquad (1.12)$$

where *w* and *s* are winter and summer concentrations, *a* is I/C molar ratio and P_s, is seasonal new production. This hypothesis also agrees with Wong (2001) findings that iodate reduction in surface water is directly proportional to nitrate reduction (uptake) by a factor F* (equation 1.9, section 1.1.4), where nitrate uptake represents new or nitrate-based production in the surface layer. This hypothesis is discussed in further detail in Chapter 4, section 4.1.

Iodate concentration as a tracer for ALBW

In this work, south of ~ 60°S, a tongue of low iodate concentration was observed and associated with Antarctic Bottom Water (AABW) presence. AABW (depth > 1000 m, temperature < 0°C) is of fundamental importance in ventilating the world's oceans, being fresher, cooler and higher in dissolved oxygen than deep waters above and penetrating from Antarctica to lower latitudes, as a tongue of high density water close to the bottom (Rintoul, 1998). AABW is formed mainly at the Weddell and Ross seas, but is also believed to have a source at the southern end of the SR3 transect, at ~ 143°E (Rintoul, 1998; Bindoff *et al.*, 2000). This locally formed AABW has been named Adélie Land Bottom Water (ALBW). ALBW has recently been confirmed to spread westwards inside the Australian-Antarctic basin, which is a deep basin (depths ~ 4000 m) extending from ~ 80°E to ~ 150°E, between the Antarctic continental shelf and the South-Indian Ridge (Rintoul, 1998; Orsi *et al.*, 1999 and Bindoff *et al.*, 2000). ALBW is believed to influence bottom waters from the south Indian and Pacific oceans and may represent as much as 25% of all AABW found in the world's oceans (Rintoul, 1998).

AABW is mostly formed in the winter, when cold, low-salinity shelf waters mix with warm, high-salinity modified circumpolar deep water (MCDW) forming high density shelf water, which is able to descend the continental slope, reaching the bottom of the ocean, forming AABW (Whitworth *et al.*, 1998). Surface shelf waters present in spring and summer normally support phytoplankton growth, with major nutrients, nitrate, phosphate and silicate being removed. As they mix with deeper shelf waters below during winter overturn, this low-nutrient signal is partially preserved (Fukamachi *et al.*, 2000). As AABW is partially formed from these waters, AABW also shows a low-nutrient signature. Although the low-nutrient signature of AABW has been documented for nitrate, phosphate and silicate, the same has not been observed for iodate or total iodine.

Iodate distribution in deep waters has been largely neglected in most studies to date, especially in the Southern Ocean. Iodate, or total iodine, concentrations in deep waters have been considered to be constant or close to constant and few references have been given to iodate distribution in different intermediate, deep and bottom water masses through different oceans or different regions within the same ocean system. In particular, iodate distribution in AABW has not been mentioned on the literature before.

In this work, I investigate the possibility that iodate concentration in AABW present along the SR3 transect is lower than iodate concentration in Lower Circumpolar Deep Water (LCDW) above, and can possibly be used to trace freshly formed ALBW, formed at the southern end of the SR3 transect. This hypothesis is further discussed in Chapter 4, section 4.2.

CHAPTER 2- EXPERIMENTAL METHODS

This chapter has been divided in three sections. Section 2.1 is a brief review of analytical methods for iodine determination in seawater. Section 2.2 is a description of the sampling procedures used to collect samples for iodine analysis and Section 2.3 describes the methods used to analyse iodate, iodide and total iodine during this work. After the results are presented in the next chapter, Section 3.3 will further discuss the performance of the analytical methods used and their influence on the results obtained.

2.1 Brief historical overview of analytical methods in the study of iodine in seawater

The aim of this section is to briefly summarise the main methods that have been used to measure iodate, iodide and total iodine in seawater during the past 50 years.

During many years there was speculation about the main species of inorganic iodine found in seawater. Already in 1916, Winkler (cited by Johannesson, 1957) reported that iodate was the major species of iodine in seawater, the remainder being iodide. But only in the mid-fifties the analytical methods for iodine determination in seawater became more precise and some understanding about iodine distribution in the oceans began.

In 1955, Sugawara *et al.* reported a new method for iodide determination in natural waters using co-precipitation of silver iodide with excess silver chloride, followed by oxidation of the precipitated iodide to iodate with bromine water; iodate reaction with cadmium iodide to liberate iodine; and spectrophotometric measurement of starch-iodine complex at 580 nm. The method required from 3 to 5 litres of seawater per sample in order to obtain measurable amounts of iodide. Using their method, in 1957 Sugawara and Terada studied iodine distribution in the Western North Pacific. They measured iodide by the method described before and total inorganic iodine by the same procedure after iodate reduction to iodide with sodium sulphite.

Matthews and Riley (1970) investigated Sugawara's *et al.* (1955) method and found that the co-precipitation of iodide never exceeded 90% of the total iodide in solution. They suggested the use of silver citrate, instead of silver nitrate, for the coprecipitation of iodide, showing that it would precipitate more than 99% of iodide. Apart from problems with the co-precipitation of iodide, they also identified problems with iodide recovery during the oxidation of precipitated iodide with bromine water. They suggested that ultrasonic agitation, rather than stirring, was necessary for a consistent high recovery of iodide. They also criticised the imprecision of starch-iodine complex measurements at the final stage, and suggested either the spectrophotometric determination of I_3^- ion at 353 nm, or the photometric micro-titration of iodide with thiosulphate using tri-iodide ion absorption to detect the end-point.

Miyake and Tsunogai (1966), Tsunogai (1971a) and Tsunogai and Henmi (1971) also used a modification of Sugawara's *et al.* (1955) method for iodide and total inorganic iodine determination described by Tsunogai (1971b). The modifications included leaving the co-precipitated iodide rest in the dark for more than 20 hours and also leaving the precipitated iodide to react with bromine water, after evaporating the solution, and letting it stand for more than 12 hours. The purity of the starch solution was also a problem, and the author suggested the used of high-amylose starch to obtain higher sensitivity during detection (Tsunogai, 1971b).

In 1957, Johannesson determined iodate in coastal waters of New Zealand. The method used involved acidification with sulphamic acid, adding potassium iodide and measuring tri-iodide ion spectrophotometrically at 355 nm. The maximum concentration of iodate in seawater he measured was of 0.034 ppm (268 nM). He believed iodate acted as a bactericidal agent being responsible for the quick death of *Escherichia coli* in seawater noticed in the studied region.

Also in 1957, Shaw and Cooper publish a paper stating that iodate was unlikely to be stable in seawater and that hypoiodous acid (HIO) was the more likely oxidised species of iodine in seawater.

Already by 1958, Sugawara and Terada had done a series of experiments and showed that there is no measurable amount of hypoiodite in seawater, and concluded that iodate and iodide are the two states of iodine in oxygenated seawater.

Johannesson (1958) also supported their results. He measured oxidised iodine in seawater and concluded that the amount of oxidising material found was too great to be anything but iodate. Shaw and Cooper (1958) then agreed with the two previous articles on the presence of iodate in seawater, but argued that still little explanation was given about the enrichment of iodine in the atmosphere.

Dubravcic (1955) used the catalytic reduction of ceric ions by iodide and performed what is believed to be the first direct determination of total iodine in seawater, from a sample from the Adriatic Sea, using 14 mL as sample volume.

Barkley and Thompson (1960b) developed an amperometric method for iodate determination in seawater. The method was based on the reaction of iodate with excess iodide in acidic samples followed by amperometric titration of iodine with thiosulfate. They also used a catalytic method for total iodine determination in seawater after some modifications of Dubravcic's (1955) method. This second method was based on the catalytic effect of iodide on the reaction between ceric and arsenous ions. The addition of arsenous acid reagent to seawater reduces all inorganic iodine species to iodide, allowing one to measure total iodine content of the sample. The disappearance of ceric ions from the solution was measured spectrophotometrically using brucine reagent. They suggested that the use of the amperometric method for iodate determination and the catalytic method for total iodine determination, with iodide being determined by difference, would be ideal for extensive oceanographic studies.

Not long after, they determined total iodine and iodate in samples from the Northeast Pacific and Arctic Ocean (Barkley and Thompson, 1960a). They found iodate representing one to two thirds of the total iodine content in the North Pacific with no trend occurring with depth or location. The iodate concentration was higher in the

Arctic samples than in the North Pacific ones. Their results differed from Sugawara and Terada's (1957), who found average total iodine of 45 μg/L (354 nM) while their average value for total iodine was 64 μg/L (504 nM).

Wong and Brewer (1974) developed another very sensitive method for iodate determination in seawater, again based on the titration of tri-iodide ions with thiosulphate, but this time using spectrophotometric detection. The coefficient of variation for iodate determination was 0.7%. Depth profiles of iodate in Atlantic Ocean waters, showed that iodate content in seawater not only varied with depth, but also with latitude. Iodate concentration in near surface waters in one equatorial station was considerably lower (247 nM) than sub-tropical stations (403 and 387 nM), which showed that better precision was necessary during iodine analysis in order to discern such differences and start to understand iodine behaviour in the oceans.

Herring and Liss (1974) developed a new method to determine iodate and total iodine in seawater using differential pulse polarography (DPP). Iodate was determined directly in seawater after addition of EDTA solution to complex Zn^{+2}, whose reduction peak interferes with the iodate peak. Total iodine was determined by the same method after oxidation of iodide with ultra-violet (UV) radiation with addition of H_2O_2 as an extra oxygen source. As later pointed out by Truesdale (1975), Smith and Butler (1979), and Butler and Smith (1980), the UV irradiation is able to oxidise not only iodide, but also organically bound iodine into iodate, which can become a critical issue when analysing surface coastal or estuarine waters.

Smith and Butler (1979), and Butler and Smith (1980) used chlorine water to oxidise iodide to iodate before determination by DPP. Chlorine water treatment oxidised iodide, but did not oxidise the organo-iodine compounds tested (Smith and Butler, 1979), and appeared to provide the concentration of total inorganic iodine after analysis. According to the authors (Butler and Smith, 1980), the organo-iodine fraction could further be determined as the difference between total inorganic iodine, determined after chlorine water treatment, and total iodine, determined by DPP after

UV irradiation followed by chlorine water treatment to destroy peroxide, which interferes with the polarographic peak. Differential pulse polarography has still been used recently to measure iodate in seawater (Brandão, 1992; McTaggart, 1994; Tian and Nicolas, 1995; Wong and Cheng, 1998; Farrenkopf, 2000; Cook *et al.*, 2000).

Takayanagi and Wong (1986) suggested the addition of sodium hypochlorite to oxidise iodide to iodate before the polarographic measurement of iodate plus iodide. The excess of hypochlorite was destroyed with sulphite. As discussed by Wong (1991), the addition of chlorine water or hypochlorite has been reported to oxidise some organo-iodine compounds, as well as iodide, to iodate. Luther and Cole (1988) reported that chemical oxidation using hypochlorite recovered 100% of iodine as iodoacetic acid, but only 50% of iodine in thyroxine. Luther and Campbell (1991) stated that hypochlorite solutions containing molecular chlorine are able to "attack" carbon-iodine bonds, in both aliphatic and aromatic compounds, liberating iodide, which is then oxidised to iodate. Wong and Cheng (1998) investigated this matter even further and concluded that, although a significant fraction of organo-iodine can be oxidised to iodate using hypochlorite, this oxidation is non-quantitative and compound-dependent. As the oxidation of dissolved organic iodine by hypochlorite appears to oxidise labile forms of organic iodine compounds, but not refractory ones (Butler, 1981), it has recently been used for the determination of total iodine in waters from a humic-rich estuary (Cook *et al.*, 2000).

Truesdale and Spencer (1974) emphasised the importance of using methods for iodate and total iodine determination onboard ship. Using the catalytic effect of iodide ions in the reaction between ceric ions and arsenous acid, they developed an automated method based on the previous Barkley and Thompson's (1960b) method. The automated catalytic method was very precise, but did not measure iodine species separately, and although it was developed for total inorganic iodine, some organically bound iodine could have also been mineralised to iodide (Truesdale, 1975). This method was further improved in later publication using new instrumentation (Truesdale and Chapman, 1976). Later on, Wong and Cheng (1998) confirmed that As^{3+} in acidic conditions is able to convert a large fraction of organo-iodine into

iodide. This conversion, however, was found to be non-quantitative, dependent on the concentration and chemical nature of the organo-iodine compounds present, and could lead to errors when estimating both the organic fraction and the iodide content of a seawater sample by difference (Wong and Cheng, 1998).

Truesdale (1975) using the automated catalytic method (Truesdale and Spencer, 1974) found what he suggested to be organically bound iodine after UV irradiation of seawater. The highest concentration measured was 5.2 μg/L.

In 1978, a new automated method was published for iodate and total iodine determinations in seawater (Truesdale, 1978a). The iodate method was based on Johannesson's previous work (1958) in measuring tri-iodide ion spectrophotometrically at 350 nm after addition of sulphamic acid and potassium iodide using a flow injection system. The first version of the method had been presented in previous work in a non-automated version (Truesdale and Spencer, 1974). Total iodine was determined after addition of bromine-water, which was removed with phenol before the analysis. He also noticed that reducing agents in the iodide reagent could affect the results by reacting with the iodine formed leading to errors in the iodate measurements. Other reducing agents present in seawater could also affect the analysis, since molecular iodine added to seawater was shown to be quickly reduced (Truesdale, 1974). Special attention was given to nitrite, and it was shown that even very small concentrations could oxidise iodide to tri-iodide (Chapman and Liss, 1977). Sulphamic acid was added to destroy nitrite, taking care to allow enough time for the reaction to take place before adding iodide reagent. Iodine-water was also used to eliminate possible natural occurring reducing agents for iodate analysis. The use of iodine-water was later condemned because it was shown to overestimate iodate concentration due to disproportionation of iodine, especially in inshore waters, where iodate concentration was lower (Truesdale and Smith, 1979).

Truesdale and Smith (1979) compared the polarographic method for iodate determination (Herring and Liss, 1974) with two colorimetric methods. The two

colorimetric methods tested involved the reaction of iodate with excess iodide in acidic medium to form tri-iodide, one including iodine-water pre-treatment (Truesdale, 1978a) and another without iodine-water. The authors recommended using either the polarographic method or the colorimetric method without iodine water as the most reliable methods for iodate determination in seawater. Even though some previous results had shown that molecular iodine was easily reduced in seawater by unknown reducing agents (Truesdale, 1974), in the colorimetric method the addition of excess iodide appeared to act as a blocking agent for the reducing process. Therefore, the pre-treatment step for elimination of reducing agents became unnecessary.

As the necessity for better methods for direct measurement of iodide in seawater were in high demand, Wong and Brewer in 1976 published a new method for iodide determination using neutron activation analysis. The method involved the separation of iodide from most other anions in seawater with a strongly basic anion-exchange column, iodide elution with sodium nitrate, co-precipitation with palladium (II) and filtration of the precipitate. The filter paper was then made into a pellet for neutron activation analysis. Although the method included long sample preparation steps, it gave a precision of ± 5%, and detection limit around 1 nM. Using this method for iodide and photometric micro-titration for iodate determination, Wong and Brewer (1977) measured iodide and iodate in anoxic basins. Their results showed that in lower pE zones, iodide concentrations increased rapidly and iodate concentration decreased to zero, showing opposite trends to that on oxygenated waters.

In 1988, Luther *et al.* published a new method for direct determination of iodide in seawater by cathodic stripping square wave voltammetry (CSSWV). This method is very sensitive with detection limit of 0.1-0.2 nM and did not require sample pre-treatment, only the addition of a small amount of surfactant. Sample analyses are relatively quick (compared with earlier methods for iodide determination), normally around 30 minutes per sample. This method helped improve the understanding of iodine chemistry, especially in the open ocean, where iodide concentration is lower, and poorer precision of iodide calculated by difference could compromise the results.

Apart from oxygen, the method's only interference is sulphide, which is only a problem in anoxic waters.

Wong and Zhang (1992a,b) used sulphite to remove dissolved oxygen from the sample prior analysis of iodide by CSSWV and iodate by DPP. This procedure shortens the time of analysis up to 20 minutes, and in acidic conditions iodate can also be reduced to iodide by sulphite, so that total inorganic iodine can be determined as iodide (Wong and Zhang, 1992b). Wong and Cheng (1998) later found that sulphite is able to break the carbon-iodine bond and liberate iodide from the dissolved organic iodine fraction at the pH of seawater. Because at this pH this reaction is very slow, no iodide increase was noticed if the sample was analysed immediately after sulphite addition. However, in acidic conditions, sulphite was able to promptly liberate some iodide from the dissolved organic iodine fraction and could lead to an overestimation of the total inorganic iodine concentration (Wong and Cheng, 1998). Campos (1997) also suggested iodate reduction with ascorbic acid followed by iodide measurement by CSSWV as a good alternative for total inorganic iodine determination.

Nakayama *et al.* (1985) developed a new method for iodide determination in seawater using a flow-through electrode. In this method iodide is oxidised to molecular iodine and adsorbed onto a carbon electrode. The iodide is then eluted from the carbon electrode and is detected at an Ag_3SI electrode. This method is very sensitive with detection limit of 1 nM and was used to measure iodide in deep waters of the Japan Sea and Japan Deep (Nakayama *et al.*, 1989). The electrode is not commercially available, which restricts its use.

Butler and Gershey (1984) determined iodide in seawater by ion-exchange chromatography with potentiometric detection using an iodide-selective electrode. Total inorganic iodine and total dissolved iodine were also determined after reduction of iodate with ascorbic acid, and UV irradiation followed by treatment with ascorbic, respectively. The detection limit for iodide with this method was 15 nM. The iodide chromatographic peak suffered some interference from bromide and chloride peaks.

Matrix-elimination ion chromatography (IC) was first used to separate iodide in seawater by Ito and Sunahara (1990). Excess of chloride in the eluent was used to suppress chloride interference from samples. McTaggart *et al.* (1994) measured iodide in coastal waters using matrix-elimination IC and direct UV detection at 226 nm. The detection limit of 10 nM, however, limited its use to coastal or tropical seawater samples.

Brandão *et al.* (1995) used matrix-elimination ion chromatography with post-column reaction detection to determine iodide in seawater with detection limit of approximately 6 nM. Details of this method are discussed in Section 2.2.

Butler (1996) emphasised the importance of doing measurements at sea and the use of automated techniques for different iodine species in seawater. He believed that the automated flow injection analysis method (Truesdale, 1978a) was still the most convenient method for iodate measurement at sea, with some limitations in coastal and estuarine samples where the high organic content of waters can interfere with the analysis. He also recommended the use of ion-chromatography with post-column reaction detection (Verma *et al.*, 1992; Brandão *et al.*, 1995) as the best available option for real-time iodide analysis at sea, because both its sensitivity and readiness to be automated.

Recently, Hu and Haddad (1998) used a new electrostatic IC method to separate and measure iodide in saline samples with UV detection at 210 nm. Their detection limit was less than 6 nM. They used an octadecylsilica (ODS) stationary phase coated with a zwitterionic surfactant. This type of surfactant contains both positively and negatively charged functional groups, but carries no formal net charge itself, and it has been shown to interact with inorganic anions. The main advantage of this technique is the low interference of matrix ions, such as chloride, which show little or no retention, while polarisable ions, such as iodide, show good retention and separation. This new method has been used successfully to analyse iodide in seawater samples (Hu *et al.*, 1999a,b).

Ito (2001) also measured iodide in seawater using UV detection (226 nm) after separation in a semi-micro ODS column coated with cetyltrimethylammonium. The detection limit was less than 4 nM for a sample injection volume of 0.5 mL. Iodide interacted with the column by both electrostatics and hydrophobicity and it was shown to be well separated from chloride and bromide, without peak broadening. The author used a mobile phase of sodium perchlorate and sodium chloride in a sodium phosphate buffer.

Although the main methods for iodate, iodide and total iodine analysis in seawater have been described above, other methods have also been used for individual studies of iodine in seawater. The catalytic effect of iodide on the reduction of iron (III) thiocyanate complex with spectrophotometric detection has been used either as an automated (Oguma *et al.*, 1993) or a manual method (Sivaraman and Rajeswari, 1983). Also, the adsorption of iodine species on to charcoal and subsequent detection using neutron activation analysis has been used (Woittiez *et al.*, 1991).

2.2 Sampling Procedures

Samples were collected on board Research Vessel *Aurora Australis* on three different cruises. The first cruise started in January 1994 (au9407), the second in December 1994 (au9404) and the third in July 1995 (au9501) (Rosenberg *et al.*, 1995, 1996, 1997). Table 2.1 shows dates, number of samples analysed and oceanographic sections sampled for these cruises.

All the water samples were collected from 10-L General Oceanics Niskin bottles, carefully cleaned for nutrient sampling (Rosenberg *et al.*, 1995). Niskin bottles were deployed on a 24-bottle rosette containing a General Oceanics Mark IIIC Conductivity Temperature Depth (CTD) probe controlled by shipboard computer. While CTD data was collected continuously, Niskin bottles were only closed on their way up. Normally, the first bottle was fired at the bottom of the cast and the other firing depths selected from data obtained by the CTD on its way down. The rosette was first stopped at each pre-selected depth and then fired (Rosenberg *et al.*, 1995). Once on board, the rosette was kept in a small enclosed laboratory room from where the water samples were drawn.

Sampling from the Niskin bottles followed a pre-determined sample order according to sample preservation. Iodine followed nutrient sampling, after dissolved gases, dissolved organic carbon (DOC), dissolved oxygen (DO), dissolved inorganic carbon (DIC) and salinity. Special care was taken during sampling to avoid being in the proximity of potassium iodide used for DO fixation and $HgCl_2$ used for DIC sample preservation.

Duplicate seawater samples for iodate determination were taken in 12-mL polypropylene screw-cap tubes, used as supplied, after rinsing twice with sample. Iodide was sampled in 100-mL screw-cap polypropylene bottles (Nalgene). Each bottle had been pre-washed overnight in Extran 0.5 % (Merck), rinsed well with Milli-Q water, air dried; and was rinsed three times with seawater prior taking the sample. After sampling, all sample containers were immediately refrigerated at 4°C

Table 2.1 Details for the three cruises sampled for this work and number of samples analysed for iodate and iodide.

Cruise	Start date	End date	Sections sampled	IO_3^- samples analysed	I^- samples analysed
au9407	01/01/1994	01/03/1994	SR3, PET	723	nil
au9404	13/12/1994	02/02/1995	SR3, S4	1058	190
au9501	18/07/1995	09/08/1995	SR3	685	101

and kept in the dark until being analysed on board, or back in the laboratory in Tasmania. Tests conducted here showed that iodate concentration in seawater samples did not change significantly after four months of storage in these conditions. Iodide samples analysed on board and then twelve months later did not show any significant changes.

2.3 Analytical Methods

2.3.1 Determination of Iodate in Seawater by Automated Flow Injection Analysis

2.3.1.1 Introduction

Iodate was determined using the automated flow injection procedure by Truesdale and Smith (1979). The method is based on the reaction of iodate with sulphamic acid in presence of excess iodide and measurement of iodonium ion, I_3^-, spectrophotometrically at 350 nm. Sulphamic acid addition is used to combat nitrite interference. This method was first studied by Johannesson (1958). Further studies were done by Truesdale and Spencer (1974), who developed a manual procedure in which seawater sample was first mixed with potassium iodide and sulfamic acid solutions and the absorption measured after 1 minute at 350 nm. Later Truesdale (1978a) automated the same procedure, which enables the method to be used aboard ship.

In this work, a flow injection analysis system set up by Butler and Plaschke (unpublished) was used and it included some minor modifications of the autoanalyser manifold proposed by Truesdale and Smith (1979).

2.3.1.2 Equipment

A Technicon Autoanalyzer II equipped with a Technicon Autoanalizer II single-channel colorimeter with 352-nm filter and a chart recorder, YEW Type 3056 pen recorder, were used throughout the work.

2.3.1.3 Reagents

All reagents and standards were prepared using distilled water that had been passed through a Millipore Milli-Q water purification system.

1. Sulphamic acid

Technical grade sulphamic acid was used and purified according to standard procedures (Appendix 1). A solution containing 10 % (w/v) of purified sulphamic acid was prepared daily.

2. Potassium iodide

A solution containing 5% (w/v) KI (Analytical Reagent –A.R., Fluka) in 0.2 % (w/v) NaOH (A.R., Fluka) was prepared daily for analysis.

3. Artificial seawater

A solution containing 39‰ (w/v) NaCl (A.R., Merck) was prepared as sample carrier. The solution was prepared typically once a week and filtered through 0.45-μm HA Millipore filters, which reduced the baseline noise.

4. Blank reagent

A solution containing 5 % (w/v) NaCl in 0.2 % (w/v) NaOH was used instead of the KI solution to run the blank signal for each group of seawater samples after the end of the analysis.

5. Iodate standards

A stock standard solution containing 1g IO_3^- as I/L was prepared from potassium iodate salt. KIO_3 (A.R., Merck) was dried in the oven at 100° C for 1 hour, 1.6864 g weighed after cooling, dissolved in Milli-Q water and made up to 1 L in a volumetric flask. This solution was kept in the dark at 4° C and used to prepare a 10 mg/L (78.8 μM) working standard every second day. From the working standard, low-concentration standards of 0, 25, 50, 75 and 100 μg/L (0, 197, 394, 591 and 788 nM) were prepared daily using micropipettes directly into 10 mL of artificial seawater pipetted inside sample tubes.

2.3.1.4 Procedures

Before analysis the sample tubes were left at room temperature (20° C) and the duplicates were only analysed for samples which showed some abnormal peak shape or unusual results. Every eight samples or standards a sample tube containing only Milli-Q water was introduced as a wash to avoid build up of reagents and salt in the system. The standards of 0, 25, 50, 75 and 100 μg/L (0, 197, 394, 591 and 788 nM) of iodate-iodine were prepared in solution of 39‰ (w/v) NaCl and run before the samples. After the last standard two wash tubes were sampled.

The schematic of the system used is shown on Figure 2.1. Milli-Q water first washes the system (with exception of the autosampler), before the reagents and then the NaCl carrier solution is introduced. While the system is being washed with Milli-Q, the NaCl carrier solution recycles back into its container after passing through the autosampler only. The reagents are introduced into the system following the Milli-Q

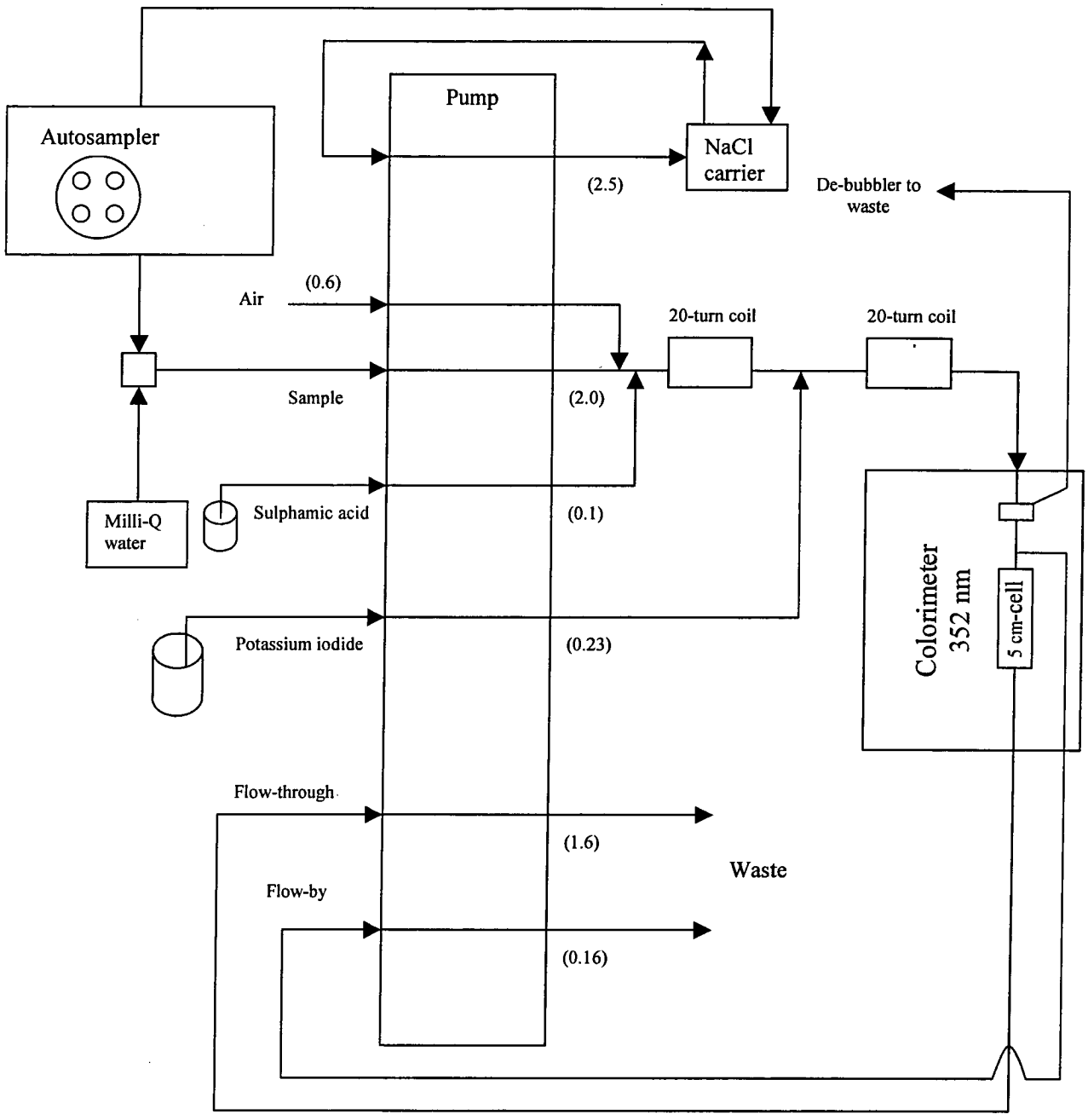

Figure 2.1 Schematic of flow injection system used for iodate determination modified from Truesdale (1978a).

water. When starting to run the samples, one would have a first baseline for Milli-Q water, a second one for Milli-Q plus reagents, and then a third baseline for the carrier solution plus reagents. The baselines for these different solutions are indicated in Figure 2.2.

2.3.1.5 Analytical performance

Normally up to 48 samples would be analysed in each run, after that the standards would be measured again to start a new run. A blank run, using the blank reagent instead of potassium iodide reagent, both described in Section 2.3.1.3, took place after each run to measure absorption by other compounds other than iodine. Normally, three surface, three intermediate and three deep-water samples from each station (total 18 samples) were picked for this run. Generally the blank signal was the same for any sample in a particular day, suggesting that it was mostly dependent on the reagents or on the equipment, or both, rather than the samples. In some surface coastal waters, however, higher blank values were noticed. These values were typically associated with noisy peak signals probably caused by the high content of organic matter in these waters.

The precision result for a typical seawater sample was 464 ± 2 (± 0.4 %) nM for n=6, which is an equivalent precision to that previously reported by Truesdale (1978a). Here precision is related to short term precision, precision estimate obtained on the same day of analysis, or within the same run. The calibration curve was linear from 0 to 100 μg/L (0 to 788 nM) and had a correlation coefficient of 1.0000. All the results were measured using strip-chart plots, which could have added up to ± 0.5% to the imprecision. Sample absorption peaks were typically 9 to 11 (± 0.05) cm high.

Although the short term precision of the method is relatively good within each run, the variation of the results for this method from day to day, or long term precision, seemed to be higher than ± 0.4%. Farrenkopf (2000) noticed differences from 10 up to 40% in results for same samples analysed on different days. Such day to day variability, or long term precision, will be discussed further at the end of this chapter.

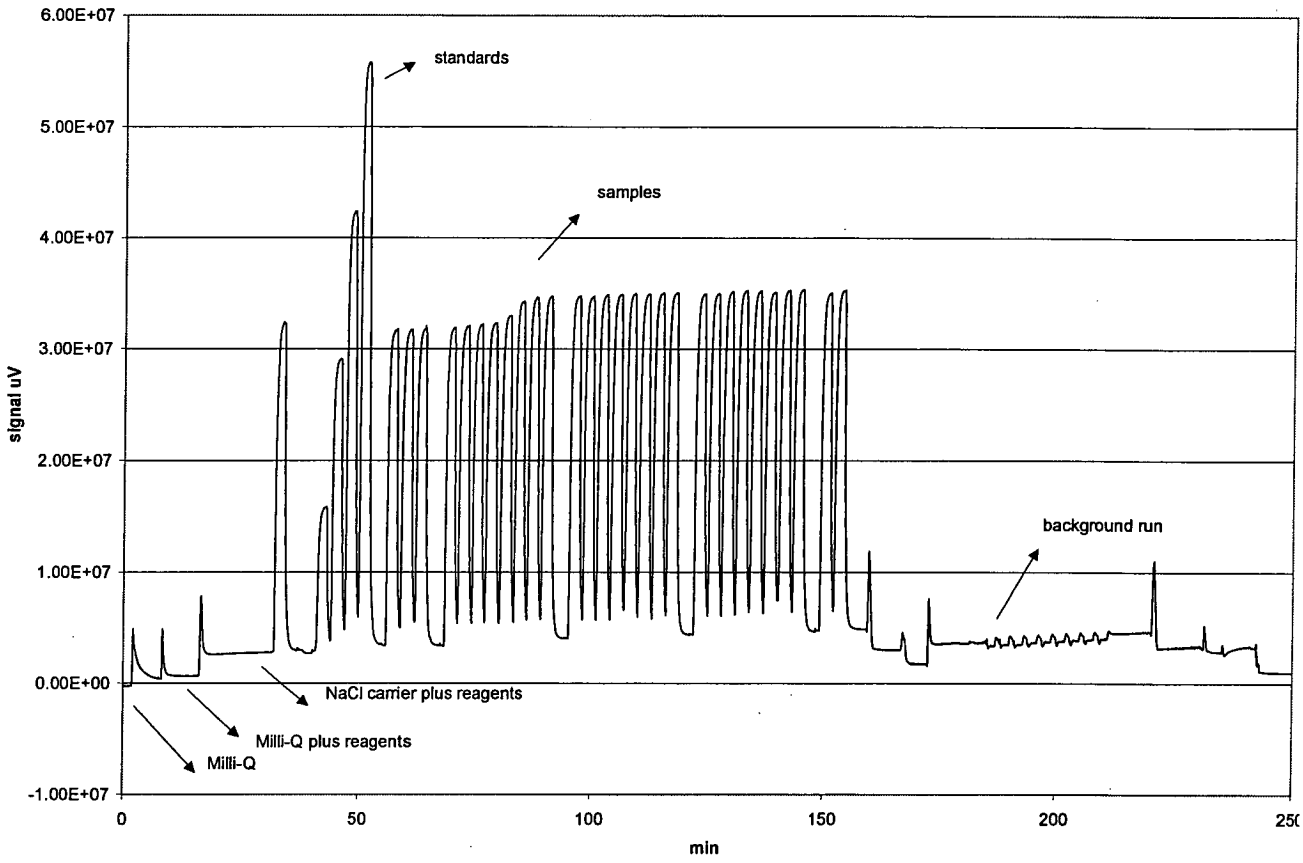

Figure 2.2 – Plot showing iodate sample and standard peaks originated from automated flow-injection analysis. Three baselines can be seen in the left side of the plot. The first is from Milli-Q water; the second after the introduction of reagents; and the third after Milli-Q water had been substituted by the NaCl carrier. The background or blank run can also be seen on the right hand side of the plot.

The baseline usually rose ~ 1 cm per 2-hour period, but this did not seem to affect the results. Sometimes the same sample measured again at the end of the run would show slightly lower or higher values, although still under ± 0.4 % variation from the initial measurement.

Some interference effect was also noticed with surface coastal samples, probably caused by UV absorption of organic matter. These samples also had a much higher blank. The top of the peaks was noisy instead of smooth, which added to the imprecision of their measurement. Fortunately, only few samples showed such interference problems, as most samples were collected in the open ocean.

In the two first cruises (au9407 and au9404), all samples were analysed on board, within 24 hours, and in the last cruise (au9501) they were analysed in the lab, within four months. The first samples analysed in the laboratory were kept in the fridge and re-analysed four months later. No significant variation was noticed for these samples, indicating that the four months between collection and analysis did not seem to have caused any increase or decrease in iodate concentration, as it had been observed before by Butler (1981) and McTaggart (1994).

The analytical equipment proved to be very robust and reliable, running 6 to 8 hours daily for up to four weeks at times without problems, both on board ship and in the laboratory. It was also easy to set up, clean and maintain. The method's reproducibility of ± 0.4% was satisfactory, and the calibration curve was linear for the range of samples analysed (Truesdale, 1978a). The reagents were relatively easy to prepare, which contributed to make this method a good choice for shipboard analysis.

2.3.2 Determination of Iodide by Ion-Chromatography

2.3.2.1 Choice of method

The voltammetric method for iodide in seawater developed by Luther *et al.* (1988) is very sensitive, with detection limit between 0.01 and 0.03 μg/L, and is by far the most popular method for iodide in seawater. However, the use of a hanging mercury drop electrode at sea in rough weather may be problematic. The equipment is also difficult to automate and sample analyses are time consuming (~45min/sample).

Nakayama *et al.* (1985) also developed a very sensitive method for iodide in seawater, using a flow-through iodide selective electrode. The method is automated, but the instrumentation they used is not readily available and appears quite complex.

The use of ion-chromatography (IC) for iodide determination offered some advantages over the above mentioned methods. Iodide elutes late in anion exchange chromatography and in ion interaction chromatography, separating well from the main seawater anions Cl^-, NO_3^- and SO_4^{-2}, and also from interferences, such as Br^-. The main problems with determination of iodide in seawater by IC were the injection of high amounts of chloride interfering with chromatographic efficiency (broad peaks) and the lack of sensitivity (small peaks). The use of a matrix-elimination technique, where chloride is added to the eluent, eliminated the chloride interference problem (Marheni *et al.*, 1991). The sensitivity problem was also addressed by combining the matrix-elimination technique with a selective post-column reaction (PCR) for iodide described by Buchberger (1988).

The method used in this work was then modified from previous work, in which iodide was determined by IC with post-column reaction using chloramine T (Buchberger, 1988). This method is very sensitive with detection limit reaching the lower μg/L range, but it is not as sensitive for saline samples. To avoid interference from chloride a matrix-elimination technique was also used by adding chloride to the mobile phase (Marheni *et al.*, 1991). The use of matrix-elimination coupled with a

sensitive post-column reaction method resulted in a method for determination of iodide in seawater samples with a detection limit as low as 0.8 μg/L (6.3 nM).

Iodide was thus determined by ion chromatography using a procedure modified especially for the analysis of iodide in Southern Ocean waters. The method is based on the detection of the blue-coloured complex iodide produces with 4,4'-bis(dimethylamino) diphenylmethane ("tetrabase") in the presence of N-chlorosuccinimide, after being well separated from bromide. Iodide was separated from bromide using a Dionex AS-11 column, using tetrabase in 20% methanol, 0.4 ml/L methanesulfonic acid, and 0.1 M NaCl as the mobile phase, and 1.5 g/L N-chlorosuccinimide solution in a buffered solution of succinic acid and succinimide at pH 4 as post-column reagent (PCR). The detection was carried out at 605 nm (Brandão *et al.*, 1995).

2.3.2.2 Conditions of Analysis and Equipment

The IC instrumentation consisted of two Waters 510 dual-piston pumps, an LKB 2157 autosampler, a Dionex AS 11 column, a Waters Temperature Control Module, a knitted reaction coil made from Teflon tubing (114cm x 0.5mm I.D.), a Waters model 450 Variable Wavelength Detector and a Waters Maxima Chromatography Data Workstation. The second pump was also fitted with a pulse dampener. The schematic of the system can be seen in Figure 2.3.

The flow rates used were 0.9 mL/min for the mobile phase and 0.3 mL/min for the post-column reagent. The reaction coil was kept inside the temperature control module at 45° C and the detection wavelength was 605 nm. The PCR reagent was kept inside an insulated container with ice during analysis, and in the fridge at all other times to avoid deterioration of n-chlorosuccinimide (P. Fagan, personal communication, 1994). The mobile-phase flask was always wrapped in aluminium foil, and kept in the fridge when not in use to avoid deterioration of the tetrabase reagent through exposure to light.

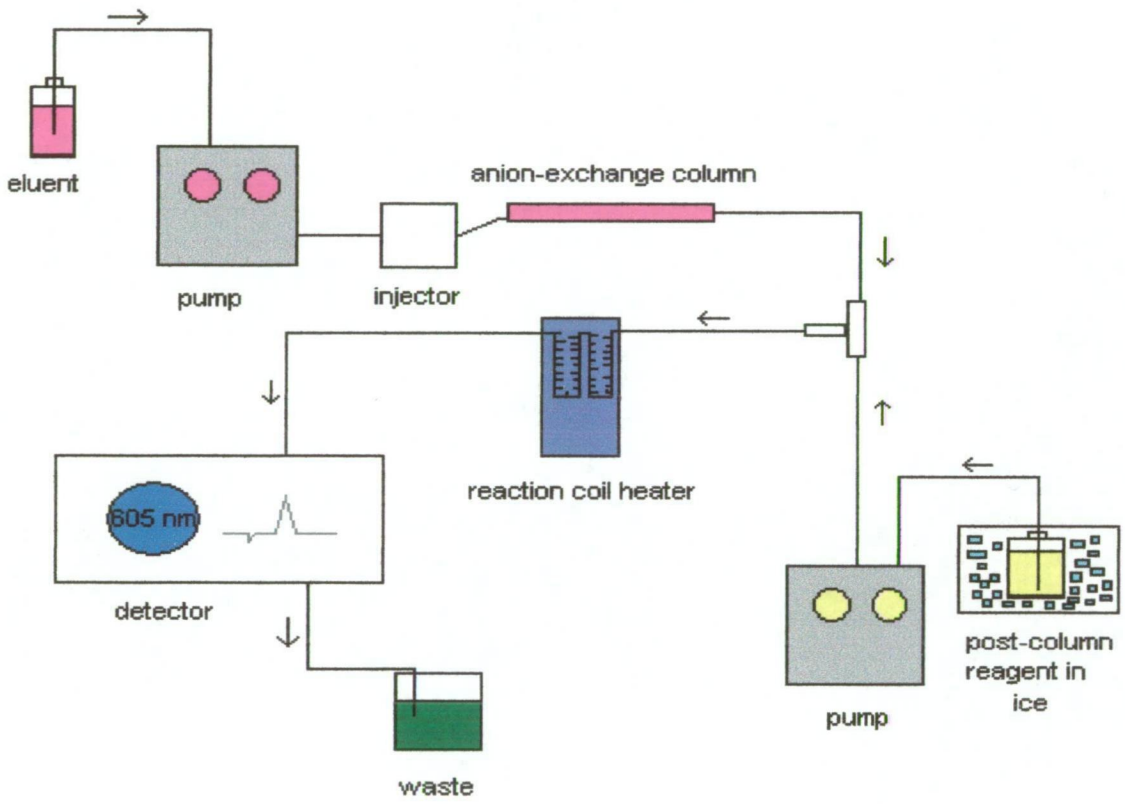

Figure 2.3- Schematic of ion-chromatographic system for iodide and total iodine determination using post-column reaction detection.

2.3.2.3 Reagents

1. Mobile phase

The mobile phase was prepared by dissolving 0.8 g of 4,4'-bis(dimethyl-amino) diphenylmethane (A.R., Merck) in 200 mL of methanol (Chromatography grade, Merck) and adding it to a solution containing 0.4 mL methanesulphonic acid (A.R., Fluka) and 5.84 g NaCl (A.R., Merck) in 700 mL of Milli-Q water. The tetrabase was first dissolved in methanol and then added to the solution with pH below 4, to avoid precipitation. The solution was then filtered through a 0.45-μm membrane filter and degassed in an ultrasonic bath for 15 min. Best results were obtained by preparing 500 mL of tetrabase reagent every second day.

2. PCR

1.5 g of n-chlorosuccinimide (A.R., Aldrich) and 15 g of succinimide (A.R., Aldrich) were added to a buffer solution containing 11.8 g of succinic acid, made up to 1.0 L and pH adjusted to 4.0 with NaOH. As a routine, 1.0 L of buffer solution would first be prepared containing 14.74 g of succinic acid, 18.76 g of succinimide and 2.33 g of NaOH, which was then filtered, degassed and kept in the fridge. When needed, 0.375g of n-chlorosuccinimide would be dissolved in 50 mL of Milli-Q water added to 200 mL of the prepared buffer and filtered. The n-chlorosuccinimide (NCS) solution is not stable for very long and should always be kept in the cold and dark, and discarded every 4 to 5 days. The final PCR solution was only degassed prior to the addition of NCS to avoid decomposition of this reagent by ultrasound (P. Fagan, personal communication, 1994), and no problems were evident from this procedure.

3. Standards

All iodide standards were prepared in a 0.56 M NaCl (A.R., Merck) solution, as an artificial seawater matrix. Standards of 1, 2.5 and 5 μg/L (7.9, 19.7 and 39.4 nM)

were prepared fresh every day from a working iodide solution of 1 mg/L (78.8 nM), prepared every week from the stock solution. The stock solution of 1.0000 g I^-/L of KI (A.R., Merck) was kept in the refrigerator.

2.3.2.4 Optimisation of the method

One of the first steps during the optimisation of this method was to substitute the chloramine T reagent with a more stable one. The use of N-chlorosuccinimide-succinimide (NCS) reagent as a source of hypochlorite was first proposed by Lambert *et al.* (1975) and later by Fagan and Haddad (1991) in the post-column detection of cyanide by IC. According to these authors, if kept refrigerated in the dark, the NCS reagent can last for two or more weeks. This reagent is also prepared in a succinic acid/ succinimide buffer at pH 4, which has a very good buffer capacity at the right pH for the reaction with tetrabase.

The strong blue colour formed in the reaction of tetrabase with free hypochlorite is not stable, and quickly decomposes into a green and finally brown colour with some precipitated being formed. So a careful adjustment of the pH had to be done. The tetrabase reagent in itself is unstable at pH higher than 5, and forms a precipitate. Thus the PCR reagent was kept at pH 4 with a small addition of NaOH, and the mobile phase was prepared in methanesulfonic acid with a pH below 4, so that the final post-column reaction pH was around 4, in order to avoid any precipitation in the reaction coil.

The length of the reaction coil was also tested. Best results were obtained using 114-cm coil of 0.5-mm I.D. (Table 2.2). The reaction coil was made of Teflon tubing knitted on a stainless steel mesh and can be seen on Figure 2.4.

The optimum flow rates were 0.9 and 0.3 ml/min for the mobile phase and NCS reagent, respectively.

Table 2.2- Results for iodide injection with variable reaction coil lengths (10 μg/L iodide standard; 130 μl injection). Reaction coil length that gave highest peak area and height is shown in **bold** letters.

Reaction coil length (cm)	**Peak Area (10^6 μV.s)**	**Peak Height (10^4 μV)**	**Reaction Coil Volume (μL)**	**Approx. Reaction Time (s)**
38	0.39	1.37	77	4
76	1.97	5.73	154	8
114	**2.66**	**7.34**	**231**	**12**
152	2.48	6.74	308	15

Table 2.3- Temperature variation for reaction coil (10 μg/L iodide standard, 200 μL injection).

Temperature (°C)	**Peak Area (10^6 μV.s)**	**Peak Height (10^4 μV)**	**Noise Height (10^4 μV)**
35	0.24	0.54	0.10
45	0.44	0.84	0.11
55	0.91	1.62	0.11
65	1.42	2.28	0.20

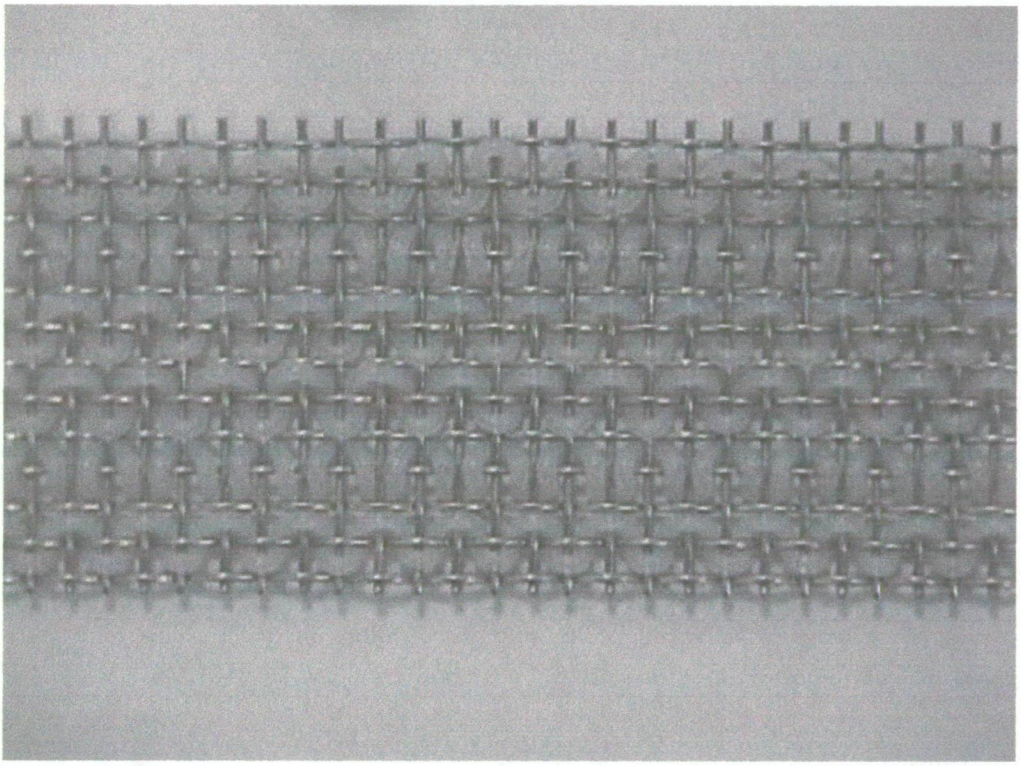

Figure 2.4- Knitted reaction coil used for iodide and total iodine determination by ion chromatography with post-column reaction. The reaction coil was made of Teflon tubing (1.4 m, 0.5 mm I.D.) knitted through a stainless steel mesh (~ 5mm).

The tetrabase concentration was also increased from the original 0.4 g/L up to 0.8 g/L, which produced nearly a three-fold increase in the peak area (from 0.239×10^6 to 0.690×10^6 μV s for a 79–nM standard).

The effect of temperature on the reaction was also investigated. Temperatures from 35° up to 65°C were tested for tetrabase concentration of 0.4 g/L (Table 2.3). For the higher tetrabase concentration (0.8 g/L), the peak area doubled as temperature increased from 35° to 45°C, but there was only a 20% increase after that at 55°C. At higher temperatures, with the rapid increase in the reaction rates, the products of reaction can precipitate before leaving the system, causing blockage and possible damage to the reaction coil or detector. The temperature of 45°C was then chosen for being a good compromise between peak area increase, low baseline noise, and the absence of precipitates in the reaction coil.

Possible interference of thiocyanate on the separation of iodide was checked, and concentrations up to 1.5 mg/L did not show any significant effect. The effect of injecting samples with high chloride concentration in the chromatographic column was also investigated. The number of theoretical plates (N) of a chromatographic column is often a good indicator of separation efficiency (Haddad and Jackson, 1990). N is calculated from the retention time (t_R) and the width of the peak at 4.4% of the peak height ($w_{4.4\%}$) according to Haddad and Jackson (1990):

$$N = 25 \times (t_R / w_{4.4\%})^2$$

The higher the number N, the more efficient is the separation. Figure 2.5 shows how the number N (per metre of column) for iodide peak varied with increasing NaCl concentration in the iodide sample. It was clear that the injection of high salinity samples affected the separation efficiency by producing broader peaks (lower value of N). The volume of injection was also tested (Figure 2.5) and as a compromise between separation efficiency (higher N value) and sensitivity (higher injection volume) the volume of injection chosen was 150 μL.

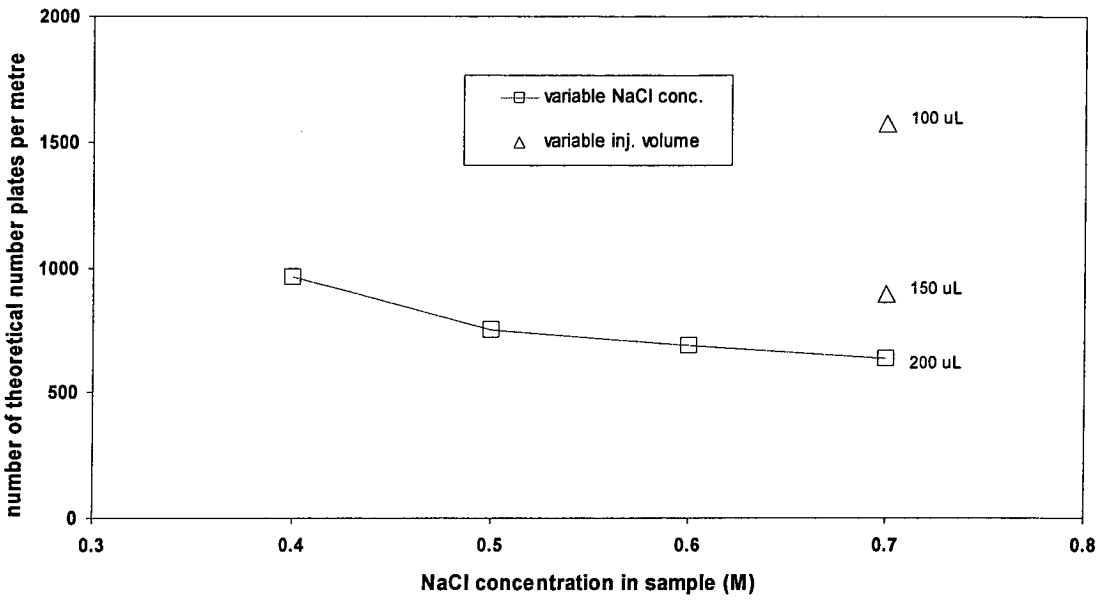

Figure 2.5 – Variation of number of theoretical plates per metre of chromatographic column for iodide peak with variable injection volume (Δ) and variable NaCl concentration in the sample matrix (□).

2.3.2.5 Analytical performance

This matrix-elimination IC method was used to analyse a total of 291 seawater samples for iodide. A typical chromatogram can be seen on Figure 2.6. The systemwas used on board RSV *Aurora Australis* during au9404 cruise and a total of 107 samples were analysed on board. The system proved to be robust and well-suited for use at sea.

The main difficulty with this technique was the high baseline noise caused by the second HPLC pump, the post-column reaction pump. To solve this problem, some authors have used pressurised injection of PCR (Vinall, 1991), but for this work some problems were found in keeping the pressure constant as the reagent was being used. A Reagent Delivery Unit (Waters) was also tested, but it had a similar problem regarding pressure stability. It was decided to compromise some of the sensitivity and use a HPLC dual piston pump to deliver the PCR. The use of pulse dampeners after the PCR pump reduced the baseline noise, as did a 10-m back-pressure coil made from Teflon tubing (0.23 mm I.D.) knitted onto a metallic grid. The use of syringe pumps for PCR might be a possible solution for this noise problem, and it should be considered in future work.

The detection limit for the method was 0.8 μg I^-/L (6.3 nM), when the method was first optimised. However, it later increased to 2.5 μg/L (20 nM), because of baseline noise problems with the pumps that could not be fixed at that time. The relative standard deviation was better than 4 % for iodide concentration of 5 μg/L (39.4 nM) (n=5).

A small signal resulting from iodide present in the sodium chloride salt used to prepare the standards was found. However, this signal was typically at the detection limit, and often it could not be measured accurately. So the most recent measured blank value was subtracted from the standards, whenever the blank signal was below the detection limit, during a determined analysis.

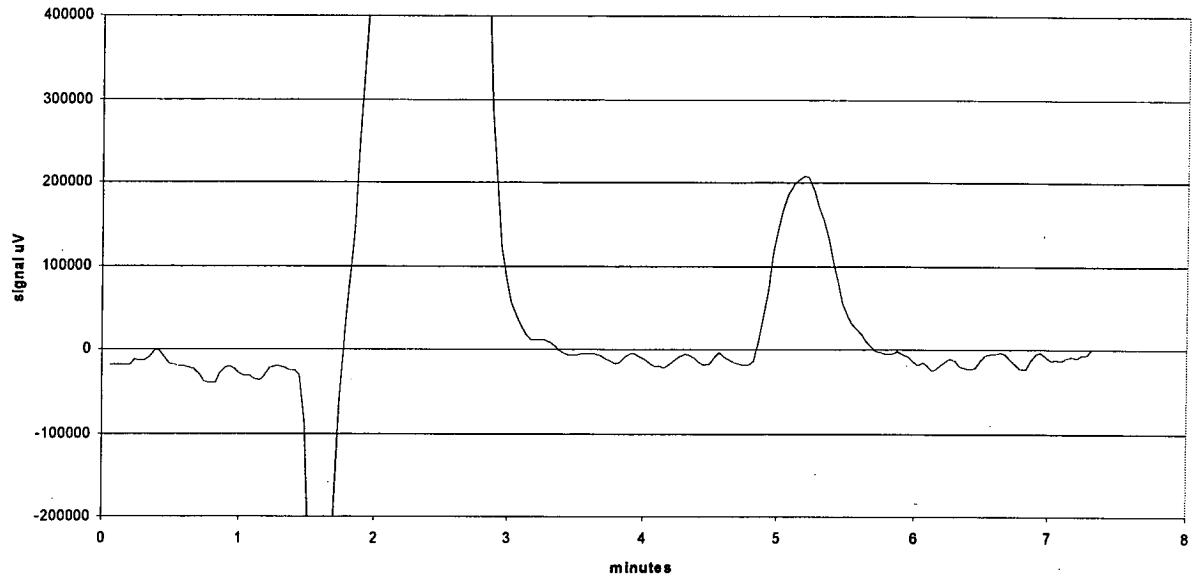

Figure 2.6- Typical chromatogram of iodide in seawater sample showing iodide peak (at ~ 5.2 min) well separated from bromide peak (off scale at ~ 2.5 min). Iodide concentration in the samples was 30 nM.

2.3.2.6 Baseline noise and estimation of detection limit

Many of the samples were found to be very close to the detection limit of the method, so care was taken to define the detection limit rigorously. From 291 samples analysed only 149 were above the detection limit, as determined using a macro subroutine developed by Dr. Mirek Macka (School of Chemistry, University of Tasmania). The subroutine runs inside a Macintosh compatible software called Igor. With this subroutine it was possible to measure the baseline noise (N) within 95% confidence level, such that N= 3s,where s is the noise's standard deviation. It was then decided to define the detection limit, DL, as twice the baseline noise, 2N, so DL=2N. Any measured iodide concentration below DL has been plotted in white, and presented in Chapter 3. Figure 2.7 shows an example of a peak absorbance that is just above the detection limit. The detection limit was then calculated separately for each chromatogram, because the baseline noise varied during a day of measurements.

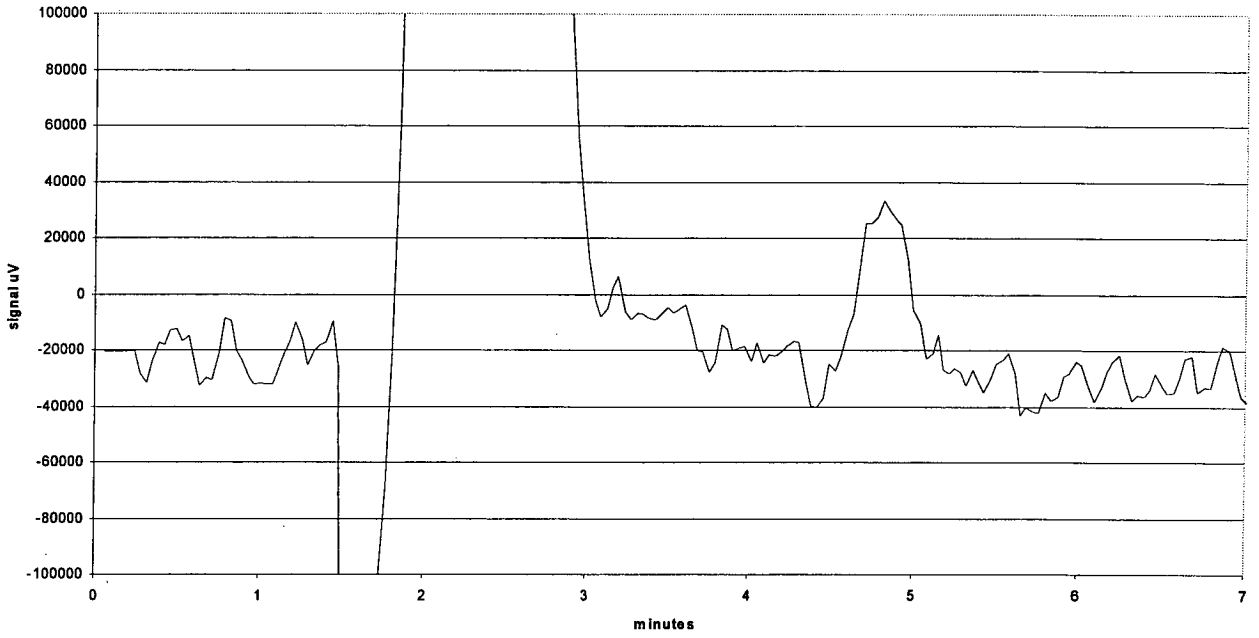

Figure 2.7 - Chromatogram showing iodide separation in seawater sample at 200 m depth. Bromide peak was eluted first and is off scale (at ~ 2.5 min). Iodide peak is just above detection limit at concentration of 11 nM (at ~ 4.9 min).

2.3.3 Determination of iodide by Cathodic Stripping Square Wave Voltammetry (CSSWV)

2.3.3.1 Introduction

The determination of iodide by CSSWV followed the method first introduced by Luther *et al.* (1988) using Triton –X100 addition to improve iodide peak shape as it oxidises on the mercury drop. The most important thing about this method is its high sensitivity, which has only been approached by that of Nakayama et al (1985), which uses a proprietary selective electrode that is not readily available. The use of voltammetry for iodide determination for this work was carried out in order to provide a comparison with the IC method described in the previous section.

2.3.3.2 Conditions of Analysis and Equipment

The system was set up using a Metrohm 663 VA stand electrode coupled with a PAR 384 B polarographic analyser using an interface developed at CSIRO Marine Labs by Paul Boult. The Metrohm electrode is more robust than the PAR 303, allowing the use of larger sample volumes which increases method sensitivity. The Metrohm unit also has a superior mercury delivery system, based on inert gas pressure rather than gravity.

In this method, the sample is first poured into the cell and weighed to minimise handling. Roughly 10 g of sample were used, with 1 μL of surfactant Triton X-100 (1 %) added per gram of sample. The sample was then purged with argon for 20 min, and the deposition time varied from 40 to 240 s, depending on the height of the peak obtained. The voltage scan was run from -0.10 V to -0.75 V, with 100 Hz frequency and 20 mV pulse height.

2.3.3.3 Reagents

1. Triton X-100 solution

A 1% (v/v) solution was prepared by adding 100 μL of Triton X–100 (Laboratory grade, Sigma) to 100 mL of Milli-Q water every four days. It was kept in the fridge while not in use.

2. Iodide stock solution

A solution containing 1000 mg I^-/L was prepared using KI (A.R., Merck), dried at 100°C for 1 h, in Milli-Q water. This solution was used for 12 months.

3. Iodide working standards

Solutions containing 1 or 5 mg/L (78.8 or 394 nM) of iodide were prepared fresh every four days using the iodide stock solution.

2.3.3.4 Analytical performance

The iodide concentration of seawater by CSSWV samples was determined after two standard additions. The coefficient of variation for five consecutive iodide determinations was 4.1% at 20 μg/L (158 nM) level and 9.5% at 3 μg/L (23.6 nM) level.

The results obtained by CSSWV for iodide concentration in seawater samples were compared with results from the IC method. The results of the methods comparison are plotted in Figure 2.8 and concentration values can be seen in Appendix I for samples from two oceanographic stations. From Figure 2.8, the results obtained by the two different methods appear to be in agreement with a R^2 of 0.9528. Results obtained by IC, according to the slope of the linear regression, were on average nearly 20% lower than the ones obtained by CSSWV. In the lower nM range

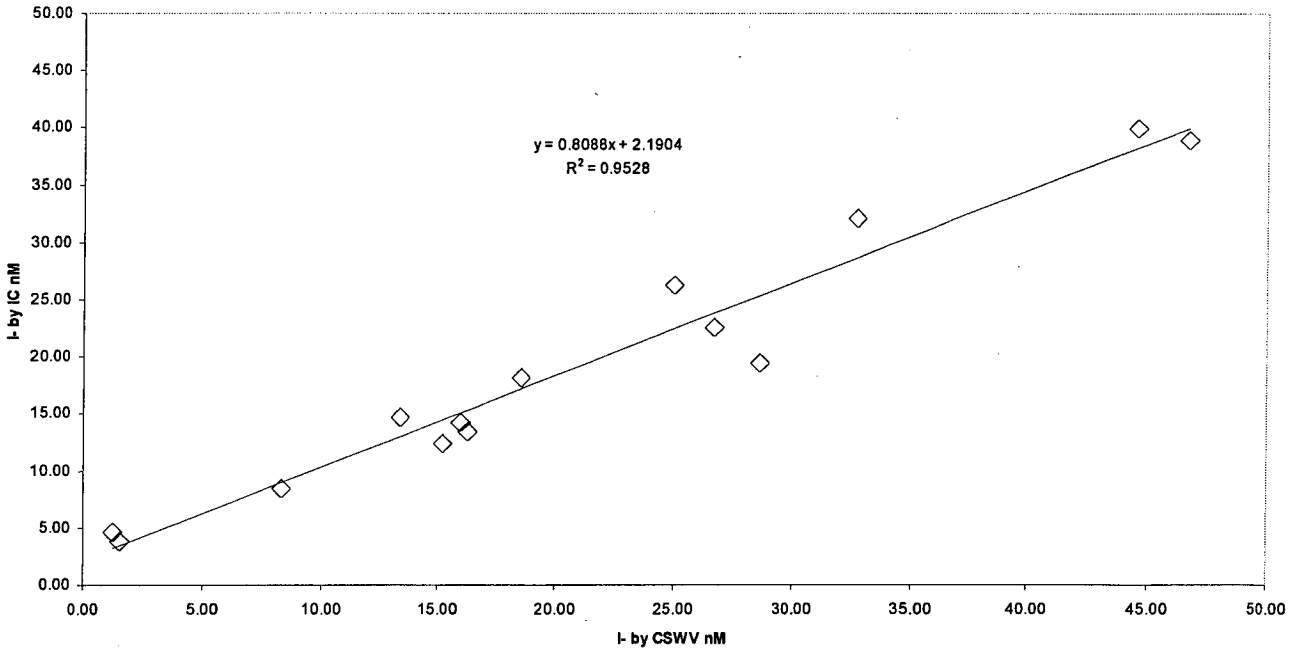

Figure 2.8- Iodide determination by ion-chromatography (IC) plotted against iodide determination by cathodic stripping square wave voltammetry (CSSWV).

(<5 nM), however, with IC results close to their detection limit, the two values by CSSWV were lower than the equivalents from IC. However, on a sample-by-sample basis, if the two samples with lowest concentration were ignored, the average sample value of IC determination is 91 ± 12% of that obtained from CSSWV. This difference may possibly be explained by the time of six months elapsed between samples analysed by IC, and those by CSSWV, but with only 14 samples analysed for this comparison, however, it is difficult to drawn any more conclusions at this point. More samples would need to be analysed by the two methods to confirm this trend.

The lowest concentration measured by CSSWV was 1.26 nM iodide followed by 1.53 nM iodide for the same station near the bottom of the cast. These concentrations were well below the IC detection limit of 6.3 nM and show that ideally the IC detection limit should be around 1 or 0.5 nM to give a complete view of iodide distribution in waters from the studied region. The highest concentration measured was 46.7 nM iodide, near the surface.

Unfortunately, after one month of work the 384 B polarographic analyser developed what appeared to be an electronic problem and no further samples were analysed.

2.3.4 Determination of Total Inorganic Iodine by Ion-Chromatography

2.3.4.1 Introduction

It was originally planned to measure total iodine so as to estimate the concentration of organic iodine in the Southern Ocean surface waters by difference. Quite commonly total iodine measurements involve oxidation of all iodine species to iodate either chemically, using hypochlorite (Takayanagi and Wong, 1986), or photochemically, using UV irradiation (Butler and Smith, 1980) followed by differential pulse polarography (DPP) determination of iodate. With the unserviceability of electrochemical instrumentation to measure samples by DPP, a

new procedure was used to measure total *inorganic* iodine by ion-chromatography (IC) instead of total iodine.

In this new procedure, iodate plus iodide were determined by IC after iodate reduction with ascorbic acid at pH 2. The IC method used is described in section 2.3.2.

The reduction of iodate to iodide in seawater with ascorbic acid in the presence of HCl has previously been used for voltammetric or polarographic measurements (Campos, 1997). However these electrochemical methods required buffering the samples after the reduction step back to their original pH. Apart from the addition of extra reagents to buffer the sample, another disadvantage of such methods, when compared with IC, is the difficulty in being automated and used for shipboard analysis.

In this study, total inorganic iodine was determined by IC after a rapid reduction of iodate with ascorbic acid in the presence of HCl. The ascorbic acid is able to reduce iodate to iodide, but will not reduce organic iodine (Butler, 1981) so the fraction measured is most likely to contain only the inorganic species iodate and iodide.

2.3.4.2 Procedures

To each 5 mL of seawater sample, 5 mL of Milli-Q water, 100 μL of 6 M HCl and 50 μL of 0.2 M ascorbic acid were added, the sample was mixed for 1 minute and then 100 μL injected into the IC system.

The IC was carried out using a Dionex AS-11 anion-exchange column. Ascorbic acid did not interfere with the iodide separation or peak shape. The system was set up as the previously described post-column reaction detection method for iodide analysis (Section 2.3.2). The samples were injected manually using a 7125 Rheodyne injector, and the reaction coil was kept at 35°C.

2.3.4.3 Reagents

1. HCl 6M

The solution was prepared by diluting 100 mL of 12 M HCl (A.R., Merck) in 100 mL of Milli-Q water.

2. Ascorbic Acid 0.2 M

The solution was prepared by dissolving 3.522 g of Ascorbic Acid (A.R., Merck) in approximately 50 mL of Milli-Q water and making it up to 100 mL in a volumetric flask.

Other reagents were prepared as in Section 2.3.2.3

2.3.4.4 Analytical performance

The procedure described above was used to determine total inorganic iodine in seawater samples from the Southern Ocean. The total inorganic iodine concentration ranged from 393 to 500 nM, and the values are consistently lower than those obtained by adding iodate and iodide results that were obtained independently. These differences will be further discussed in section 3.3.4. A total number of 130 samples were analysed. A typical chromatogram can be seen on Figure 2.9.

The relative standard deviation on repeat measurements in seawater was better than 3% at 230 nM concentration level (n=5).

Iodide standards were compared with equivalent iodate standards and any resulting differences were within the method's analytical uncertainty, showing that iodate was quantitatively reduced to iodide under the conditions employed. Further discussion on the results is presented in section 3.3.4.

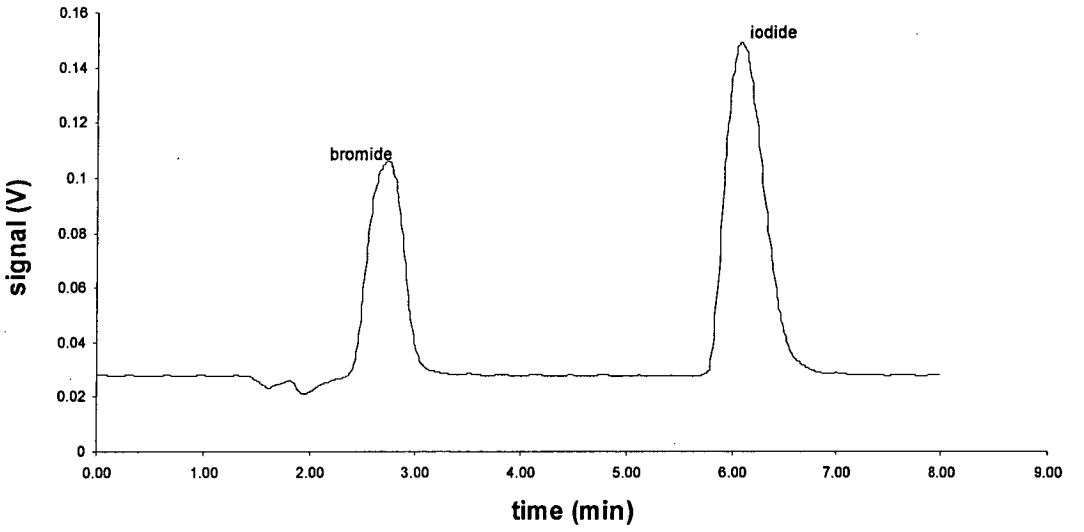

Figure 2.9- Typical chromatogram for total iodine in seawater sample of Antarctic region. Total iodine was measured as iodide after iodate reduction with ascorbic acid. Sample had been diluted by 50%. Total iodine concentration was approximately 240 nM.

This procedure proved to be a rapid and effective method for determining total inorganic iodine in seawater, requiring minimal chemical treatment of the samples. The products from ascorbic acid reduction (including iodide from iodate) showed to be stable for at least 24 hours. The analytical system can also be automated, and the equipment is robust enough for shipboard use.

CHAPTER 3- IODINE DISTRIBUTION IN THE SOUTHERN OCEAN

This chapter has been divided in three sections. Section 3.1 introduces the major oceanographic and biogeochemical features of the Australian sector of the Southern Ocean. Section 3.2 presents iodate, iodide and total inorganic iodine depth-profiles an some contoured sections for the several transects studied in the region; and Section 3.3 discusses the implications of the analytical methods used for iodine determination on the results obtained.

3.1 Area of Study

All the sampling for this work was concentrated on the Australian section of the Southern Ocean as part of the World Ocean Circulation Experiment (WOCE). The WOCE section SR3, from Tasmania to Antarctica, was sampled three times for iodine (Figure 3.1)— twice over the austral summer (January 1994 and 1995) and once during the austral winter (July-August 1995). Two other transects were also sampled: the Princess Elizabeth Trough (PET), longitudinal section leaving east of Prydz Bay, Antarctica (65°S, ~ 85°E) to 57°S (January 1994); and the WOCE S4, meridional section along the 62°S line from Casey station (110°E) to the Balleny Islands (162°E) (January 1995).

3.1.1 The Antarctic Circumpolar Current

The Antarctic Circumpolar Current (ACC) constitutes the main part of the Southern Ocean. The ACC is the world's largest ocean current, carrying around 137 Sverdrups (1 Sv = 10^6 m^3 s^{-1}) only within its main eastward flow, between 50°S and 53°S, as measured on the SR3 section (Rintoul and Bullister, 1999).

The ACC flows mainly from west to east around the Antarctic continent and it communicates with the three major ocean basins: Atlantic, Indian and Pacific Ocean.

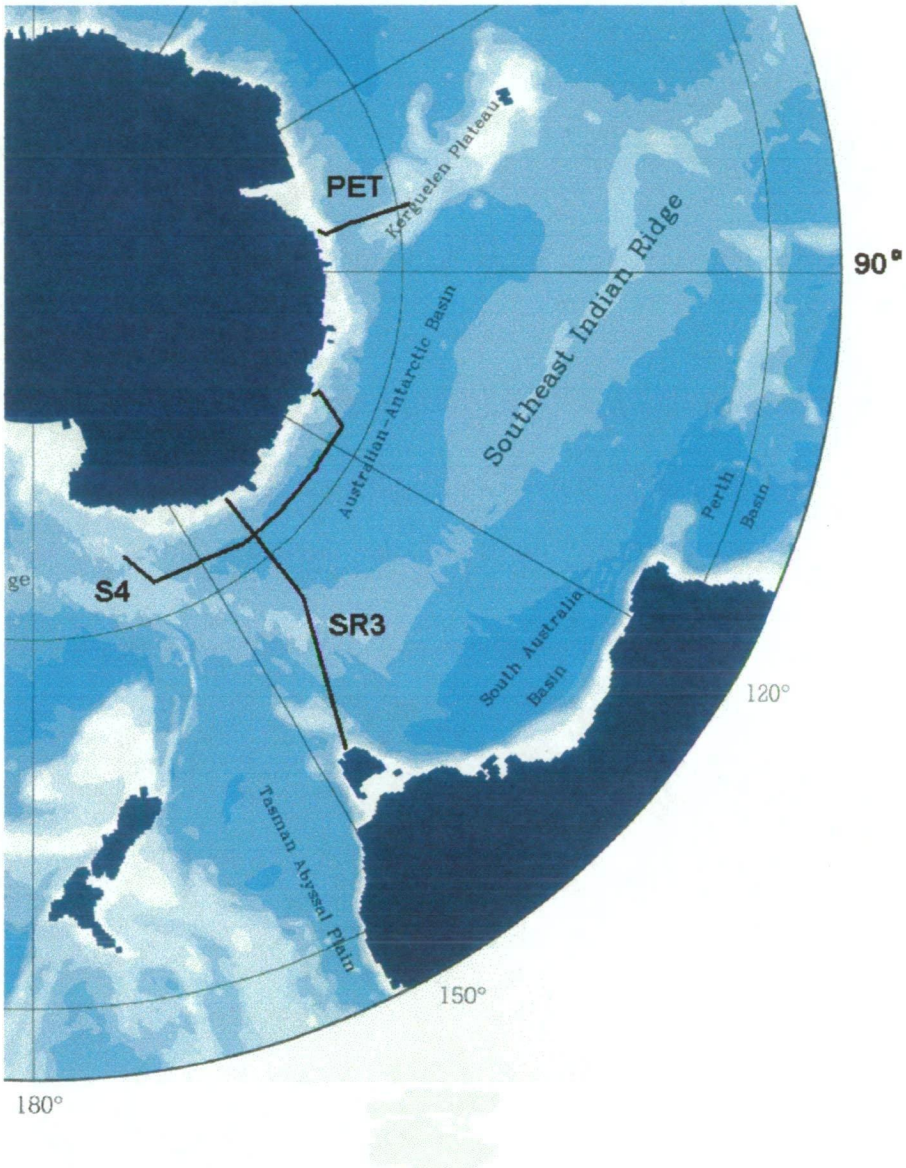

Figure 3.1- Map of the Southern Ocean showing Australian sector with main bathymetric features and the WOCE SR3, S4 and PET transects sampled for this work. Different colour shades indicate isobaths from 1000 m to 4000 m depth. Longitude of meridians shown are °E, and the two parallels shown are 30°S, crossing the south of Australia, and 60°S, closer to the Antarctic continent.

The ACC connects each of these ocean basins forming a network of ocean currents, known as global thermohaline circulation. This global circulation transports a large amount of heat between different regions of the planet, being very important in regulating global climate, influencing patterns of rainfall and temperature (Rintoul *et al.*, 2001).

The ACC is limited to the north by the Subtropical Front (STF), at around 40° to 46°S, which separates warm and saltier subtropical waters from colder and fresher subantarctic waters. Its southern limit is between about 64°S and 65°S, where the westward Antarctic coastal current starts, but is not so clearly marked (Orsi *et al.*, 1995). The ACC is also largely influenced by the bathymetry. South of Australia, at approximately 145°E, the Southeast Indian Ridge turns to the southeast. The intense flow of the ACC in the ridge's north flank also turns to the southeast as a result (Patterson and Whitworth, 1990).

Before the 1990's only two circumpolar surveys had been conducted in the Southern Ocean: the Discovery cruises in the 1930's led by George Deacon, and the Eltanin expeditions in the 1960's led by Arnold Gordon. Most of the data about the volume transport along the ACC published in the 1970's was obtained in places where the ACC is bathymetrically directed: to the south of Australian and New Zealand and in the Drake Passage (the waterway lying between the Antarctic Peninsula and South America– Patterson and Whitworth, 1990). In the 1990's with the need for more detailed information on the Southern Ocean circulation, many measurements of the ACC were made as part of the World Ocean Circulation Experiment (WOCE). One of the aims of the WOCE was to measure the ACC in parts of the Southern Ocean other than the Drake Passage (Rintoul *et al.*, 2001).

South of Australia, most of the WOCE measurements were conducted in conjunction with the Australian National Antarctic Research Expeditions (ANARE) program. As part of the program, the WOCE SR3 section from Tasmania to Antarctica was repeated six times between 1991 and 1996, covering each season of the year (Rintoul *et al.*, 2001). Along the transect, full-depth profiles were taken every 55 km for

temperature, salinity, oxygen and major nutrients (nitrate, phosphate and silicate) (Rosenberg *et al.*, 1995, 1996, 1997). These data provided important new insight into the ACC transport and hydrography (Rintoul *et al.*, 2001)

The ACC is not a homogeneous current, but consists of two or three narrow jets of large eastward transport, which form fronts (Rintoul and Bullister, 1999). These fronts are normally deep reaching, and separate the Southern Ocean in different zones with relatively uniform properties and weak transport.

3.1.2 Southern Ocean fronts south of Australia

The Southern Ocean consists of several different zones, but with relatively uniform characteristics within each. These zones are separated by regions of large gradients of temperature and salinity, known as fronts.

The major fronts in the Southern Ocean from North to South are: the Subtropical Front (STF), the Subantarctic Front (SAF) and the Polar Front (PF). The regions between the fronts are named the Subantarctic Zone (SAZ), between STF and SAF, the Polar Frontal Zone (PFZ), between the SAF and the PF, and the Antarctic Zone (AZ) south of the PF (Figure 3.2).

As mentioned earlier, the STF (previously known as the Subtropical Convergence) separates warm and salty subtropical waters from cool and fresh subantarctic waters. Along the SR3 section, the drop in salinity from >35.0 to < 34.8 from north to south marks the STF. This change occurs in the upper 300-600 m between 44° and 46°S, at the SR3 section. There is also a drop in upper-water column temperature, with subtropical waters being warmer than 11.5° C (Rintoul and Bullister, 1999). The STF is not observed in the Drake Passage, so it is not a circumpolar feature (Patterson and Whitworth, 1990). General criteria for identifying STF, SAF and PF, between 0° and 150°E in the Southern Ocean, were also summarised in Belkin and Gordon (1996).

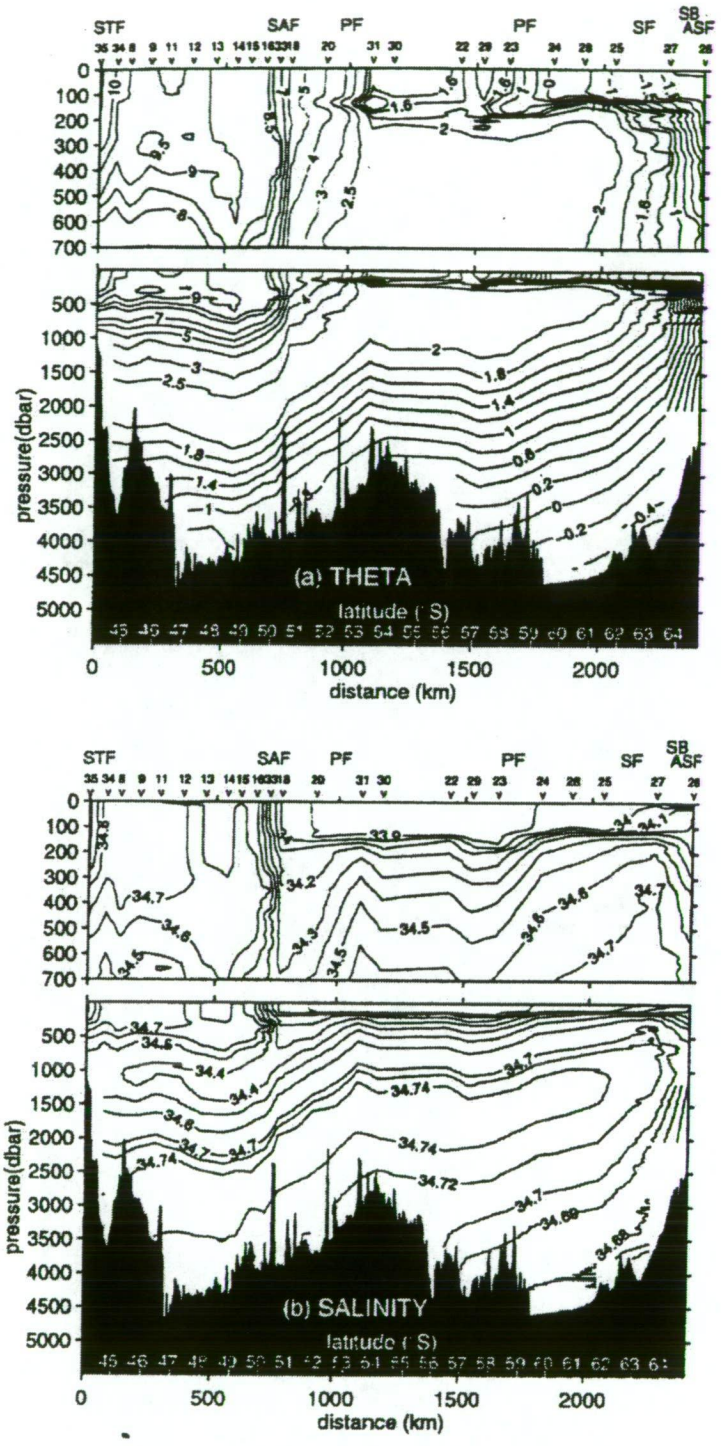

Figure 3.2- Temperature (a) (°C) and salinity (b) contoured distributions along the WOCE SR3 section during a late winter cruise (October 1991). The main fronts are marked on the top of the graph: Subtropical Front (STF), Subantarctic Front (SAF), the northern and southern branches of the Polar Front (PF), the Southern Antarctic Circumpolar Current Front (SF), the Southern Boundary of the Polar Front (SB) and the Antarctic Surface Front (ASF) (from Rintoul and Bullister, 1999).

Along the SR3, between 50° and 52°S, another front separates subantarctic surface waters (SASW) from fresher and cooler Antarctic Surface Water (AASW) further south. This front is the Subantarctic Front (SAF), and, in contrast to the STF, the SAF reaches from the surface to the sea floor, and strong gradients in salinity and temperature can be seen throughout the water column (Figure 3.2).

There are several criteria, which may be used to identify the SAF. Here, the SAF was placed immediately north of the salinity contour line of 34.20 in the upper 300 m of the water column (Orsi *et al.*, 1995; Rintoul and Bullister, 1999). The position of the SAF also varies seasonally (Rintoul *et al.*, 2001).

The third well-known front in the Southern Ocean is the Polar Front (PF). The PF typically marks the northern limit of the 2°C isotherm at 200 m depth (Orsi *et al.*, 1995; Rintoul and Bullister, 1999). In the SR3 sections, this places the PF between 53° and 54°S. In some parts of the Southern Ocean the PF appears to be split in two, and this is exactly what has been noticed along the SR3 transect. These two branches are called the northern Polar Front (PF-N), defined as before, and the southern Polar Front (PF-S), which is typically defined by the rapid deepening of the temperature minimum layer between 57° and 59° S along the SR3 (Rintoul and Bullister, 1999). The PF-S, however, is not found all around the Southern Ocean, so it is not circumpolar (Orsi *et al.*, 1995).

Another front that has been identified as circumpolar in extent is the Southern ACC Front (SACCF). Orsi *et al.* (1995) defined the SACCF as the southern limit of the 1.8°C isotherm, along the temperature maximum line, at 500-m depth. Although most of the transport within the ACC occurs along the SAF and the PF, the transport along the SACCF also has to be accounted for in the estimate of total transport for the ACC (Orsi *et al.*, 1995). Along the SR3 the SACCF is found approximately at 63°S (Rintoul and Bullister, 1999).

South of the SACCF, one last feature also appeared to be circumpolar. This is the southern limit of the oxygen minimum layer of the Upper Circumpolar Deep Water

(UCDW). This feature has been defined as the Southern Boundary of the ACC (SB) (Rintoul and Bullister, 1999). Along the SR3 sections, the SB is very close to the SACCF at ~ 64°S.

South of the SB, along the SR3 transect, the isopleths of temperature and salinity again slope downward at the Antarctic continental slope, marking the edge of the Antarctic Slope Front (ASF) (Figure 3.2). The ASF separates cold shelf water from waters offshore and also marks the northern limit of the westward flow around the Antarctic Continent (Rintoul and Bullister, 1999).

3.1.3 Main water masses in the Southern Ocean south of Australia

Several water masses are formed in the Southern Ocean. These newly formed water masses normally have high concentration of dissolved oxygen, and, as they spread to lower latitudes, they help ventilate the ocean's intermediate and bottom layers. Most major water masses are formed by overturning circulation. Along the divergent fronts, strong winds force surface waters to diverge, allowing the upwelling of deep saline waters. Some of these deep waters mix with fresher and colder waters to produce high-density bottom water, while the remainder will form less dense, fresher intermediate water (Rintoul *et al.*, 2001).

Some of the most important water masses present in the Australian sector of the Southern Ocean will be briefly described below.

3.1.3.1 Subantarctic Mode Water (SAMW)

The SAMW is present in the SAZ, between the STF and the SAF, from the surface, in the winter, or sub-surface, in the summer, down to 450-600 m depth. This well-oxygenated and vertically homogeneous water mass is formed in the Southern Ocean during deep winter mixing, and is very important in ventilating subtropical lower thermocline waters (Rintoul and Trull, 2001).

Although apparently a very homogeneous water mass (potential density = 26.85-26.95), three different modes were actually identified within the SAMW during a winter section along SR3 (Rintoul and Bullister, 1999). A first "warm mode" was identified in its northern part, between the STF and approximately 47°S, with warmer (9.5°C) and saltier (34.73) waters. A second "cool mode" was noticed in the surface mixed layer down to 300 m, from ~ 48° S to ~ 49°S, with cooler (~ 8.8°C) and fresher (~ 34.58) waters. And a third "subsurface temperature maximum mode" was identified beneath the "cool mode", which was warmer (9.1°C) and saltier (34.66) than the surface mixed layer. Rintoul and Bullister (1999) suggested that the cool mode was formed by mixing and advection of cooler and fresher waters coming from the SAF in the upper 100 m, while the warm mode was formed due to input of warmer and saltier waters from the southern Tasman Sea.

Along SR3, and as far west as 140°E, the northern part of the SAZ is characterised by a westward flow, while the southern part follows the main eastward flow of the ACC. This causes the SAMW layer, within the SAZ, to have an anticlockwise recirculation pattern (Rintoul and Trull, 2001).

3.1.3.2 Antarctic Surface Water (AASW)

The surface waters south of the northern branch of the Polar Front (PF-N) are known as Antarctic Surface Water (AASW), being colder and fresher than surface waters further north. Although AASW extends south to the Antarctic continent, its salinity and temperature change across the fronts.

The mixed layer south of the PF is shallower than further north, with winter mixed layers rarely deeper than 150 m. This shallow winter mixing, in contrast with the deep winter mixing in the SAMW, causes poor ventilation and isolation of intermediate and deep waters below, which has important implications for carbon and nutrient cycling in the Southern Ocean (Rintoul and Bullister, 1999; Rintoul and Trull, 2001).

During the summer, with the warming of AASW, a strong thermocline is formed below the surface on top of a temperature minimum layer. This temperature minimum layer is sometimes called Winter Water and is a remnant from deeper winter mixing (Rintoul and Bullister, 1999). Along the SR3 sections, a weak winter water layer can be observed from ~ 53° to 59°S, between the northern and the southern branches of the Polar Front (Figure 3.2).

3.1.3.3 Antarctic Intermediate Water (AAIW)

Below the SAMW, in the SAZ, a salinity minimum layer is known as Antarctic Intermediate Water (AAIW). Although the low-salinity (< 34.4) AAIW appears to sink and flow northward from south of the SAF under SAMW, this is not the case (Figure 3.2). AAIW north of the SAF, along the SR3 section, showed to be very poor in oxygen, thus has not been recently ventilated. This AAIW was probably mixed with older water from the Tasman Sea and recirculated back into the SAZ (Rintoul and Bullister, 1999).

3.1.3.4 Upper Circumpolar Deep Water (UCDW)

The Circumpolar Deep Water (CDW) can be divided in two groups: the Upper Circumpolar Deep Water (UCDW) and the Lower Circumpolar Deep Water (LCDW). The former is characterised by an oxygen-minimum and nutrient-maximum layer. UCDW is formed from saline deep waters coming from the Indian and Pacific Oceans into the Southern Ocean (Callahan, 1972; Rintoul and Bullister, 1999).

The deep-water circulation in the Southern Ocean seems to follow the main surface eastward flow of the ACC (Deacon, 1984). North of the SAF, in the northern part of the SAZ, however, UCDW follows AAIW and SAMW in a westward flow (Rintoul and Bullister, 1999).

In the SAZ, UCDW layer is below AAIW at 1500-2000 m depth. It becomes shallower further south, reaching 1000 m depth at the PFZ, and 500 m depth at the

AZ. In the proximity of SACCF (~ 63°S), along the SR3 section, UCDW is immediately below AASW at depths < 300 m.

The southern limit of UCDW has also been identified as the southern most point of circumpolar circulation to pass through the Drake Passage, marking the southern boundary of the ACC (SB) (Orsi *et al.*, 1995).

3.1.3.5 Lower Circumpolar Deep Water (LCDW)

Lower circumpolar deep water (LCDW) is characterised by a salinity-maximum core beneath UCDW. Its origins can be traced to North Atlantic Deep Water (NADW), which enters the Southern Ocean through the Atlantic (Callahan, 1972).

Along the SR3 section, LCDW layer is deeper in the SAZ at ~ 3000 m, becoming shallower through the PFZ and AZ.

LCDW is also important in the formation of bottom water. At the end of the SR3 section, it mixes with cold and fresher shelf water from Wilkes-Adélie coast to form denser bottom water (Rintoul and Bullister, 1999).

3.1.3.6 Antarctic Bottom Water (AABW)

A late winter section along the SR3 in 1991 (Rintoul and Bullister, 1999) confirmed previous results showing that high oxygen and fresh Antarctic Bottom Water (AABW) was formed along Wilkes—Adélie coast, between 140°E and 150°E, in Antarctica (Gordon and Tchernia, 1972). New evidence suggests that up to 25 % of all AABW around the globe may be formed in this sector of the Antarctic continent, between 142.5° and 145.5°E (Rintoul, 1998).

The formation of bottom water in that region is enhanced by a coastal polynya, the Mertz polynya. This polynya ensures that large amounts of ice are formed each year causing the increase in salinity noticed in shelf waters. These cold and saline shelf

waters appear to have the right density to form the AABW found in the abyssal plains of the Southern Ocean south of the Southeast Indian Ridge, crossed by the SR3 section (Rintoul *et al.*, 2001). AABW also appears to be formed, episodically, near Prydz Bay, at around 80°E on the Antarctic coast (Wong *et al.*, 1998).

The bottom water formed off Adélie Land is called Adélie Land Bottom Water (ALBW) (Rintoul, 1998). ALBW is very high in dissolved oxygen, colder and fresher than LCDW above, being very important in ventilating the deep ocean. After formation, ALBW flows westward into the Australian-Antarctic Basin. Once in the Australian-Antarctic Basin, ALBW will move west until the Princess Elizabeth Trough, and then will go north, along the Kerguelen Plateau, and then east, following the Southeast Indian Ridge, forming a clockwise circulation pattern. However, ALBW will not cross the Southeast Indian Ridge to mix with bottom waters from the Southeast Pacific Basin (Orsi *et al.*, 1999).

3.1.4 Major nutrients distribution in the Australian sector of the Southern Ocean

The distribution of the major nutrients, nitrate, phosphate and silicate, in the Southern Ocean also show strong north to south changes. Pronounced changes are observed across the fronts, while more homogeneous distribution are seen in the zones between the fronts (Figure 3.3).

North of the STF, in the Subtropical Surface Water (STSW), nitrate, phosphate and silicate are typically depleted in the summer. Nutrient concentrations are low in the summer, due to a shallow mixed layer of 50 m and the abundance of light. In the winter, deep mixing (down to 400 m) increases nitrate concentration from close to zero to about 5 μM. While phosphate concentrations are also renewed with winter mixing from 0.3 to approximately 0.8 μM, silicate also increases, but to a lesser extent, from 1.4 to 3 μM (Rintoul and Trull, 2001).

South of the STF, along the SR3 section, in the Subantarctic Surface Water (SASW), nitrate and phosphate concentrations are higher than in the STSW. In the summer, a

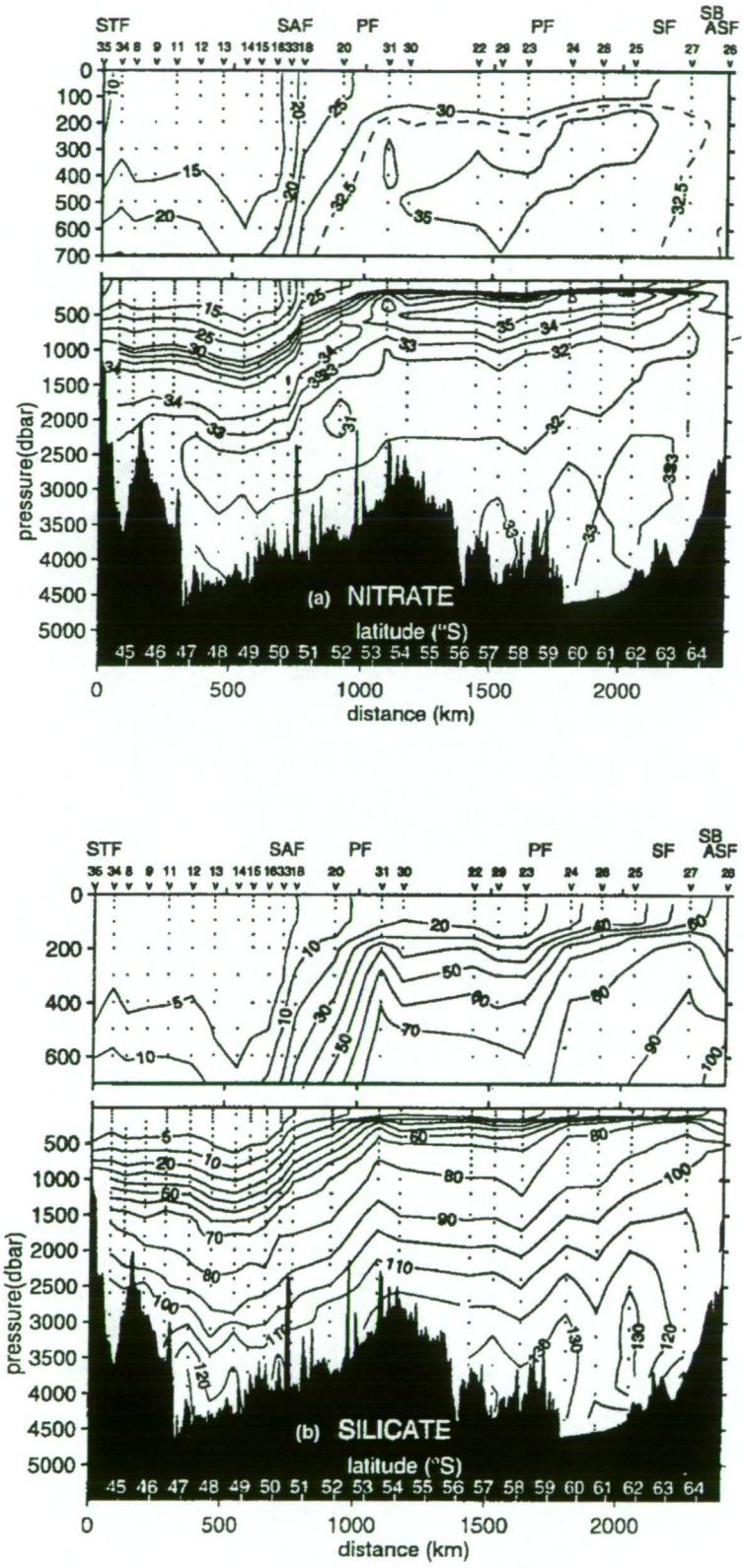

Figure 3.3- Nitrate (a) and silicate (b) contoured distribution (μM) along WOCE SR3 section during a late winter cruise (October 1991). Adapted from Rintoul and Bullister, 1999.

shallow mixed layer is also formed, and nitrate concentrations vary from 8 to 10 μM, while phosphate concentrations are below 0.8 μM. In the winter, deep mixing renews nitrate and phosphate concentrations in surface waters to about 12-16 μM and 0.9-1.2 μM, respectively. In the SAZ, silicate concentrations are low in the surface and in the winter mixed layer below (SAMW), and do not vary much from summer to winter, averaging 4 μM (Rintoul and Trull, 2001; Lourey and Trull, 2001).

Across the SAF, another large change in nutrient levels is observed. Nitrate increases from about 10 to 20 μM, while phosphate increases from about 0.8 to 1.6 μM in the summer mixed layer. Silicate increases from about 2 to 4 μM along the SAF. Between the SAF and the PF-N, in the PFZ, nutrient depletion from summer to winter is not as high as within the SAZ (Lourey and Trull, 2001). Within the PFZ, nitrate and phosphate continue to increase southward, while silicate increases noticeably only south of the PF-S (Figure 3.3).

South of the PF-N, in the winter section depicted in Figure 3.3 (Rintoul and Bullister, 1999), nitrate concentrations are lower than 30 μM in the surface until the SACCF, where they increase above 30 μM. In the summer nitrate concentrations for the same region along the SR3, are typically lower than 30 μM (Popp *et al.*, 1999). Phosphate also follows the same pattern, with surface concentrations lower than 2.2 μM until south of the SACCF in the winter, and summer concentrations typically lower than 2 μM for the same region (Popp *et al.*, 1999; Rintoul and Bullister, 1999).

Silicate, however, has a different distribution. It is depleted in the surface from the STZ, through the PFZ, with little increase through the fronts when compared to nitrate and phosphate. It continues to be depleted between the two Polar Fronts, but south of 59°S its concentration increases from 8 to above 22 μM in the surface during the summer, and from 10-20 μM to 20-30 μM during the winter (Popp *et al.*, 1999; Rintoul and Bullister, 1999).

Silicate depletion in the SAZ, in relation to nitrate and phosphate may be a co-limiting factor on phytoplankton growth in this region, along with iron (Boyd *et al.*,

1999). In the SAZ and PFZ, along the SR3, coccolithophores are very common, but south of the PF-N, in colder Antarctic waters, diatoms are dominant (Popp *et al.*, 1999). Iron addition experiments have shown that addition of iron in the silicate rich AZ-S, at 61°S 140°E, favoured the growth of larger, higher silicified diatoms; while it is believed that iron addition during mid-summer in silicate poor surface waters of the PFZ or IPFZ would lead to a dominance of smaller and lighter silicified diatoms (Trull *et al.*, 2001).

Nutrient concentrations also vary with longitude in this sector of the Southern Ocean, due to changes in hydrography, primary production and algal communities. Along the PET transect (~ 80°E), nutrient depletion in surface waters was higher than at the SR3 at the same latitude. Higher chlorophyll *a* concentrations were also found along the PET, in comparison to the SR3 transect, at the same latitude (Popp *et al.*, 1999). In a large survey between 80°E to 150°E, from about 63°S to the ice edge, measured chlorophyll *a* concentrations were higher in the west, than in the east (Wright and van den Enden, 2000), and nitrate and phosphate depletion in the mixed layer, in relation to winter water below, was also higher in the west than in the east part of the survey (Strutton *et al.*, 2000).

3.1.5 Carbon uptake and primary production in the Southern Ocean south of Australia

The Southern Ocean is a large sink of CO_2 from the atmosphere. Two main processes are involved in effectively removing CO_2: physical dissolution in cold waters and sinking to form intermediate or bottom waters (the solubility pump), and the so-called "biological pump" with biological uptake of CO_2 and removal to deep waters as sinking organic matter.

The main area of carbon uptake in the Southern Ocean is the Subantarctic Zone (SAZ) (Rintoul *et al.*, 2001). In the summer months, the shallow mixed layer promotes high primary production in the area, which combined with mixing with subtropical waters generates a carbon sink of approximately 1 Gt C yr^{-1} for the entire circumpolar SAZ, one of the largest sinks of the world's oceans (Metzl *et al.*, 1999).

South of 55°S, the carbon sink is smaller than in the SAZ, but still significant. It was estimated that the net sink of CO_2 in this region was around 0.1 to 0.2 Gt C yr^{-1} (Rintoul *et al.*, 2001).

The biological uptake of CO_2 along the Southern Ocean is not homogeneous. The zone between 110°E and 150°E, within the Australian sector, is known for its low productivity. In contrast, the sea-ice zone off Prydz Bay (~ 80°E) has a very high productivity. These differences seem to be related to local circulation patterns, such as circulation of Antarctic shelf waters offshore from Prydz Bay; differences in physical properties such as salinity, temperature and mixed layer depths; and the occurrence of meanders along the ACC north of Prydz Bay, among others (Rintoul *et al.*, 2001; Popp *et al.*, 1999). Other factors, such as iron supply from melting ice may also be of importance (Martin *et al.*, 1990).

Arrigo *et al.* (1998) measured primary production in the Southern Ocean on a monthly basis using coastal zone colour scanner (CZCS). They divided the Southern Ocean in five geographic sectors according to longitude, namely the Weddell Sea, the South Indian Ocean, the Southwestern Pacific Ocean, the Ross Sea and the Bellingshausen-Amundsen Sea. The Southwestern Pacific Ocean sector (90°—160°E) was found to be an area with the second lowest annual primary production in the Southern Ocean with 724 Tg C yr^{-1}, above only the South Indian Ocean sector (20°–90°E) with 630 Tg C yr^{-1}.

Along the SR3 line, from Tasmania to Antarctica, primary production varies considerably between the various zones bounded by the ocean fronts (Rintoul *et al.*, 2001).

In the Subtropical Zone (STZ), from 44° to ~ 46°S, primary production values in the summer averaged 1760 mg C m^{-2} d^{-1} in open waters (Griffiths *et al.*, 1999). In the winter primary production averaged 690 mg C m^{-2} d^{-1} (Rintoul *et al.*, 2001). With shallow mixed layer in the summer and moderately deep mixed layer in the winter, nutrient supply is easily renewed each year from the near zero concentrations during the summer following the spring bloom.

South of the STF, in the SAZ, the spring blooms start in November. After deep winter mixing, which forms SAMW, the mixed layer is warmed up in the surface and a shallow mixed layer of SASW is formed. This shallow mixed layer allows abundant algal growth and primary production in the summer is around 940 mg C m^{-2} d^{-1}. In the winter, primary production is lower, about 390 mg C m^{-2} d^{-1}. Nitrate levels, although decreasing during summer, remain high all year round (Rintoul *et al.*, 2001). The presence of high nitrate concentrations combined with low chlorophyll characterises the Southern Ocean as a high-nutrient, low-chlorophyll (HNLC) zone. With the abundance of nitrate and phosphate, the presence of low levels of iron, and possibly the low levels of silicate also, are believed to limit phytoplankton growth in subantarctic waters (Boyd *et al.*, 1999; Sedwick *et al.*, 1999).

Between the SAF and PF-N, in the PFZ, the winter mixed layers are around 120 m, but light may become a limiting factor of primary production at these higher latitudes. In the summer, again a shallow mixed layer (~ 60 m) is formed and primary production increases, although nitrate is typically very high all year. Summer production values were around 490 mg C m^{-2} d^{-1}, while winter values were not much lower at 380 mg C m^{-2} d^{-1} (Rintoul *et al.*, 2001). Between the PF-N (54°S) and the PF-S (59°S), a sub-surface chlorophyll maximum is noticed in the summer, following the spring bloom (Parslow *et al.*, 2001). In the PFZ, iron and silicate may again play roles in limiting summer production (de Baar *et al.*, 1997; Franck *et al.*, 2000).

In the Antarctic Zone, between the PF-N and around 62°S, the lowest values of primary production for the SR3 transect are observed. In the summer, this zone, as related before, is characterised by a sub-surface temperature minimum layer, known as "winter water" (Rintoul *et al.*, 2001). This temperature minimum layer sometimes is also observed during winter, if the surface waters are not cooled enough to promote deeper mixing (Rintoul and Bullister, 1999). In this zone, production in the winter (360 mg C m^{-2} d^{-1}) can even be higher than in the summer (270 mg C m^{-2} d^{-1}). Biomass is also very low year round (Rintoul *et al.*, 2001). Here, again, with elevated

silicate levels south of 59°S, iron is likely to be an important limitation on algal growth (Martin *et al.*, 1990).

South of around 63°S, in the so-called Seasonal Sea-Ice Zone, primary production in the summer was higher than further north. In late spring and summer a shallow pycnocline is formed by ice melting, with summer production being around 840 mg C m^{-2} d^{-1}. Winter production, due to deep winter mixing and light limitation is very low at 185 mg C m^{-2} d^{-1} (Rintoul *et al.*, 2001). Close to the SACCF at around 64°S the divergence of waters brings higher nutrient concentration and possibly iron to the surface waters, which might contribute, in combination with meltwater from sea-ice and the stable shallow surface waters to the increase in algal growth observed in this region, south of this front.

3.2 Iodate, iodide and total iodine distribution along the WOCE SR3, S4 and PET transects

3.2.1 SR3 section during the winter cruise, July 1995 (au9501)

During the austral winter (July-August) of 1995 (cruise au9501) the WOCE repeat section SR3, from Tasmania to Antarctica, was sampled for iodate and iodide (Figure 3.1). All the stations sampled for iodine can be seen in Appendix II.

Figures 3.4a and b show temperature and salinity distribution for the SR3 section during au9501. The first features to be noticed are the fronts. The Subtropical Front (STF) was located ~ 45.8°S during this cruise. The Subantarctic Front (SAF) was located at ~ 51.8°S. Between these two fronts, in the Subantarctic Zone (SAZ), one can see a nearly uniform water mass between the surface and around 600 m depth. This feature is the Subantarctic Mode Water (SAMW), which is formed by deep winter mixing and can be well identified in this winter contour. Further south, just before 54°S, is the Polar Front (PF), or, more correctly, its northern branch, the Polar Front North (PF-N). Between the SAF and the PF-N is the Polar Frontal Zone (PFZ). Below the surface in the PFZ, one can see in Figure 3.4b a low salinity (<34.4)

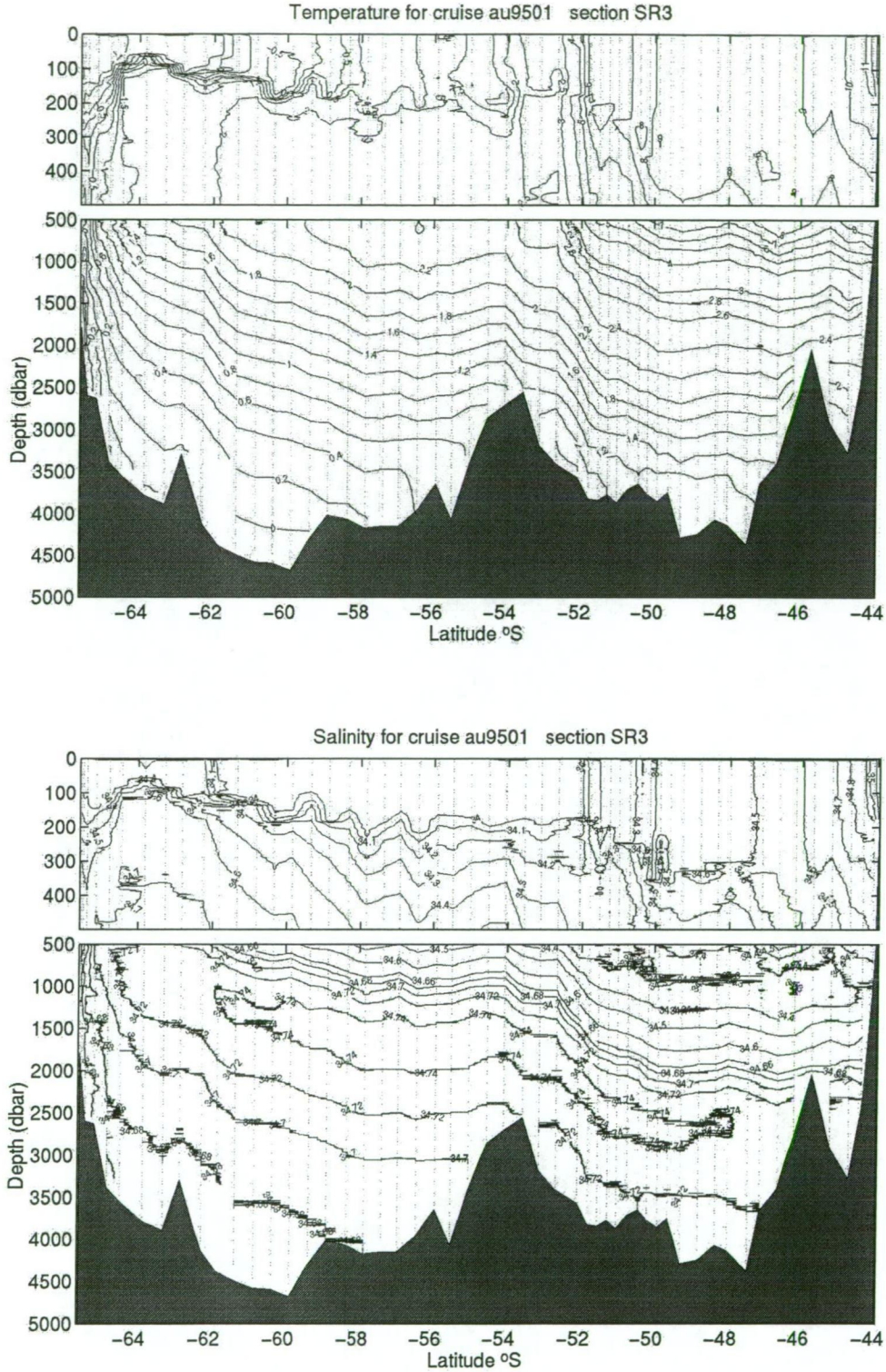

Figure 3.4- Temperature (°C, **a**) and salinity (**b**) contoured sections of the SR3 section during cruise au9501, July 1995. Note higher latitudes in the left hand side of the plot.

tongue becoming deeper in the SAZ, below SAMW. This is the Antarctic Intermediate Water (AAIW).

Still within the SAZ, on the salinity section, below 2000 m, Lower Circumpolar Deep Water (LCDW) can be seen, with salinities >34.7 ‰. Between AAIW and LCDW lies the Upper Circumpolar Deep Water (UCDW), the oxygen minimum layer. In the PFZ, LCDW is shallower, between 1500 and 2000 m, and so is UCDW. South of the PF-N starts the Antarctic Zone (AZ), with typically colder and fresher surface waters. In the PFZ and in the AZ, the winter mixed layer was a lot shallower than at the SAZ, reaching 200 m depth at maximum. At ~ 58°S is the southern branch of the PF, the PF-S. Between the PF-N and PF-S is the newly named Inter-Polar Frontal Zone (IPFZ) (Parslow *et al.*, 2001), in the northern part of the AZ. In this zone, UCDW is much shallower at around 600 m depth. Below UCDW, the LCDW salinity maximum layer extends from below 1000 m down to 3500 m depth. At around 63°S is the southern Antarctic Circumpolar Current front, or SACCF; and at ~ 64°S the southern boundary of the ACC, or SB, marks the southern limit of the ACC eastward transport. The SB is also the southernmost limit of the UCDW oxygen minimum layer. Between the SACCF and the SB is a seasonal sea-ice zone. From the Antarctic continental slope, waters with temperatures below 0°C, salinity <34.7, and high dissolved oxygen sink the bottom of the Southern Ocean below LCDW to form Antarctic Bottom Water (AABW).

3.2.1.1 Iodate distribution

Iodate depth profiles obtained for the au9501 cruise can be seen in Figure 3.5a-f.

Iodate concentrations were typically lower in the surface and higher at depth. Normally, the bottom of the surface mixed layer coincided with a break in the iodate profile between 200 and 300 m depth. Below this feature, iodate generally increased quickly down to approximately 1000 m, and then showed a small increase towards the bottom, unless there was a change in the water mass, in which case a small decrease in iodate concentration was noticed, coinciding with bottom water.

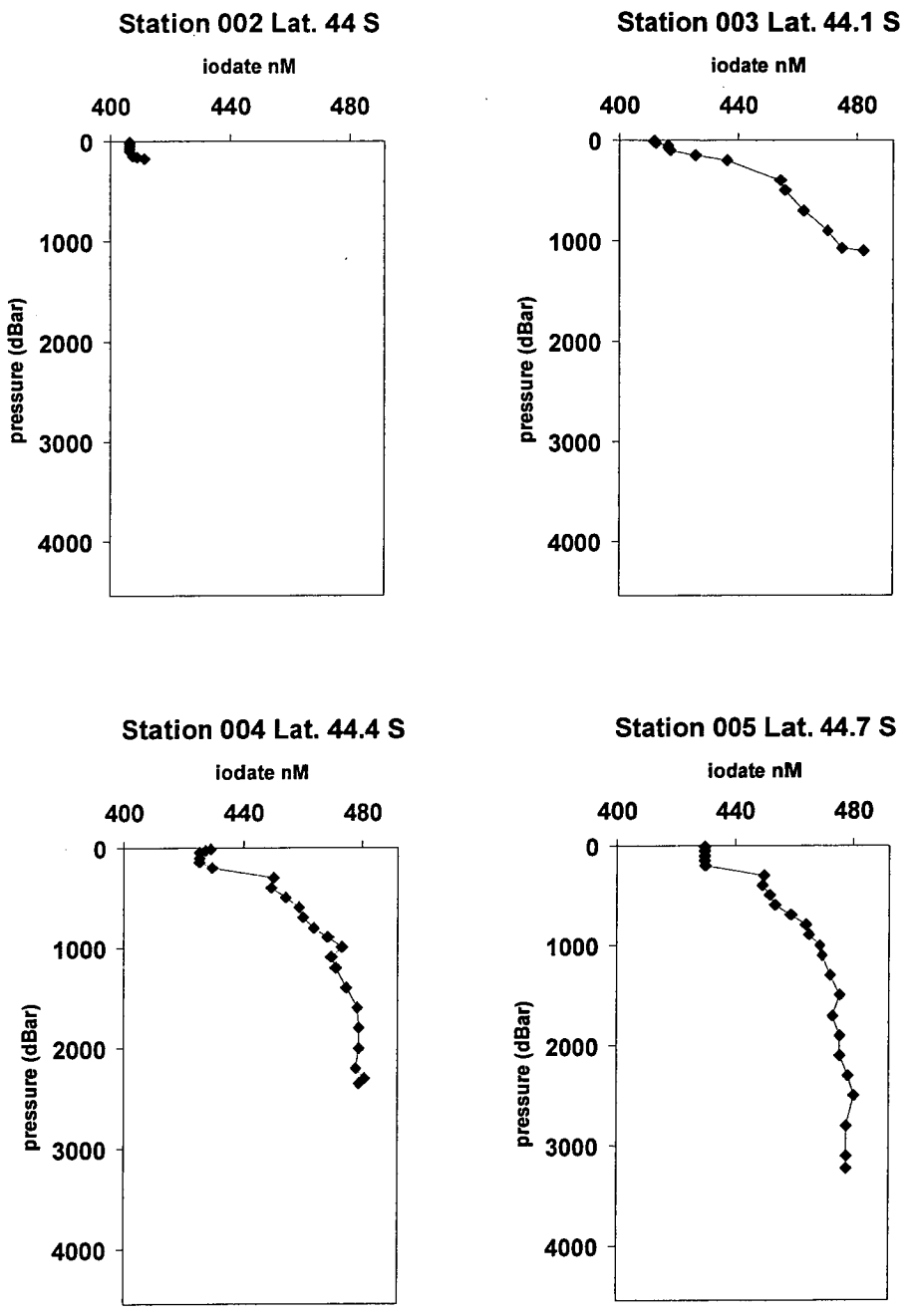

Figure 3.5a- Iodate distribution during cruise au9501 in the Subtropical Zone (STZ) Stations.

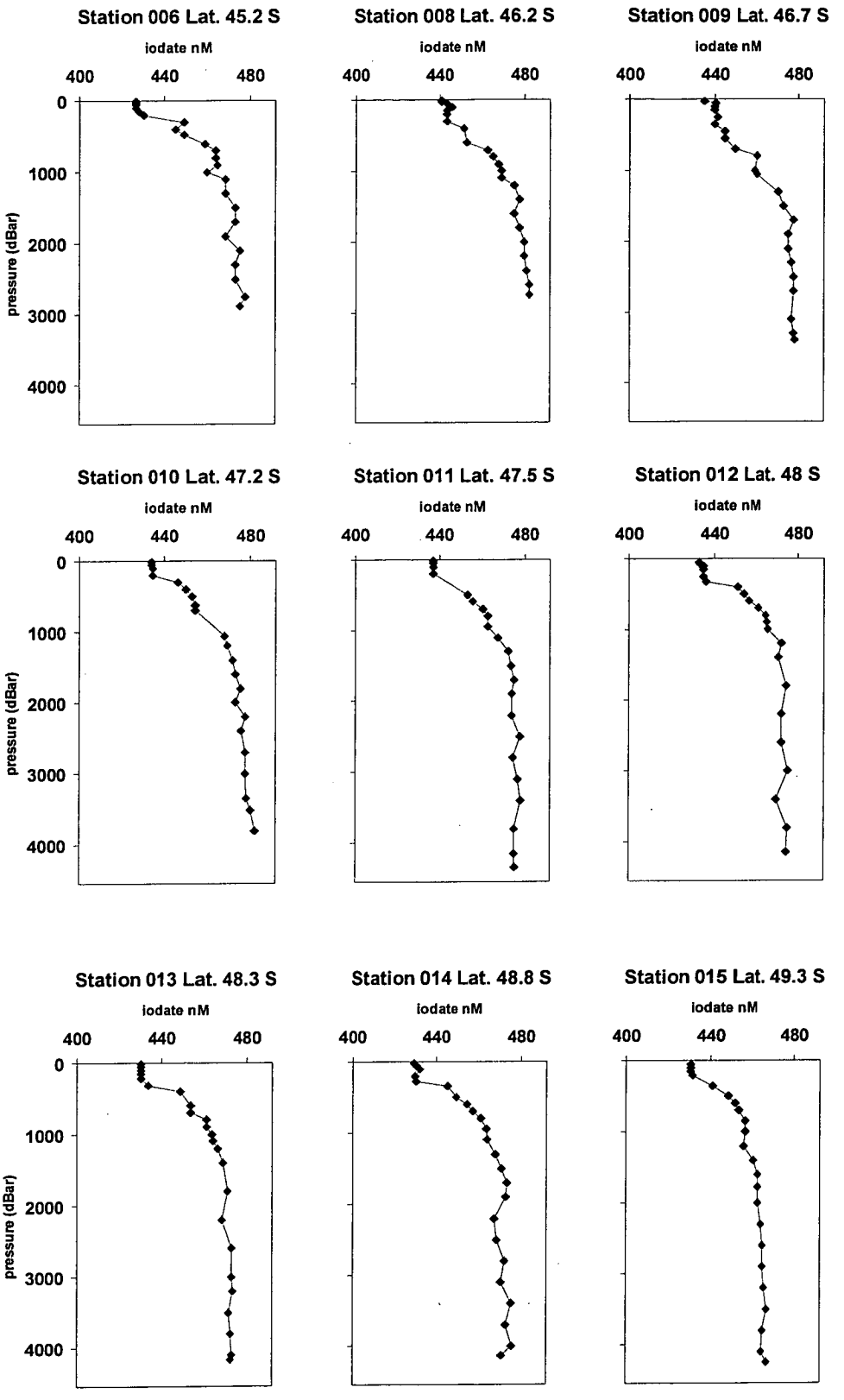

Figure 3.5b- Iodate distribution during cruise au9501 (July 1995) along the SR3 section in the Subantarctic Zone (SAZ) Stations.

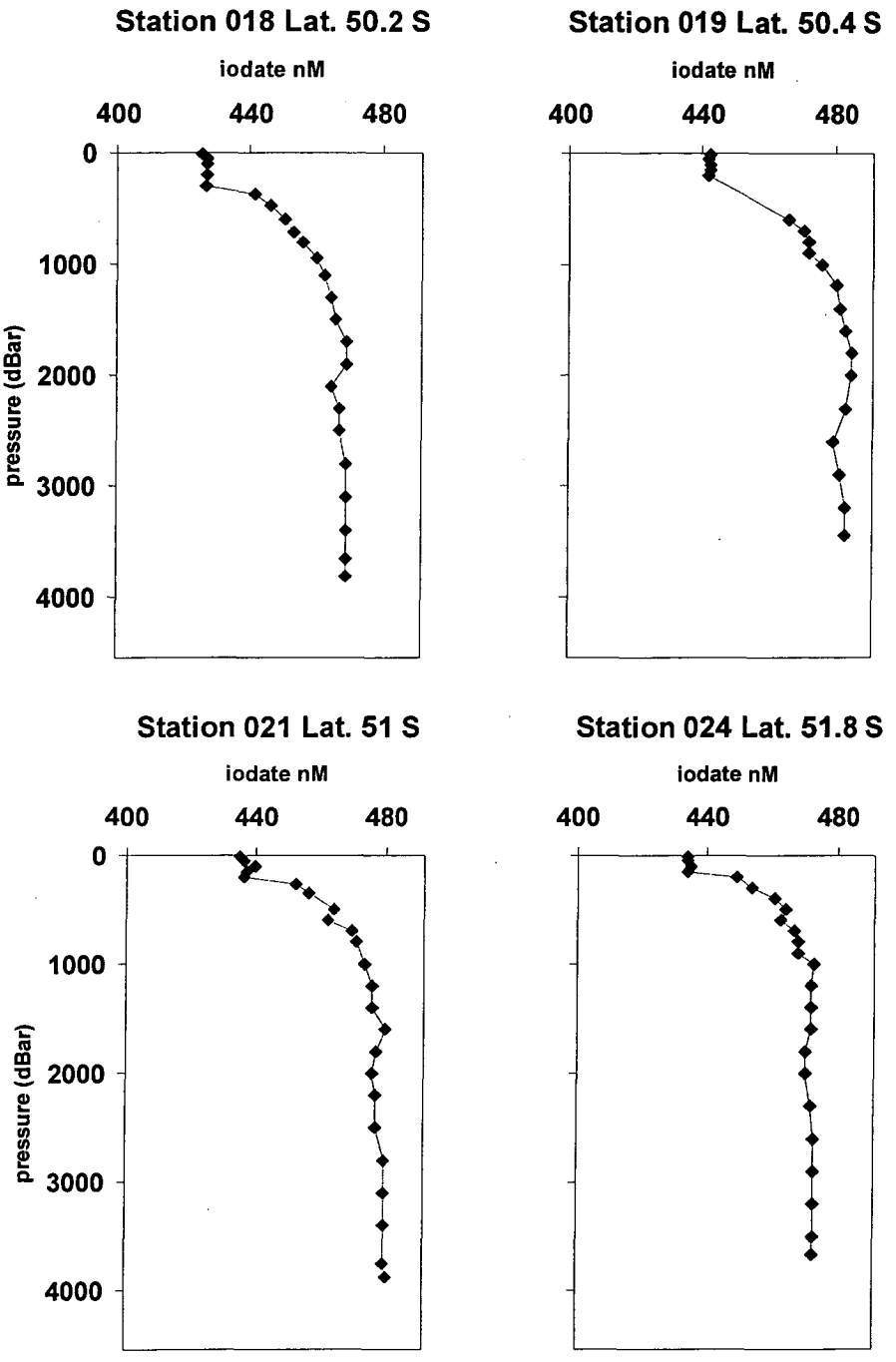

Figure 3.5c- Iodate distribution during cruise au9501 (July 1995) along the SR3 section in the Subantarctic Zone (SAZ) Stations (cont.).

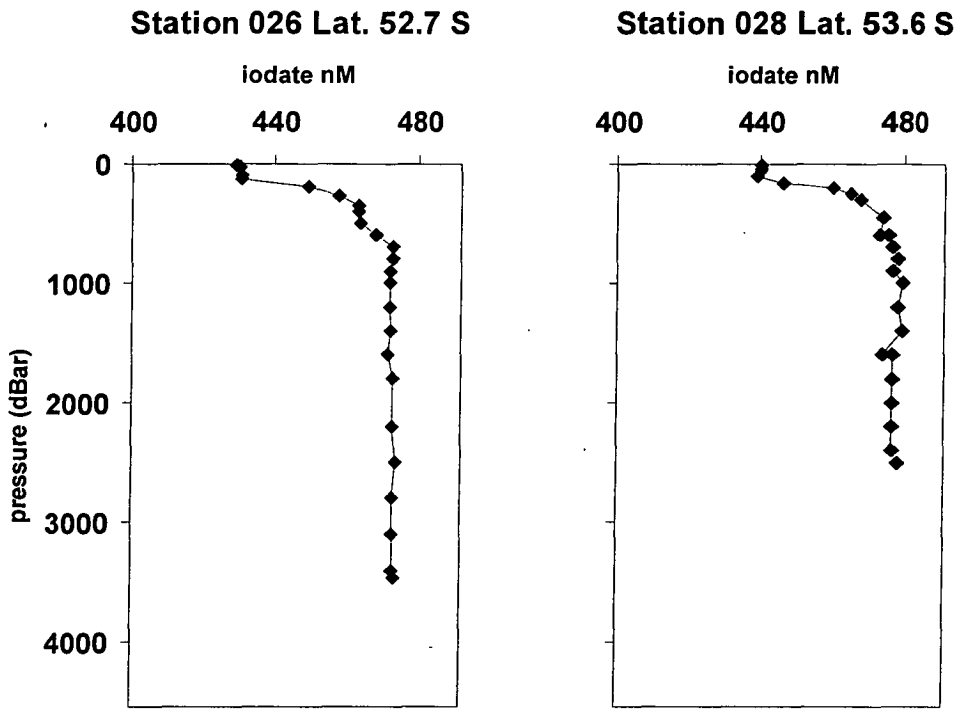

Figure 3.5d- Iodate distribution during cruise au9501(July 1995) along SR3 section in the Polar Frontal Zone (PFZ) Stations.

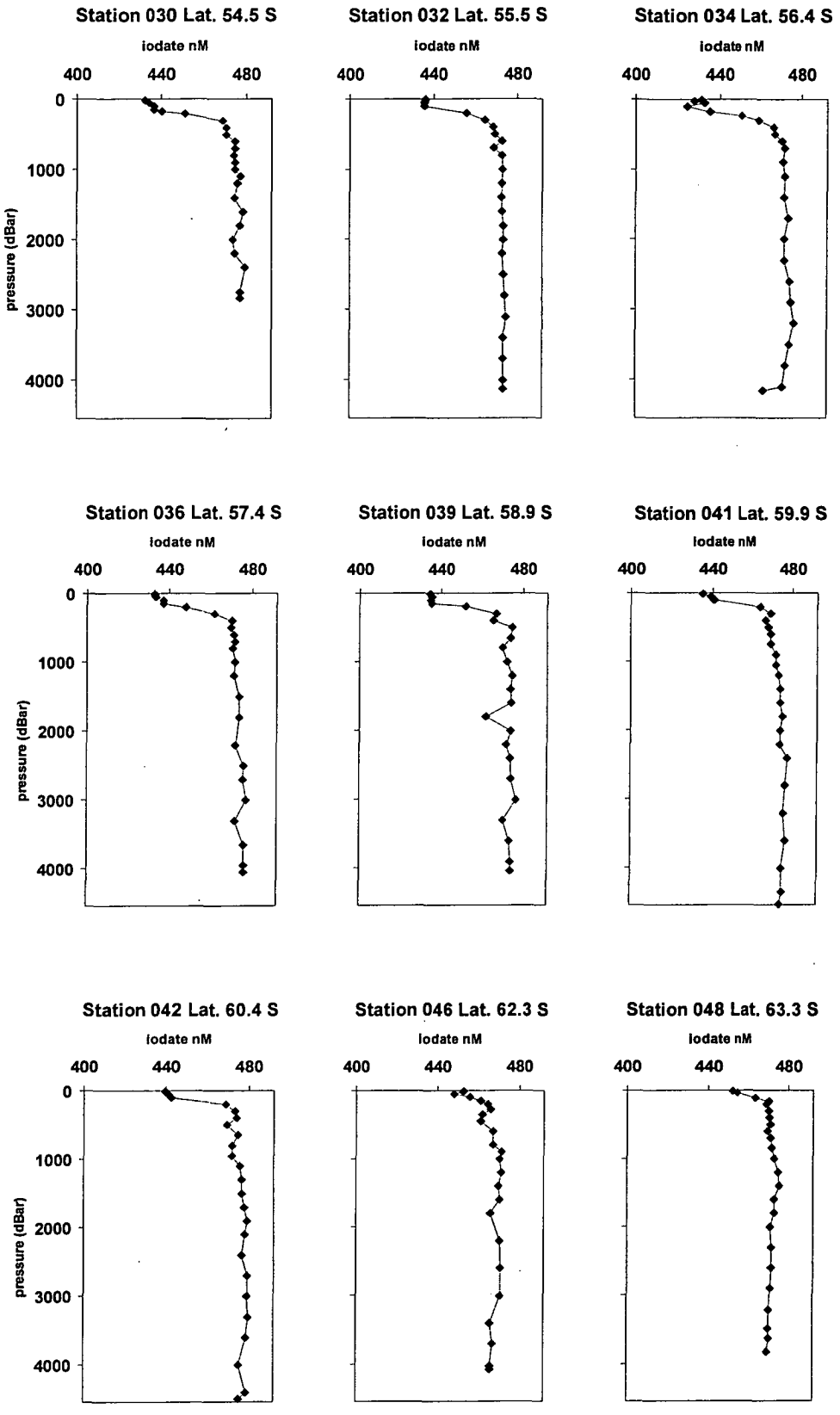

Figure 3.5e- Iodate distribution during cruise au9501 (July 1995) along the SR3 section for stations in the Antarctic Zone (AZ) .

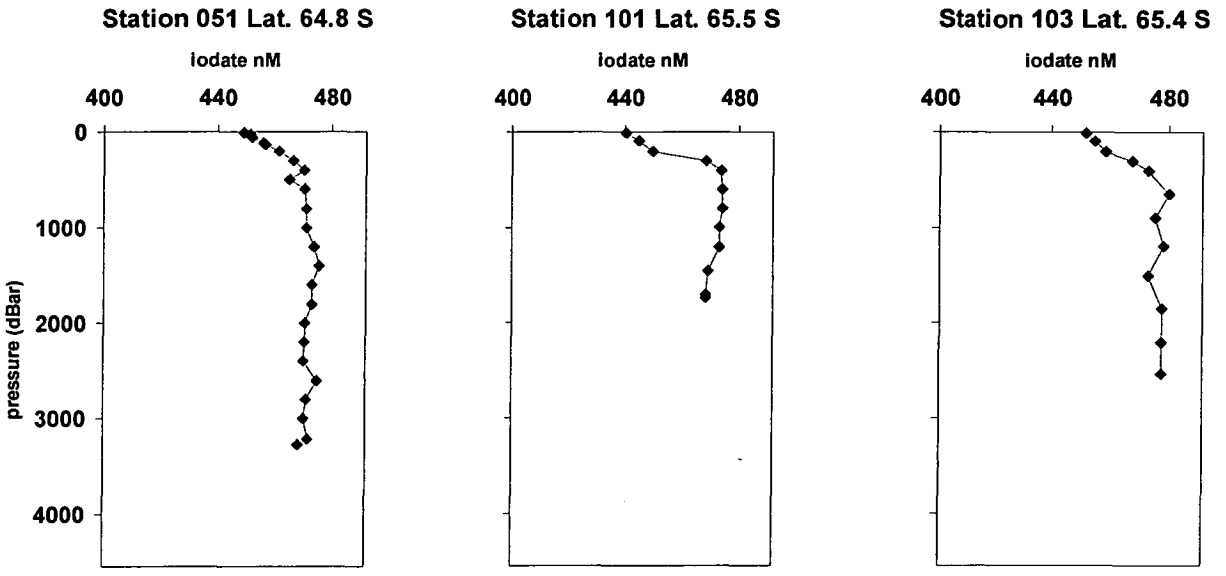

Figure 3.5f- Iodate distribution during cruise au9501(July 1995) along SR3 section for stations in the Antarctic Zone (AZ).

Stations 2 to 5 were in the Subtropical Zone (STZ) (Figure 3.5a). For stations 4 and 5, in the surface, a 200-m deep surface mixed layer can be seen, with homogeneous iodate concentrations, being characteristic of winter advection. The STF was found between stations 5 and 6, with a large drop in temperature and salinity in the top 300 m. In the SAZ (Figure 3.5b and c) a deeper mixed layer can be seen in the iodate plots. Station 9 shows deep winter mixing of iodate down to nearly 800 m, marking the core of the SAMW. For the next stations the mixed layer becomes shallower until the PF, between stations 24 and 26. In the PFZ and AZ (Figure 3.5d to e) the surface mixed layer was typically shallower than 200 m. From station 32 southwards, waters with salinity lower than 34.7 were found below the LCDW. Those waters are Modified Lower Circumpolar Deep Water (MLCDW) and were formed from the contact of LCDW with AABW sinking to the ocean floor from the Antarctic slope. At some stations, lower iodate concentrations were found for these waters. At station 34, for example, a break in the iodate profile can be seen at the bottom (> 4000 m), corresponding to the presence of MLCDW. At stations 41, 42, 48 and 51, a break close to the bottom of the iodate profile corresponds to AABW presence. The southern branch of the polar front, the PF-S, was found between stations 36 and 39. The SACCF was found between stations 46 and 48, and the SB between stations 48 and 51. From station 46 southwards, iodate concentration in surface waters was consistently higher than further north (> 450 nM), with exception of station 101. The lower concentration of iodate at station 101 compared to other polar stations was also matched by a lower concentration for nitrate (not shown) for this winter section.

In the contour plot for iodate data obtained during au9501 cruise (Figure 3.6) some key features can be observed. There is an obvious increase in iodate concentration southwards both in the surface and deep waters. The lowest concentrations of iodate (400-410 nM) are in surface waters (shallower than 200m) just south of Tasmania and coincide with Subtropical Surface Waters (STSW). Just south of 45°S latitude the shallow STF can be seen, with steep gradients separating STSW from SAMW. Further south, around 50°S of latitude, deeper steep gradients can be seen, and they coincide with the SAF. Between the STF and the SAF, in the SAZ, iodate concentration was less than 450 nM down to 500 m depth. From 500 m down to 1500m, iodate concentration increased slowly up to 470 nM.

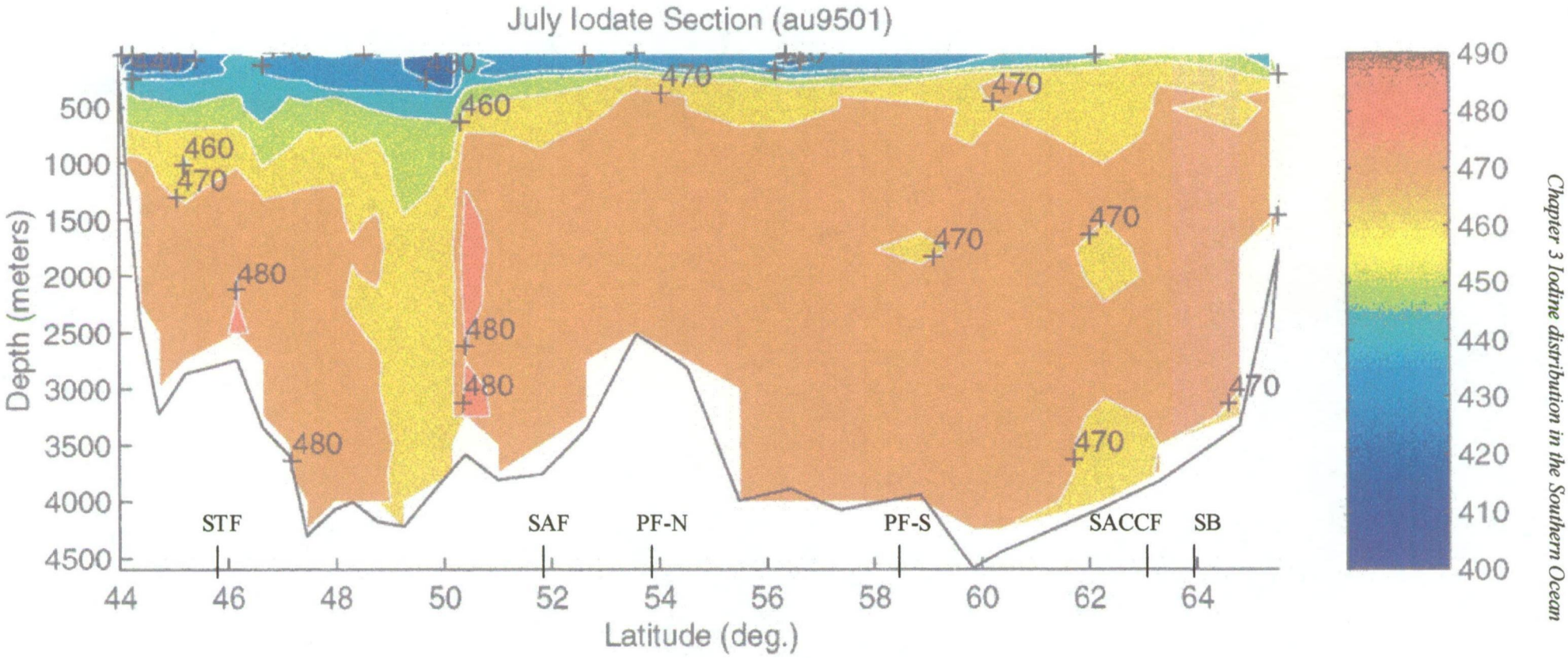

Figure 3.6- Iodate contoured section along SR3 transect during cruise au9501 (July 1995). The approximate positions of the oceanic fronts are indicated.

Another front further south is the PF-N, which was situated around latitude of 54° S for au9501. On the contour plot again (Figure 3.6), a shallow steep gradient in iodate concentration can be seen. In the PFZ, between the SAF and the PF-N, low salinity AAIW is probably formed below the surface, and extends northwards below SAMW. The PF-N also marks the northern most point for Antarctic Surface Water (AASW). The main characteristic of the AZ, south of the PF-N, in the iodate contour plot is the steep gradient between the mixed layer (<200 m) and the AAIW below. Iodate concentrations at those latitudes were typically above 430 nM in the surface, and increased quickly with depth, reaching 465 nM between the depths of 200 and 300 m. The AAIW layer, below AASW, became thinner southwards until 60°S. At this latitude, UCDW lays just below AASW, and iodate gradients between the surface and deep waters became even steeper.

Again, at around 63°S latitude, iodate contour lines were compressed towards surface waters. This feature seemed to coincide with the southernmost front within the ACC, the SACCF.

Iodate concentrations in the surface south of 64°S ranged from 437 to 457 nM. South of this latitude, as the continental slope starts to rise, iodate concentrations were slightly lower in the water column. Waters with iodate concentration below 473 nM can be seen sinking down the continental slope and they coincided with cold AABW, which here dives below the high salinity LCDW.

A large vertical patch of iodate concentration < 470 nM, which can be seen in the iodate contoured section from ~ 49°S to ~ 50.5°S. This patch is not related to any other physical or chemical parameter distribution and is not believed to be a true feature, but an analytical artefact, and it will be discussed later in section 3.3.

3.2.1.2 Iodide distribution

During the au9501 cruise, water samples were also taken and analysed for iodide along the SR3 section. Details of stations and samples analysed can be seen in Appendix II.

Figures 3.7a and b show depth profiles for iodide along the SR3 line for cruise au9501. Iodide concentrations were generally highest in the upper mixed layer, decreasing to values near or below the detection limit in deeper waters.

Stations 2 and 3 are in the core of the STZ and had surface iodide concentrations around 60 nM. Station 5 is on the STF and iodide concentration in the surface was already smaller than 40 nM. At stations 15 and 21, with the approach of the SAF, iodide concentrations in the surface (< 200 m) were all below 40 nM. For stations 28 and 36, a distinct sub-surface iodide maximum was observed at around 95 and 150 m depths, respectively. These winter iodide maxima may be remnant features of the reported sub-surface chlorophyll maximum between 53° and 58°S on the SR3 section, which are normally found around 60 m in the summer, but can become deeper (100 m or more) by late summer/autumn (Parslow *et al.*, 2001). At Station 28, an iodide maximum coincided with iodate minimum at 95 m. Stations 36 and 42 also presented the lowest iodide concentration measured (above the detection limit) for near surface waters for the winter cruise, 20 nM. Further south, iodide results were unfortunately below the detection limit of ~ 20 nM. At station 48, measured surface iodide concentration was below the detection limit at 17 nM, one of the lowest results so far recorded for iodide in ocean surface waters (Campos, *et al.*, 1999).

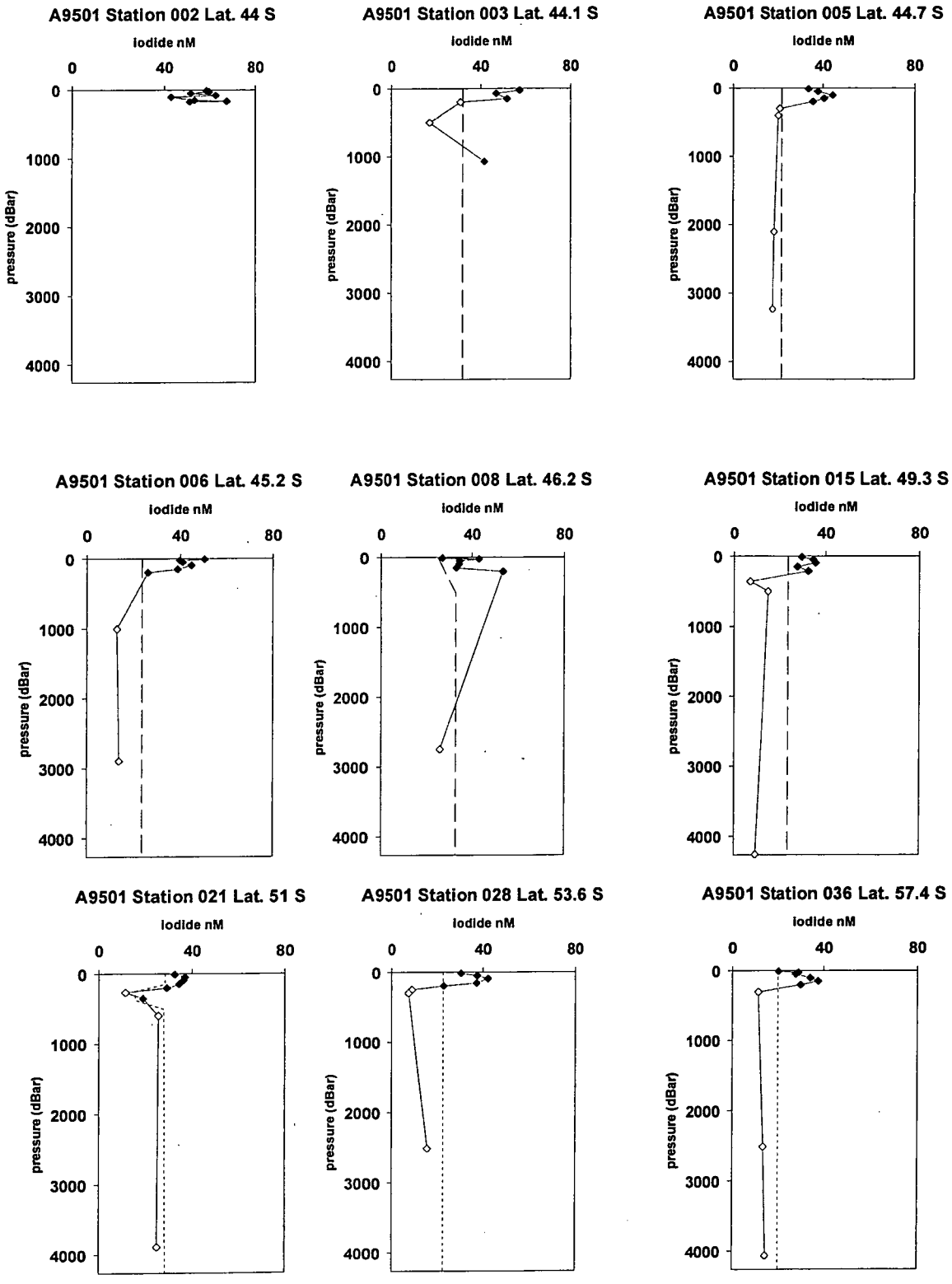

Figure 3.7a- Iodide depth profiles for cruise au9501 (July 1995) along SR3 section. The dotted line represents the detection limit; ◆ represents iodide values above the detection limit; and ◇ represents iodide values below the detection limit.

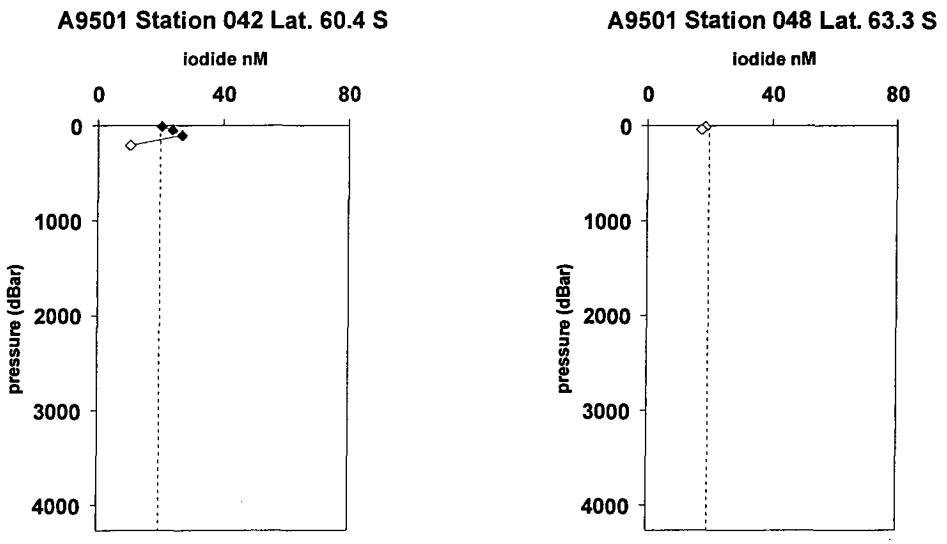

Figure 3.7b- Iodide depth profiles for cruise au9501 (July 1995) along SR3 section (Cont.). The dotted line represents the detection limit; ◆ represents iodide values above the detection limit; and ◇ represents iodide values below the detection limit.

3.2.1.3 Total inorganic iodine distribution

Some samples collected for iodide along the SR3 au9501 winter transect were also analysed for total inorganic iodine (total iodine).

The results are shown in Figure 3.8. Total iodine concentration was measured after reduction of iodate with ascorbic acid, as described in Chapter 2, and the results represent the inorganic iodine fraction, iodate plus iodide. It was then expected total iodine results would be higher than iodate in the surface, becoming closer to iodate concentration in deep waters, where iodide concentrations are very low. The results obtained were lower than the expected concentrations. Total iodine values were higher than iodate values in surface waters in all stations, except two. At station 8, near surface water total iodine value was very close to iodate concentration, contradicting iodide concentration of 30 nM found. Also at station 36, total iodine results were all lower than iodate concentrations measured directly. For the other stations (2, 6, 15, 28, 101 and 103) total iodine was higher than iodate in the surface and either approached iodate concentration in deep waters (stations 6, 101 and 103) or was lower than iodate in deep waters (stations 15 and 28). For all the stations, except 101 and 103 with no iodide measurements, measured iodate values plus measured iodide values were higher than measured total iodine values.

These results lead one to believe that total iodine results were influenced by incomplete detection of iodine forms.

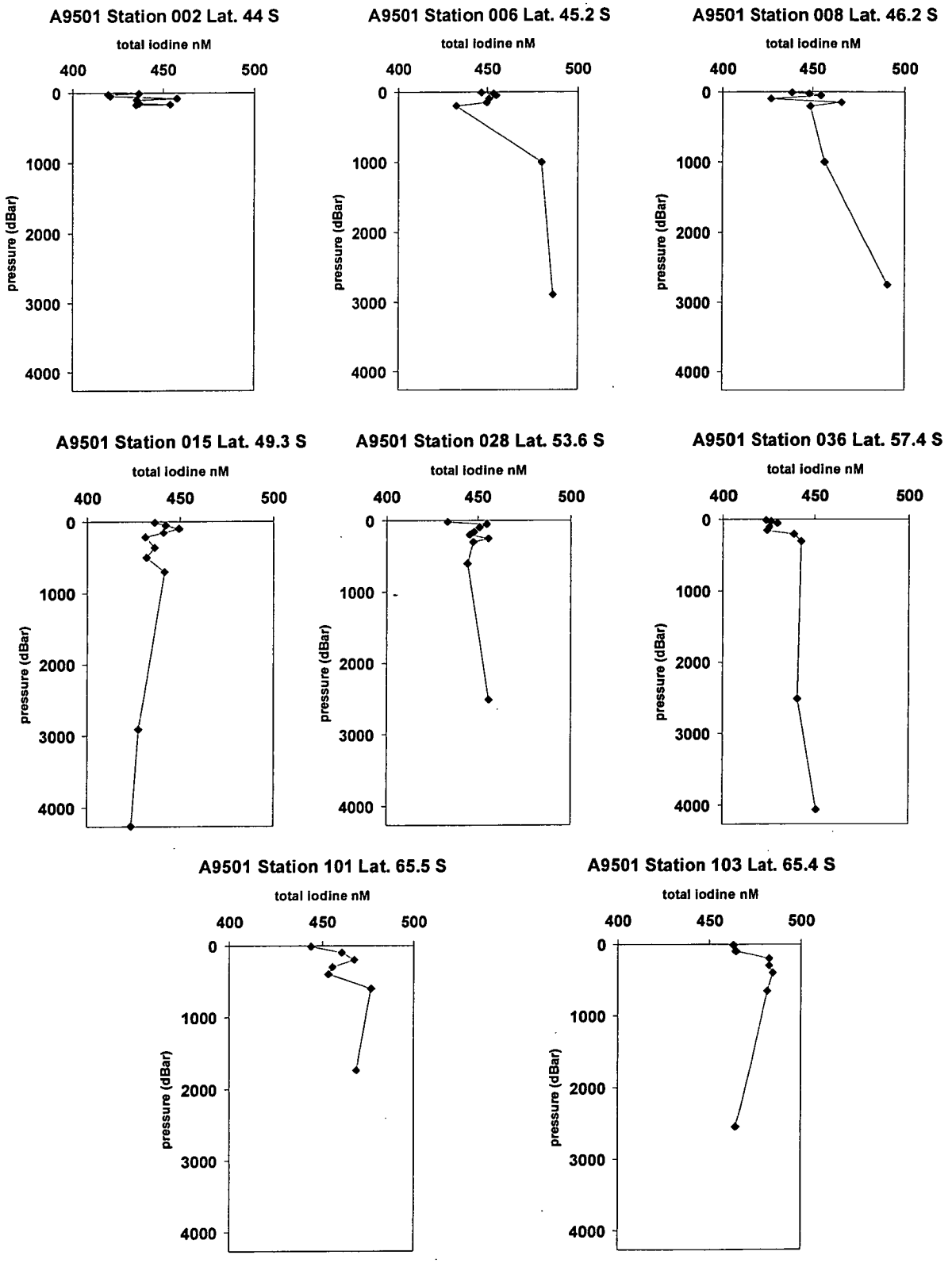

Figure 3.8- Total inorganic iodine depth profiles for cruise au9501 (July 1995) along SR3 section.

3.2.2 First summer cruise, austral summer 1994 (au9407)

Two sections were covered during this cruise in January and February 1994: the repeat section SR3 and the PET section (Figure 3.1). Details of stations sampled and samples taken can be seen in Appendix II. Only iodate was analysed during this cruise, since the method for iodide determination by IC was still being developed.

3.2.2.1 The SR3 section

The salinity and temperature distributions along the SR3 line during au9407 cruise are depicted in Figure 3.9.

In Figure 3.9b, the abrupt change in salinity from 34.9 to 34.7 at ~ 45.6°S marked the STF. And again, the change at ~ 51°S from 34.4 to 34.2 marked the SAF. Between those two fronts, within the SAZ, waters with salinity < 34.4 and temperatures < 9°C were observed in the upper 200 m as a result of a large eddy in the region at that time (Popp *et al.*, 1999). With the summer warming, a shallow (< 100 m) surface layer of Subantarctic Surface Water (SASW) was formed above the SAMW. At 53.6°S, the PF-N marked the northern limit of the 2°C sub-surface isotherm at 200 m, while at ~ 59°S the PF-S can be seen with isotherms becoming again steeper towards the south. Further south, the southern limit of the surface temperature maximum layer warmer than 1.8° C marks the SACCF at ~ 64°S. Very close to that is the southern limit of UCDW, marking the SB of the ACC, at 64.3°S. At this longitude, the ACC is very close to the Antarctic continental shelf. This fact brings important implications for the ventilation of CDW due to contact with newly formed AABW (Orsi *et al.*, 1995).

Iodate distribution along the SR3 during au9407

Iodate results for cruise au9407 (January 1994) are shown in Figure 3.10. Details of stations sampled and samples taken are given in Appendix II.

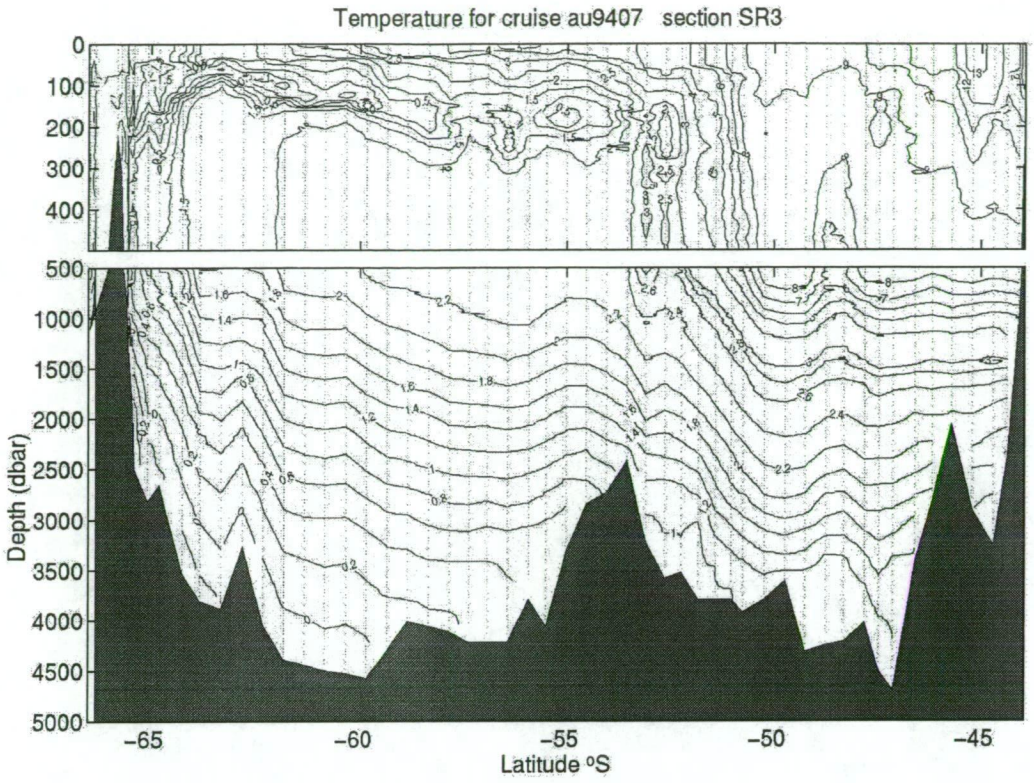

(a)

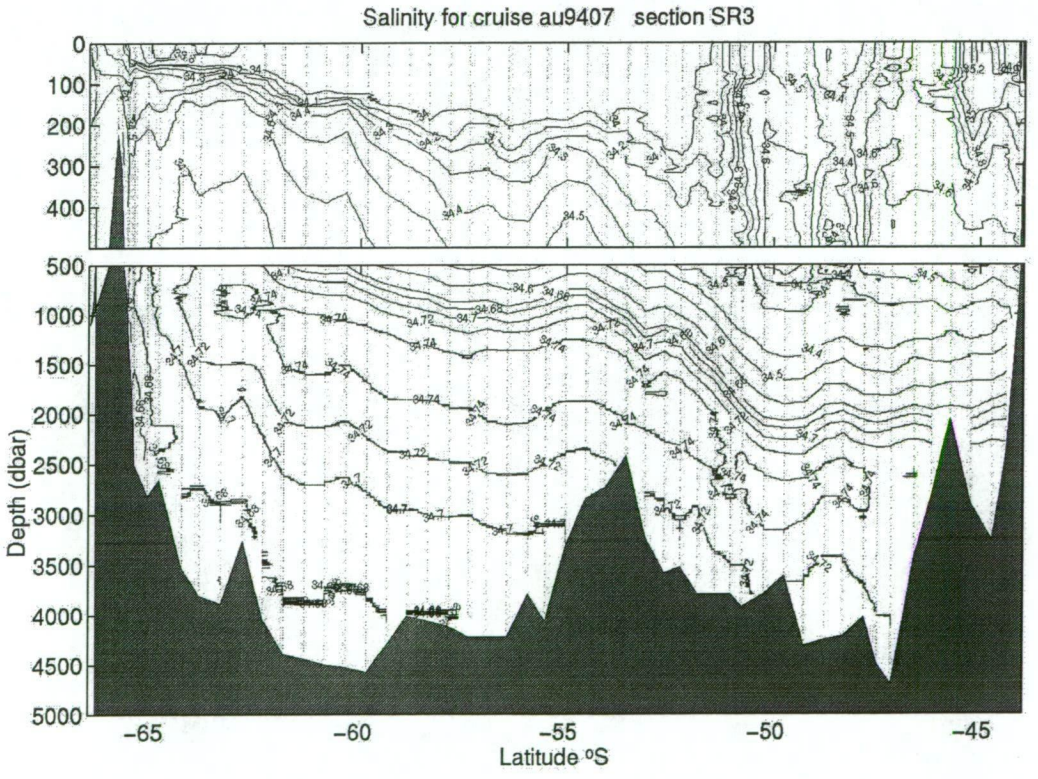

(b)

Figure 3.9- Temperature (°C, **a**) and salinity (**b**) contoured sections along SR3 transect during cruise au9407 (January 1994).

In the STZ (Figure 3.10a), iodate depletion in the surface was very pronounced (concentrations 397-438 nM). From 200 m, iodate increased steadily down to 600 m depth. Iodate concentration of 397 nM was recorded for station 003 at 30 m depth, being the lowest iodate concentration measured during this work.

In the SAZ (Figure 3.10b) iodate concentrations were higher in the surface (419-440 nM) than further north. With the arrival of summer, SASW is formed on top of SAMW. Looking at iodate profiles on Figure 3.10b, one can see that iodate is depleted in the SASW (top 100 m) in relation to SAMW below (150 to ~ 600 m). Also, iodate concentration in the surface increased more quickly than within the more homogeneous SAMW. Below 500-600 m depth, a break in the profiles coincided with the low salinity tongue of AAIW. At station 15 a series of "steps" are noticeable on iodate profile. They coincided with the following changes in water masses: 0-100 m SASW, 100-600 m SAMW, 700-1300 m AAIW, 1500-2100 m UCDW and below 2700 m LCDW.

In the PFZ (Figure 3.10c) the surface mixed layer was deeper than further north, reaching 200 m. At station 25 (Figure 3.10d), iodate was homogeneously distributed within the Polar Frontal Zone Surface Water (PFZSW), on the top 200 m of the profile, with a concentration of ~ 436 nM, also higher than further north. With the absence of SAMW, UCDW was closer to the surface at ~ 1000 m depth, which can also be observed in the iodate profiles. At stations 36 and 38 (Figure 3.10d), within the IPFZ, an iodate minimum can be seen at 50 m. This iodate minimum coincided with a silica minimum and a chlorophyll maximum at the same depth, suggesting a biological origin (Popp *et al.*, 1999). At stations 36 to 48, AAIW can still be distinguished below AASW, extending down to 300-400 m. At stations 52/53, however, AAIW is no longer present and UCDW came up to 300 m depth. At stations 58 and 60, UCDW was at 150 m depth, immediately below AASW. The SACCF was located at ~ 64°S. Station 60 was also the last station sampled for iodate where UCDW was observed, being the last station sampled for iodate within the ACC for the SR3 section. For this section, cruise au9407, in January 1994, the SACCF and the SB were both close together at ~ 64°S. Stations 63 and 65 were approaching the continental slope and AABW can be seen in the iodate profiles at

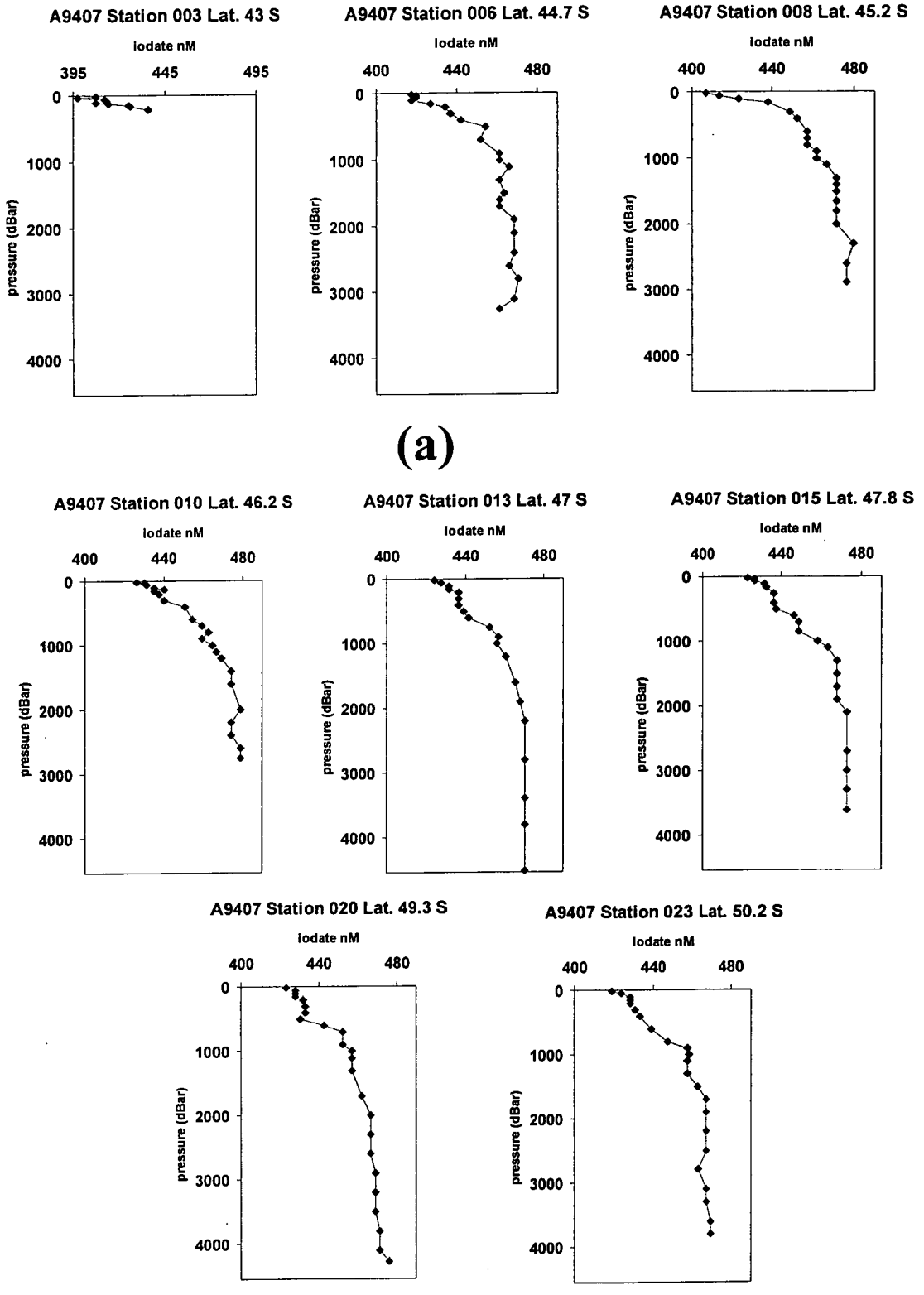

Figure 3.10a and b- Iodate distribution during cruise au9407 in the Subtropical Zone (STZ) stations **(a)** and Subantarctic Zone (SAZ) stations **(b)**.

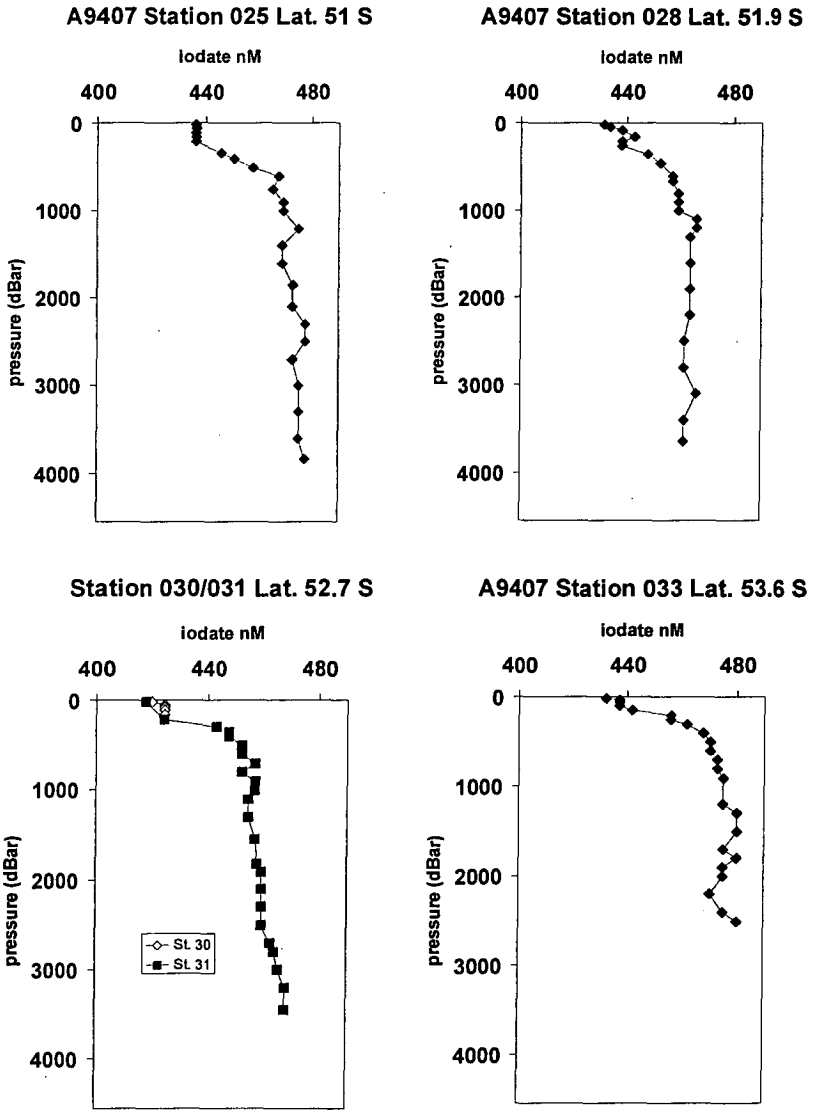

Figure 3.10c- Iodate distribution during cruise au9407 (January 1994) along the SR3 section in the Polar Frontal Zone (PFZ) stations.

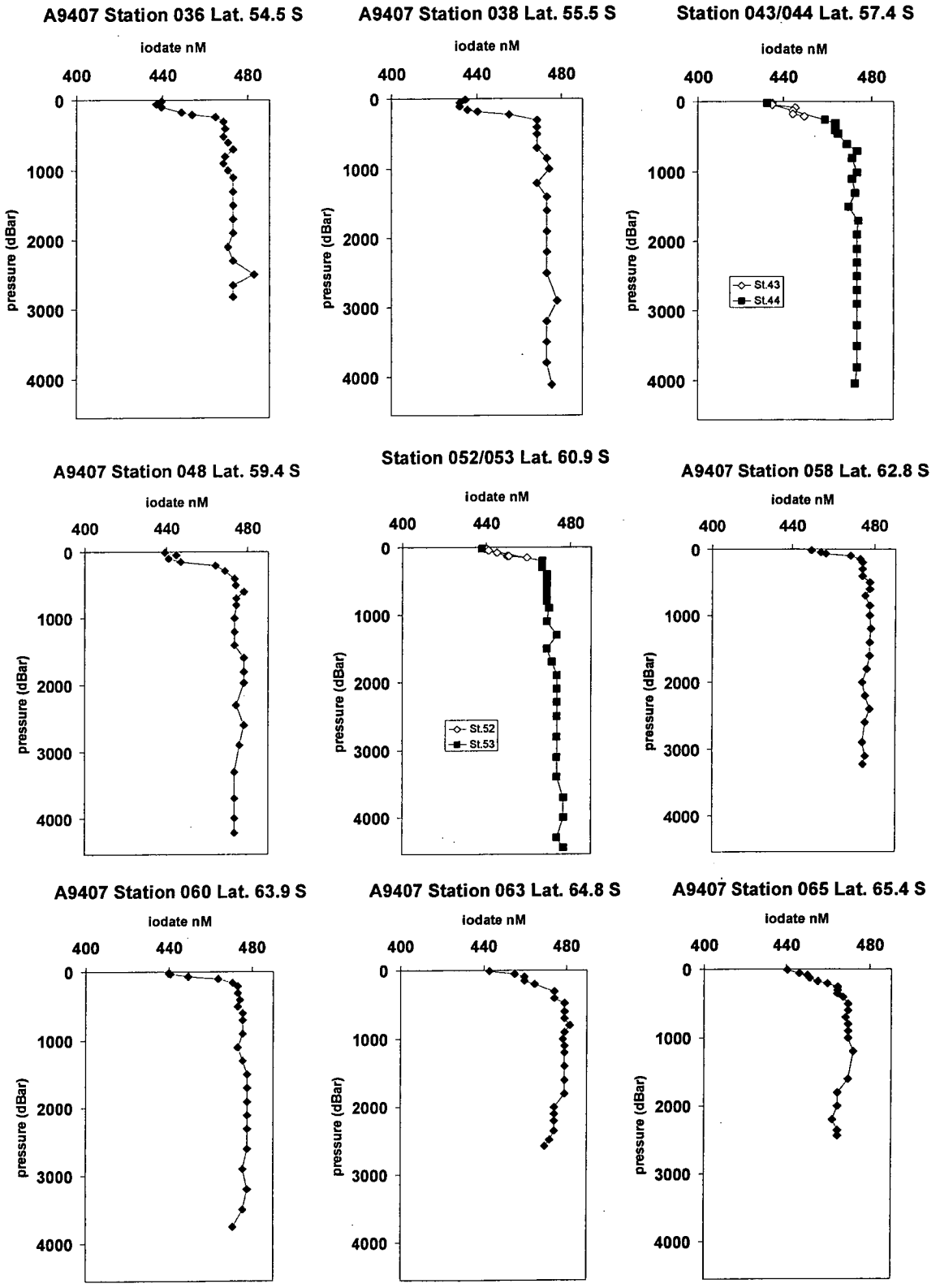

Figure 3.10d- Iodate distribution during cruise au9407 (January 1994) along the SR3 section in the Antarctic Zone (AZ) stations.

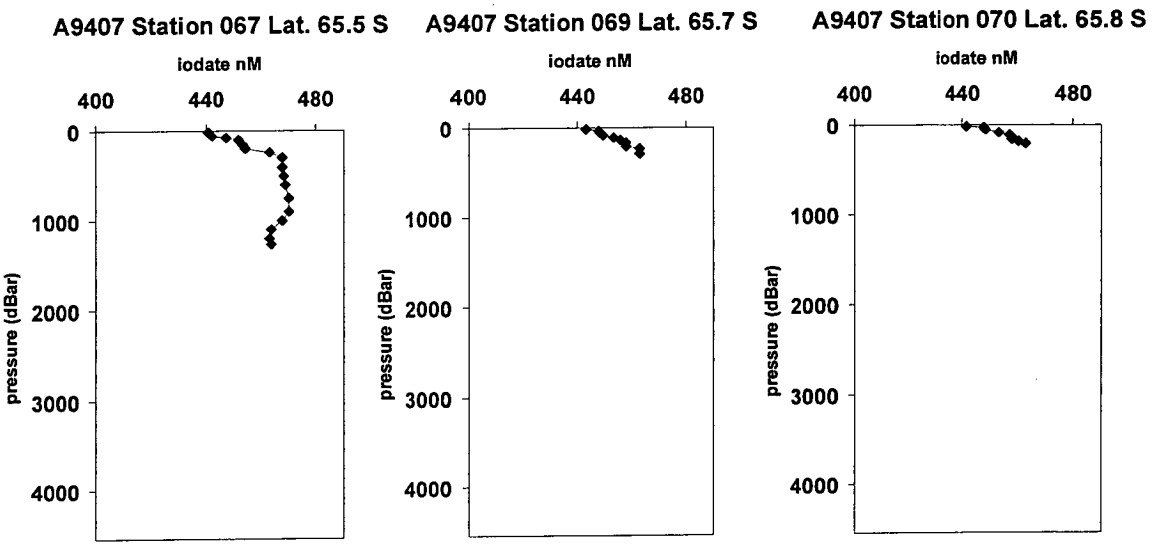

Figure 3.10e- Iodate distribution during cruise au9407(January 1994) along SR3 section in the Antarctic Zone (AZ) stations (cont.).

2000 m and 1600 m depth, respectively, with lower concentrations than LCDW above. At station 67 (Figure 3.10e), on the Antarctic continental slope, lower concentrations of iodate were also seen below 1000 m, as slope water descended to form bottom water. The last two stations, 69 and 70, were sampled over the Antarctic continental slope, approaching the continental shelf, and showed iodate concentrations all higher than 440 nM increasing steadily with depth.

On the iodate contour plot (Figure 3.11) the SAF can be seen with steep concentration gradients approaching 51°S latitude. North of the SAF, SAMW was within the 450 nM iodate contour line. Further south, approaching 54°S, another shallower change in contour gradient marked the PF-N. At 63°S, one can notice deep water coming closer to the surface, with the 460 nM contour line following approximately the upper limit of UCDW. Waters with iodate concentration < 470 nM can be seen on the contour plot cascading down the Antarctic continental slope. These slope waters would later form AABW after reaching the ocean floor.

3.2.2.2 The PET section

During cruise au9407, in January and February 1994, the Princess Elizabeth Trough section, east of Prydz Bay (Figure 3.1) was also sampled for iodate. Details of stations and samples taken can be seen in Appendix II.

Distribution of salinity and temperature along the PET section are shown on Figure 3.12. This section showed some features that were distinct from the SR3 section at same latitude. Due to the melting ice, very low salinity waters (< 33.6) were found in the upper 50 m, close to the Antarctic continent. The UCDW extended further south than in the SR3, marking the Southern Boundary of the ACC (SB) at ~ 64.6°S. The SACCF was located at 62.7°S. Remnant sub-zero temperature water ("winter water") was found below the surface between 62° and ~ 63.5°S, isolating surface waters from CDW.

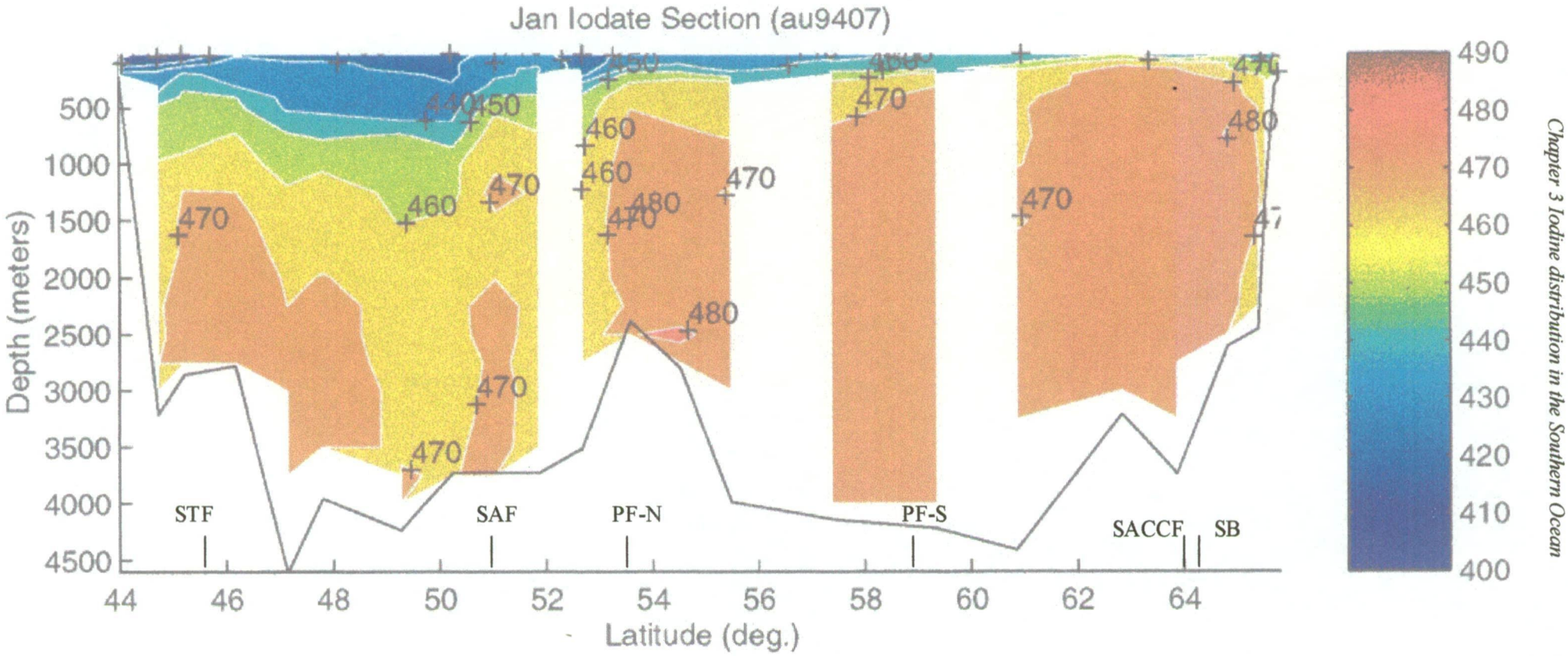

Figure 3.11- Iodate contoured section along SR3 section during cruise au9407 (January 1994). Approximated positions of oceanic fronts are indicated.

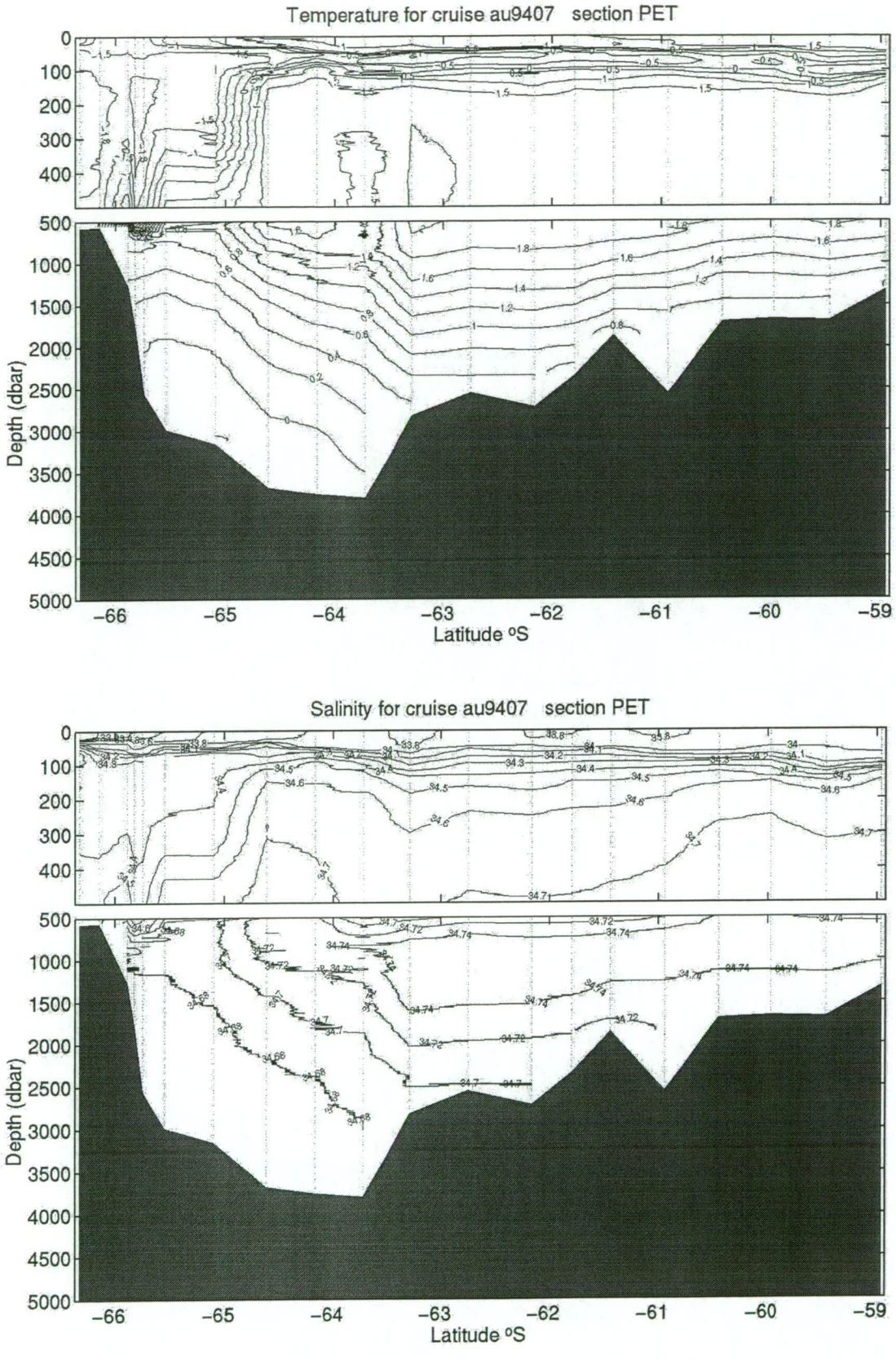

Figure 3.12- Temperature (°C, **a**) and salinity (**b**) contoured sections along PET transect during cruise au9407 (January 1994).

Iodate distribution along PET during au9407

Iodate profiles for the PET section are shown on Figure 3.13. Most profiles also differ from those at the same latitude at the SR3 section. At stations 76, 78, 79 and 81, iodate concentration in the near surface was low (~ 420 nM), partly due to dilution caused by meltwaters. With the SB between stations 81 and 85, a dramatic change in the iodate profile can be seen, with UCDW bringing high iodate waters closer to the surface at station 85. Within the ACC, stations 85 to 99, iodate profiles were very similar, with high depletion in the surface down to 200 m depth and near constant concentration below that. Surface depletion of iodate also was more intense in this section, especially from stations 92 to 99, than at the SR3 section for this cruise at same latitude. At station 92 (62.2°S, PET), iodate depletion from the surface down to 160 m was 38 nM, versus 24 nM at station 58 (62.8°S, SR3, au9407) (Figure 3.10d). Nitrate also showed higher depletion along PET than along SR3, au9407. At station 92, nitrate surface depletion was 14.5 μM, versus 5.3 μM at station 58, from the near surface down to 160 m. Also at the PET transect, AABW presence was not so noticeable on iodate profiles as it was for some stations on the SR3.

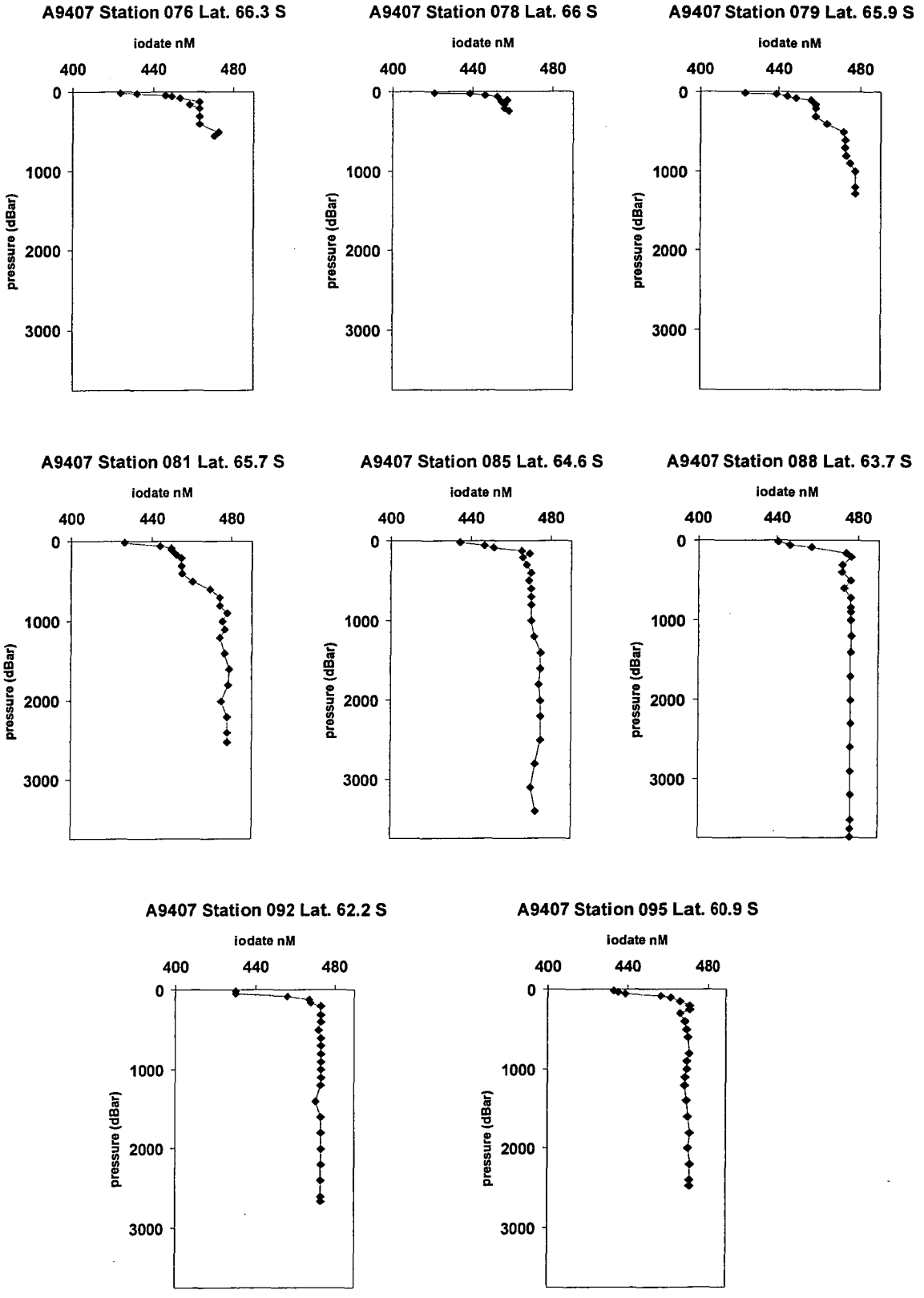

Figure 3.13a- Iodate distribution during cruise au9407 (January 1994) along PET section.

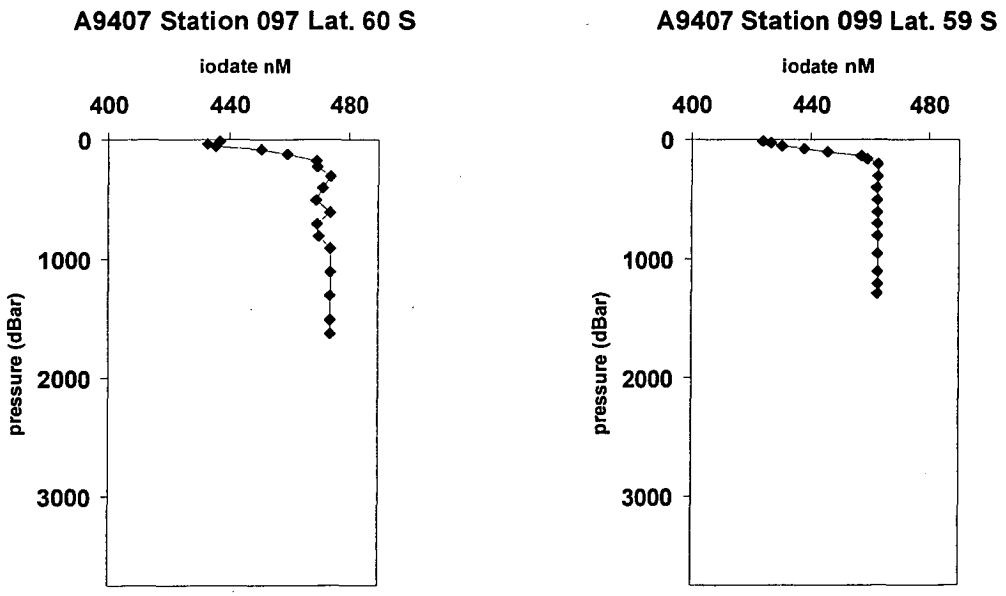

Figure 3.13b- Iodate distribution during cruise 9407 along PET section.

3.2.3 Second summer cruise, austral summer 1995 (au9404)

During cruise au9404 in January 1995, two transects were sampled for iodate and iodide. First, was the WOCE S4 line along the Antarctic continent at ~ 62°S from 110°E to 162°E (Figure 3.1), and second, was the WOCE SR3 line, this time from south to north.

3.2.3 .1 The S4 section

Salinity and temperature distributions for this section are shown in Figure 3.14.

The section started at 110°E, with first station offshore from the Australian Antarctic Station Casey. With sea ice still present during early summer 1995, surface salinities were above 34.0 and surface temperatures below 0° C at stations 6 and 7. At the western end of the section, at around 62.5°S and 114.5°E, the end of UCDW marked the Southern Boundary of the ACC. From there on, the section went east, approximately following the 62°S latitude line until 137°E. Along the 62°S line, the section was hydrographically homogeneous. Lower surface salinities (< 33.9) and near surface temperatures below 1°C were observed along this part of the section, from ~ 114° to 137°E. Other features observed here were: (1) a sub-zero sub-surface temperature layer from ~ 50 to ~ 100 m depth; (2) temperatures higher than 1.8° C below the sub-zero layer down to 700 m depth; and (3) sub-zero temperatures again close to the bottom (below 3,800 m depth) characterising AABW. East of 137°E, the section moved south, following the Antarctic coastline. Surface salinity started to drop slowly, reaching values below 33.0 at station 47. In surface waters, temperatures also dropped from above to below 0°C at station 45. Between stations 47 and 48, at 63.4°S 159.5°E and 64°S 160°E, respectively, the section crossed the Southern Boundary of the ACC. The last part of the section approached the continental shelf and sub-zero temperatures can be seen on the surface, with slightly higher salinities of ~ 33.5.

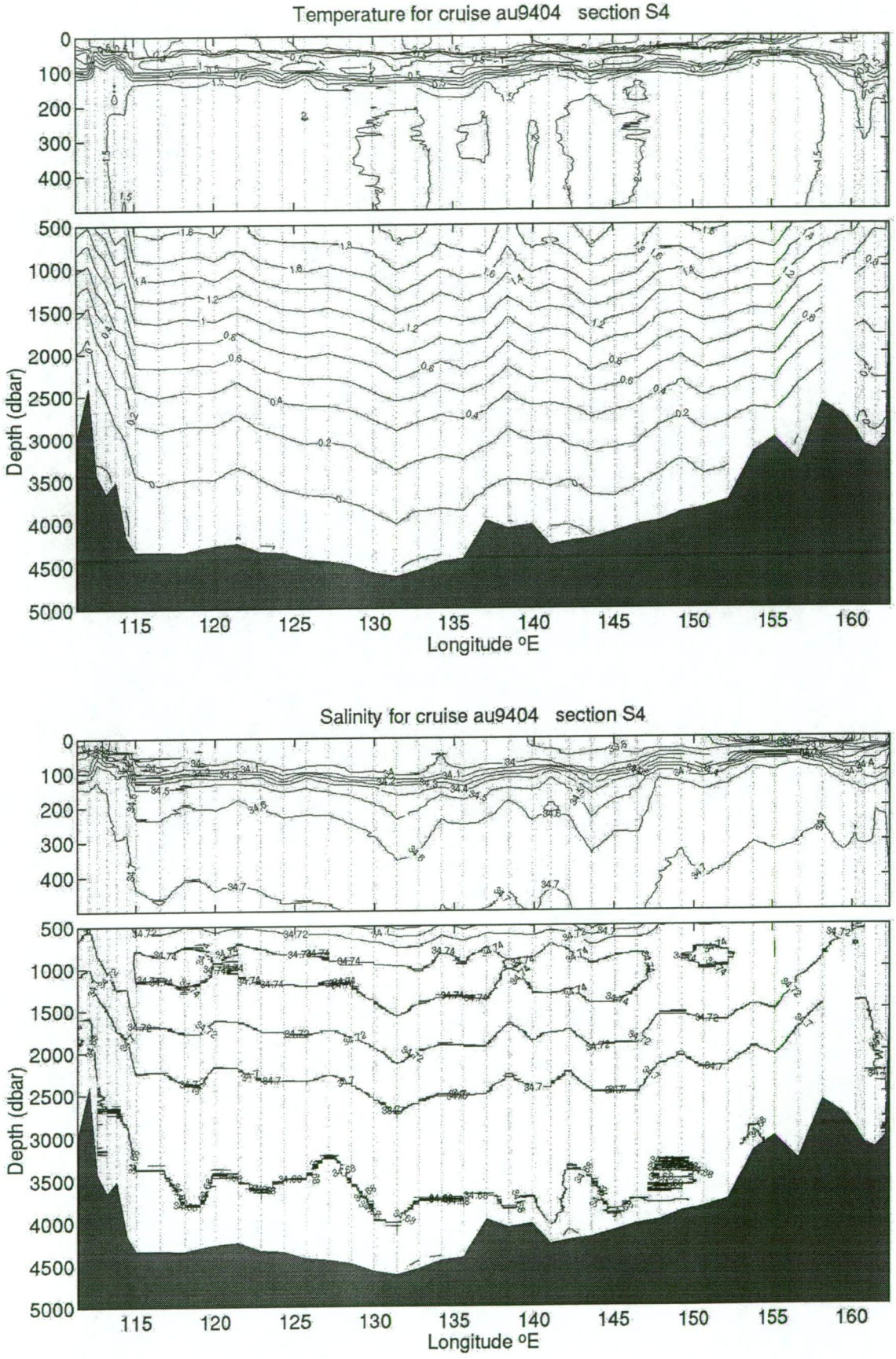

Figure 3.14- Temperature (°C, **a**) and salinity (**b**) contoured sections along S4 transect during cruise au9404 (January 1995).

Iodate distribution along S4 during au9404

As for salinity and temperature, iodate distribution varied mostly at the beginning and at the end of the section, remaining mostly the same along the 62°S line. Figure 3.15 shows the iodate results obtained for S4 transect during au9404, in January 1995. Sampling dates, positions and number of samples taken are presented in Appendix II.

At stations 6 and 7, at the west end of the section, surface iodate concentrations were high at 465 and 467 nM, respectively (Figure 3.15a). These values were the highest surface iodate concentrations measured for all the cruises in this study. These high values of iodate can probably be explained by the high salinities in surface waters observed near Casey, due to the presence of forming sea ice, which also limited algal production. At station 10, salinity was lower and iodate concentrations were also correspondingly lower at the surface.

The transect left 66°S at station 6 and crossed the SB between stations 13 and 17, at around 63.5°S. At station 13, the very shallow surface layer (< 100 m) that can be observed in the iodate profile (Figure 3.15a) was characteristic of the proximity of the Southern Boundary (SB). At station 17 and beyond, the surface mixed layer was around 200 m deep, which can also be observed in the iodate profile. From station 17 to station 30 (Figure 3.15a,b), with the transect along 62°S latitude, iodate profiles were all very similar, with a shallow mixed layer (~ 200 m deep). Iodate depletion in relation to deep waters for these stations was also restricted to this shallow mixed layer, consistent with salinity distribution. From station 30 the section started to head south and crossed the SACCF between stations 43 and 47. At station 43 (Figure 3.15b), a very shallow mixed layer can be observed in the iodate profile, consistent with the proximity of the fronts. Again the SB was crossed, this time between stations 47 and 50. From station 47 onwards (Figure 3.15b,c), iodate depletion in the mixed layer, in relation to deep waters, became more intense. Iodate concentrations in the near surface were all below 440 nM. At station 47, there is a clear depletion of iodate at the surface, which was caused partially by a patch of low salinity (< 33.0) in

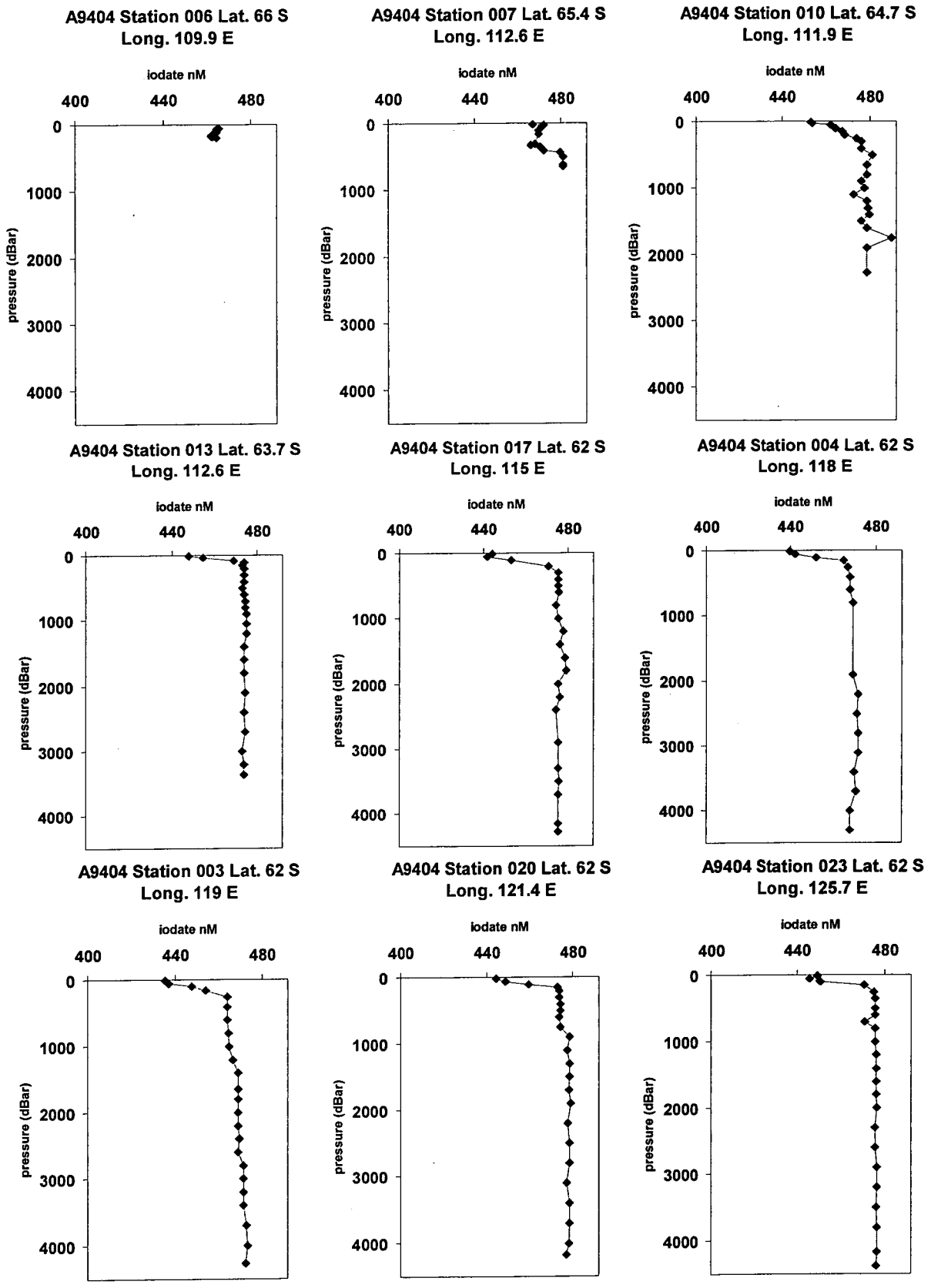

Figure 3.15a- Iodate distribution during cruise au9404 (January 1995) along S4 section.

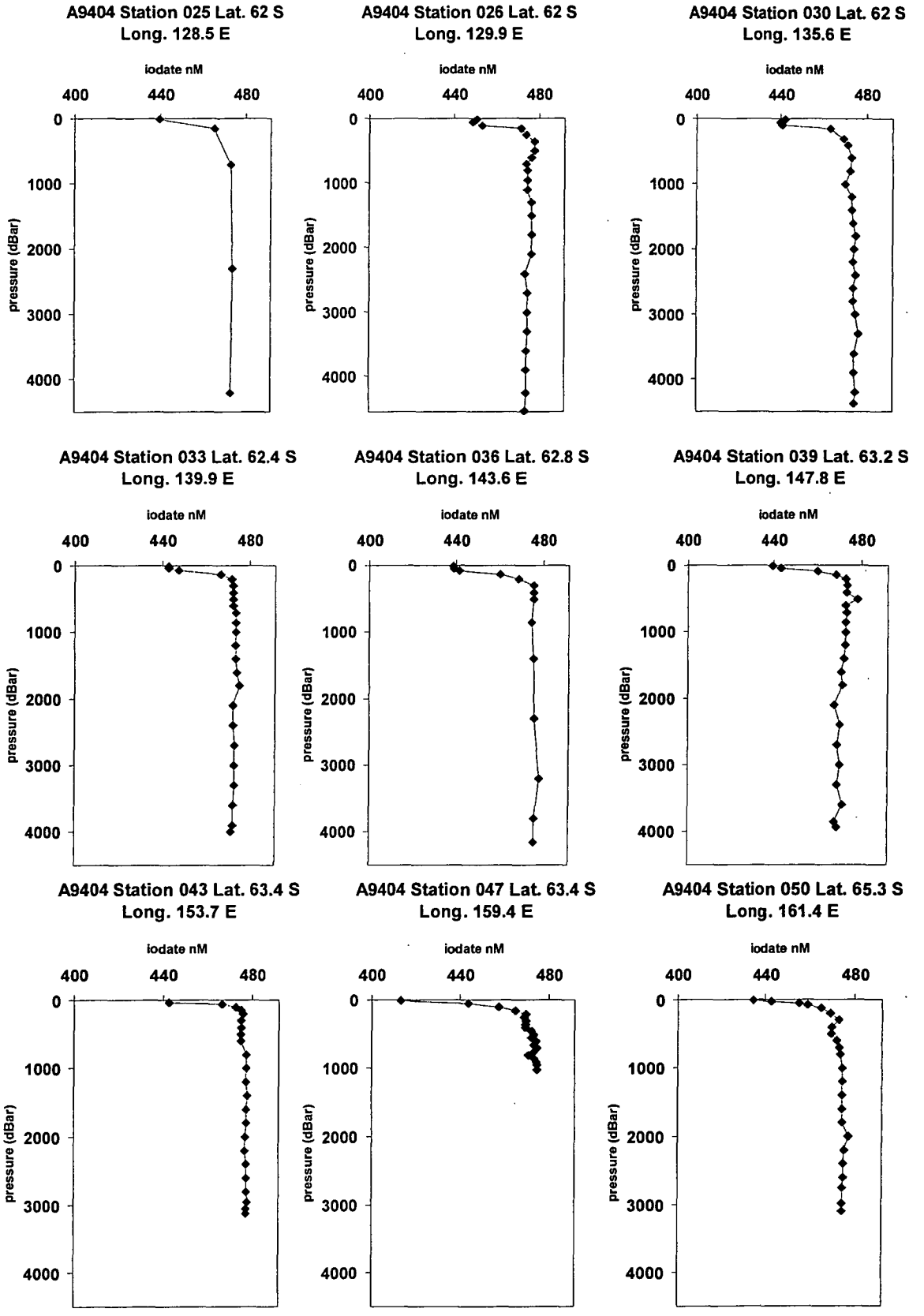

Figure 3.15b- Iodate distribution during cruise 9404 along S4 section.

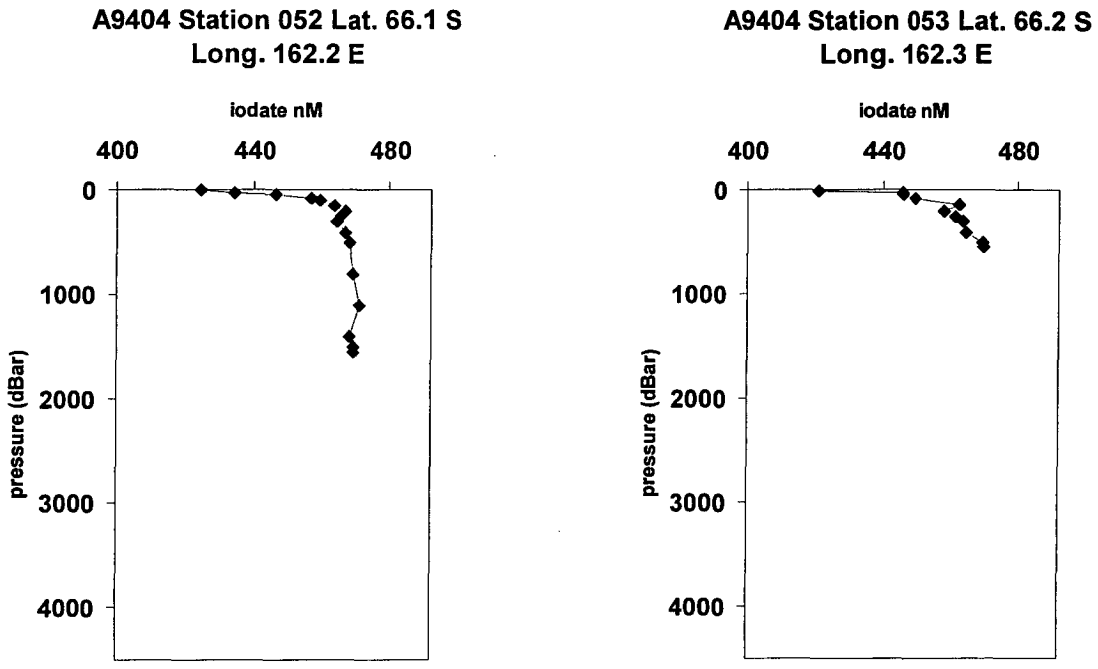

Figure 3.15c- Iodate distribution during cruise au9404 along S4 section.

the region. The iodate value measured at the surface of 413 nM at station 47, when normalised to salinity at 50 m (34.136) still showed a lower concentration of iodate (430 nM), than surface iodate at station 50 (434 nM). High dissolved oxygen at near surface was also noticed for these stations. Stations 52 and 53 (Figure 3.15c) also showed iodate depletion combined with high dissolved oxygen and low nutrients at the surface, suggesting recent high levels of biological production. These two stations were closer to the Balleny Is, which may have contributed to the proposed increase in productivity at those stations.

Iodide distribution along the S4 section during au9404

During cruise au9404, iodide was also measured at nine stations along the WOCE S4 line. Depth profiles for iodide are shown in Figure 3.16.

Iodide concentrations were typically higher in the surface decreasing towards the bottom. Iodide values were normally below the detection limit for depths greater than 200 m, with exception of stations 7 and 50. At station 7 iodide values of ~ 15 nM were measured down to 354 m depth. At station 50, iodide value of 7 nM was measured at 3095 m depth. Also at station 7, the highest value of 38 nM for iodide for this section was measured at the near surface. At station 3, iodide sub-surface maximum coincided with dissolved oxygen sub-surface maximum at 53 m, suggesting biological production. The lowest value of iodide in a surface sample for all the cruises was measured at station 33, 15 nM at 12 m depth.

3.2.3.2 The SR3 section

During cruise au9404 in January 1995, the WOCE repeat section SR3 was again sampled for iodate and iodide (total iodine). Contoured salinity and temperature distributions for the SR3 section during the cruise are shown in Figure 3.17.

The STF was located at ~ 46°S and SAF at ~ 51.5°S. At the southern end of the SAZ (~ 50°S) a meander of the SAF can be seen, with steep gradients just before the front itself. At 53.6° S is the PF-N. South of the PF-N, warm and fresher AASW can be

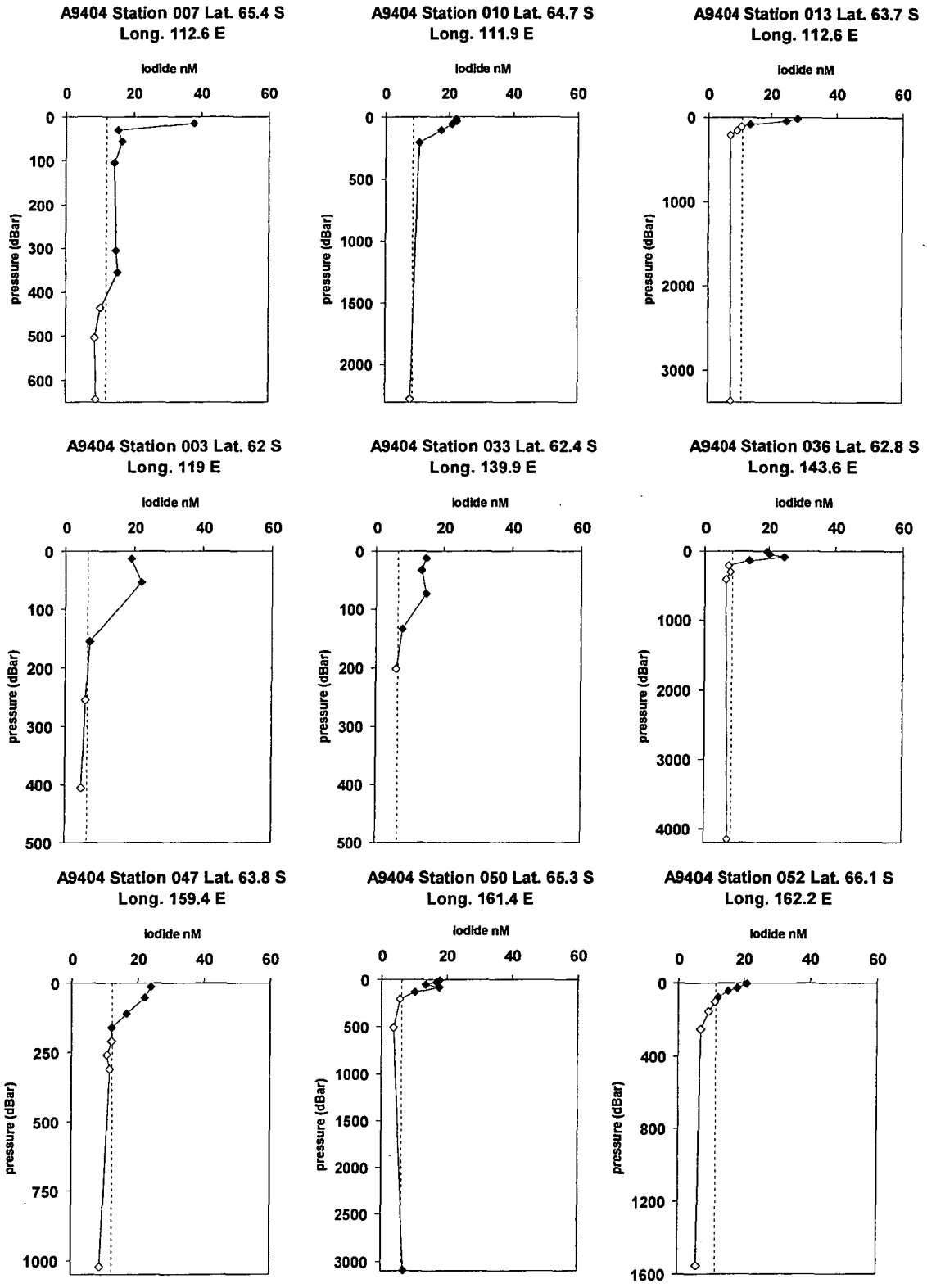

Figure 3.16- Iodide depth profiles for cruise au9404(January 1995)along S4 section. The dotted line represents the detection limit; ◆ represents iodide values above the detection limit; and ◇ represents iodide values below the detection limit.

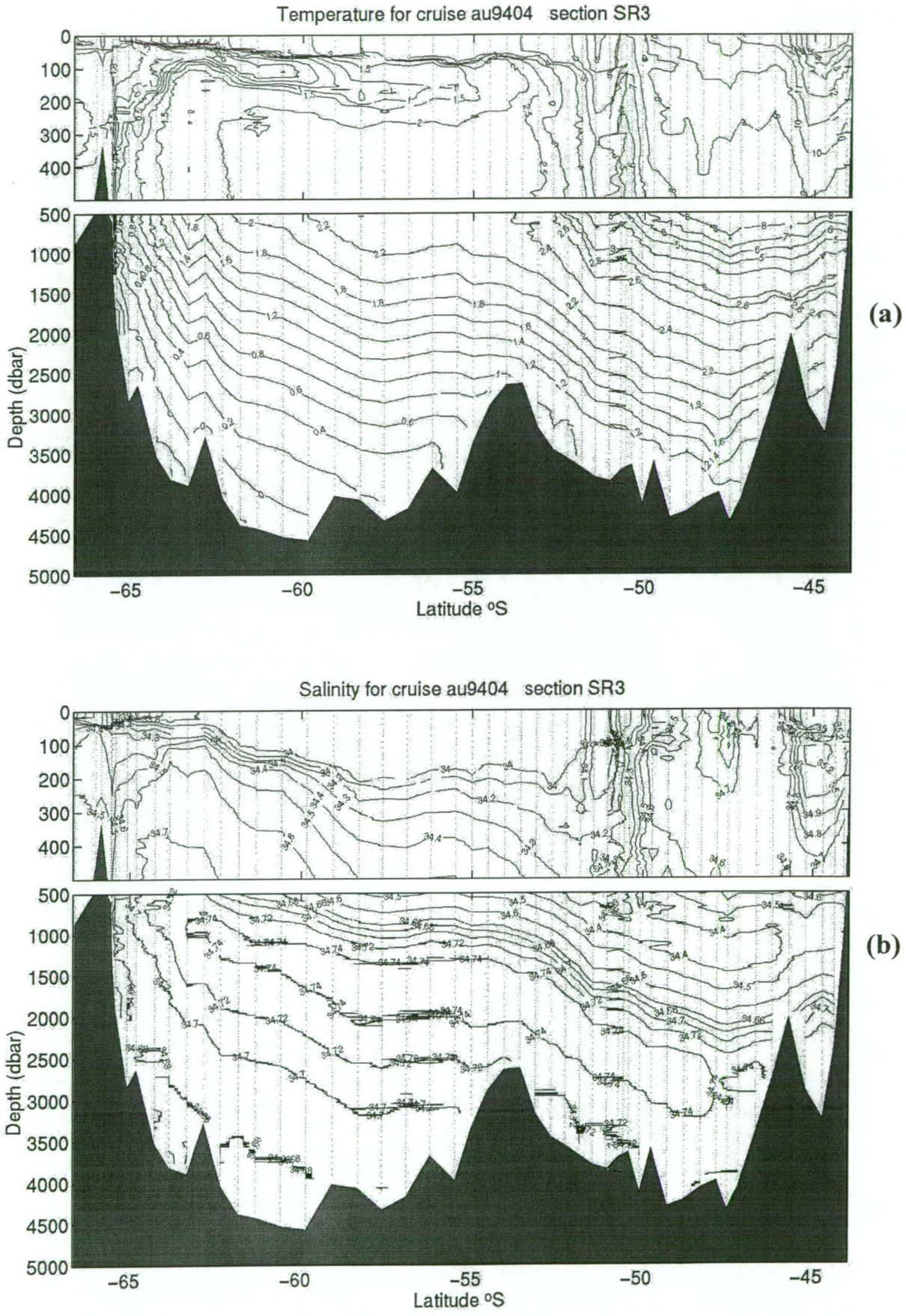

Figure 3.17- Temperature (°C, **a**) and salinity (**b**) contoured sections along SR3 transect during cruise au9404 (January 1995).

seen on the upper 100 m, while some cold "winter water" sits below from 100 to 300 m. At ~ 59°S the PF-S was located, and at ~ 63.5°S the SACCF. AABW, dense and cold (< 0° C), can be seen near the bottom, reaching as far north as 56.5°S, the southern slopes of the Southeast Indian Ridge.

Iodate distribution along the SR3 section during au9404

Samples were analysed for iodate along the WOCE repeat section SR3 during January 1995, cruise au9404. Results are shown on Figure 3.18a-e. More details about station numbers, dates and samples taken can be seen in Appendix II.

Iodate depth profiles within the STZ were similar in shape to those of cruise au9407 (Figure 3.18a). Surface concentrations below 420 nM increased gradually down to ~ 1500 m, with little increase at greater depths.

Within the SAZ iodate profiles were also similar to the previous summer for that region (Figure 3.18b). The upper 100 m, showing summer warming and formation of SASW, are clearly noticeable on iodate plots for stations 100 to 93, with iodate depleted in the surface. Below SASW, SAMW is also distinguished from iodate profiles with nearly constant concentration from 100 m down to ~ 700 m depth. Stations 91 to 88 were within the SAF and its meander and showed different iodate profiles. With the deepening of the surface mixed layer and the thinning of the SAMW, iodate concentrations increased steadily towards deeper waters.

In the PFZ, PFZSW showed iodate concentrations increasing gradually down to 200 m depth (Figure 3.18c). Below the surface layer, iodate concentrations increased steeply down to 500 m depth within AAIW, below which iodate concentrations became nearly constant within UCDW and LCDW.

Between the northern and the southern branch of the PF, in the IPFZ, iodate profiles changed slightly again (Figure 3.18d). Here, with AAIW becoming thinner below AASW, the contrast between iodate concentrations in the surface (< 200 m) and the high iodate concentrations within UCDW below was even more dramatic. At stations

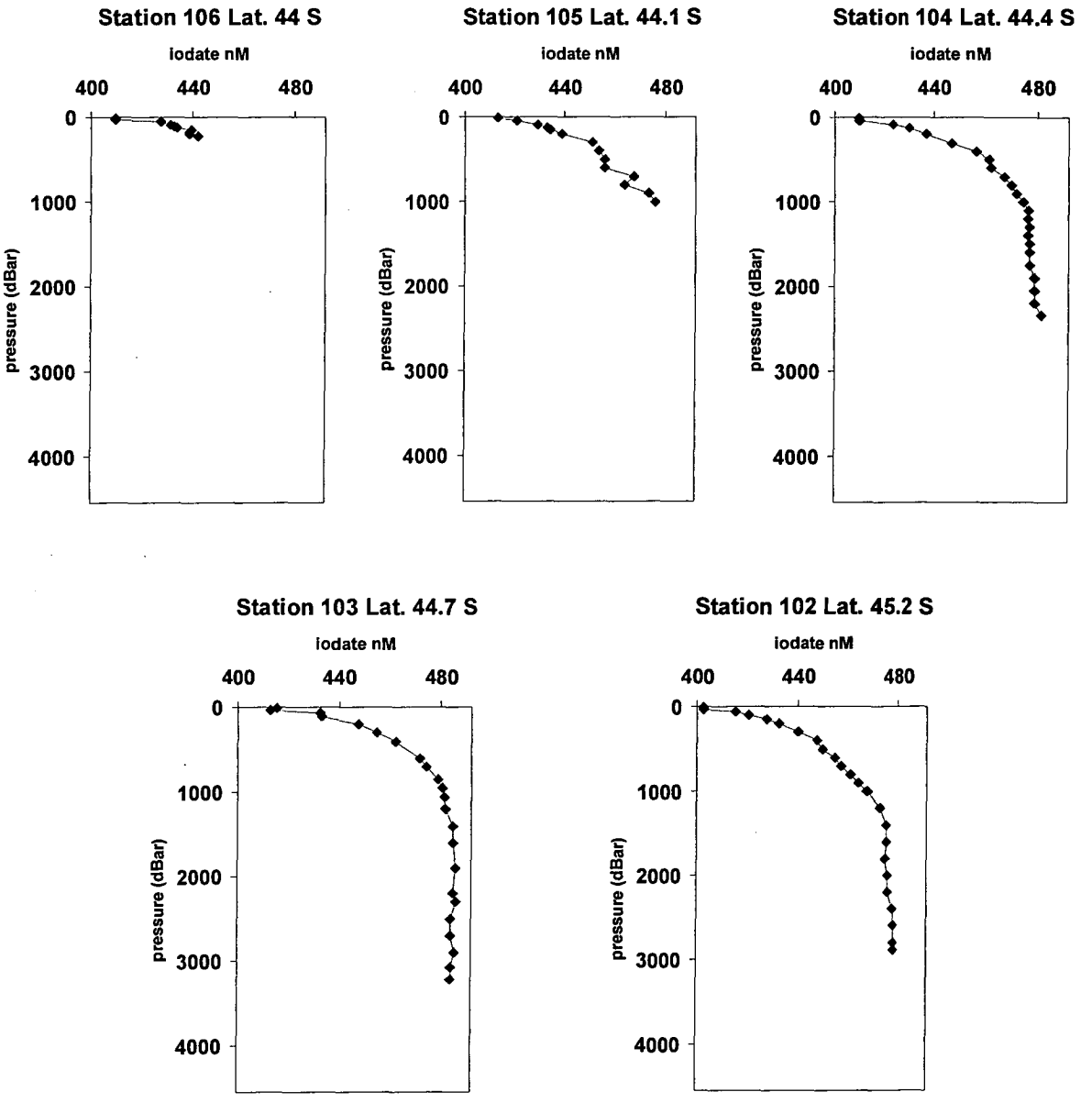

Figure 3.18a - Iodate distribution in the Subtropical Zone (STZ) stations along SR3 section during cruise au9404.

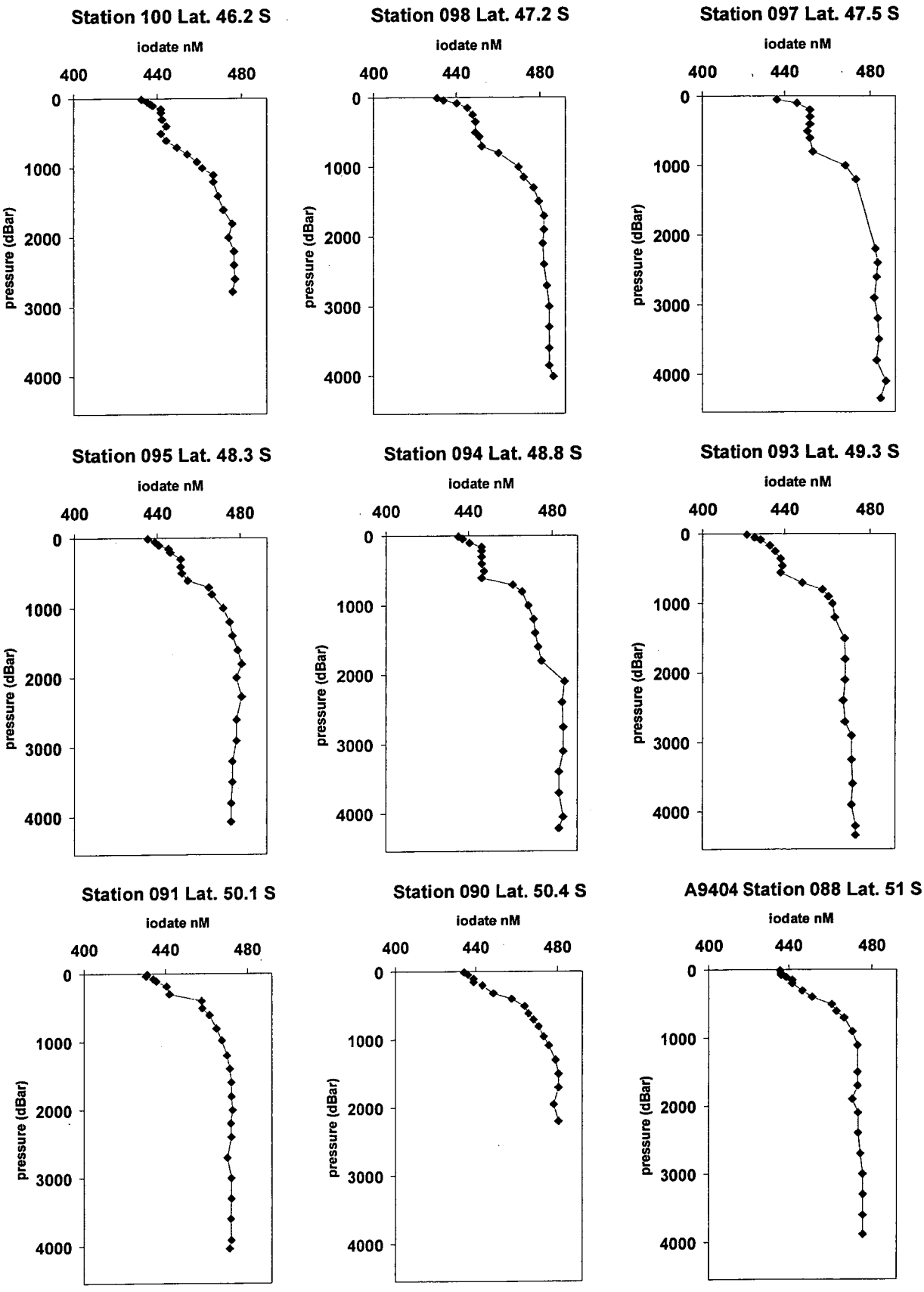

Figure 3.18b- Iodate distribution during cruise au9404 (January 1995) along the SR3 section in Subantarctic Zone (SAZ) stations.

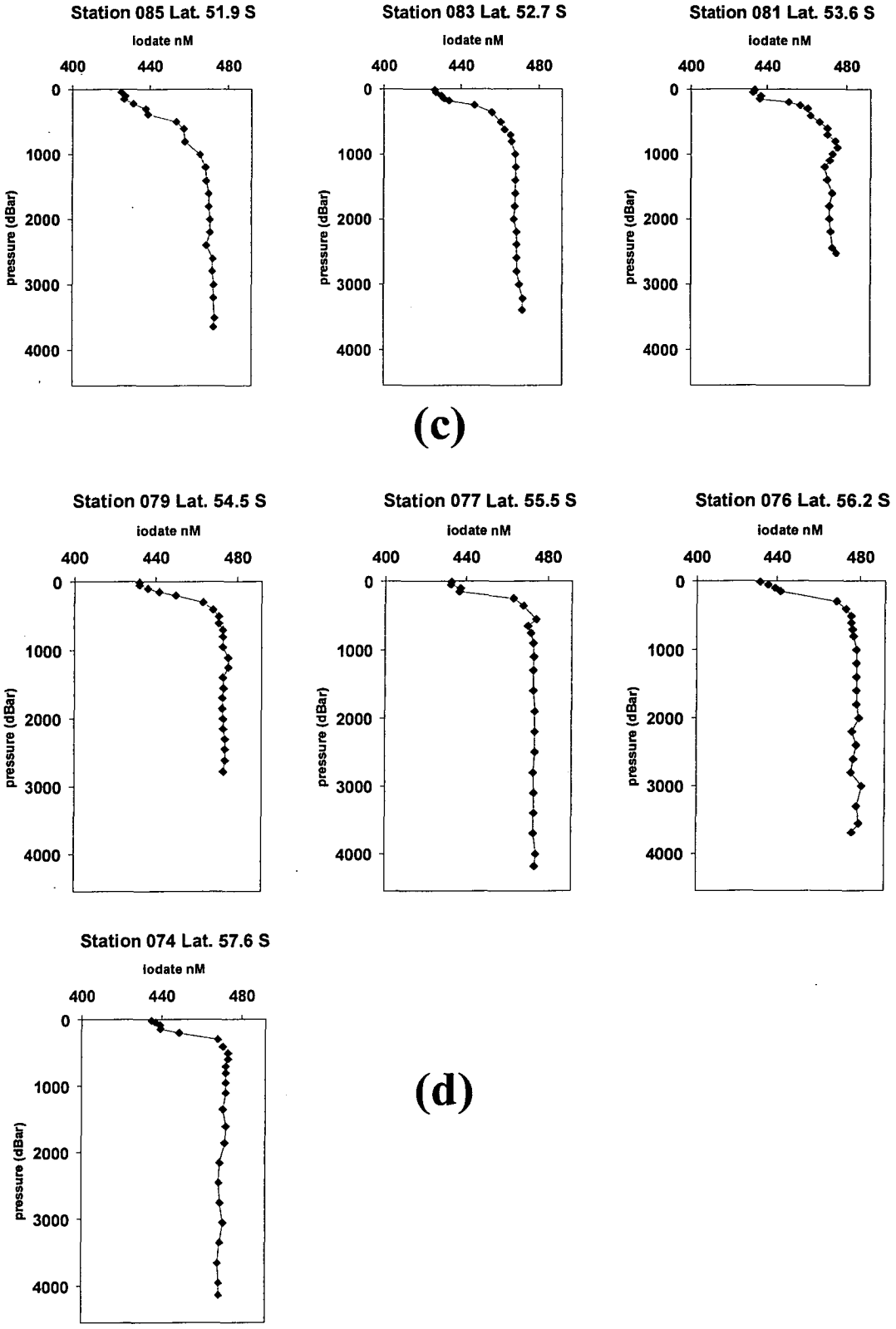

Figure 3.18c and d- Iodate distribution during cruise au9404 (January 1995) along the SR3 section in the Polar frontal Zone (PFZ) **(c)** and in the Inter Polar Frontal Zone (IPFZ) stations **(d)**.

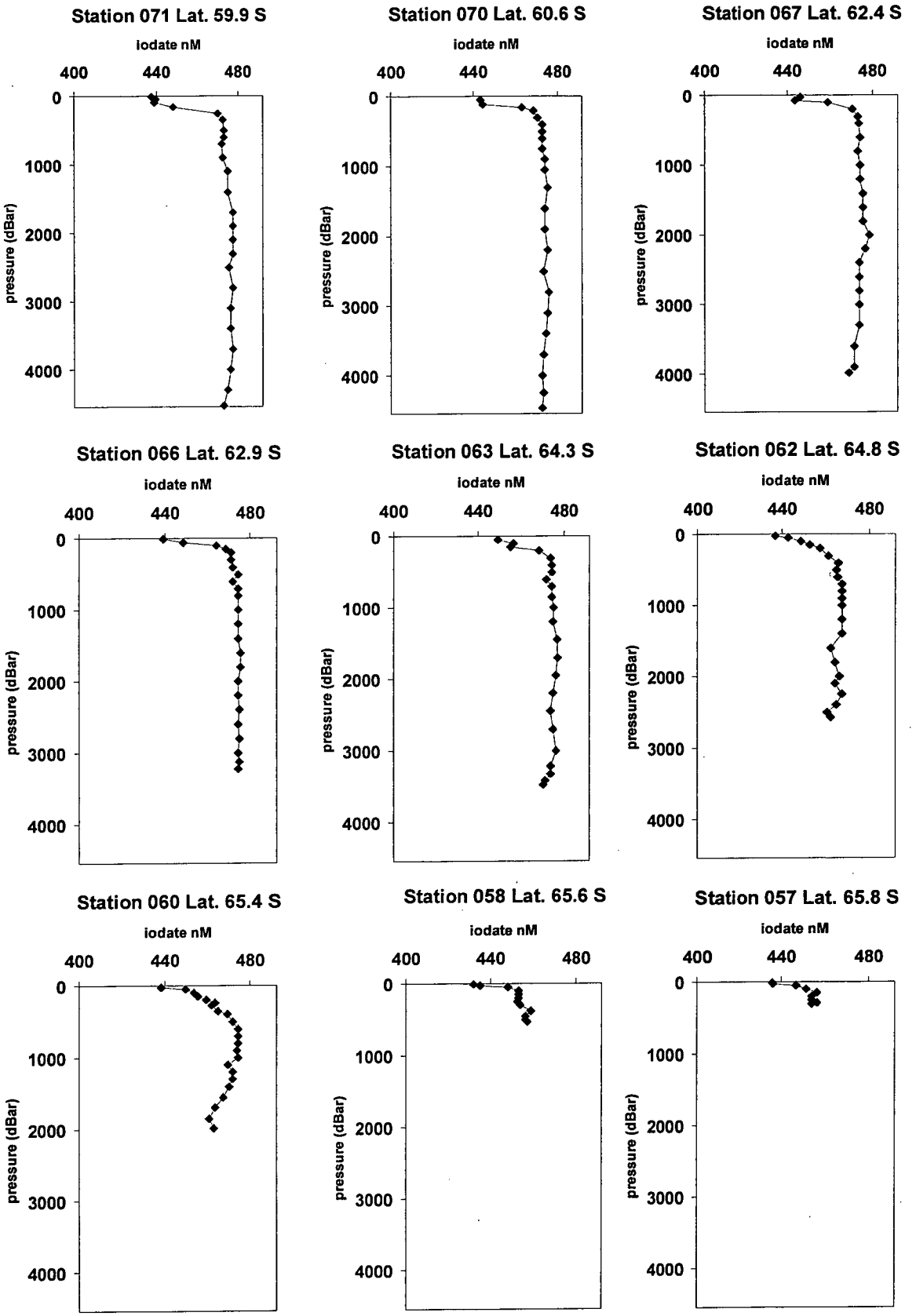

Figure 3.18e- Iodate distribution during cruise au9404 (January 1995) along SR3 section in the Antarctic Zone (AZ) stations.

81 and 77, an iodate minimum at 50 m depth coincided with silica minimum (both stations) and phosphate minimum (only station 77) at the same depth, suggesting possible biological uptake.

Past the PF-S, in the southern part of the AZ (Figure 3.18e), stations 71 to 66 showed similar iodate profiles, with depletion in the shallow surface mixed layer and near constant values below 100 to 200 m. At station 66, the shallowing of the surface layer seen in the iodate profile is characteristic of the proximity of the SACCF. At station 63, an oxygen minimum layer of UCDW was still identified, but not at the next station, 62. This feature marked the Southern Boundary of the ACC (SB) at around 64.5°S. From station 62 to station 57, iodate profiles were again different, with a less steep break between the surface layer and the deep-water concentrations. AABW was present close to the bottom from station 71 southwards, with lower iodate concentration than LCDW above.

A contoured section of iodate distribution along the SR3 section during au9404 can be seen on Figure 3.19. Although some analytical irregularities produced some unexplained vertical patches, which will be discussed later in section 3.3, some of the fronts and water masses can still be observed in the iodate contoured section. The SAF and its meander can be distinguished between 50° and 52°S. Between 54° and ~ 59°S, the IPFZ can be seen with its nearly horizontal contours.

At ~ 63°S the SACCF is clearly distinguished, with surface layer being compressed and deep water with higher iodate concentrations reaching 100 m depth. Lower iodate concentration water can also be noticed descending down the continental slope, corresponding to AABW.

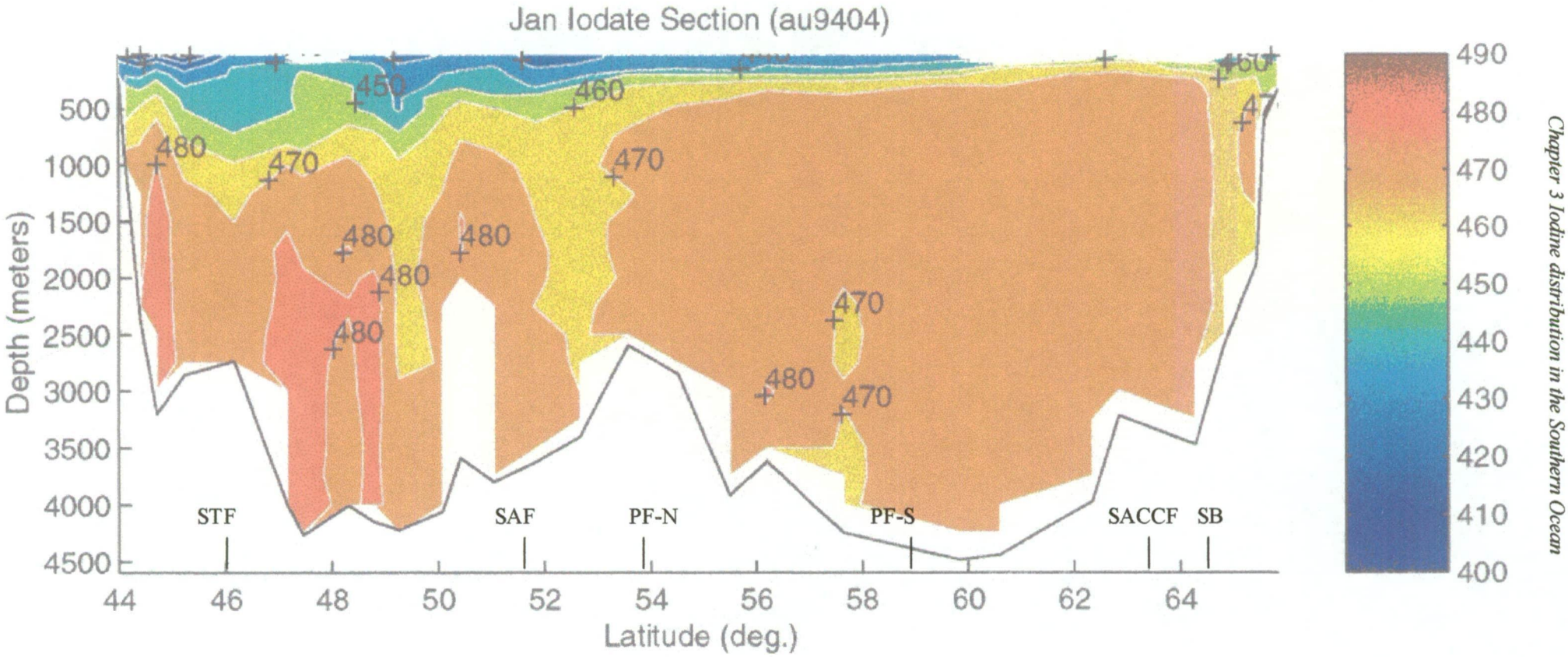

Figure 3.19- Iodate contoured section along SR3 transect during cruise au9404 (January 1995). The approximate positions of the oceanic fronts are indicated.

Iodide distribution along the SR3 section during au9404

Results from iodide measurements by IC along the SR3 transect can be seen in Figure 3.20. Iodide concentrations were generally higher in the surface, and decreased towards deep waters. Below 500 m depth, only very few samples were above the detection limit. At station 93, with the lowest detection limit of 5 nM and deeper mixing caused by the SAF, iodide concentration was measured at the detection limit at 3000 m. At station 91, iodide concentration of 8 nM was measured near the bottom of the profile.

In the STZ, at stations 106 to 103, iodide was generally higher in the surface than further south, with exception of station 100, which also had higher iodide concentration in the SAZ. At stations 81 and 77, a sub-surface iodide maximum was noticed at 100 and 50 m depth, respectively (Figure 3.20b). At station 77, the iodide maximum coincided with iodate, phosphate and silica minima at the same depth, suggesting iodide increase could be related with biological uptake of nutrients.

Station 33, at 62.2°S, for both S4 and SR3 transect, with 15 nM of iodide at 12 m depth, had the lowest iodide concentration for a surface sample recorded for all the sections analysed in this work, as well one of the lowest values ever reported in the Southern Ocean (compare with Campos *et al.*, 1999).

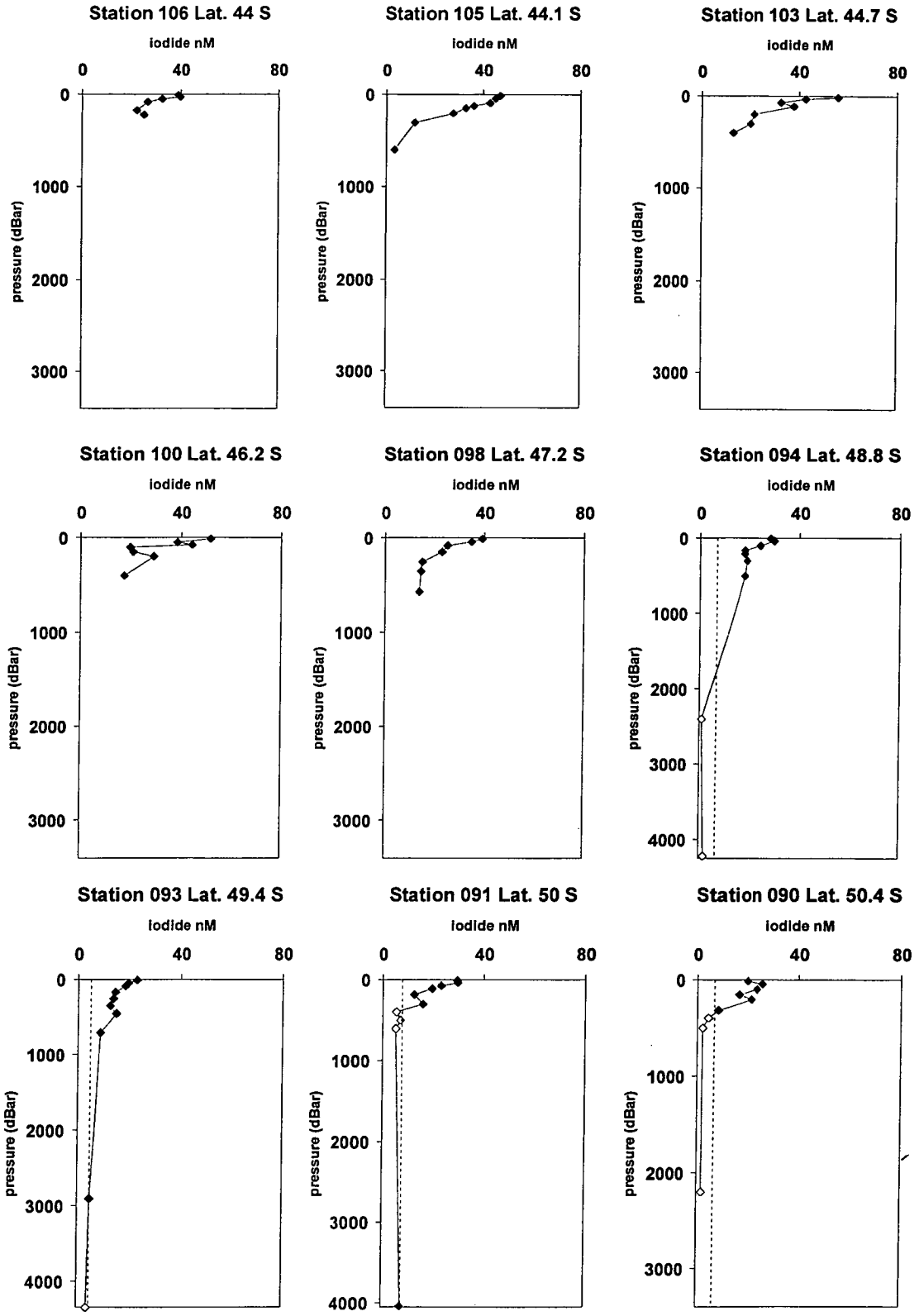

Figure 3.20a- Iodide depth profiles for cruise au9404 (January 1995) along SR3 section. The dotted line represents the detection limit; ◆ represents iodide values above the detection limit; and ◇ represents iodide values below the detection limit.

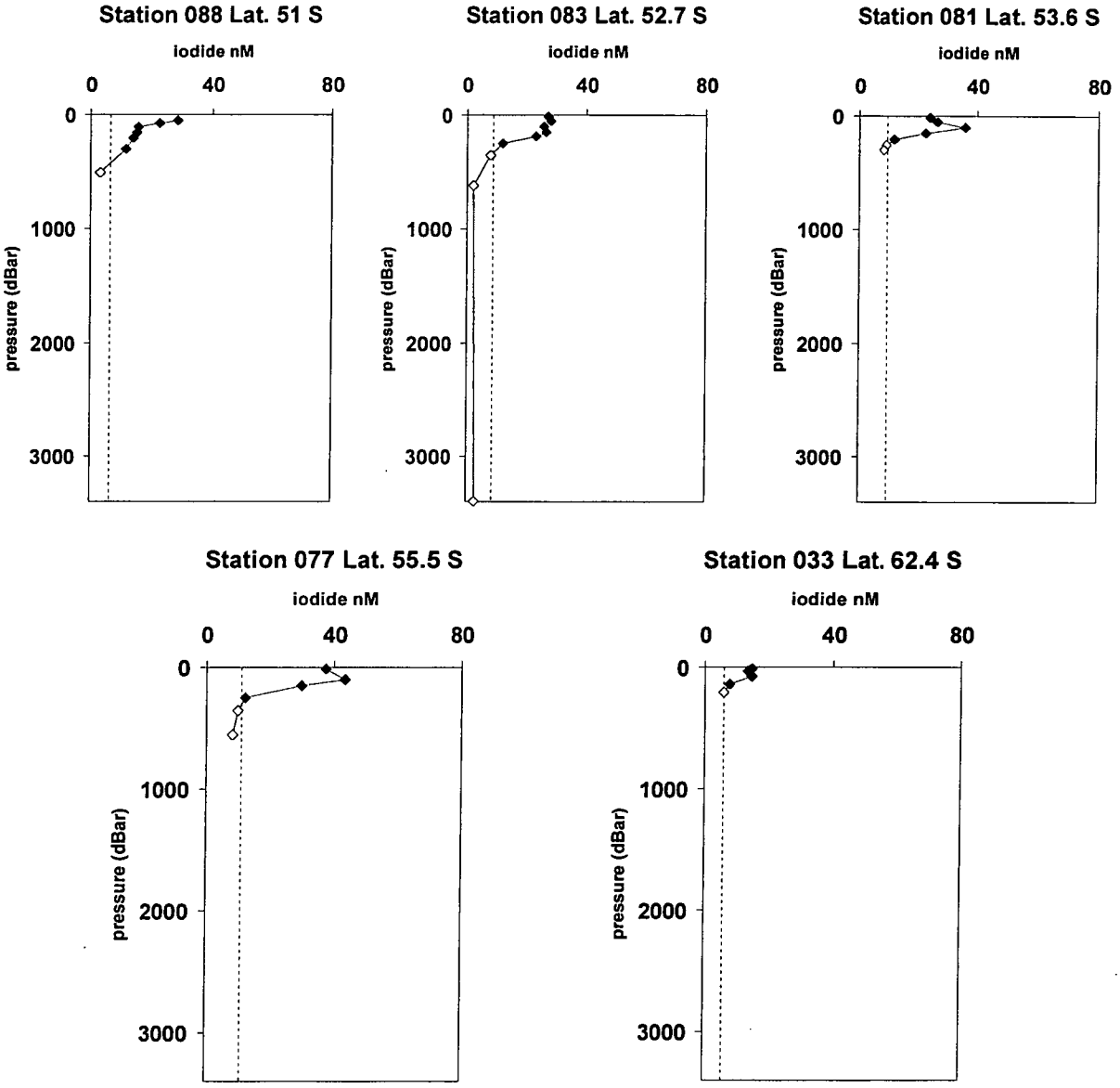

Figure 3.20b- Iodide depth profiles for cruise au9404 (January 1995) along SR3 section (Cont.). The dotted line represents the detection limit; ◆ represents iodide values above the detection limit; and ◇ represents iodide values below the detection limit.

Total inorganic iodine distribution along the SR3 section during au9404

Total iodine was measured directly by IC for 8 stations along the SR3 section during January 1995, cruise au9404. The results are shown in Figure 3.21.

In general the distribution of total iodine was similar to iodate, with lower concentrations in surface waters increasing towards the bottom, but again lower than iodate plus iodide. When compared with iodate distribution, the majority of profiles of total inorganic iodine showed higher values than iodate in the surface, tending to closer values to iodate in deep waters. At stations 100 and 93, however, total inorganic iodine in the surface was lower than iodate. At station 100, all results were lower than iodate, including the deep waters. At station 93, most results from 10 to 500 m depth were lower than iodate, but deep water values were higher than iodate.

Total iodine minus iodate values were generally lower than iodide values measured directly. This confirms the trend noticed in the au9501 cruise results, suggesting that total inorganic iodine results were an underestimation of the true values.

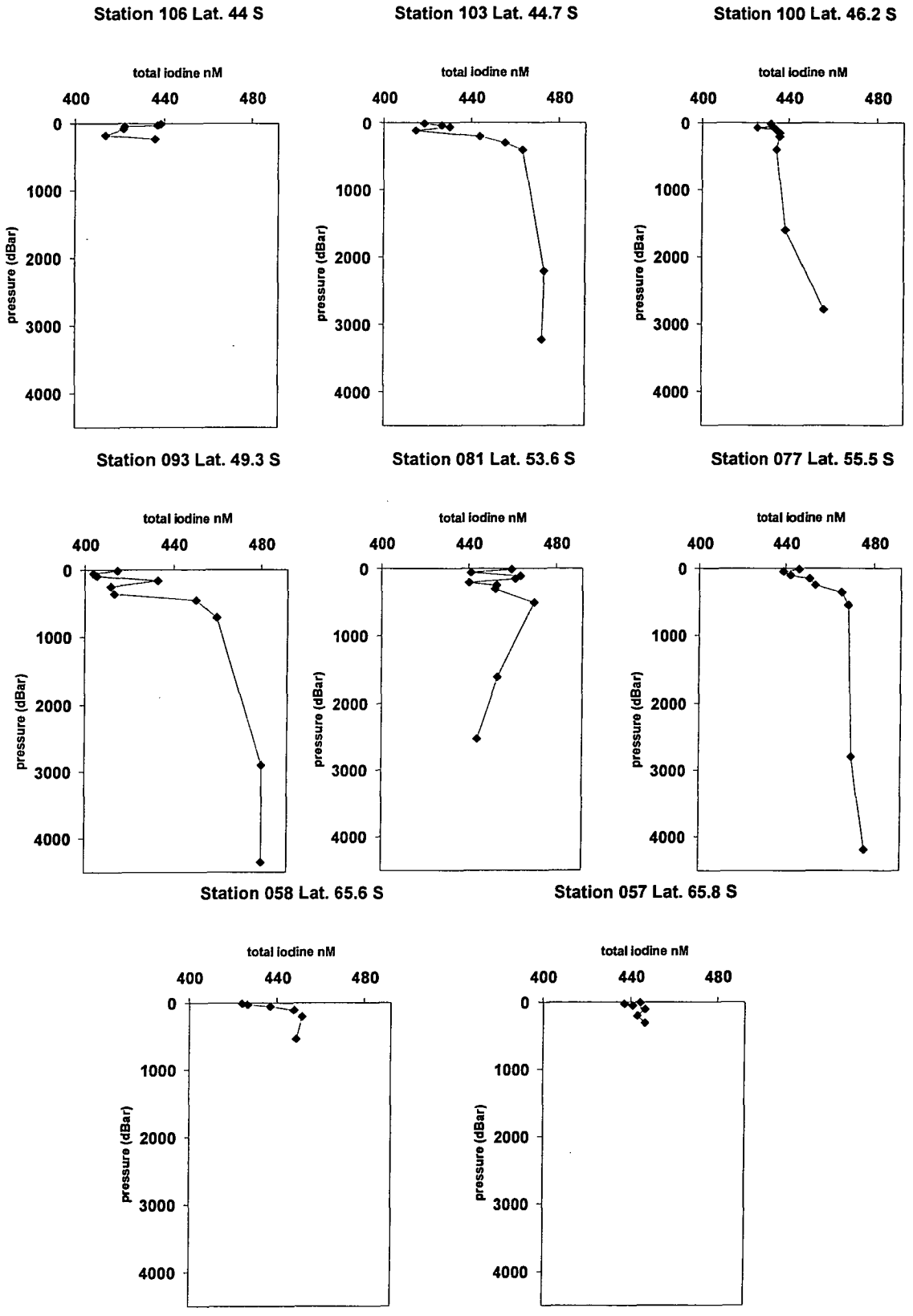

Figure 3.21- Total inorganic iodine depth profiles for cruise au9404 (January 1995) along SR3 section.

3.3 The analytical methods for determination of iodate, iodide and total iodine in seawater and their influence on the observed results

3.3.1 Iodate results as determined by flow injection analysis

Contoured iodate concentrations, as shown previously in Section 3.2, presented a sometimes patchy distribution along the SR3 section, which was not explained by any known oceanographic features. These vertical patches seem to be related to different days of analysis, as two stations were analysed per day, on average. These results were carefully examined and although there seems to be a variation from day to day, this variation failed to be quantified. Same samples analysed in four consecutive days showed coefficient of variation between ± 0.3 to 0.6 % (Table 3.1). However, looking at the contoured iodate distribution (Figures 3.6, 3.11 and 3.19) the variation appeared to be higher than the short term precision, calculated in one day, of 0.4% (see Section 2.3.1.5) or the long term precision measured in the four consecutive days (0.3-0.6%). McTaggart (1994) used Truesdale's (1978a) precision estimate of 0.4% for his analysis. Farrenkopf (2000) reported a precision of ± 5% for the determination of iodate by the same Truesdale's (1978a) method. This method is well known for its high precision, but reports suggest that the true reproducibility, or long term precision, is not as high. Farrenkopf (2000) reported frozen samples analysed in different days giving results varying from ± 10 to 40% for two determinations. Truesdale *et al.*(2000) reported the use of analytical control standards through the entire analysis of his data set (typically 10 replicates per day), probably during several days. The coefficient of variation for analysis of those standards was 4.3%, with each analysis having a probable accuracy of 5% for each analysis. For this work, I shall consider a maximum analytical error of ± 1% for each sample, from the worst coefficient of variation result of ± 0.6% for iodate sample analysis performed on different days.

McTaggart *et al.* (1994) and Truesdale and Smith (1979) also compared the colorimetric method with the polarographic method (Herring and Liss, 1974) for iodate determination in seawater. They found that the polarographic method results

Table 3.1- Standard deviation and coefficient of variation for five iodate samples from station 25 (cruise au9404) analysed by flow injection analysis. Samples were measured in four consecutive days of analysis during the cruise.

Sample number	Depth (m)	Average concentration in nM (n=4)	Standard deviation (nM)	Coefficient of variation (%)
23	50	439.6	1.2	0.27
20	250	465.2	2.9	0.63
15	800	472.9	1.9	0.40
7	2600	473.7	1.7	0.35
1	4441	472.9	1.9	0.40

for iodate were on average 8 nM higher than the ones measured by the automated colorimetric method. McTaggart *et al.* (1994) corrected all their measured iodate results by subtracting 8 nM. However, Farrenkopf (2000) found good agreement between fresh seawater samples analysed by both methods.

Here, all the analyses for iodate were carefully examined. Quality and freshness of reagents, standard preparation, calibration curve, peak measurement were all examined without finding an obvious reason for the patchy distribution of iodate. Low and variable temperatures in the ship laboratory might have had some influence, or variations within the photometric cell. As the variation appears to get worse from the first to the third cruise, an equipment problem is a possible explanation. In order to be able to eliminate such daily variations, a sample of well-known concentration can be measured daily, as suggested by Truesdale *et al.* (2000) and Truesdale and Bailey (2000). This way, the variation can be quantified as a part of the method's precision, once precision values calculated from sample repeats on the same day of analysis do not seem to reflect the daily variation between samples. Unfortunately this was not done as part of this work, and, instead, an analytical correction, described in the next sub-section, was then applied to the iodate dataset along most the SR3 transect.

3.3.2 Analytical correction of iodate data along the SR3 transect

One of the main aims of this work was to look at seasonal variations of iodate concentration in surface waters of the Southern Ocean. The seasonal variations in the Southern Ocean iodate concentration, especially south of Subtropical Front, appear to be very small, normally smaller than 10 nM (see Section 4.1), which would easily be masked by the abovementioned daily variations caused by some unknown analytical problem. In an effort to "correct" the iodate data for such variations, an "analytical correction" was applied to most of the raw iodate data along the SR3 transect.

In order to apply this analytical correction, one assumption was made: iodate concentration in the high salinity core of Lower Circumpolar Deep Water (LCDW) at the SR3 section would not vary during the sampling period (18 months), except due to salinity change. The high salinity core of LCDW originates from North Atlantic Deep Water (NADW), which is very low in CFCs (Rintoul and Bullister, 1999) and at least 60 years old when entering the Southern Ocean (England, 1995). If iodate concentration in the core of LCDW was constant during the 18-month period of sampling (from January 1994 until July 1995), then the variation observed in the iodate data in the core of the LCDW reflects the effect of the unknown analytical problem. Here an attempt was made to correct iodate concentrations on a station-by-station basis using a variable multiplicative factor, in order to obtain a constant salinity-normalised iodate concentration in LCDW. The multiplication factor was chosen instead of an addition/subtraction one, because I believe that changes in instrument sensitivity, not offset, have caused the observed problem, affecting the slope of the calibration curve. Thus the use of a multiplication factor was more appropriate here.

Iodate values for the core (highest salinity) of LCDW for all the three cruises (one value per station, total of 71 stations) were normalised to same salinity (34.741) and averaged, resulting in a Normalised Average Iodate value for the Core (NAIC) of LCDW of 474.5 ± 5 nM. The salinity value of 34.741 (± 0.009) used was obtained averaging the highest salinity value (core of LCDW) for the 71 stations where LCDW was detected. The NAIC value was then compared with the salinity Normalised Iodate value for the Core (NIC) of LCDW at each station. The ratio NAIC/NIC produced a correction factor F for each station. The analytical correction was then applied to the iodate data by multiplying the iodate concentrations for each station by the value of F calculated for that station (Table 3.2). For instance, as in Table 3.2, a NIC value for station 5 of au9501 was 478.0 nM, so F would be 474.5/478 or 0.992747. All iodate data points for that station were then multiplied by F to obtain the corrected iodate values for station 5, au9501. As a result, because F <1, all iodate corrected data for that station were smaller than the original values.

Table 3.2- Analytical correction applied to iodate values at station 5, cruise au9501. Iodate and salinity values in bold are those of LCDW. Iodate and salinity values in italics are the core values within LCDW.

Original iodate values (nM)	**Salinity**	**Iodate value (nM) normalised to average LCDW core salinity (34.741)**	**Correction Factor F for station 5 (au9501):** Average of LCDW core iodate values (n=71) normalised to salinity 34.741 divided by normalised iodate core value for this station (474.5/478.0)	**Corrected iodate values (nM):** Original iodate values multiplied by F
429.5	34.801			426.4
429.5	34.801			426.4
429.5	34.807			426.4
429.5	34.791			426.4
429.9	34.783			426.8
449.8	34.699			446.5
449.3	34.630			446.1
451.8	34.578			448.5
453.7	34.511			450.4
458.6	34.482			455.2
463.4	34.469			460.0
464.3	34.436			460.9
468.2	34.417			464.8
469.2	34.390			465.8
472.1	34.444			468.7
475.5	34.534			472.0
473.0	34.608			469.6
475.5	34.675			472.0
475.5	**34.709**			**472.0**
478.3	**34.723**			**474.9**
480.3	**34.730**			**476.8**
477.9	***34.733***	***478.0***	0.992747	***474.4***
477.9	**34.732**			**474.4**
477.9	**34.726**			**474.5**

The correction factor F was calculated for each of the 71 stations where LCDW was present, which did not cover the entire range of the SR3 transect, but most of it. Contoured sections for the corrected iodate data (Figure 3.22) seemed to eliminate the vertical patches seen before, keeping the main frontal structure of the section. This suggests that the analytical correction successfully eliminated the effects of the unknown analytical problem described in the previous sub-section. It is surmised that the vertical patchiness was likely to have been caused by analytical imprecision from run to run, and did not arise from any oceanographic feature.

3.3.3 Iodide results as determined by ion-chromatography with post-column reaction detection

As reported in sub-section 3.2.2.2, iodide distribution along the SR3 transect during summer cruise au9404 was within expected values for the region (Campos *et al.*, 1999). Surface concentrations decreased steadily towards colder Antarctic Waters and towards deep waters. The detection limit on this cruise was less than 10 nM.

During the next cruise, au9501, the detection limit increased from <10 nM to ~ 20 nM, resulting in a higher percentage of iodide samples falling below this criterion. Also the profiles of iodide were not so smooth, showing a higher variability than in the previous voyage and suggesting inferior analytical or instrumental precision. Iodide concentrations remained nearly unchanged or became slightly higher from summer to winter for stations at the same latitude, which is similar to the observations of Campos *et al.* (1996a) for two time-series stations in the North Pacific and North Atlantic, suggesting little seasonal variation.

One of the reasons for the deterioration of the detection limit was the chromatographic system. The chromatographic system used was not the best suited for running saline eluent and highly saline samples. The pump seals were easily worn out and as a result the pump noise increased dramatically, compromising the sensitivity with the resulting high baseline noise. The separation column was also

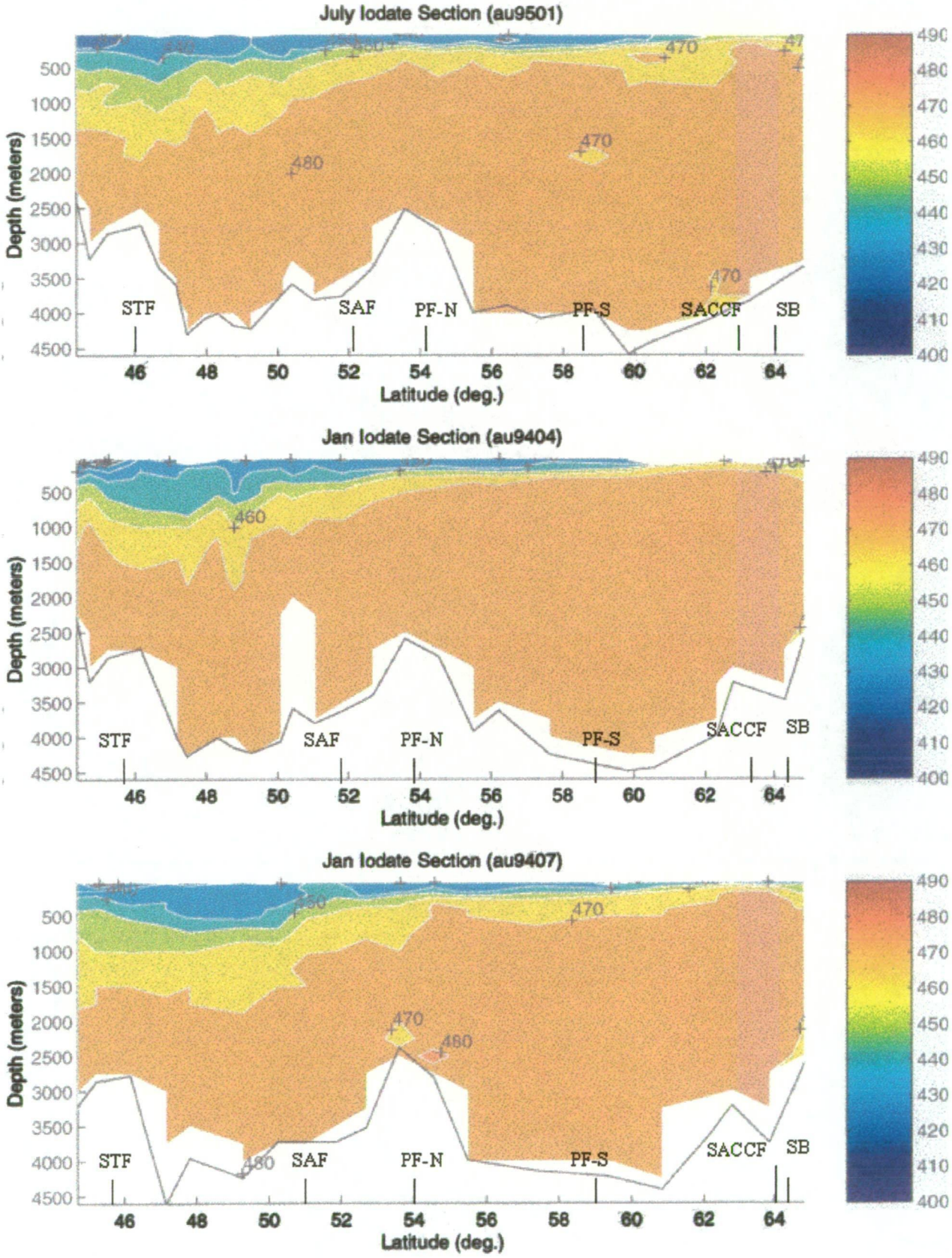

Figure 3.22 Iodate contoured sections along SR3 for cruises au9501, au9404 and au9407 after analytical correction was applied to iodate data.

well used when the last samples were analysed, and no regeneration procedure solved the problem (Dionex, 2000).

A solution for this problem would be the use of a pump that would support high salinity eluent running all day for several months. For the post-column reagent the use of syringe pumps has also been suggested (Brandão *et al.*, 1995) to help decrease the baseline noise in the detector. The separation column worked very well when new, and it is suggested here that its life span would be less than twelve months, with a new column being changed ideally every six months for continuous analysis of high salinity samples.

3.3.4 Total iodine as determined by iodate reduction with ascorbic acid followed by iodide measurement by ion-chromatography

The use of ascorbic acid to reduce iodate was used effectively by Campos (1997) and in following applications (Campos *et al.*, 1996a, 1999). Here, the efficiency of iodate reduction was tested with iodate standards in artificial seawater followed by iodide detection by ion-chromatography (see Chapter 2). Excess of ascorbic acid was used to guarantee that lack of reducing agent was not a problem. Peak areas for thus reduced iodate standards were typically smaller than peak areas for iodide standards of the same concentration, varying from 92.1 to 100 % of iodide peak area values, with average value of 97.1 ± 2.7%. The coefficient of variation for iodate and iodide standards determination varied from 0.5 to 3.4 % for two consecutive determinations, with average of 1.3%. Thus the iodate reduction may have been slightly less than 100%, based on the precision of the determinations. For seawater samples, however, the coefficient of variation was ± 2.7% (n=5).

In sub-sections 3.2.1.3 and 3.2.2.2, total inorganic iodine results were presented. It was noticed that on average total iodine values were frequently lower than the sum of iodate-plus-iodide values determined separately. The reduction step, as discussed before, could have been a problem. Another problem noticed was the steady decrease of peak area during the day for most days of analysis. As the decrease in the standard

peak area seemed to vary linearly with time (number of samples injected), a simple multiplicative correction was applied to the affected data. Even after this correction a slight decrease could still be seen from the first to the last sample analysed. The reason for this decrease in peak area is unknown, but it is believed to be related with the aging of the chromatographic column as discussed in the section above.

Although the recovery for total inorganic iodine samples was marginally less than 100%, I believe that the method described is reproducible and a good option for total inorganic iodine determination in seawater. The problems I encountered were mostly attributable to the analytical column and the chromatographic system, which could not be rectified at the time. As a result of the problems encountered, total iodine results were not considered any further in this work.

CHAPTER 4- IODATE AS A TRACER OF BIOLOGICAL AND PHYSICAL PROCESSES IN THE SOUTHERN OCEAN

This chapter has been divided in two sections. In Section 4.1, the iodate depletion in surface waters between winter and summer, along the WOCE SR3 transect, is used to estimate seasonal new production in the different oceanographic zones between Tasmania and Antarctica. In Section 4.2, the iodate lower concentration in Antarctic Bottom Water, in relation to Lower Circumpolar Deep Water above, is identified as a possible signature of this water mass at the southern end of the SR3 transect.

4.1 Using iodate seasonal depletion to estimate seasonal new production in the Southern Ocean

4.1.1 Introduction

The increase of CO_2 in the atmosphere and the possibility of climate change have led to an increase interest in studying the global carbon cycle. The Southern Ocean has been recognised as a strong sink of atmospheric CO_2 (Metzl *et al.*, 1999), emphasising the need to better understand the carbon cycle in this circumpolar ocean. The measurement of new production in the oceans is critical in evaluating the export of carbon from the euphotic zone to the deep waters. New production has been defined as being the primary production due to newly available nitrogen, such as nitrogen gas or nitrate, coming from sources outside the euphotic zone, such as deep water, the atmosphere or from land (Eppley, 1989; Platt *et al.*, 1992). Export production can be defined as the flux of organic matter from the euphotic zone, in this case being the equivalent to new production (Eppley, 1989). Measurements of new production can be made directly by using bottle incubation experiments with ^{15}N tracers or indirectly from ^{14}C primary production data. However, the use of direct primary productivity measurements has some disadvantages such as producing data that is patchy in space and time, providing a poor estimate of integrated annual production (Longhurst *et al.*, 1995; Priddle *et al.*, 1998b). Seasonal changes in nutrient concentration can also provide a measure of new production, with the advantage of providing an average production over time (Ishii *et al.*, 1998). The

ability to measure nutrients quickly and routinely would also be an advantage over primary production incubation methods. Several authors have used seasonal nutrient depletion in surface waters as an estimate of seasonal new production (Jennings *et al.*, 1984; Karl *et al.*, 1991; Minas and Minas, 1992; Bates *et al.*, 1998; Ishii *et al.*, 1998; Rubin *et al.*, 1998; Hoppema and Goeyens, 1999; Lourey and Trull, 2001). Here, for the first time, iodate depletion from winter (July) to summer (January) is used to estimate seasonal new production in the Southern Ocean. Such seasonal new production estimates are based on measuring nutrient depletion during a period of time and represent the "difference between primary production and respiration by all autotrophic and heterotrophic organisms present in a water column, and is defined as net community production (NCP)" (Ishii *et al.*, 1998), being approximately the same as new production (Minas and Minas, 1992). In a steady state condition, where the input of nitrogen into the euphotic zone is equivalent to its export from this zone, new production is equivalent to export production, with carbon being removed from the surface layer by the sinking of phytoplankton cells. However the use of nutrient depletion may underestimate export production by not taking into account nutrient resupply to surface waters (Wang *et al.*, 2001), and should be taken as conservative estimate of carbon export (Lourey and Trull, 2001).

Iodate has long been known as a micronutrient for marine phytoplankton, as seen previously in Chapter 1. Evidence of iodate uptake by marine phytoplankton suggests close coupling with iodide production (Moisan *et al.*, 1994; Udomkit, 1994). Iodide, however, remains in surface waters for a relatively long period of time. Chemical and photochemical oxidation of iodide to iodate are unlikely, probably due to the lack of available oxidants in the ocean and their slow or negligible reactivity with iodide (Luther *et al.*, 1995). Rather, iodide oxidation probably occurs by bacterial mediation or other biological mechanisms in the photic zone, but little is known about these mechanisms (Wong, 1991; Luther *et al.*, 1995).

The results found in this study, presented in Chapter 3, showed that possible changes in iodide concentration in the Southern Ocean were small and could not me measured by the analytical method used. This shows that, although iodide is formed during or as a consequence of biological cycling of iodine, it did not accumulate indefinitely in

the ocean surface, and it did not show a seasonal cycle, with unaltered concentrations from winter to summer. It is surmised that iodide was probably oxidising back to iodate at the same rate that it was formed. Iodate, on the contrary, showed a decrease from winter to summer in most stations for both summers. This is believed to be a result of the close coupling of iodate uptake and primary production in the Southern Ocean, thus allowing the use of iodate depletion to estimate seasonal new production.

In order to be able to use seasonal depletion of iodate to estimate seasonal new production in the Southern Ocean, some assumptions were made. First it was assumed that all iodate depletion measured was due to phytoplankton uptake. Second, it was assumed that the iodate input from iodide oxidation was of the same size of iodate reduction for other processes other than phytoplankton uptake, meaning that there was no net input of iodate from iodide oxidation. And last, it was assumed that the iodate pool in the surface was renewed due to deep winter mixing and that the cruise au9501 (July 1995) was also representative of the winters of 1993 and 1994. Thus:

$$\Delta I = (IO_3^-{}_w + I^-_w) - (IO_3^-{}_s + I^-_s) = a\,P_s \quad \text{(I)}, \text{ where } I^-_w = I^-_s, \text{ so}$$

$$IO_3^-{}_w - IO_3^-{}_s = a\,P_s \quad \text{(II)}$$

where *a* is a constant and represents the I/C uptake ratio of phytoplankton, and P_s is the seasonal new primary production, and *w* and *s* indices represent iodate and iodide concentrations in winter and summer. As the observed iodate depletion in the Southern Ocean was not accompanied by any measurable increase in iodide, the iodate removed is considered to have been all taken up by phytoplankton. This way the ratio IO_3^-/C uptake ratio is assumed to represent the I/C ratio in organic material.

4.1.2 Calculating iodate depletion

Iodate depletion was calculated on a station-by-station basis along the SR3 transect. Stations with same latitude (± 0.4°) were selected from summer and winter cruises. All iodate data used has been corrected according to analytical correction described in sub-section 3.3. Iodate data for both stations were then normalised to salinity of 34.363, which is the average salinity of near surface samples along SR3 line during the winter cruise 9501. Salinity-normalisation of iodate concentration is necessary to minimise the effects of dilution due to mixing of different water masses along the transect. The integrated area between the winter data and the summer data at the surface was measured down to the depth where the depletion was zero. The zero-depletion depth was calculated as the point of intersection of two straight-line segments representing the iodate concentration from summer and winter profiles (Figure 4.1). At this point:

$IO_3^-{}_w - IO_3^-{}_s = 0$ and $IO_3^-{}_w = IO_3^-{}_s$ (III)

The difference between iodate concentration in winter and iodate concentration in summer is equivalent to net value of seasonal iodate depletion. Seasonal iodate depletion was calculated integrating the area between depth profile line for summer data and depth profile line for winter data from the surface (0 m) to the zero-depletion depth. The result was given in mmol IO_3^- m^{-2} and represents iodate seasonal depletion at that latitude. Figure 4.1 shows an example of the integrated area that is equivalent to iodate depletion. Calculated iodate depletion between 9501 (July 1995) and 9407 (January 1994), and 9501 and 9404 (January 1995) are shown on Tables 4.1 and 4.2, and Figures 4.2 and 4.3, respectively. Negative depletion values were considered to be zero, with most of these in fact being close to zero.

Calculated depth-integrated iodate depletion values for summer 1994 (9407) varied from 0.081 to 2.13 mmol IO_3^- m^{-2} (Table 4.1 and Figure 4.2). The errors associated with these estimates were not small and varied from 22 to 360% of the calculated iodate depletion values. These errors (E) were calculated using the added uncertainty

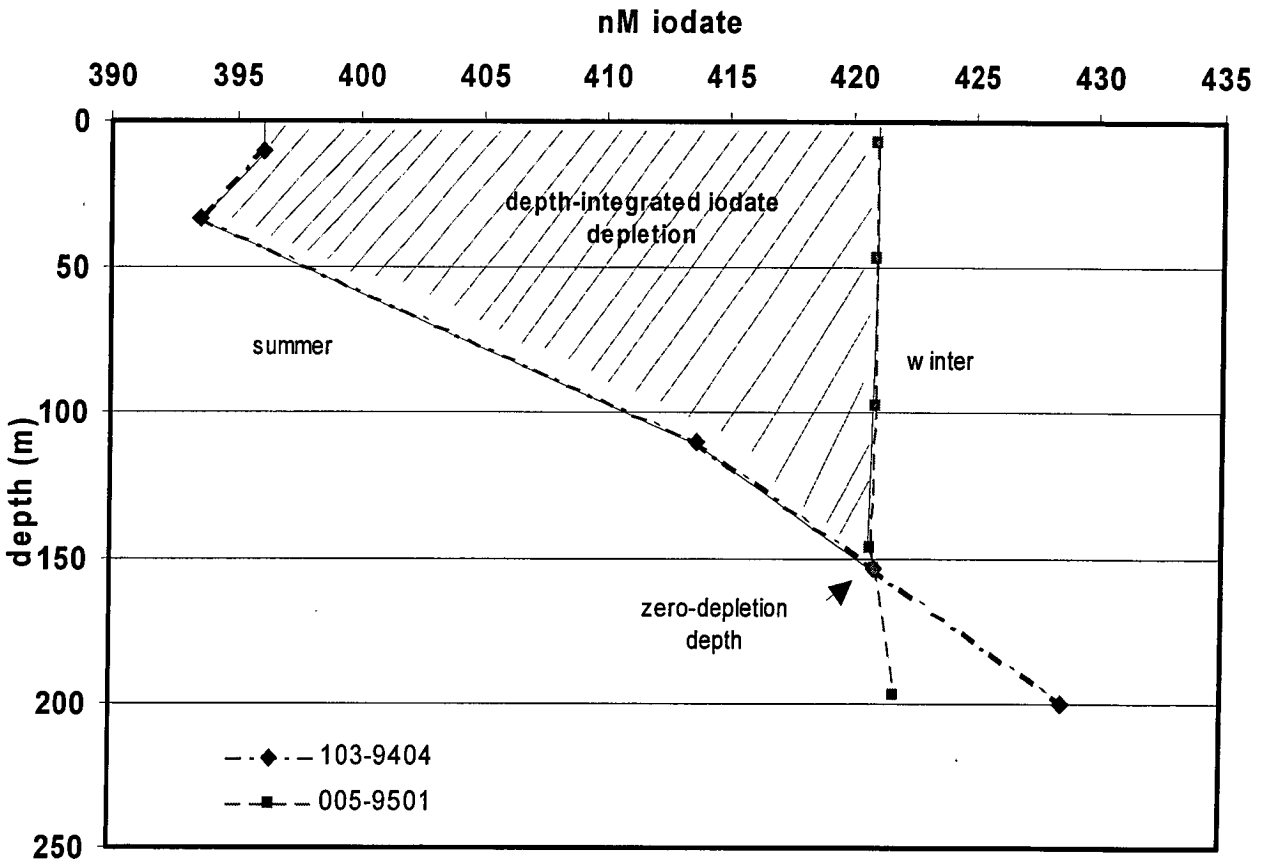

Figure 4.1- Example of integrated area, which is equivalent to depth-integrated iodate depletion between winter (005-9501) and summer (103-9404) stations located at the same latitude along the SR3 transect in the Subtropical Zone (STZ).

Table 4.1 Depth-integrated iodate depletion from winter (July), cruise au9501, to summer 1994 (January), cruise au9407, along the WOCE SR3 line, from Tasmania to Antarctica.

Zone	Station no. (9501)	Zone	Station no. (9407)	Zero depletion depth (m)	Iodate depletion ($mmol.m^{-2}$)	Latitude (°S)
STZ	005	STZ	006	132	0.607 ± 0.466	44.7
SAZ	006		008	136	2.126 ± 0.471	45.2
	008	SAZ	010	341	2.033 ± 1.244	46.2
	010		013	18	0	47.2
	012		015	250	1.087 ± 0.572	48.0
	015		020	204	1.580 ± 0.753	49.3
	018		023	257	0.703 ± 0.645	50.2
	021	PFZ	025	-	0	51.0
	024		028	-	0	51.9
PFZ	026		031	80	0.081 ± 0.243	52.6
	028		033	103	0.758 ± 0.377	53.6
AZ	030	AZ	036	-	0	54.5
	032		038	155	0.457 ± 0.580	55.5
	036		044	33	0.034 ± 0.123	57.3
	041		048	-	0	59.9
	042		053	-	0	60.6
	046		058	41	0.157 ± 0.155	62.3
	048		060	202	1.008 ± 0.582	63.3
	051		063	300	1.223 ± 1.181	64.8

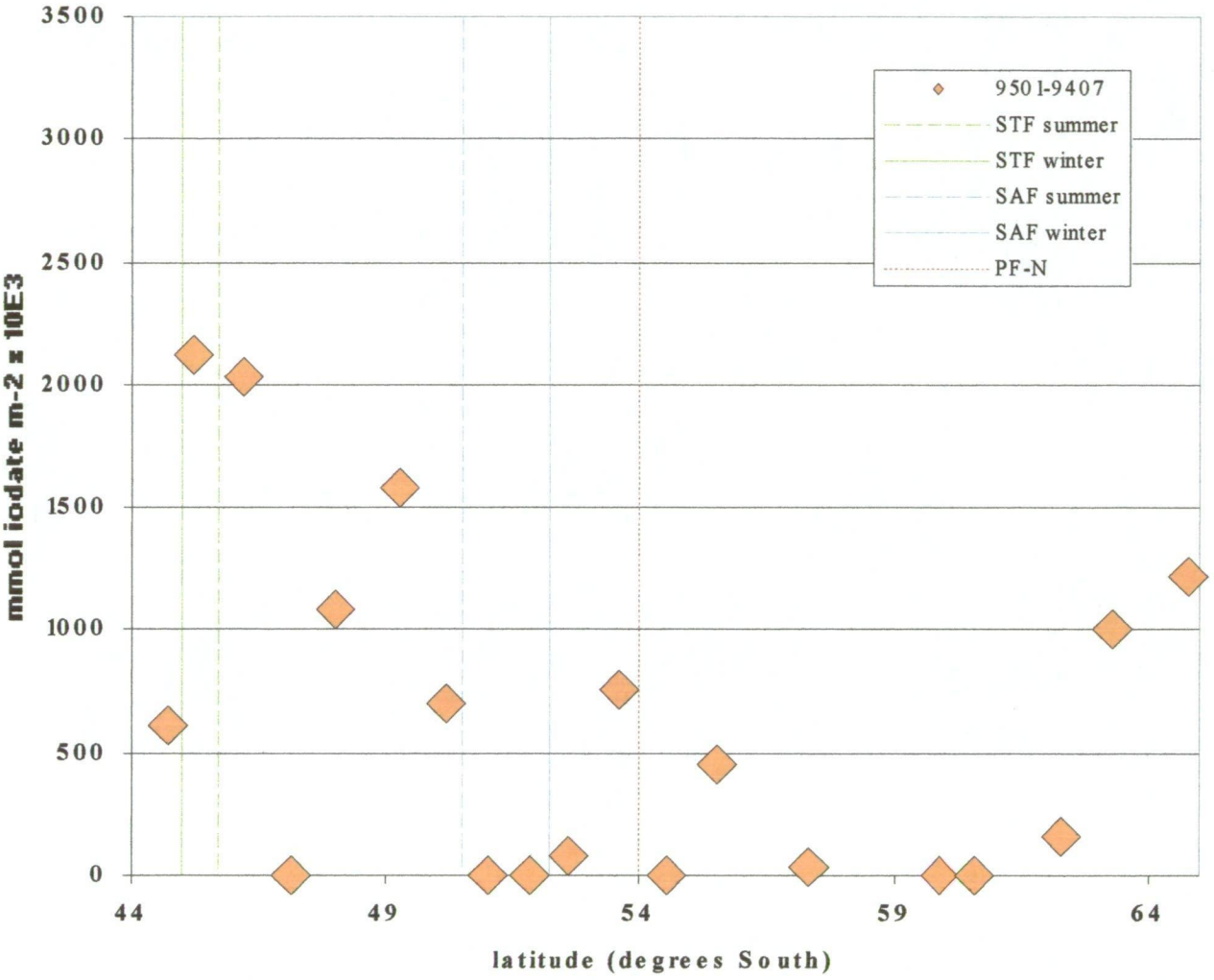

Figure 4.2- Depth-integrated iodate depletion values calculated along the WOCE SR3 transect, from Tasmania to Antarctica, between winter 1995 and summer 1994 (au9407). Vertical lines mark position of Subtropical Front (STF), Subantarctic Front (SAF) and Polar Front (PF) in winter (au9501) and summer (au9407).

of the average summer iodate value (SE) and the average winter iodate value (WE), such as:

$E = \sqrt{(SE)^2 + (WE)^2}$, multiplied by the depth (zero depletion depth).

These errors occurred because the difference between winter and summer iodate concentrations varied from 2 to 26 nM, with some values close to precision of method of ± 0.6%, which would be equivalent to ± 2.5 nM for an iodate concentration of 420 nM. However small these differences were, looking at the winter and summer depth profiles of iodate (as in Figure 4.1), it is apparent that, at a certain depth, the iodate concentration in summer increases back to the normally invariant winter values in the surface, showing that a depletion of iodate took place in surface layer between winter and summer. In Table 4.1, highest iodate depletion values (> 2 mmol.m^{-2}) were close to the Subtropical Front (STF), between 45.2° and 46.2°S. Lowest values were in the Polar Frontal Zone (PFZ) with two stations where no depletion was measured, and again at around 60°S at the Antarctic Zone (AZ), where two stations showed no significant depletion. In the Subantarctic Zone (SAZ), iodate depletion was observed to more than 200 m depth at three stations, with relatively high depletion (> 1 mmol m^{-2}) at two of them. South of 63°S, iodate depletion increased dramatically to more than 1 mmol m^{-2} for two stations, probably because of the proximity of the Southern Antarctic Circumpolar Current Front (SACCF) and the higher phytoplankton biomass associated with the area (Popp *et al.*, 1999).

Calculated iodate depletion values for summer 1995 (9404) showed some similarities to the year before (Table 4.2 and Figure 4.3). Measured depletion varied from 0.083 to 3.425 mmol IO_3^- m^{-2}. The errors associated with these estimates varied from 18 to 296% of the iodate depletion value. Again larger uncertainties were associated with the smaller depletion values, mostly in the southern part of SAZ, the PFZ and the AZ north of 63°S. As the summer before, highest values (> 1.7 mmol.m^{-2}) were in the STZ, with the highest values just before the STF. At the SAZ, iodate depletion below 200-m depth was again noticed for two stations. Still in the SAZ, three stations

Table 4.2- Depth-integrated iodate depletion from winter (July), cruise au9501, to summer 1995(January), cruise au9404, along the WOCE SR3 line, from Tasmania to Antarctica.

Zone	Station no. (9501)	Zone	Station no. (9404)	Zero depletion depth (m)	Iodate depletion ($mmol.m^{-2}$)	Latitude (degrees South)
STZ	004	STZ	104	123	1.740 ± 0.427	44.4
	005		103	154	2.310 ± 0.540	44.7
SAZ	006		102	200	3.425 ± 0.622	45.2
	008	SAZ	100	128	0.357 ± 0.470	46.2
	010		098	93	0.483 ± 0.337	47.2
	011		097	128	0.959 ± 0.467	47.5
	013		095	52	0.083 ± 0.190	48.3
	014		094	140	0.616 ± 0.511	48.8
	015		093	251	1.431 ± 0.773	49.3
	018		091	-	0	50.1
	019		090	202	0.705 ± 0.747	50.4
	021		088	-	0	51.0
	024	PFZ	085	151	0.476 ± 0.561	51.9
PFZ	026		083	-	0	52.7
	028		081	71	0.090 ± 0.267	53.6
AZ	030	AZ	079	-	0	54.5
	032		077	85	0.191 ± 0.320	55.5
	034		076	50	0.105 ± 0.186	56.2
	036		074	-	0	57.6
	041		071	-	0	59.9
	042		070	-	0	60.6
	046		067	90	0.290 ± 0.337	62.3
	048		066	101	0.773 ± 0.390	63.3
	051		062	202	0.868 ± 0.722	64.8

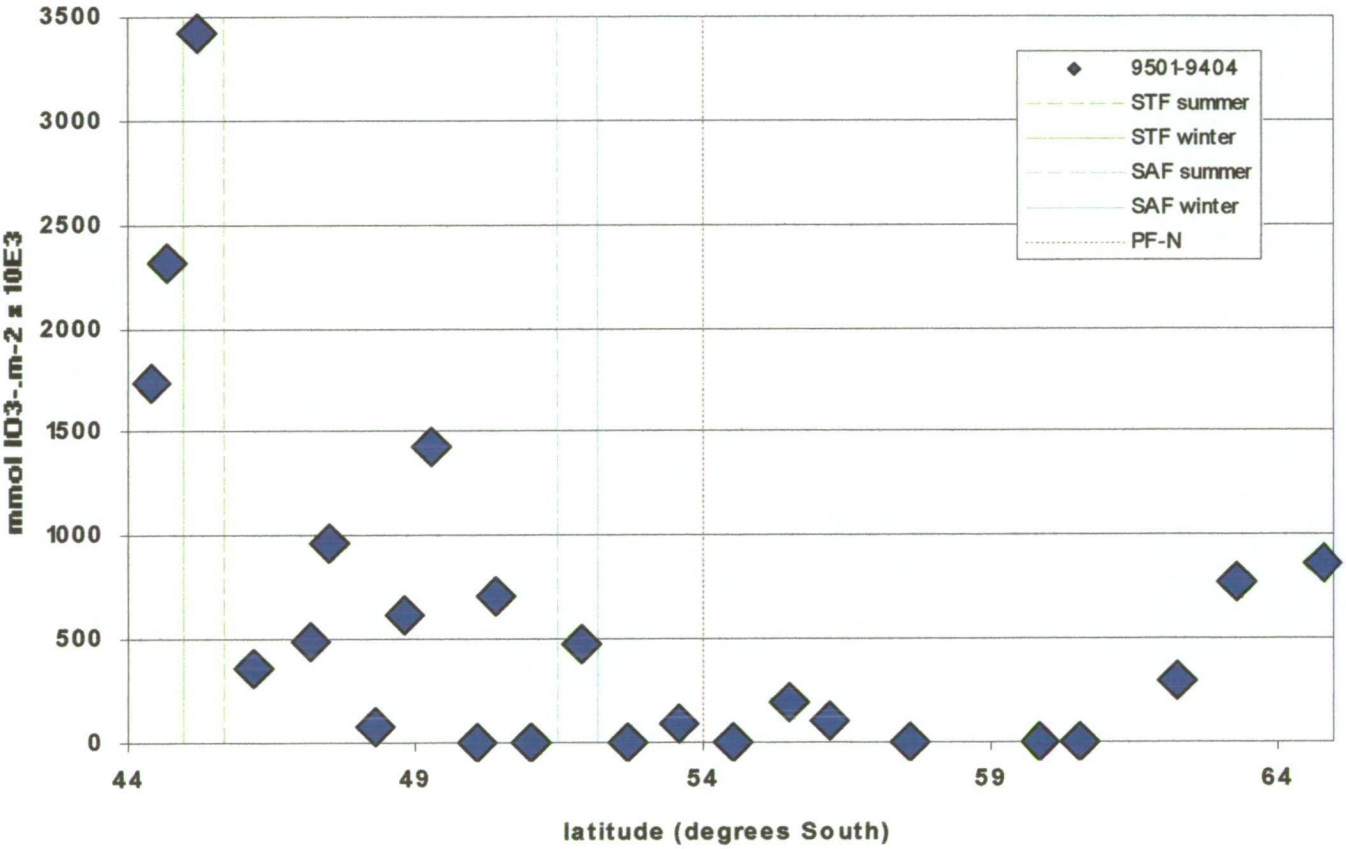

Figure 4.3- Depth-integrated iodate depletion values calculated along the WOCE SR3 transect, from Tasmania to Antarctica, between winter and summer 1995 (au9404). Vertical lines mark position of Subtropical Front (STF), Subantarctic Front (SAF) and Polar Front (PF) in winter (au9501) and summer (au9404).

showed depletion larger than 0.7 mmol IO_3^- m^{-2}. South of the Subantarctic Front (SAF) iodate depletion values decreased until 62.3°S, where they started to increase again, reaching 0.8 mmol IO_3^- m^{-2} south of 63°S, at the proximity of the SACCF.

4.1.3 Estimating I/C ratio

Wong and Brewer (1974) were the first to report iodine's strong correlation with nutrients in South Atlantic waters. They found an I/N ratio of 2.8×10^{-3}, which would give an I/C ratio of 4.2×10^{-4} from a Redfield C/N ratio of 106/16 (Redfield *et al.*, 1963). Their values were calculated based on dissolved iodate concentration in the Pacific.

Elderfield and Truesdale (1980) measured I/C ratio in planktonic material finding a value of $1.4 (\pm 0.8) \times 10^{-4}$, which agreed with their I/C value for the hydrographic data of 1.0×10^{-4}, calculated directly from the slope of the linear correlation between total iodine and phosphate normalised data.

Brandão *et al.* (1994) found an I/C of 1×10^{-3}, for a phytoplankton culture, but as pointed out by Farrenkopf (2000), their value was calculated using mass ratio and not a molar ratio as the ones estimated before. Their value translated into a molar ratio also agreed with the value of 10^{-4} reported by Elderfield and Truesdale (1980).

Farrenkopf (2000) measured the I/C ratio in fresh particulate organic material at station Aloha near Hawaii, using direct filtration and sediment traps. For large volume filtered samples I/C varied from 2×10^{-6} to 1.8×10^{-3}. A seasonal variation of this value was also noticed with highest values in May (spring) and lower values in October (autumn). For sediment trap samples I/C values varied from 6.6×10^{-7} to 9.6×10^{-4}.

Recently, Wong (2001) found that iodate/nitrate ratio should fall between values of 2×10^{-2} to 10^{-3}. Considering a Redfield C/N ratio of 6.63, this would represent an IO_3^-/C ratio between 3.0×10^{-3} to 1.5×10^{-4}.

In the Southern Ocean several authors have estimated C/N ratios and/or N/P ratios from dissolved CO_2 and nutrient depletion (Copin-Montegut and Copin-Montegut, 1978; Minas and Minas, 1992; Lourey and Trull, 2001), but no I/C calculation has been made for these waters. Most published I/C ratios have been calculated using a large amount of data from tropical and subtropical oceans. Using these ratios is unlikely to be applicable here, since a clear drop in I/N or I/P ratios south of the Subtropical Front has been observed before (Butler and Plaschke, 1988; Butler *et al.*, 1992; Campos *et al.*, 1999).

In this work I/C ratios were calculated from I/N ratios obtained directly from the slope of the best-fit line of salinity-normalised iodate data plotted against salinity-normalised nitrate + nitrite (hereafter, nitrate) data in surface waters for the two summers, using a Redfield C/N ratio of 6.63 (Table 4.3). Iodate and nitrate were normalised to salinity 34.363, which is the average salinity for surface waters along the SR3 transect during winter. Different I/N ratios were calculated for different oceanographic zones along the SR3 transect, such as subtropical zone (STZ), subantarctic zone (SAZ), polar frontal zone (PFZ) and Antarctic zone (AZ), and for different summers, 1994 and 1995. The variation of I/N ratios through different zones along the SR3 transect can be seen in Figures 4.4 and 4.5, and are listed in Table 4.3 with respective I/C values. Only surface water samples (<250 m) were used, because iodate and nutrients nitrate and phosphate are believed to recycle differently below the mixed layer (Truesdale, 1994), generating a poor correlation of deep-water data, the once-called "deep-water anomaly" (Elderfield and Truesdale, 1980).

The highest I/C value found was 4.22 (± 0.29) x 10^{-4} for the STZ on cruise 9404. Uncertainties were calculated by dividing the respective uncertainties of the I/N correlation by 6.63. At the same cruise I/C dropped to 1.80 (± 0.25) x 10^{-4} in the SAZ, suggesting that, maybe due to the higher availability of nitrate, iodate uptake by phytoplankton was lower. Still with the 9404 cruise, I/C ratio for PFZ and AZ were very similar (3.62 (± 0.46) x 10^{-4} and 3.32 (± 0.26) x 10^{-4}, respectively), suggesting similar characteristics in iodate and nitrate uptake for surface waters in those two regions.

Table 4.3- Iodate and nitrate correlation for the two summer cruises along the SR3 transect for surface samples (<250 m). I/C molar ratio was calculated from Redfield C/N molar ratio of 6.63.

cruise	zone	equation	R^2	I/C
9404	STZ	$I = 2.8 (\pm 0.2) \times 10^{-3} N + 0.3899$	0.9643	$4.22 (\pm 0.29) \times 10^{-4}$
	SAZ	$I = 1.2 (\pm 0.2) \times 10^{-3} N + 0.4165$	0.5414	$1.80 (\pm 0.25) \times 10^{-4}$
	PFZ	$I = 2.4 (\pm 0.3) \times 10^{-3} N + 0.383$	0.8098	$3.62 (\pm 0.46) \times 10^{-4}$
	AZ	$I = 2.2 (\pm 0.2) \times 10^{-3} N + 0.3866$	0.8129	$3.32 (\pm 0.26) \times 10^{-4}$
9407	STZ	$I = 2.5 (\pm 0.4) \times 10^{-3} N + 0.3992$	0.8193	$3.77 (\pm 0.59) \times 10^{-4}$
	SAZ	$I = 1.6 (\pm 0.2) \times 10^{-3} N + 0.4094$	0.7344	$2.41 (\pm 0.29) \times 10^{-4}$
	PFZ	$I = 0.6 (\pm 0.3) \times 10^{-3} N + 0.4299$	0.173	$9.05 (\pm 4.81) \times 10^{-5}$
	AZ	$I = 2.6 (\pm 0.2) \times 10^{-3} N + 0.3754$	0.8614	$3.92 (\pm 0.26) \times 10^{-4}$

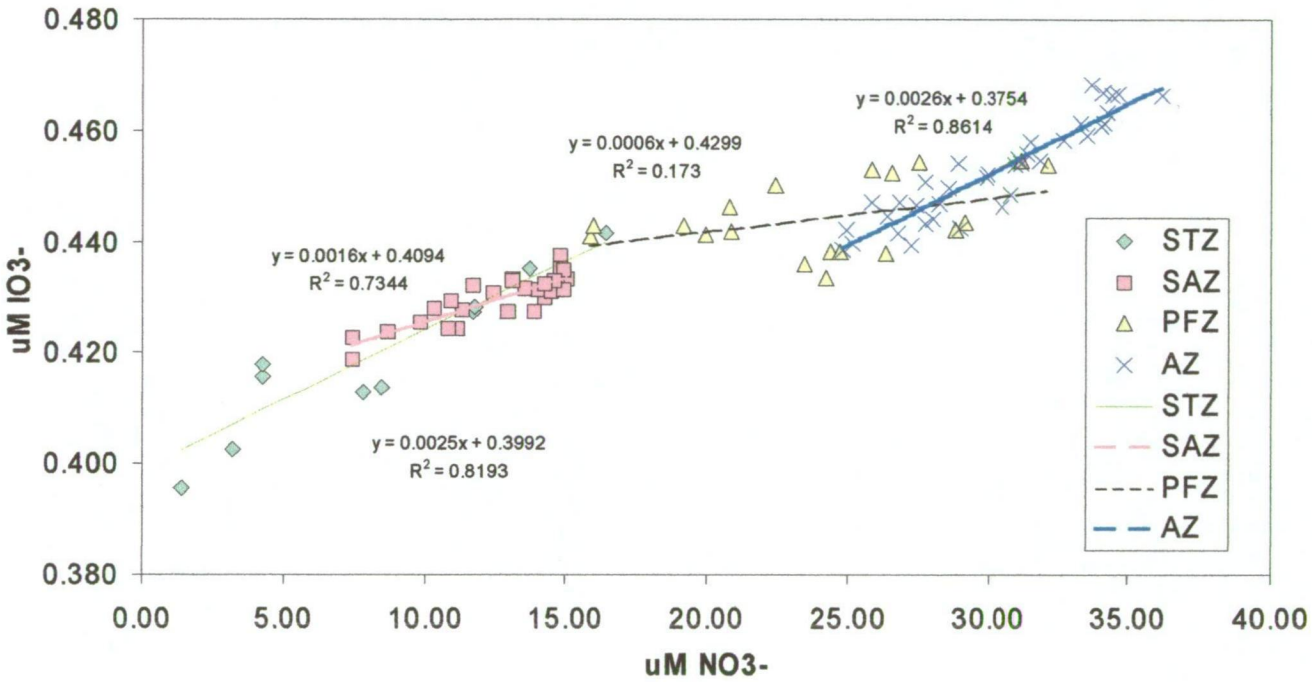

Figure 4.4- Salinity-normalised iodate data plotted against salinity-normalised nitrate data for surface waters (< 250 m) along the WOCE SR3 transect for summer 1994 (au9407). Different slopes represent different iodate to nitrate ratios in different oceanographic provinces, and were used to estimate iodine to carbon ratio in each of these provinces.

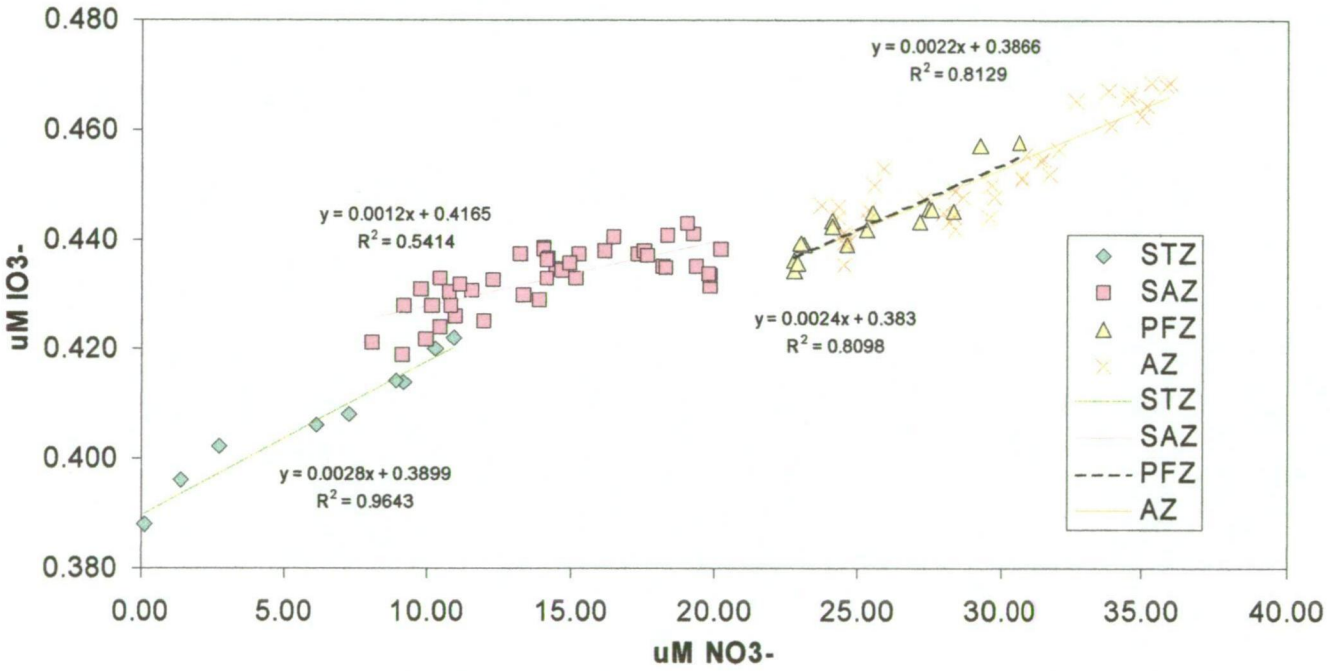

Figure 4.5- Salinity-normalised iodate data plotted against salinity-normalised nitrate data for surface waters (< 250 m) along the WOCE SR3 transect for summer 1995 (au9404). Different slopes represent different iodate to nitrate ratios in different oceanographic provinces, and were used to estimate iodine to carbon ratio in each of these provinces.

At the STZ for cruise 9407, the estimated I/C ratio was 3.77 (± 0.59) x 10^{-4}. It then dropped to 2.41 (± 0.29) x 10^{-4} at SAZ. At the PFZ, I/N correlation was very poor, with an estimated I/C of 9.05 (± 4.81) x 10^{-5}. At the AZ, however, I/N correlation was the highest for that cruise (R^2 = 0.8614) also giving the highest I/C of 3.92 (± 0.26) x 10^{-4}.

4.1.4 Estimating seasonal new production from iodate depletion

Iodate depletion values (section 4.1.2) and estimated I/C ratios (section 4.1.3) were used to estimate seasonal new production in the Southern Ocean along the SR3 transect. Depth-integrated iodate depletion values in mmol m^{-2} were divided by the estimated I/C ratio for each zone giving integrated seasonal new production in mmol C m^{-2}. Seasonal new production estimates for each station are presented on Tables 4.4 and 4.5, together with depth-integrated iodate depletion results.

For summer 1994 (9407), seasonal new production values varied from 87 (± 314) to 8436 (± 5261) mmol C m^{-2} (Table 4.4). The calculated standard deviations for these estimates were very high, varying from ± 27 to ± 300%, due to the high standard deviations from iodate depletion values. Seasonal new production estimates below 400 mmol C m^{-2} attracted the highest uncertainties. The northernmost value for seasonal new production of 1610 (± 1261) mmol C m^{-2} at 44.7°S was lower than the next one at 45.2°S of 5639 (± 1530) mmol C m^{-2} , within the STZ, and this difference was perhaps caused by the presence of less saline water (< 34.8) with higher iodate and nitrate at 44.7°S. The highest iodate depletion was within the STZ, while the highest seasonal new production value was immediately south of the STF, in the SAZ. In the SAZ, seasonal new production values were very variable with a minimum of zero at 47.2°S and a maximum of 8436 mmol C m^{-2} at 46.2°S. In the PFZ, owing to the poor correlation for I/N data (see sub-section 4.1.3), the I/C ratio from SAZ was used to calculate seasonal new production. The seasonal new production estimates within the PFZ varied from zero to 3145 (± 1609) mmol C m^{-2}, at the proximity of the Polar Front (PF). In the AZ, seasonal new production estimates were generally low, with exception of station 38 at 55.5°S with

Table 4.4 Estimated seasonal new production from depth-integrated iodate depletion between cruises 9501 (July) and 9407 (January 1994), for different zones along the WOCE SR3 line.

Zone	Station no. (9407)	Iodate depletion ($mmol.m^{-2}$)	I/C ratio	Seasonal production ($mmol\ C.m^{-2}$)	Latitude (°S)
STZ	006	0.607 (±0.466)	$3.77\ (\pm0.59) \times 10^{-4}$	1610 (±1261)	44.7
	008	2.126 (±0.471)		5639 (±1530)	45.2
SAZ	010	2.033 (±1.244)	$2.41\ (\pm0.29) \times 10^{-4}$	8436 (±5261)	46.2
	013	0		–	47.2
	015	1.087 (±0.572)		4510 (±2435)	48.0
	020	1.580 (±0.753)		6656 (±3223)	49.3
	023	0.703 (±0.645)		2917 (±2699)	50.2
PFZ	025	0	(9.05×10^{-5})	–	51.0
	028	0	$2.41\ (\pm0.29) \times 10^{-4}$	–	51.9
	031	0.081 (±0.243)		336 (±1009)	52.6
	033	0.758 (±0.377)		3145 (±1609)	53.6
AZ	036	0	$3.92\ (\pm0.26) \times 10^{-4}$	–	54.5
	038	0.457 (±0.580)		1166 (±1482)	55.5
	044	0.034 (±0.123)		87 (±314)	57.3
	048	0		–	59.9
	053	0		–	60.6
	058	0.157 (±0.155)		401 (±396)	62.3
	060	1.008 (±0.582)		2571 (±1494)	63.3
	063	1.223 (±1.181)		3120 (±3020)	64.8

1166 (± 1482) mmol C m^{-2}, and increased southwards with reasonably higher values (> 2500 mmol C m^{-2}) south of 63°S, at the proximity of the SACCF.

Seasonal primary production values estimated for summer 1995 (9404) varied from zero to 8116 mmol C m^{-2} (Table 4.5). Calculated standard deviations varied from ± 19 to ± 296%. The highest seasonal new production estimate was again at the proximity of the STF , but this time within the STZ at 45°S. STZ values were higher than the previous year, all above 4000 mmol C m^{-2}. In the SAZ, seasonal new production estimates varied from zero to 7950 mmol C m^{-2}, and peaked at 49.3°S for both summers, reflecting iodate depletion occurring to greater depths in the centre of the SAZ. In the PFZ seasonal new production varied from zero to 1315 mmol C m^{-2}, with the highest value immediately south of the SAF. In the AZ, production values varied from zero to 2614 mmol C m^{-2}, with values increasing quickly southwards, and highest values again south of 63°S, at the proximity of the SACCF.

Figure 4.6 shows the variation of estimated seasonal new production with latitude along the SR3 line for both summers (9404 and 9407), where data were available. As expected, these estimated values for seasonal new production varied along the SR3 line in a similar way to iodate depletion.

Table 4.5 Estimated seasonal new production calculated from depth-integrated iodate depletion between cruises 9501 (July) and 9404 (January 1995), for different zones along the WOCE SR3 line.

Zone	Station no. (9404)	Iodate depletion ($mmol.m^{-2}$)	I/C ratio	Seasonal production ($mmol\ C.m^{-2}$)	Latitude (°S)
STZ	104	1.740 (± 0.427)	4.22 (±0.29) x 10^{-4}	4123 (±1051)	44.4
	103	2.310 (± 0.540)		5474 (±1334)	44.7
	102	3.425 (± 0.622)		8116 (±1576)	45.2
SAZ	100	0.357 (± 0.470)	1.80 (±0.25) x 10^{-4}	1983 (±2626)	46.2
	098	0.483 (± 0.337)		2683 (±1909)	47.2
	097	0.959 (± 0.467)		5328 (±2698)	47.5
	095	0.083 (± 0.190)		461 (±1057)	48.3
	094	0.616 (± 0.511)		3422 (±2878)	48.8
	093	1.431 (± 0.773)		7950 (±4434)	49.3
	091	0		-	50.1
	090	0.705 (± 0.747)		3917 (±4186)	50.4
	088	0		-	51.0
PFZ	085	0.476 (± 0.561)	3.62 (±0.46) x 10^{-4}	1315 (±1559)	51.9
	083	0		-	52.7
	081	0.090 (± 0.267)		249 (±738)	53.6
AZ	079	0	3.32 (±0.26) x 10^{-4}	-	54.5
	077	0.191 (± 0.320)		575 (±965)	55.5
	076	0.105 (± 0.186)		316 (±561)	56.2
	074	0		-	57.6
	071	0		-	59.9
	070	0		-	60.6
	067	0.290 (± 0.337)		873 (±1017)	62.3
	066	0.773 (± 0.390)		2328 (±1189)	63.3
	062	0.868 (± 0.722)		2614 (±2184)	64.8

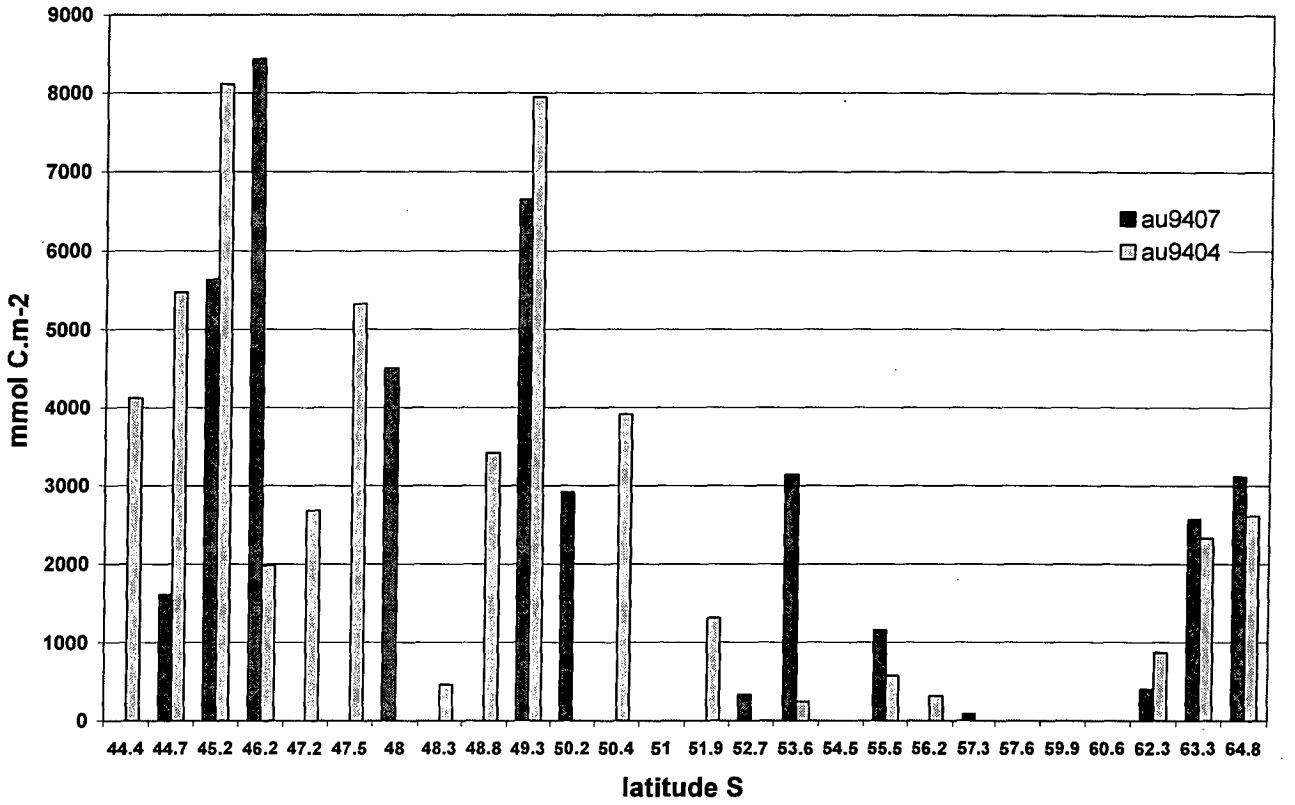

Figure 4.6- Seasonal production estimated from iodate depletion in surface waters from winter (July) to summer (January) along the WOCE SR3 transect, from Tasmania to Antarctica. Cruise au9407 was in January 1994 and cruise au9404 was in January 1995.

4.1.5 Discussion

4.1.5.1 Iodate depletion

Averaged depth-integrated iodate depletion values for both summers for each zone are shown on Figure 4.7. Standard deviations and exact values can be seen in Appendix III. These results show that depth-integrated iodate depletion was highest within sub-tropical zone (STZ) for both summers, with 1.4 and 2.5 mmol m^{-2} for cruises 9407 and 9404, respectively. The lower value of iodate depletion at 44.7°S for cruise 9407 brought the average integrated iodate depletion in the STZ down to nearly half of the average of that for next year's cruise (9404). Values considered zero represent small values that could not be measured accurately and, when used to calculate the average shown in Figure 4.7, certainly caused an underestimation of these average values.

In the SAZ, iodate depletion was less than for the STZ for both summers, and again a large inter-annual variability was noticed. This time the larger depletion of 1.1 mmol IO_3^- m^{-2} occurred in summer 1994 (9407), and the lower depletion of 0.52 mmol IO_3^- occurred in the following summer (9404). These results agree with Lourey and Trull (2001), who also found a large inter-annual variability in nitrate depletion within the SAZ from the winter cruise au9501 to summers January 1994 (au9407) and January 1995 (au9404). These authors found an average depth-integrated nitrate depletion in the SAZ of 460 (± 37) mmol N m^{-2} and of 290 (± 95) mmol N m^{-2}, for cruises au9407 and au9404, respectively.

In the PFZ, average integrated values of iodate depletion dropped further from SAZ values (Figure 4.7) and were around 0.2 mmol m^{-2} for both cruises. For summer cruise 9407, average iodate depletion in PFZ was close to 20% of the SAZ value, while for next summer, cruise 9404, the drop was not so large, with PFZ average iodate depletion close to 40% of SAZ value. Lourey and Trull (2001) also found a similar difference in nitrate depletion between the PFZ and SAZ. They found average integrated nitrate depletion values in the PFZ of 170 (± 38) mmol N m^{-2} for cruise

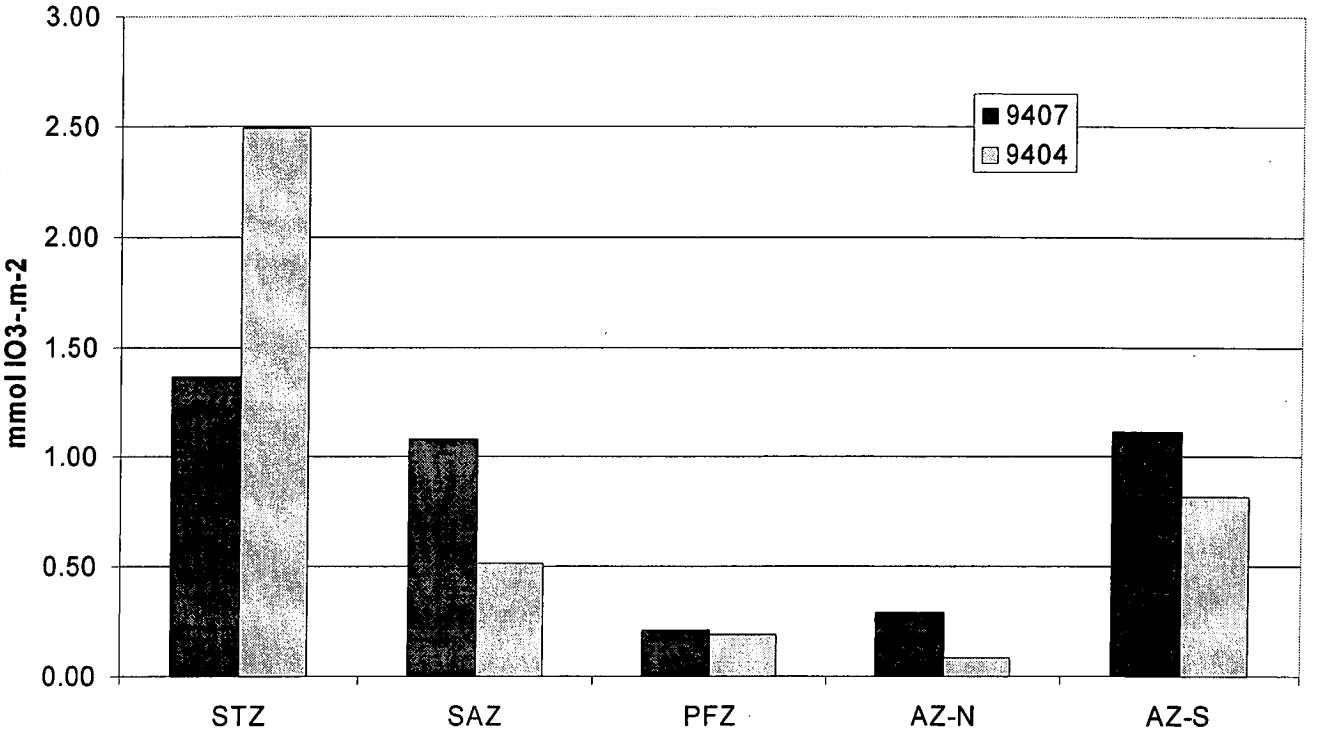

Figure 4.7- Average iodate depletion in surface waters from winter (July) to summer (January) for different oceanographic provinces along the WOCE SR3 transect, from Tasmania to Antarctica. Cruise au9404 was in January 1995 and cruise au9407 was in January 1994.

9407 and of 150 (± 57) mmol $N.m^{-2}$ for cruise 9404, which represented 37% and 52% of their SAZ estimates, respectively. Nitrate depletion will be further discussed later in the section.

The AZ here was divided in AZ north of 63°S (AZ-N) and AZ south of 63°S (AZ-S), because of the marked difference found between the two regions, especially during summer cruise 9404. With the exception of a station at 55.5°S for cruise 9407, values within the AZ-N were lower than further north, averaging 0.11 and 0.09 mmol IO_3^- m^{-2} for cruises 9407 and 9404, respectively. South of 63°S, iodate depletion increased dramatically. Popp *et al.* (1999) reported chlorophyll levels decreasing southwards along the SR3 during summer 1994, until south of this latitude, where they increased again, which is generally consistent with the trends in average integrated iodate depletion. Average iodate depletion values for AZ-S were 1.1 and 0.82 mmol m^{-2}, for cruises 9407 and 9404, respectively.

Integrated iodate depletion estimates varied a lot within each zone, which was probably caused by analytical uncertainties. Negative or zero values were all but two (station 91 at 50.1°S, cruise 9404, and station 13 at 47.2°S, cruise 9407) within the PFZ or AZ-N. According to the literature (Popp *et al.*, 1999; Lourey and Trull, 2001), primary production is typically lower within these two zones, and thus the accordingly low seasonal depletions in iodate are more difficult to quantify given the precision of the analytical method used.

Using nitrate data from cruises au9404 and cruise au9501 (Rosenberg *et al.*, 1996, 1997), nitrate depth integrated depletion from winter (9501) to summer (9404) was calculated along the SR3 transect. Nitrate values were normalised to same salinity (34.363) and integrated to the same depth as iodate depletion values for the same stations. Iodate and nitrate depletions were plotted together in Figure 4.8. It appears that iodate depletion varied more than nitrate depletion along the SR3, which was probably caused by the iodate depletion values being closer to the detection limit than nitrate depletion values. However similar trends can be noticed for both nutrients in Figure 4.8. Both iodate and nitrate showed higher depletion in the

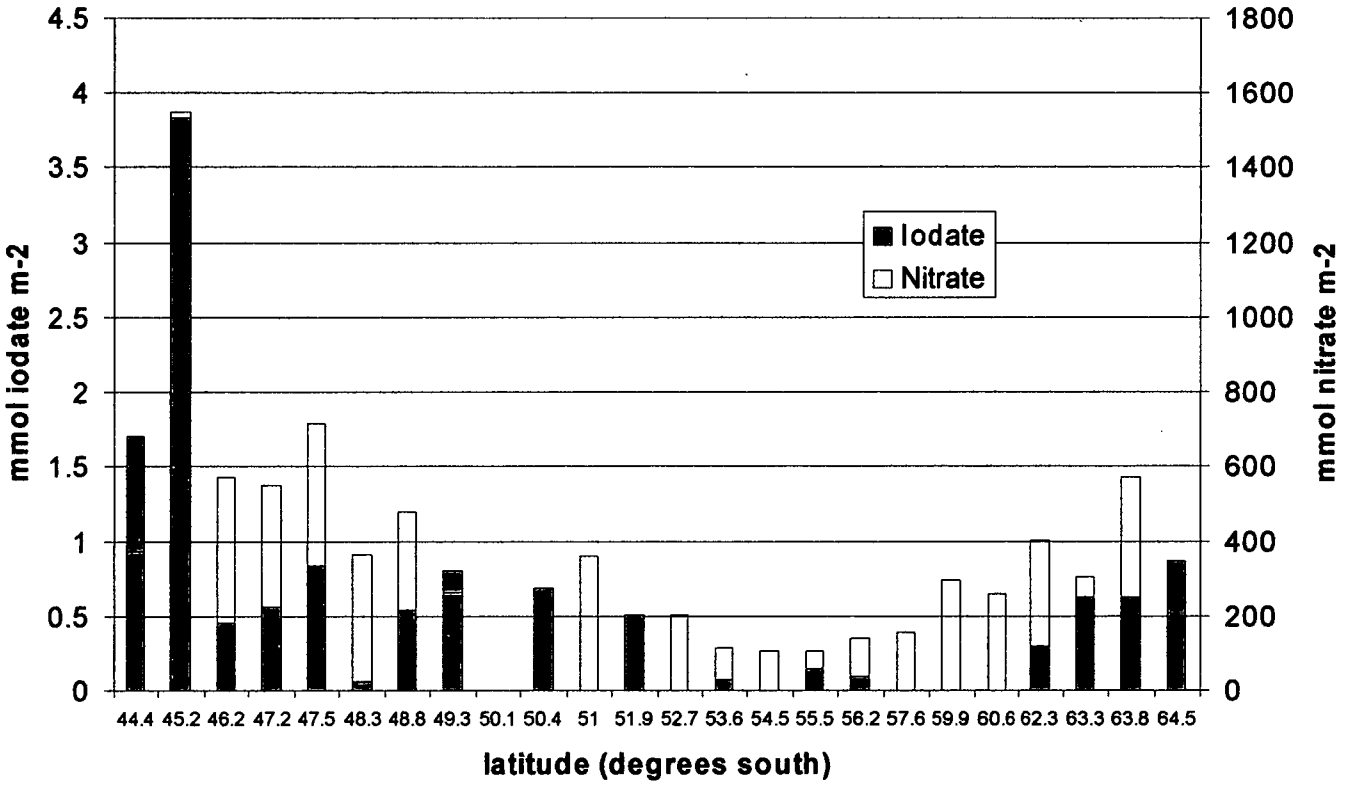

Figure 4.8- Iodate and nitrate depletion in surface waters from winter (July) to summer (January 1995, au9404) along the WOCE SR3 transect, from Tasmania to Antarctica.

subtropical zone, a small increase again at 47.5°S, a generally low depletion between the PF at 53.6°S and 59.9°S and an increase south of 62°S.

Overall, averaged integrated iodate depletion variation has agreed with Lourey and Trull's (2001) nitrate depletion variation both for SAZ and PFZ along the SR3, and with nitrate depletions calculated here showed in Figure 4.8. Also with increased biomass reported south of 63°S (Popp *et al.*, 1999), it seems reasonable to assume that seasonal nutrient depletion would be also higher in that region when compared to PFZ and AZ north of 63°S, which was also confirmed by nitrate depletion shown in Figure 4.8.

4.1.5.2 I/C ratios

I/C ratio values were estimated for the Southern Ocean for the first time in this study. The results, calculated indirectly from iodate/nitrate ratio in surface waters, suggest that I/C ratio not only varies between different regions in the Southern Ocean, but also varies on an annual basis (Table 4.3). As it has been observed before (Butler and Plaschke, 1988; Butler *et al.*, 1992; Campos *et al.*, 1999; Truesdale *et al.*, 2000), there is a change in I/C or I/N values south of the STF. Butler *et al.* (1992) suggested that iodate is either "assimilated or regenerated (or both) differently in subtropical and subantarctic waters". Truesdale *et al.* (2000) believed that the variation in I/N ratio in surface waters, which they observed throughout the Atlantic along different latitudes, is part of a hyperbolic relationship, where the IO_3^-/NO_3^- ratio in surface waters is proportional to nitrate concentration at 200 m, but not linked directly to nitrate biological uptake. On the other hand, Campos *et al.* (1999) suggested that the low iron levels of the Southern Ocean, causing low nitrate reductase activity in this high nitrate low chlorophyll (HNLC) zone, would directly affect iodine cycling in Subantarctic and Antarctic waters, because of the lack of nitrate reductase to reduce iodate.

In this work, I/C ratios (calculated from iodate/nitrate ratio in surface waters) dropped from 4.22×10^{-4} in Subtropical waters to 1.8×10^{-4} in Subantarctic waters,

more than 50%, for cruise 9404. For cruise 9407 the drop in I/C ratio from 3.7 x 10^{-4} (STZ) to 2.41 x 10^{-4} (SAZ) was not so intense, it still confirms that there is a change in iodate/nitrate assimilation rate that should not be ignored. It is also worth noticing that the excellent agreement normally found between iodate versus nitrate plots in Subtropical surface waters, with R^2 normally larger than 0.9, was not observed in Subantarctic waters (Truesdale *et al.*, 2000; Campos *et al.*, 1999, Table 4.3). This fact shows that the entire iodate/nitrate relationship changes south of the STF, and not only the iodate/nitrate uptake ratio by phytoplankton. These changes could have been caused by one or more factors such as:

(a) low iodate uptake by phytoplankton due to high nitrate concentration;

(b) increased competition for nitrate reductase, which preferentially reduces nitrate rather than iodate in presence of high nitrate concentrations;

(c) low nitrate reductase activity caused by low iron levels, affecting iodate reduction rates;

(d) changes in the planktonic community from the STZ to the SAZ, which would reflect on iodine absorption/reduction rates;

(e) changes in nitrogen uptake, with more reduced (NH_4^+, N_2 after fixation) species being taken up by phytoplankton in the STZ.

Campos *et al.* (1999) also noticed a dramatic change in iodine/nitrate relationship south of the STF in the South Atlantic. Measured iodide/nitrate ratios dropped from 29 x 10^{-3} in the Subtropical Gyre to 2.35 x 10^{-3} in the Subtropical Frontal Region. Their estimated I/C ratios were 3.5 x 10^{-4} in the Subtropical Frontal region, 2.7 x 10^{-4} in the SAZ, 2.4 x 10^{-4} between the SAF and the Scotia Sea (~56°S), 3.8 x 10^{-4} in the Scotia Sea (56°-61°S) and 3.6 x 10^{-4} in the Weddell Sea (south of 61°). These values are in good agreement with the ones estimated by this study, and also show a decrease from Subtropical to Subantarctic waters, with an increase of I/C again in more productive Antarctic waters.

Although I/C ratios calculated here using iodate (instead of total iodine) were higher than Elderfield and Truesdale (1980) value of 1×10^{-4}, I/C ratios for STZ were consistent with Wong and Brewer's (1974) I/C ratio of 4×10^{-4} for subtropical waters in South Atlantic. Jickells *et al.* (1988) also believed that an I/C ratio of 1×10^{-4} was an underestimated value for the seasonal changes they noticed in iodate speciation in the Sargasso Sea. Farrenkopf (2000) also showed that I/C in particulate material in the North Pacific can be variable, and was also higher than Elderfield and Truesdale's (1980) estimate for most filtered particulates. Wong and Hung (2001) also showed that, in subtropical waters of the southern East China Sea, iodate plotted against iodide concentrations had a close relationship, with $r^2=0.87$ and slope of -1.06 ($\pm$ 0.06), showing that iodide production was closely coupled with iodate uptake/reduction. Based on these findings, later Wong (2001) argued that iodate depletion, and *not* total iodine depletion, was directly related to new or nitrate-based production, because iodate and nitrate are taken up by phytoplankton at some ratio during nitrate uptake and almost all iodate taken up was exuded as iodide. Using iodate depletion and iodate/nitrate ratio to estimate new production, as done in this work, are in agreement with Wong's (2001) and Wong and Hung's (2001) findings.

As suggested by Wong (2001), and used before by other authors (Wong and Brewer, 1974; Elderfield and Truesdale, 1980), the iodate/nitrate uptake ratio can be obtained directly from the slope of iodate versus nitrate plot in surface waters. Using the iodate-to-nitrate depletion ratio from nitrate and iodate depletions between winter 1995 (9501) and summer 1995 (9404) calculated here (Figure 4.8), $(I/C)_d$ ratios were recalculated, using a Redfield C/N ratio of 6.63, and compared with previous $(I/C)_s$ values obtained from the slope of iodate against nitrate plot. $(I/C)_d$ are ratios obtained from iodate to nitrate depletion ratios divided by 6.63, and $(I/C)_s$ are ratios obtained previously directly from the slopes of iodate against nitrate concentrations plotted for surface waters, also divided by 6.63 (Figure 4.5, Table 4.3). All $(I/C)_d$ ratios obtained for stations along SR3 for cruise 9404 are shown in Figure 4.9, and average $(I/C)_d$ ratios within each zone are compared to $(I/C)_s$ in Table 4.6. In Figure 4.9, I/C ratios in the STZ were all above 3.7×10^{-4}, and south of 46.2°S, at the STF, I/C ratios were all, but two (at 49.3°S and at 55.5°S), below 2.8×10^{-4} until 63°S. South of 63°S I/C values increased and reached 6.3×10^{-4} at 64.8°S. In Table 4.6 averaged $(I/C)_d$ values

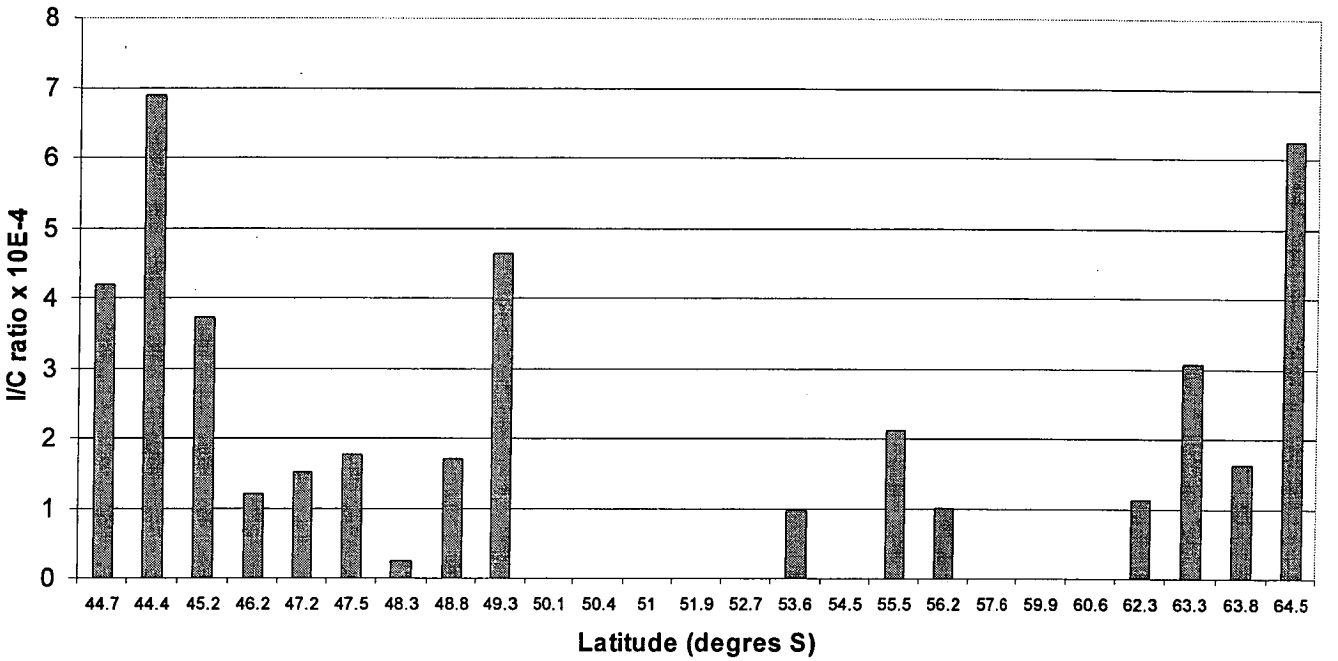

Figure 4.9- Iodine to carbon ratios calculated from iodate to nitrate depletion ratios in surface waters from winter (July) to summer (January 1995, au9404) along the WOCE SR3 transect, from Tasmania to Antarctica. Iodate and nitrate depletion were presented in Figure 4.8.

Table 4.6- Comparison between I/C ratios calculated from iodate/nitrate depletion ratio $(I/C)_d$ and from the slope of iodate against nitrate plot for surface waters along the SR3 transect for cruise 9404.

Zone	$(I/C)_d$	$(I/C)_s$
STZ	$4.94 (\pm 1.3) \times 10^{-4}$	$4.22 (\pm 0.29) \times 10^{-4}$
SAZ	$1.85 (\pm 0.93) \times 10^{-4}$	$1.80 (\pm 0.25) \times 10^{-4}$
PFZ	0.96×10^{-4}	$3.62 (\pm 0.46) \times 10^{-4}$
AZ-N	$1.41 (\pm 0.47) \times 10^{-4}$	$3.32 (\pm 0.26) \times 10^{-4}$
AZ-S	$3.65 (\pm 1.74) \times 10^{-4}$	$3.32 (\pm 0.26) \times 10^{-4}$

had large standard deviations varying from 26 to 50% of values. $(I/C)_d$ value for PFZ was the only $(I/C)_d$ ratio obtained for that zone, because either iodate or nitrate depletion were zero. $(I/C)_d$ dropped to less than half its value from the STZ to the SAZ, and appears to have dropped again from the SAZ to the PFZ and AZ-N, increasing to values closer to the STZ in the AZ-S. These variations generally agreed with variations observed before for $(I/C)_s$. The only exceptions were that of PFZ and AZ-N. In the PFZ, only one value for $(I/C)_d$ was obtained and was probably not representative. In the AZ only one value of $(I/C)_s$ was calculated for this entire zone, while $(I/C)_d$ average value shown in Table 4.6 was calculated for AZ-N and AZ-S separately. These findings support the idea that using iodate/nitrate ratio obtained directly from the slope of the line of best fit for iodate data plotted against nitrate data for surface waters in summer give results similar to using the iodate/nitrate depletion ratio. The former possibly brings some advantage because data loss of the latter associated with lack of measurable iodate or nitrate depletion is not encountered.

The I/C ratios calculated here seemed to reflect the differences in iodate depletion for different zones to a certain extent. For cruise 9404, higher depletion in subtropical waters was associated with higher I/C, and lower depletions corresponding to a lower I/C ratio were observed in Subantarctic waters. I believe that both iodate depletion and I/C ratio variations reflect the changes in the community of microorganisms present along the SR3 transect, and that none of these is a dominant factor. Since I/C and iodate depletion vary with productivity levels, there is a potential to used them as indicators of new production in different zones of the Southern Ocean, and more data will be necessary to confirm this trend.

The drop in the I/C ratio from the STZ to the SAZ also happened concomitantly with a drop in dissolved levels. Dissolved iron levels south of Tasmania dropped quickly from ~0.8 nM in the STZ to < 0.11 nM in the SAZ, and appear to be a limiting factor for primary production south of STF (Sedwick *et al.*, 1997, 1999). As iron is an essential element in the enzyme for nitrate reduction, namely nitrate reductase (De Baar *et al.*, 1997), and iodate reduction in surface waters seems to be dependent on this same enzyme (Wong and Hung, 2001), the drop in iron levels south of the STF

may also be affecting iodate uptake by phytoplankton. As iron levels appear to increase again in the proximity of the SACCF, due to the presence of deep water immediately below the surface layer (Sohrin *et al.*, 1999; Franck *et al.*, 2000; Measures and Vink, 2001), iodate and iodate/nitrate uptake may also increase there in response to increased iron availability.

Another important factor that can affect I/C ratio is the reported large variability of C/N ratio in the Southern Ocean. As I/C ratios here were calculated using Redfield C/N/P ratio of 106/16/1, they will change if C/N varies. Copin-Montegut and Copin-Montegut (1978) measured C/N ratio in particulate organic matter around the southwest Indian Ocean and the Southern Ocean around Kerguelen Is. For the Subtropical zone C/N ratios were similar to average phytoplankton (C/N=6.6), but C/N ratios of 5.9, 5.6 and 5.7 were found for SAZ, PFZ and AZ, respectively. If these lower C/N values had been used in this study, it would have yielded higher I/C ratios for these three zones. However, the variations observed between different zones would still exist, with I/C for SAZ, PFZ and AZ increasing 11 to 18% of their original values shown in Table 4.3. In addition, C/N ratios as high as 10.1 have been reported for marginal ice zones in Antarctica (Karl *et al.*, 1991).

4.1.5.3 Seasonal new production estimated from iodate depletion

Average values of estimated seasonal new production along the SR3 transect are presented in Figure 4.10. Standard deviations and exact values can be seen in Appendix IV. For January 1994 (cruise au9407), average seasonal new production values varied from 740 to 4508 mmol C m^{-2}, for AZ-N and SAZ, respectively. For January 1995 (cruise au9404), average seasonal new production values varied from 252 to 5904 mmol C m^{-2}, at AZ-N and STZ, respectively.

For cruise 9407, the results in the STZ were affected by the intrusion of waters with salinities >34.8 at 44.7°S, and so estimated production was lower than in the SAZ. Results from both summers for waters south of the STF varied in a similar way, with highest values in the SAZ decreasing southwards until 63°S, at the proximity of the SACCF, where average seasonal new production increased again.

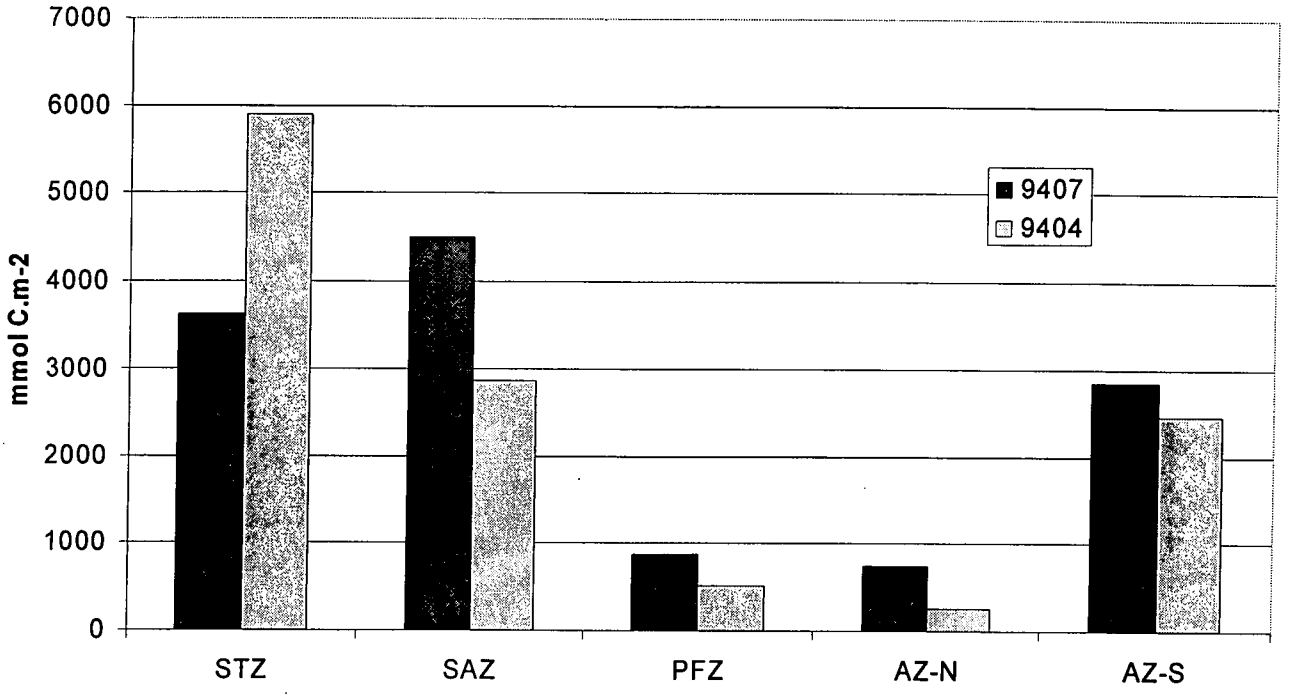

Figure 4.10- Average estimated seasonal production calculated from iodate depletion in surface waters in different oceanographic provinces along the WOCE SR3 transect, from Tasmania to Antarctica.

In the PFZ, for cruise 9407, the plotted average production value of 870 mmol $C.m^{-2}$ was estimated using I/C from SAZ (2.41×10^{-4}), instead of calculated value for PFZ (9.1×10^{-5}) due to the poor linear correlation of I/N plot for that zone. With the exception of STZ, January 1994 (9407) average seasonal new production values were higher than January 1995 (9404) for all other zones.

Table 4.7 shows a comparison between seasonal new production along the SR3 transect for SAZ and PFZ estimated from nitrate depletion (Lourey and Trull, 2001) and from iodate depletion. Both seasonal new production estimates were calculated from the differences between nutrient concentrations from winter cruise au9501 (July 1995) and summer cruises au9407 (January 1994) and au9404 (January 1995). Seasonal new production estimated from iodate depletion was higher than that estimated from nitrate depletion in the SAZ. In the PFZ, the opposite trend was observed, although considering the higher standard deviations iodate depletion-based results in this zone, results were not dissimilar. Lourey and Trull's (2001) estimates were also calculated from interpolated nitrate concentrations along the SR3 transect, and not on a station by station basis, as iodate depletion calculations were. However, their estimates of seasonal new production from nitrate depletion were higher for January 1994 (9407) than for January 1995 (9404), which agrees with the estimates of seasonal new production derived from iodate depletion calculated in this work.

Nitrate depletion calculated by Lourey and Trull (2001) gives slightly different results than nitrate depletion calculated here, on a station-by-station basis. Average new production estimates obtained from nitrate depletion as calculated here are shown in Table 4.8 and compared to average production estimates obtained by iodate depletion using the same method. Looking at Tables 4.7 and 4.8, it is evident that there are differences between the two methods used to calculate nitrate depletion. Seasonal production value for SAZ on 9404 calculated by Lourey and Trull (2001) in Table 4.7 was lower than the one calculated here in Table 4.8. In the PFZ, the opposite trend was noticed. Seasonal production values calculated from iodate depletion appear closer to the ones shown in Table 4.8, obtained from nitrate depletion calculated here. It is evident from that the differences observed between Lourey and Trull's (2001) production estimates and the ones calculated here from

Table 4.7 Comparison between depth-integrated seasonal production estimates along the SR3 transect calculated from nitrate (Lourey and Trull, 2001) and iodate depletions, based on a Redfield C/N ratio of 6.63.

Zone	Cruise	Production estimate from nitrate depletion (mmol C m^{-2})		Production estimate from iodate depletion (mmol C m^{-2})	
		Average	Std deviation	Average	Std deviation
SAZ	au9407	3050	245	4508	3268
	au9404	1923	630	2860	2654
PFZ	au9407	1127	252	870	1525
	au9404	995	358	521	699

Table 4.8 Average seasonal new production estimates calculated from nitrate depletion on a station-by-station basis from July 1995 (9501) to January 1995 (au9404), using a Redfield C/N ratio of 6.63.

Zone	New production estimate from NO_3^- depletion (mmol C m^{-2})	Standard deviation (mmol C m^{-2})	New production estimate from IO_3^- depletion (mmol C m^{-2})	Standard deviation (mmol C m^{-2})
STF	6371	3905	5904	2317
SAZ	2433	1252	2860	8025
PFZ	709	473	521	1725
AZ-N	1391	626	252	1510
AZ-S	2402	927	2471	2487

iodate depletion are partly related to the method used to calculated those depletions in the first place. In Table 4.8 production estimates calculated from iodate depletion were lower that estimates from nitrate depletion at the PFZ and AZ-N, due to the higher number of zero iodate depletions measured at these zones. It appears that as iodate depletion is very close to the standard deviation of the analytical method used, its use to estimate seasonal production in zones with low nutrient depletion may produce underestimated values.

Seasonal new production estimates in the Southern Ocean from nutrient and dissolved inorganic carbon (DIC) depletion have been done by several other groups (Jennings *et al.*, 1984; Minas and Minas, 1992; Karl *et al.*, 1991; Bates *et al.*, 1998; Ishii *et al.*, 1998; Rubin *et al.*, 1998; Hoppema and Goeyens, 1999; Lourey and Trull, 2001). These results are summarised in Table 4.9.

Despite the large uncertainties of seasonal production values calculated in this study, a comparison of seasonal new production estimates from iodate and nitrate depletion shows that values estimated here are within the range of previously reported values. In the SAZ, values calculated here were above the upper limit of Lourey and Trull's (2001) results for the same period (Table 4.9), but closer to the lower limit of the estimates derived from DIC depletion by Metzl *et al.* (1999) over a six-month period (3040-8333 mmol C m^{-2}). Longhurst *et al.* (1995) estimated primary production values from satellite data were 5000 mmol C m^{-2} for the SAZ and 5875 mmol C m^{-2} for the Southern Ocean for a six-month period, both values also above average values reported in this study. Minas and Minas's (1992) results of 2520 mmol C.m^{-2} were averaged along their transect, and are around 30 % higher than our average for the whole SR3 transect (excluding STZ) of 1884 mmol C.m^{-2}. Average results obtained here for the Antarctic Zone south of SACCF (AZ-S) were comparable to the ones obtained by Ishii *et al.* (1998) and Rubin *et al.* (1998) for the same region.

Table 4.9 Seasonal production estimates for different regions of the Southern Ocean based on nutrient or DIC (dissolved inorganic carbon) depletion in comparison to estimates from iodate depletion.

Region	NO_3^- depletion (mmol $N.m^{-2}$)	C/N	Seasonal production from nitrate (mmol $C.m^{-2}$)	Seasonal production from DIC (mmol $C.m^{-2}$)
Weddell Sea (a)	300	5.64	1691	
Indian sector 48°-62°S, ~65°E (b)	380	6.63	2520	
Bransfield Strait (c)	827	10.1	8410	8410
Ross Sea polynya (d)	96-599	6.67	642-3992	
Indian sectors 30°-140°E, 63°-68°S (e)	79-532	6.3-9.3		833-4000
Pacific sector 163°E-70°W, ~67°S (f)	134-448	6.9		780-2892
Weddell Sea (g)	~40-720	5.7	~228-4104	~200-4500
Australian sector				
SAZ – SR3 (h)*	510 ± 65	6.6	3400 ± 430	
PFZ – SR3 (h)*	250 ± 53	5.6	1400–1600	
SAZ – SR3 (i)		6.63	3684	
PFZ – SR3 (i)		6.63	696	
AZ-N- SR3 (i)		6.63	496	
AZ-S – SR3 (i)		6.63	2659	

(a) Jennings et al. (1984)
(b) Minas and Minas (1992)
(c) Karl et al. (1991)
(d) Bates et al. (1998)
(e) Ishii et al. (1998)
(f) Rubin et al. (1998)
(g) Hoppema and Goeyens (1999)
(h) Lourey and Trull (2001). * nitrate depletion values from July-March
(i) Brandão, this study. Seasonal production estimate from iodate depletion from July- January.

The use of iodate depletion in the Southern Ocean to estimate seasonal or net community production in the Southern Ocean gave highly variable results. However, average values obtained here for seasonal new production in the Southern Ocean in different zones were close to other estimates reported in the literature. Iodate/nitrate relationship also shows the potential to be a good indicator of new production in the Southern Ocean, with higher I/N ratios corresponding to zones of higher production. More studies are necessary to indicate if this variation is related to either or both of iron availability and changes in phytoplankton communities.

4.2 Iodate distribution in deep and bottom water masses of the Australian sector of the Southern Ocean

4.2.1 General comments

In Chapter 3, looking at iodate *vs.* depth profiles along the SR3 for latitudes higher than 60°S, one observes a decrease, sometimes sharp, in iodate concentration below 1000 m depth (Figures 3.5e,f; 3.10d,e and 3.18e). In most cases the observed decrease corresponded to the presence of either Modified Lower Circumpolar Deep Water (MLCDW) or Antarctic Bottom Water (AABW), below the salinity maximum of Lower Circumpolar Deep Water (LCDW). MLCDW is formed as a result of LCDW mixing with denser AABW below, and is defined here as waters with salinities < 34.7 and temperatures > 0°C, between LCDW and AABW. Here, this decrease in iodate concentration towards AABW is carefully examined to test the hypothesis, from Section 1.3, that this observed decrease is not just due to the observed decrease in salinity, but due to real inherent differences in iodate concentration between AABW and LCDW.

AABW is responsible for the ventilation of abyssal layers of the world's oceans, bringing cold, fresh and oxygen-rich waters formed along the Antarctic Coast, mainly in the Weddell and Ross Seas, to the bottom of the oceans (Rintoul, 1998). AABW present along the SR3 transect is believed to be formed off Adélie Land, in the vicinity of the Mertz Polynia (between 142°E and 145°E), from where it spreads westwards into the Australian-Antarctic Basin (Rintoul, 1998). This so-called Adélie Land Bottom Water (ALBW) is colder, fresher and higher in oxygen than Ross Sea Bottom Water (RSBW), which enters the Australian-Antarctic Basin from the east. ALBW may contribute to as much as 25% of the global volume of bottom water (temperature < 0°C) in the world's oceans (Rintoul, 1998).

Here, iodate concentration in AABW along the WOCE SR3 and S4 transects (see Chapter 3, Figure 3.1) is compared to concentrations in the MLCDW and LCDW water masses above to examine the possibility of using iodate as a tracer of AABW,

particularly for ALBW. Estimated precision for iodate determination in this study is ± 0.6%, which for iodate concentration of 472 nM is ± 2.8 nM.

LCDW originates from North Atlantic Deep Water (NADW) entering the Southern Ocean through the southwestern Atlantic Ocean (Orsi *et al.*, 1995), and is older than AABW, being enriched in iodate and silicate, because of the decomposition of sinking organic matter and siliceous shells. However, unlike silicate, iodate is not associated with the hard shells of phytoplankton and is quickly recycled mostly within the mixed layer (Wong and Brewer, 1976, Elderfield and Truesdale, 1980, Truesdale, 1994). Also, iodate typically does not show a sub-surface maximum like nitrate and phosphate do in Pacific waters (Truesdale, 1994). Typical iodate profiles in the Southern Ocean (see Chapter 3, Figure 3.5) increase quickly with depth down to 500 —1000 m, then either continue to increase very slightly towards the bottom, with a maximum close to the bottom of the profile, or remain close to constant below a certain depth. However, in profiles along the SR3 section south of 60°S, where deep waters fresher than 34.7 (MLCDW) start to appear below the salinity maximum of LCDW, iodate concentrations reach a maximum and start to decrease towards the bottom, below this maximum. This bottom layer of lower iodate concentration is associated with the presence of AABW, which, in mixing with higher salinity LCDW, forms MLCDW at the southern part of the SR3 section.

4.2.2 Distribution of iodate, salinity and temperature at stations along the SR3 transect where AABW was identified

AABW presence is defined along the SR3 transect as being deeper than 1000 m and colder than 0°C (Gordon and Tchernia, 1972). All iodate concentration data used here has been corrected using the analytical correction explained previously in Section 3.3. As the correction has only been applied to stations where LCDW was present, some stations at the southern end of the SR3 transect have not been used in the following analysis. All data used come from three cruises along the SR3 transect: au9501, au9404 and au9407. More details about station positions and dates of sampling can be seen in Appendix II.

T-S diagrams for cruises au9501, au9404 and au9407 can be seen in Figures 4.11a, b and c, respectively. T-S diagrams are an important tool used to identify different water masses. A total of 15 stations from these cruises have been used. Salinity maxima of LCDW (~34.746) are prominent on the right hand side of each of the plots. As the temperature decreases and the salinity drops to below 34.7, MLCDW is present approximately between T = 0.5°C and T = 0°C. Below T = 0°C, AABW is present, and the observed change in the slope of T-S at this point is characteristic of ALBW (Rintoul, 1998). Salinities below 34.7 in the warmer (upper) part of the plots are characteristic of Upper Circumpolar Deep Water (UCDW) lying above LCDW.

Temperature *vs.* iodate concentration were plotted to observe if iodate variation with temperature follows that of salinity, changing between different water masses. Temperature *vs.* iodate plots for cruises au9501, au9404 and au9407 are shown in Figures 4.12a, b and c, respectively. Temperature *vs.* iodate plots had some similar features to the T-S plots, although there is more scatter in the trends, probably reflecting the poorer precision in the iodate measurements. In the upper part of the plot, both iodate and salinity increased sharply with decreasing temperatures up to a maximum, then started dropping, not so steeply, towards colder waters. However, salinity maxima occurred between 1.5° and 2°C for most stations, within LCDW, while iodate maxima occurred deeper in the water column for all stations except one (station 46, 9501). In most stations, seven out of 15, iodate maxima were between T = 0.5° and T = 1°C (below LCDW salinity maxima at ~ 1.5°C). In five other stations, iodate maxima were between the temperatures of 0° and 0.5°C (within MLCDW), at two others between 1° and 1.5°C, and at only one station iodate maximum was above the 1.5°C isotherm. Iodate also behaved differently from the major nutrients nitrate and silicate. Silicate maxima and nitrate second maxima (not shown) for nearly all stations were between the temperatures of 0° and 0.5°, within MLCDW. Iodate concentration in AABW also dropped quickly at the most southerly stations for the three cruises (st.51-9501, st.62-9404 and st.63-9407). Iodate concentrations for station 46, cruise 9501, appear to be lower than for the other stations, and no explanation, other than analytical imprecision, can be given to these results.

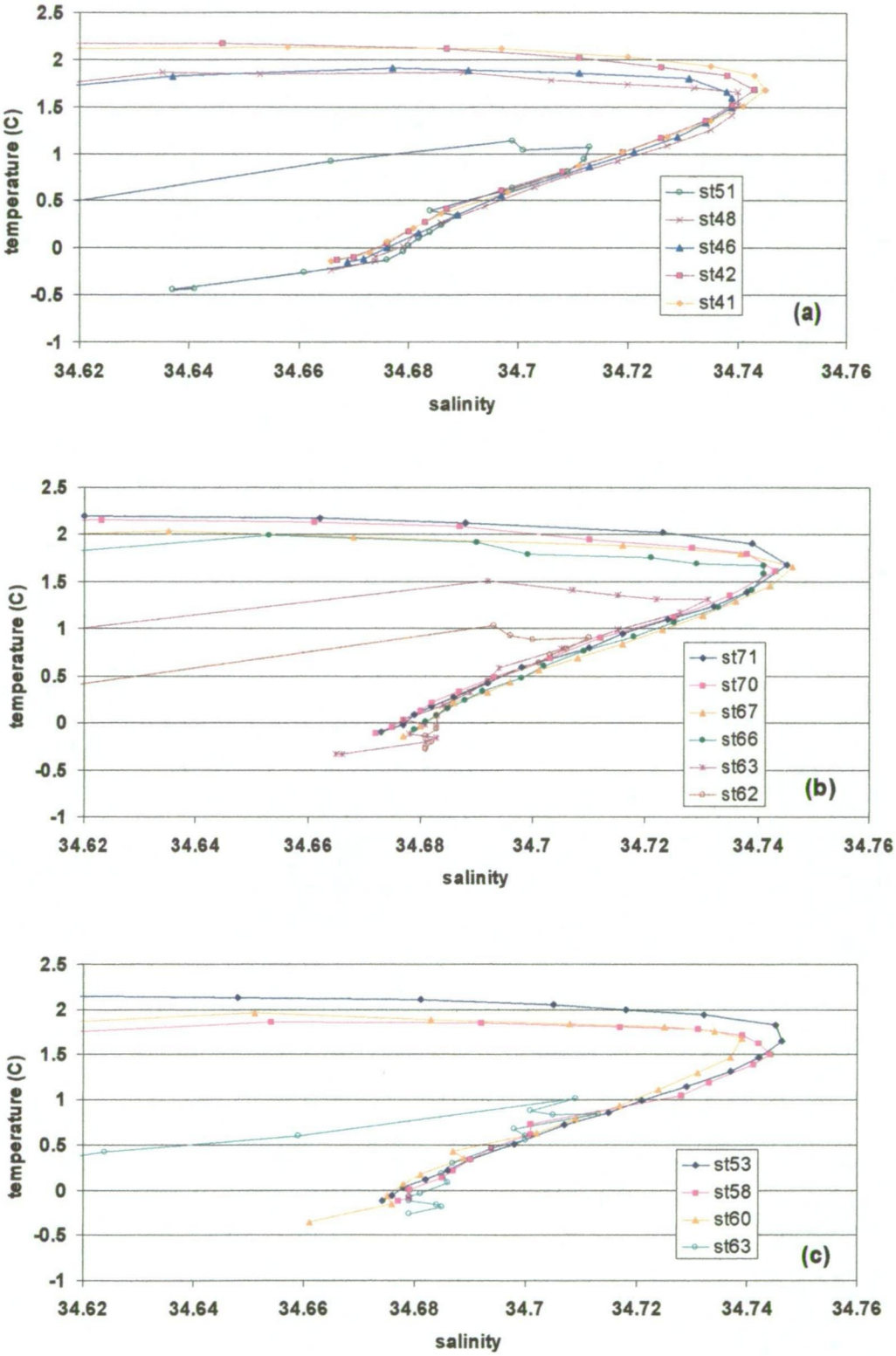

Figure 4.11- T-S curves for stations where Antarctic Bottom Water (AABW) ($t < 0°C$, depth > 1000 m) was identified in the southern part of the SR3 transect. Cruise au9501 **(a)**: station 41 at 59.9°S and station 51 at 64.8°S. Cruise au9404 **(b)**: station 71 at 59.9°S and station 62 at 64.8°S. Cruise au9407 **(c)**: station 53 at 60.9°S and station 63 at 64.8°S.

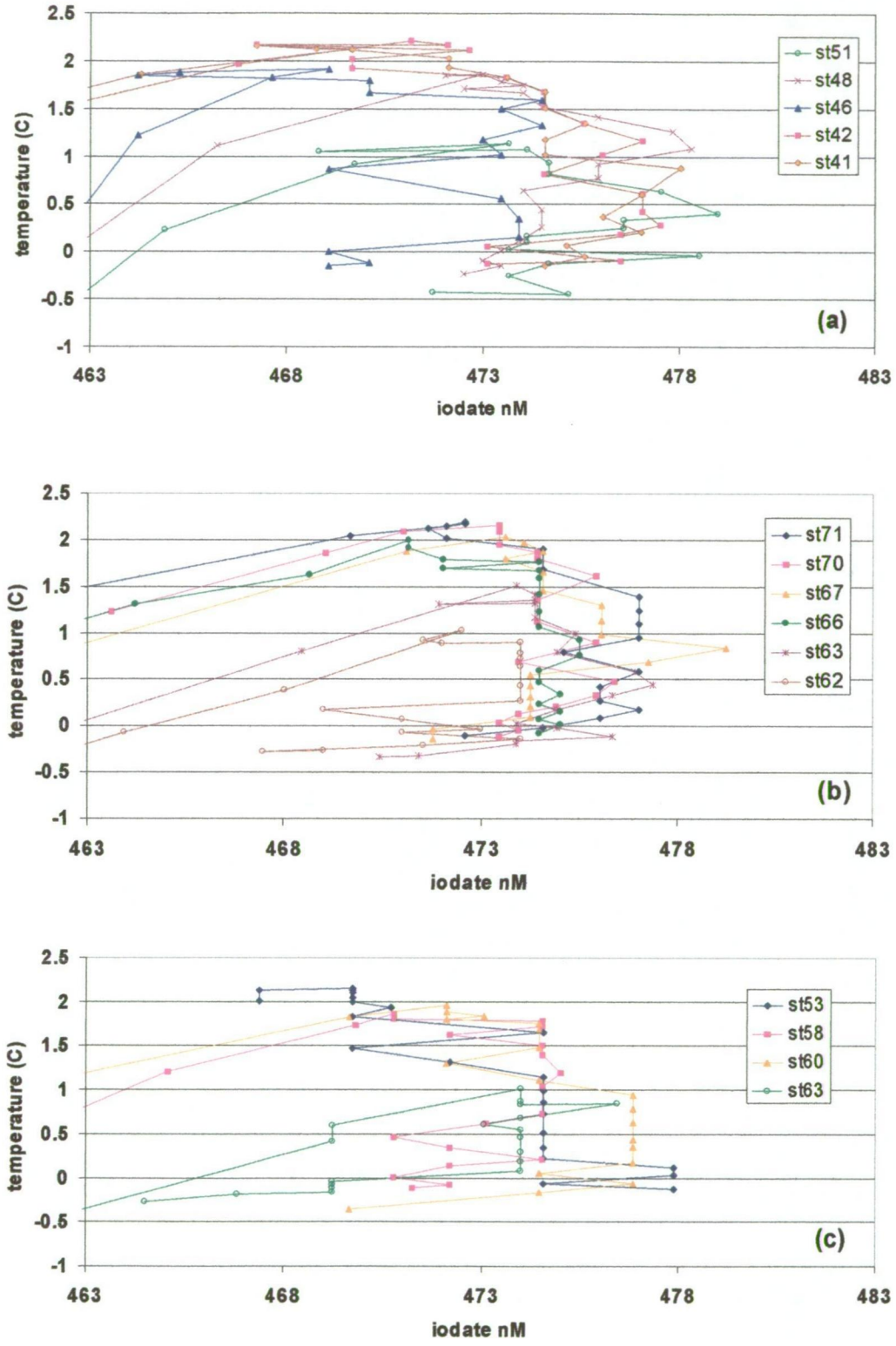

Figure 4.12- Temperature *vs.* iodate curves for stations where Antarctic Bottom Water (AABW) (t < 0°C, depth > 1000 m) was identified in the southern part of the SR3 transect. Cruise au9501 **(a)**: station 41 at 59.9°S and station 51 at 64.8°S. Cruise au9404 **(b)**: station 71 at 59.9°S and station 62 at 64.8°S. Cruise au9407 **(c)**: station 53 at 60.9°S and station 63 at 64.8°S.

Iodate *vs.* salinity plots can be a helpful tool in observing how iodate concentration changes as salinity changes between different water masses. Figures 4.13a, b and c show plots of iodate *vs.* salinity for the three cruises (9501, 9404 and 9407, respectively). Iodate concentration increased from UCDW (salinities from 34.5 to 34.7, at the bottom half of each plot) until the salinity maximum of LCDW. Below the salinity maxima (at the top half of the plot), iodate concentration continued to increase for most stations, with two exceptions: stations 63, cruise 9407 and 62, cruise 9404. These two stations are located at 64.8°S and both have their salinity maxima at 34.71, lower than most stations, marking the southern limit of LCDW. Only at these stations iodate maxima coincided with salinity maxima. Overall, iodate maxima was located between salinities 34.682 and 34.738. Below the iodate maxima, as salinity typically continued to drop, iodate concentration dropped to values sometimes lower than the ones found in UCDW (as in st.62-9404, st.60-9407 and st.63-9407). From iodate versus salinity plots (Figures 4.13a,b and c), it is apparent that iodate relationship with salinity is a very complex one, and iodate variation in these deep-water masses results from factors other than salinity changes alone.

Through iodate *vs.* salinity plots, one observes that iodate does not vary linearly with salinity, and continues to increase below the salinity maxima despite the decrease in salinity, with a sometimes-sharp decrease towards bottom waters. In order to confirm that iodate variation is due to differences in source water characteristics and/or in in-situ processes, rather than due to salinity changes, iodate concentrations were normalised to constant salinity (34.7) and plotted again against temperature (Figures 4.14a, b and c) and salinity (Figures 4.15a, b and c).

In the temperature *vs.* salinity-normalised (hereafter normalised) iodate plots (Figures 4.14a to c) very little change is observed compared with the non-normalised iodate plots. The only feature to notice is the dislocation of the normalised iodate maxima to deeper and colder waters, with seven out of 15 stations with maxima between 0 and 0.5°C within MLCDW. The sharp decrease in iodate concentration at the end of the transects can still been noticed (st.51-9501, st.62-9404 and st.63-9407).

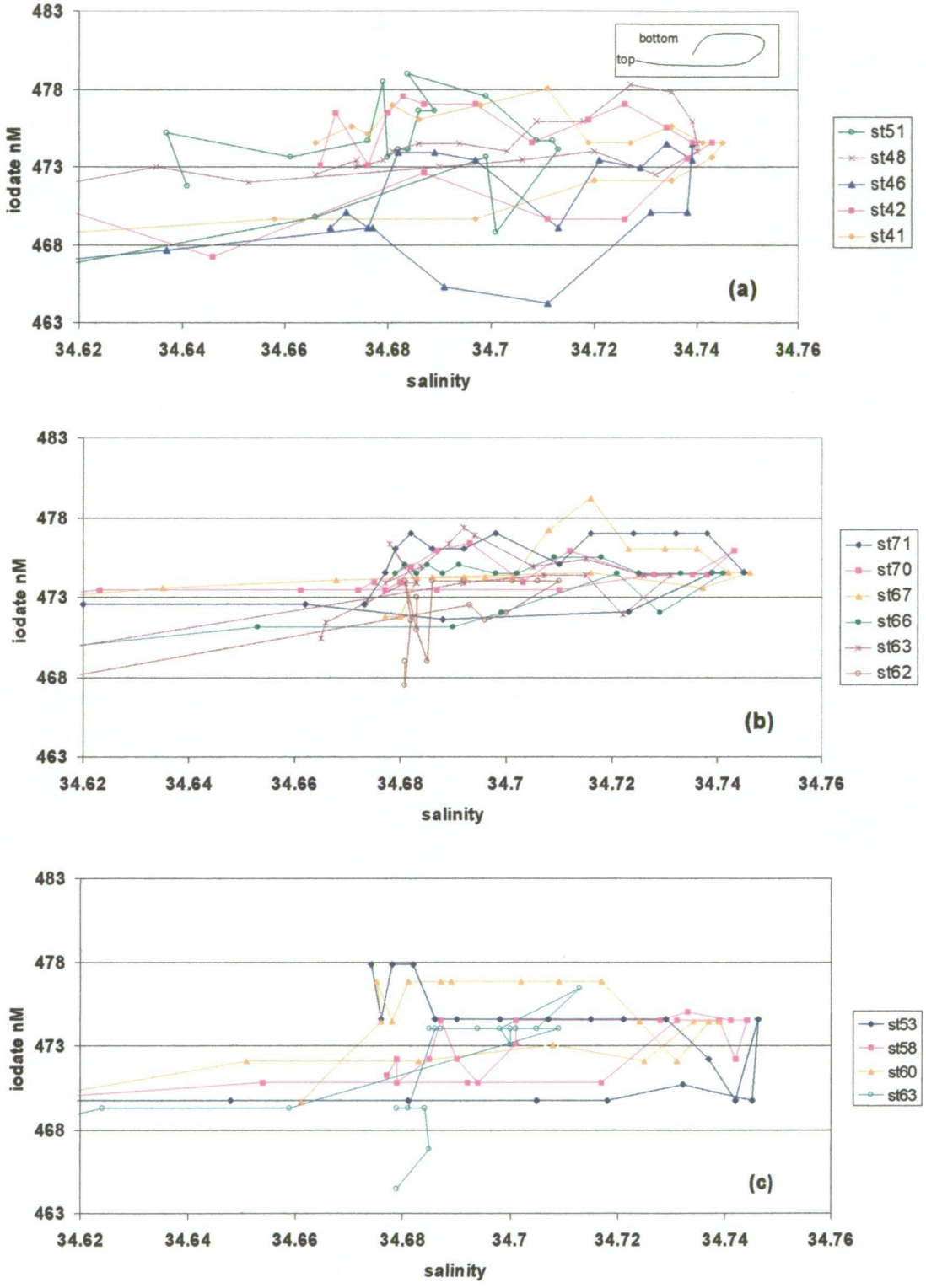

Figure 4.13- Iodate *vs.* salinity curves for stations where Antarctic Bottom Water (AABW) (t < 0°C, depth > 1000 m) was identified in the southern part of the SR3 transect. Cruise au9501 **(a)**: station 41 at 59.9°S and station 51 at 64.8°S. Cruise au9404 **(b)**: station 71 at 59.9°S and station 62 at 64.8°S. Cruise au9407 **(c)**: station 53 at 60.9°S and station 63 at 64.8°S.

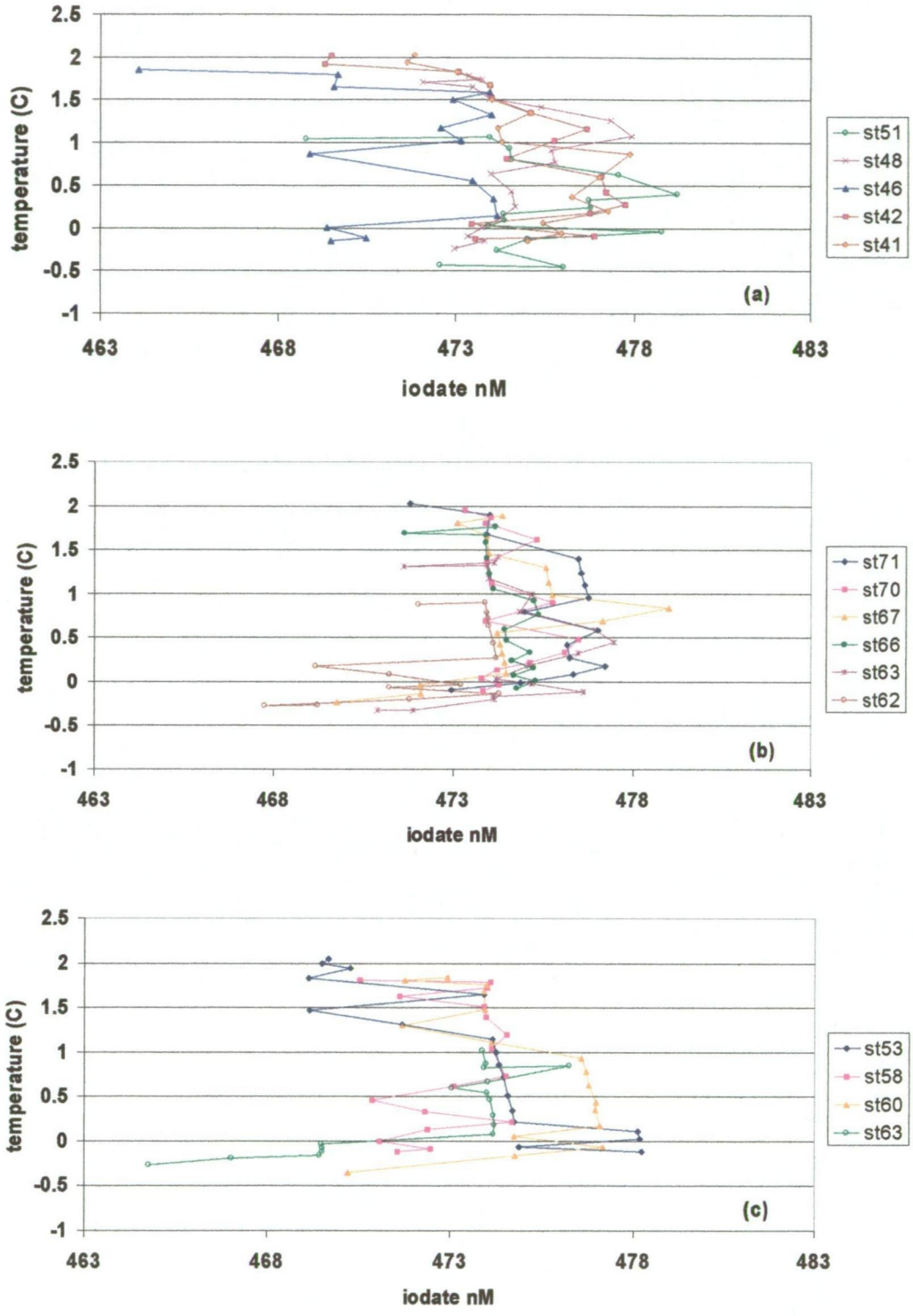

Figure 4.14- Temperature *vs.* salinity-normalised iodate curves for stations where Antarctic Bottom Water (AABW) (t < 0°C, depth > 1000 m) was identified in the southern part of the SR3 transect. Cruise au9501 **(a)**: station 41 at 59.9°S and station 51 at 64.8°S. Cruise au9404 **(b)**: station 71 at 59.9°S and station 62 at 64.8°S. Cruise au9407 **(c)**: station 53 at 60.9°S and station 63 at 64.8°S. Only LCDW, MLCDW and AABW are shown in these plots.

In the salinity *vs.* normalised iodate plots (Figures 4.15a to c), again very little change from non-normalised iodate plots can be noticed. As iodate maxima were dislocated to deeper waters, the salinity range was also displaced to lower values, with normalised iodate maxima for all stations lying between the salinities of 34.674 and 34.727. The normalised iodate plots demonstrate that the small changes observed in salinity between different water masses do not seem to affect the iodate pattern of decreasing concentrations toward bottom waters.

Over the years, since Elderfield and Truesdale (1980) introduced the idea of "rationalised" iodine and iodate values, normalisation of iodine concentration to a constant salinity has been used by several groups (Jickells *et al.*, 1988, Butler *et al.*, 1992, Truesdale, 1994, Truesdale *et al.*, 2000), and dismissed by others (Campos *et al.*, 1996a, Campos *et al.*, 1999, Farrenkopf, 2000). However, it is important to be cautious about the normalisation of nutrient data (including iodine) to same salinity, especially when dealing with different water masses. As LCDW and AABW are two independently formed water masses, they are expected to have their own characteristic temperature, salinity and nutrient (including iodine) concentration. In normalising iodine concentration, for instance within AABW, to salinity 34.7, iodate concentration in that water mass will artificially increase and no longer represent the measured concentration. Within the same water mass, general normalisation may function in correcting possible dilution/concentration effects and is especially useful when dealing within the surface layer, as done in section 4.1 earlier. However, the normalisation of iodine through different deep-water masses only assumes that water masses are a dilution (or concentration) of one-another, ignoring their own particular properties, origins and age. Here, non-normalised data will be presented in the following analysis (sections 4.2.3 and 4.2.4). The normalisation of iodine values will only be used as a comparison, to check on possible changes that could have been caused by the observed salinity changes. In normalising the iodate data, one can remove the effect of the salinity variation on iodate concentration, meaning that after normalisation the observed changes in iodate distribution are independent from salinity changes.

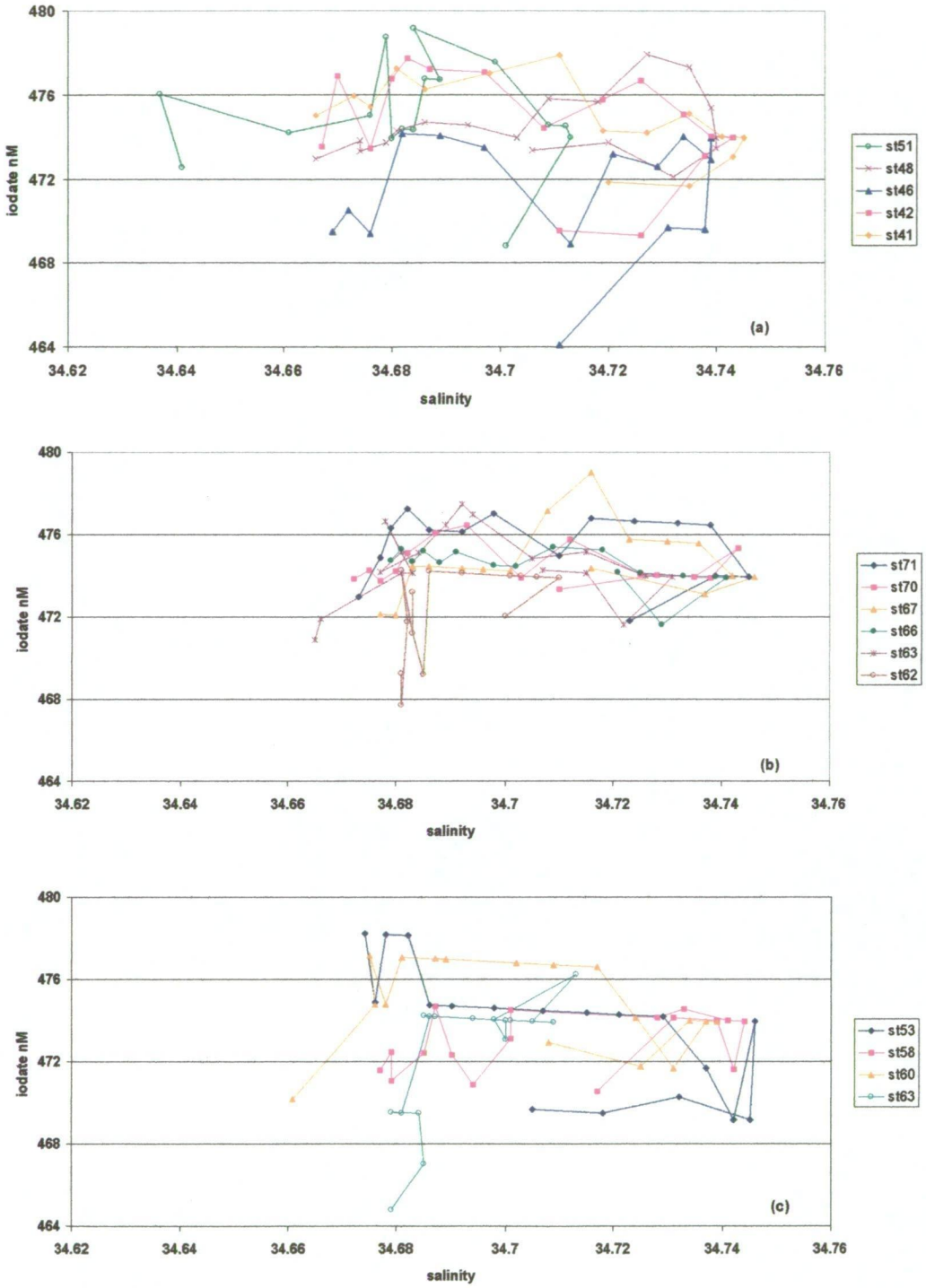

Figure 4.15- Salinity *vs.* salinity-normalised iodate curves for stations where Antarctic Bottom Water (AABW) (t < 0°C, depth > 1000 m) was identified in the southern part of the SR3 transect. Cruise au9501 **(a)**: station 41 at 59.9°S and station 51 at 64.8°S. Cruise au9404 **(b)**: station 71 at 59.9°S and station 62 at 64.8°S. Cruise au9407 **(c)**: station 53 at 60.9°S and station 63 at 64.8°S. Only LCDW, MLCDW and AABW are shown in these plots.

4.2.3 Measuring differences in iodate concentration between deep and bottom waters

4.2.3.1 The SR3 transect

As iodate concentration values seem to show a large variability, average values for each deep and bottom water masses were calculated and are compared, in order to test the hypothesis that iodate concentration in AABW is lower than in LCDW, independently of salinity changes between these two water masses.

Average iodate values for AABW, MLCDW, LCDW and UCDW for all the three cruises are listed on Table 4.10. Average iodate values were calculated for all the stations where that particular water mass was found along the SR3 transect. Water mass separation was made according to Orsi *et al.* (1995), Rintoul and Bullister (1999) and S. Rintoul (personal communication, 1999). AABW samples were defined as having pressure greater than 1000 dbar and temperatures below 0°C. LCDW samples were defined as having salinity greater than 34.7. MLCDW samples were defined as being deeper than LCDW, having salinities below 34.7 and temperatures greater than 0°C. UCDW samples were defined as being immediately above LCDW, having a dissolved oxygen minimum of less than 4.5 mL/L (200 μM) and salinities between 34.5 and 34.7.

Average values in Table 4.10 show that iodate concentration in AABW is 2 nM lower than in MLCDW and LCDW above and that average iodate concentration in MLCDW and in LCDW are very similar. This difference is smaller than the 0.6% precision value for iodate determination, but are proved to be statistically significant, considering that it is a difference between two average values of a relatively large number of samples. In order to establish if iodate concentration in AABW is lower than MLCDW and LCDW a Student's *t*-test (two-tailed) was used. The *t*-test confirmed that average iodate concentration for AABW is lower than the average iodate concentration for MLCDW at 99.9 % confidence level. The *t*-test also confirmed that average iodate concentration for AABW is lower than the average

Table 4.10-Average values of iodate concentration (*average values of salinity-normalised iodate concentration*) for different water masses for three cruises (au9501, au9404 and au9407) along the SR3 transect.

Water mass	**Average iodate concentration (nM)**	**Standard deviation (s) (nM)**	**Number of samples (n)**
AABW	472.4 (*472.8*)	3.0 (*3.0*)	48
MLCDW	474.4 (*474.6*)	2.4 (*2.4*)	113
LCDW	474.4 (*474.0*)	2.2 (*2.2*)	546
UCDW	472.2 (*473.4*)	2.7 (*2.7*)	228

iodate concentration for LCDW at the 99.9 % confidence level. Although the differences are small, they are statistically significant, which was confirmed by the *t* values found. In improving the reproductibility of the method for iodate determination, average iodate concentration for each water mass would fall in a closer envelope of values, and probably would result in a difference larger than 2 nM between AABW and LCDW. Most differences between iodate concentrations in AABW and in LCDW on a station-by-station basis were certainly higher than 2 nM, as is evident from the temperature versus iodate plots (Figures 4.12a to c).

Average normalised iodate concentrations for AABW, MLCDW, LCDW and UCDW are shown between parenthesis in Table 4.10. Normalised values varied from non-normalised values from 0.2 (MLCDW) to 1.2 (UCDW) nM of iodate. Although these changes are small, they are of the same order as the 2 nM difference between iodate concentration in deep and bottom water measured above. Differences in the average iodate concentration between AABW and MLCDW, and AABW and LCDW, decreased from 2 nM to 1.8 and 1.2 nM, respectively, after normalisation. Although the differences are small, *t*-tests again confirmed that this difference is statistically significant with average normalised iodate value for AABW being significantly lower than both normalised MLCDW and normalised LCDW at the 99.9% confidence level. This confirms the hypothesis that iodate concentration in AABW, along the SR3 transect, is lower than iodate concentration in LCDW and that this difference is independent from salinity variations.

4.2.3.2 The S4 transect

The lower iodate concentration in AABW relative to overlying MLCDW and LCDW was more noticeable in profiles along the SR3 transect than along the S4 transect (see Figure 3.15).

The S4 transect (cruise au9404) was parallel to and offshore of the Antarctic coast at approximately 63°S, from ~ 110°E to ~ 162°E (see Figure 3.1). Iodate concentrations from AABW, MLCDW and LCDW along the S4 transect were averaged and

compared, as for the SR3 transect. Iodate concentrations were also corrected according to the analytical correction described in section 3.3, based on the variability of the iodate concentration in the core of LCDW along the S4 transect. Average iodate values for the whole transect are presented in Table 4.11.

Although the number of iodate samples measured per water mass was smaller than in the SR3 section, *t*-tests between AABW and MLCDW or AABW and LCDW showed that the differences observed in iodate concentration were not significant, with a 50 % chance of being part of the same distribution curve. This result contrasts with results for the SR3 section and suggests that AABW inside the Australian-Antarctic basin may have different properties, or different origins along the coastline, other than Wilkes-Adélie Land between 138° and 158°E. This agrees with reported properties (temperature, salinity, dissolved oxygen and CFC content) of AABW inside the Australian-Antarctic Basin, which show that a strong signature of newly formed bottom water is found near the Mertz Polynya source, close to the south end of the SR3 transect (Rintoul, 1998; Bindoff *et al.*, 2000).

Average normalised iodate values for the S4 transect are again presented in parenthesis in Table 4.11. After normalisation, AABW average iodate value became 0.9 nM higher than LCDW. A *t*-test confirmed that the average normalised iodate value for AABW was higher than the average normalised iodate value for LCDW at the 98% confidence level. This again agrees with results previously described that the average iodate value for AABW along the S4 transect is actually slightly higher than average iodate value for LCDW for this same transect, in contrast with results along the SR3, described in sub-section 4.2.3.1, where average iodate value in AABW was found to be significantly lower than average iodate value in LCDW.

As the S4 transect covered a large extent of the Antarctic coast, stations are now considered in three sub-groups, in relation to the source of Adélie-Land Bottom Water (ALBW), from 138°E to 158°E (Rintoul, 1998), in an effort to better identify the source of the low iodate signal. The first sub-group of stations is west of 138°E, the second from 138°E to 158°E, and the third east of 158°. Averages for AABW,

Table 4.11- Average values of iodate concentration (*salinity-normalised iodate concentration*) for different water masses along the S4 transect (cruise au9404).

Water mass	**Average iodate concentration (nM)**	**Standard deviation (s) (nM)**	**Number of samples (n)**
AABW	473.7 (*474.0*)	2.8 (*2.8*)	38
MLCDW	474.1 (*474.3*)	2.4 (*2.4*)	52
LCDW	473.4 (*473.1*)	1.8 (*1.9*)	143

MLCDW and LCDW were then calculated for each of these sub-groups and are listed on Table 4.12.

Although limited by the small number of samples of ALBW, results in Table 4.12 seem to suggest that only ALBW (present between 138° and 158°E) show iodate concentration lower than the corresponding LCDW above it. ALBW was also lower than AABW to the west and to the east. Calculated *t*-tests between average iodate values for AABW and MLCDW or AABW and LCDW, for the three sub-groups on Table 4.12, showed that both AABW west of 138° and AABW east of 158° were not statistically different either from MLCDW or from LCDW (inside the same sub-group). However, *t*-test showed that the average iodate value for ALBW, sub-group 138° to 158°E, was statistically lower than the average iodate value for LCDW at the 95% confidence level. Iodate values for the three sub-groups of AABW were also compared using a *t*-test. Average iodate value for ALBW, between 138° and 158°E, was statistically lower than both AABW to the west and to the east, at the 95% and 90% confidence levels, respectively.

Average salinity-normalised iodate values are listed in Table 4.12, beside non-normalised values, in parenthesis. Little change again was noticed between normalised and non-normalised average values for iodate in different water masses. Again, as for the non-normalised data, normalised average iodate concentration in AABW was slightly lower than normalised average iodate concentration in LCDW only for the sub-group where ALBW is present, between 138° and 158°E. For the other sub-groups, west of 138° and east of 158°, AABW were slightly higher than LCDW, within each sub-group. A *t*-test again confirmed that average normalised iodate concentration for ALBW was different from both AABW to the west and to the east of the Wilkes-Adélie Land (138° to 158°E) at the 95% and 85% confidence levels, respectively.

Table 4.12 Average iodate values (*average salinity normalised iodate values*) for different water masses in three different sub-sections along the S4 transect, from 118°E to 162°E.

Water Mass	Average iodate value (nM)	Standard deviation (nM)	Number of samples
West of 138°E			
AABW	474.2 (*474.5*)	2.8	28
MLCDW	474.7 (*474.9*)	2.5	34
LCDW	473.6 (*473.3*)	1.9	74
138°E to 158°E			
ALBW	471.8 (*472.1*)	1.9	8
MLCDW	472.8 (*473.0*)	1.7	16
LCDW	473.2 (*472.8*)	1.6	34
East of 158°E			
AABW	474.6 (*474.6*)	0	2
MLCDW	474.9 (*474.9*)	0.4	2
LCDW	473.2 (*473.0*)	1.9	35

4.2.4 Comparison of results and discussion

Results presented in Sub-section 4.2.3 suggested that the low iodate signal, although small, is present predominantly near the source of ALBW, between 138° and 158°E, including the southern end of the SR3 section. Here in this sub-section, iodate results from the S4 section are compared with two most southerly stations from the SR3 section and three stations further west from the PET section (~ 85°E, see Chapter 3, Figure 3.1), where AABW was identified, in order to further investigate the findings from the previous sub-section.

Figure 4.16 shows the three sub-groups of AABW as previously divided along the S4 in Sub-Section 4.2.3.2. Station 10 (64.7°S, 111.9°E) belongs to section S4, but has not been corrected using the analytical correction, because of the absence of LCDW, and was thus not included in the "west of 138°E" sub-group. Station 60 and 65 (65.4°S, 139.8°E), belong to section SR3, cruises 9404 and 9407, respectively, and also were not considered before because of the absence of LCDW at that latitude. PET is a longitudinal transect across the Princess Elizabeth Trough and starts from the Antarctic coast east of Prydz Bay at ~ 85°E (see Section 3.1, Figure 3.1). PET data points are from stations 81, 85 and 88 (cruise 9407) at latitudes 65.7°S, 64.6°S and 63.7°S, respectively.

Figure 4.16a shows AABW distribution according to iodate and temperature. Highest iodate concentrations were found in AABW from station 10 (clear triangles), PET stations (clear diamonds), and one station (station 3, S4 transect, au9404, Figure 3.15) in particular from the "west of 138°E" sub-group at 62°S, 119°E (dark diamonds). Despite the high variability of iodate concentrations, it appears that ALBW points (light squares) have lower iodate concentrations than the "west of 138°E" sub-group, as pointed out before (Table 4.12), as do Stations 60 and 65 points (clear circles and squares). Stations 60 and 65 deepest points also had the lowest iodate concentrations (<465 nM) and the lowest temperatures (<-0.4°C). The higher concentration of iodate (>480 nM, dark diamonds) for AABW at station 3, at 62°S 119°E, could have been caused by an analytical problem. However, silicate

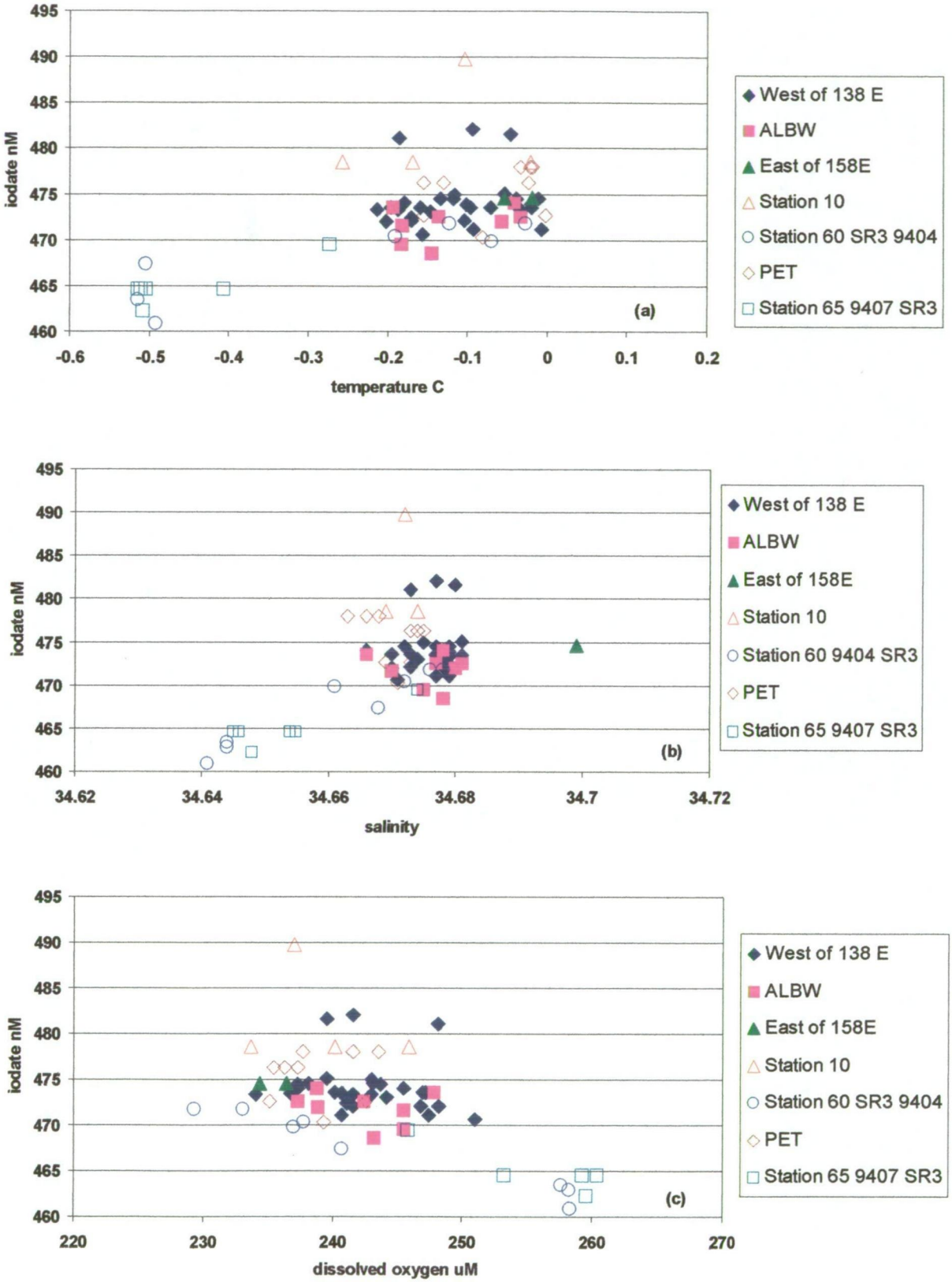

Figure 4.16- Iodate concentration for Antarctic Bottom Waters (AABW) (t < 0°C, depth > 1000 m) along the S4, SR3 (two stations only) and PET transects *versus* temperature **(a)**, salinity **(b)** and dissolved oxygen **(c)**.

profiles for this station (not shown here) also showed concentrations increasing in AABW, which may be a local feature of nutrient distribution at that particular site not related to salinity or temperature changes. Silicate contour for a longitudinal section off the Antarctic coast along 120°E in a more recent expedition (Bindoff *et al.*, 2000) showed that the low silicate (< 115 μM) signal near the bottom did not extend north of 63.5°S.

In Figure 4.16b, two overlapping points for AABW from one station east of 158° (dark triangles) show the influence of high-salinity Ross Sea Bottom Water (RSBW) (Rintoul, 1998), also with iodate concentrations higher than 474 nM. Lower salinities again coincided with lower iodate concentration for SR3 stations 60 and 65 (clear circles and squares), showing the fresh and cold characteristics of ALBW (Rintoul, 1998).

Figure 4.16c shows iodate variation with dissolved oxygen content in AABW. Most data points seem to fall between 233 and 248 μM of dissolved oxygen, with most of PET (clear diamonds) and AABW east of 158° (dark triangles) data points near the lower range (< 237 μM). Iodate concentration appear to drop as dissolved oxygen increases for ALBW (light squares), with an even more dramatic drop observed for the southerly SR3 stations (clear circles and squares), showing the high dissolved oxygen (>253 μM) and low iodate contents (<465 nM) of freshly-formed ALBW.

AABW data points for SR3 stations 60 and 65 (clear circles and squares, Figure 4.16) appear to have a good linear correlation with temperature, salinity and dissolved oxygen. These data points are the closest ones to ALBW origin, at the end of the SR3 section, and showed the largest iodate variation in all AABW plotted on Figure 4.16. It appears that the closer the data points were to the source, the stronger the iodate signal.

The lower concentration of iodate in AABW in relation to LCDW shows that this water has been recently ventilated, or in recent contact with the atmosphere (Fukamachi *et al.*, 2000). During summer months, the growth of microalgae

decreases the concentration of iodate and other nutrients (nitrate, silicate and phosphate) in surface shelf waters, which later in the winter will mix with Modified Circumpolar Deep Water (MCDW) to form AABW. Cold shelf water (SW) (< -1.7°C) inside the Adélie Depression is believed to mix with warmer high-salinity MCDW to form ALBW, which is dense enough to reach abyssal depths inside the Australian-Antarctic Basin (Rintoul, 1998; Orsi *et al.* 1999, Bindoff *et al.*, 2000). Although it is known that AABW is formed from two major source waters, MCDW and SW, the complete sequence of processes leading to its formation is not fully understood (Orsi *et al.*, 1999). SW (T = -1.7°C, salinity = 34.523) was present at the bottom (306 m) of Station 57, au9404, with iodate concentration of 454 nM. This iodate concentration is ~10 nM higher than iodate concentration in the surface in the summer, but it is still up to 10 nM lower than iodate concentration coming from offshore. So the relatively lower iodate concentration in SW also seems to reflect the uptake of iodate from the surface, as surface waters over the continental shelf mix with waters below to form SW in the winter. No iodate data for stations on the Antarctic continental shelf for the winter cruise were collected in order to confirm this. MCDW (T = 0.454°C, salinity = 34.69) was present at station 60 at 800 m, au9404, with iodate concentration of 474 nM. If, for instance, in a very simplistic approach, these observed SW and MCDW mix in equal amounts, the final iodate concentration would be 464 nM, which is very close to the measured iodate concentration of 463 nM for AABW found at the same station 60 (Figure 4.16, clear circles). However, SW with salinities higher than the one exemplified here (34.523) are needed to form ALBW, and these SW are found further inshore at the bottom of Adélie Depression (salinity > 34.6) (Rintoul, 1998), but no iodate data is available for these waters.

The influence of surface waters in bottom waters can also be observed by the good linear relationship between iodate and nutrients in freshly formed ALBW. AABW iodate data from station 60 (clear circles, Figure 4.16) showed a good linear correlation with both nitrate (R^2 = 0.9321) and silicate (R^2 = 0.9673). This linear relationship was not so good between iodate and nutrients for ALBW (light squares, Figure 4.16) with correlation coefficients dropping to 0.7440 and 0.5891, for nitrate and silicate, respectively. It appears that the further away from the source of AABW,

the poorer the correlation between iodate and nutrients. This feature may be explained by the surface water characteristics of freshly formed AABW, one of these being a good correlation between iodate and nutrients, being diluted out as it mixes with MLCDW, which shows the same typical poor correlation between iodate and nutrients as LCDW lying above it (Truesdale, 1994). The fact that iodate concentration in AABW may reflect biological uptake in the source water shows its potential as a biogeochemical tracer, with the possibility of tracing back dissolved CO_2 intake occurring in surface waters due to biological production close to the source of that specific bottom water. And perhaps iodate concentration in AABW would be able to indicate where that particular water was formed, or the primary productivity that was occurring in the source region.

Normalised-iodate data points for AABW were also plotted against temperature, salinity and dissolved oxygen and are shown on Figure 4.17. Again, there is little difference between non-normalised and normalised iodate data.

The variation of iodate concentration in AABW along the Australian-Antarctic Basin, considered here, from 85°E to 162°E, seems to be clearly related to ALBW formation and circulation within the basin. Wong *et al.* (1998) described low-salinity (< 34.68) bottom waters along a longitudinal section at Princess Elizabeth Trough at 80°E, which had characteristics of AABW local to the Australian-Antarctic Basin, and probably originated from Adélie Coast. Rintoul (1998) also showed that T-S curves for AABW at the PET transect (~ 85°E) are characteristic of Australian-Antarctic Basin bottom waters. According to Orsi *et al.* (1999), low salinity (<34.68) ALBW is formed along Wilkes-Adélie Coast (120°-160°E), then flows cyclonically along the southern and western rims of the Australian-Antarctic Basin, reaching as far as 90°E before turning back to flow to the east at lower latitudes. Although iodate variation was very small, it appeared that iodate concentration in bottom waters inside the Australian-Antarctic Basin increased the further away they were from their source in Adélie Land. At the end of the SR3 transect, the low iodate signal in AABW was stronger, decreased west of 138°E, and was not noticeable further west at 85°E at the PET transect. The apparent increase in iodate content in AABW from east to west along the Australian-Antarctic Basin might be related to an increase in

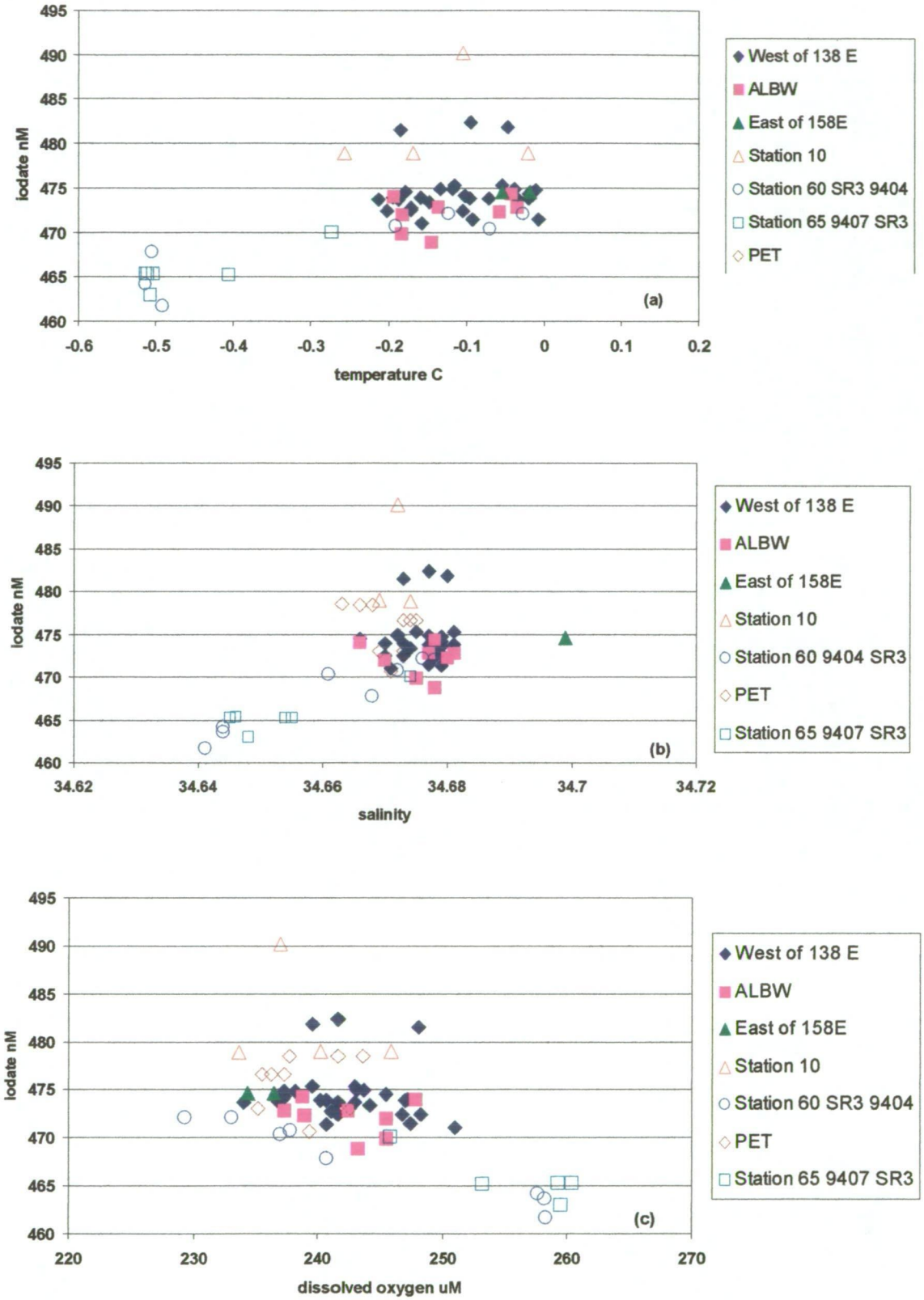

Figure 4.17- Salinity-normalised iodate concentration for Antarctic Bottom Waters (AABW) (t < 0°C, depth > 1000 m) along the S4, SR3 (two stations only) and PET transects *versus* temperature **(a)**, salinity **(b)** and dissolved oxygen **(c).**

salinity, as it would be expected if mixing with high iodate-high salinity LCDW was occurring. Bindoff *et al.* (2000) noted that bottom waters become progressively warmer and saltier to the west of 150°E, inside the Australian-Antarctic Basin. However, the increase in iodate concentration at PET (clear diamonds) is possibly related to the observed decrease in dissolved oxygen content in those waters, as salinity in AABW for the PET stations shown in Figure 4.16 is, on average, lower than ALBW (light squares) in the proximity of 140°E. AABW along the PET (clear diamonds) presents lower dissolved oxygen and higher iodate than ALBW, but lower salinity (Figure 4.16b and c). This apparent increase in iodate concentration in AABW at the PET then seems likely to be caused by respiration, with consumption of dissolved oxygen and remineralisation of iodine as iodate from organic matter, and not only by mixing with MLCDW above. Broecker *et al.* (1985) observed a good linear relationship between phosphate and dissolved oxygen for deep and intermediate ocean waters which appear to be constant for waters from the major ocean basins. On the other hand, if there are other sources of AABW between 80° and 138°E, they do not appear to have the same low iodate signature as ALBW. No strong signature of freshly formed AABW has been noticed in temperature, salinity, dissolved oxygen or CFCs along the same region (Bindoff *et al.*, 2000). The increase in iodate concentration in AABW, from Adélie Land to the west, inside the Australian-Antarctic Basin, suggests that, as ALBW enters the basin and travels westwards, it becomes older, with higher iodate and lower dissolved oxygen values, which is supported by Orsi *et al.* (1999) findings using CFCs as water mass tracers.

As most of the work published on iodine so far focuses in surface waters, no other results for iodate concentration in AABW are known. Campos *et al.* (1999) measured iodate in the western Weddell and Scotia Seas and reported concentrations of iodate, close to 500 (± 5%) nM, in deep waters. Cheng *et al.* (1993) reported one depth profile of iodate at 62.8°S, 80°E, where iodate concentration decreased between 500 and 1000 m, but no relation to water masses was made. It may be possible that both WSBW (from Campos *et al.*, 1999) and RSBW (as shown by the one station east of 158°E) do not have the low-iodate signature, which appears to be characteristic of freshly formed ALBW. Silicate contours for a longitudinal section in the South Atlantic along 40°W (Reid, 1989) showed a decrease in concentration close to the

bottom for a small part of the section between ~ 61° and 62°S, while silicate continue to increase towards the bottom for most of the waters with temperature below zero, here defined as AABW. This signal of lower nutrient concentration in bottom waters was not seen in the next contour further east at 30°W for both silicate and phosphate (Reid, 1989). This implies that the low nutrient signal observed by Reid (1989) in WSBW does not extend very far. In contrast, the low nutrient signal in ALBW, seen here for iodate, may extend further away from its source, maybe helped by the bathymetry inside the Australian Antarctic Basin. Silicate sections at near-bottom depths at the western Ross Sea (Mantyla and Reid, 1983) also showed low silicate (< 100 μM) distribution restricted to areas close to the source.

The decrease in iodate concentration associated with AABW described here has not been reported before. Looking at normalised and non-normalised iodate versus salinity plots, it was clear that iodate did not vary linearly with salinity through different water masses, but showed a complex relationship. Normalised and non-normalised average iodate values in AABW along the SR3 transect were statistically lower than normalised and non-normalised average iodate values in LCDW. These results demonstrate that the differences in iodate concentration between AABW and LCDW are a result of different source properties, including different iodate concentrations, and are independent of salinity changes.

Salinity and temperature are very good indicators of water mass distribution, but as emphasised by England and Maier-Reimer (2001), chemical tracers are of help in providing information about water mass formation and circulation that could not be obtained from temperature and salinity alone. The iodate cycle is also closely related to the carbon cycle, as seen before in section 4.1, and can provide other useful information as a biogeochemical tracer. Broecker *et al.* (1985) used "initial" phosphate concentration or PO_4^* ($PO_4^* = PO_4 + (O_2/175) - 1.95$ μmol/kg) as a conservative tracer to show the origin and flow patterns of LCDW in the Southern Ocean. Along the southern end of SR3, the low iodate signal also appear to be stronger than the low nitrate signal for AABW, with average nitrate concentration in LCDW being lower than its average concentration in AABW, the same occurring for silicate. This maybe explained by the differences in biogeochemical behaviour

between iodate and the other nutrients, with iodate being mostly recycled in the surface layer after biological uptake, nitrate being only partly recycled in surface waters and silicate dissolution occurring mostly in deep waters. Weiss *et al.* (1979) also found that silicate concentration in bottom waters from the Weddell Sea was non-conservative, with enrichments of up to ~ 35 μM coming mainly from interaction of these bottom waters with the bottom, and was not a good indicator of mixing processes between water masses.

The results of this study show that iodate concentration was on average statistically lower in AABW than in LCDW, which was noticeable mainly closer to the source of ALBW, between 138° and 158°E, and especially at the most southerly stations at the SR3 transect. According to iodate-depth profiles shown in Chapter 3 (Figure 3.15), west of 138°E, along the S4 transect, the low-iodate signal in AABW appeared only at some stations, and at 85°E, along the PET transect (Figure 3.13), iodate-depth profiles increased monotonically towards the bottom. East of 158°E, only one station was analysed for iodate at 162°E, and, again, iodate increased monotonically with depth with no distinction between deep and bottom water masses. Further studies, ideally making use of improved analytical precision and accuracy for iodate determination, are required to confirm these conclusions. Although there are no certified standards for iodine in seawater, inter-laboratory comparisons can help in determining approximate accuracy of the results. In addition to these iodate will also need to have discrimination beyond other tracers.

Although iodate measurements by flow injection analysis reported here contain a small analytical uncertainty, the need to measure very small differences in iodate concentration requires improving the long term precision of this method —as discussed before in section 3.3. This analytical improvement may turn iodate into a useful tool as a AABW tracer in the Southern Ocean. Iodate can easily be included as a commonly-measured hydrographic parameter, measured along with nitrate, silicate and phosphate by an autoanalyser, and may possibly, depending on analytical improvements, be of some help in understanding the origins and circulation patterns of AABW, especially ALBW within the Australian-Antarctic Basin.

CHAPTER 5- CONCLUSIONS

The main aim of this thesis was to study the distribution of iodate and iodide in the Australian sector of the Southern Ocean. This was achieved by the work described in this thesis. Analytical methods for determining iodine species were also carefully reviewed. It was decided that the existing method of Truesdale (1978a) could be modified successfully to produce a viable shipboard procedure for the Southern Ocean studies. However, for iodide it was judged necessary to develop a new method for direct measurement of the species that was compatible with conditions on board ship. A new method using ion chromatography with post-column reaction detection was successfully developed and used for shipboard analysis. Samples analysed during the second cruise (au9404) had a better detection limit than samples analysed from the third cruise (au9501). This could have been caused by the aging of the analytical column or equipment, due to constant injection of saline eluent and samples, causing an increase in the background signal. The use of syringe pump to deliver the post-column reagent has been suggested to decrease the baseline noise and improve the detection limit (Brandão *et al.*, 1995). However, in the future, electrostatic IC methods using zwitterionic surfactant-coated ODS columns, such as the one used by Hu and Haddad (1998) and Hu *et al.* (1999a,b), if automated, may provide a quicker and cheaper method for shipboard measurement of iodide in seawater samples.

Water-column iodate concentrations were measured along three different transects, one of these being the WOCE SR3 line, which was repeated three times in two different seasons. The SR3 section crosses the major water masses of the Southern Ocean and has thus provided a good opportunity to observe iodate variation among these. Iodate distributions confirmed earlier results, showing a sharp increase in surface waters south the subtropical front (STF) at ~46°S. Looking at the iodate *vs.* depth profiles in Chapter 3, it was also apparent that iodate distributions in both surface and deep waters varied in different water masses. Iodate distributions in intermediate, deep and bottom waters has not received much attention in previous studies. Here, important features were noted, including an iodate concentration decrease in bottom waters and an iodate depletion in surface waters in the winter mixed layer, in relation to deep waters, which may help us better understand the

marine biogeochemistry of iodine. In previous studies, iodate depletion in surface waters was related to deep water masses, mostly below 500 m depth. In the winter profiles depicted here, it appears that iodate depletion in surface waters (in relation to deep waters) is a permanent feature throughout the year, and thus may not be directly related to annual productivity events. However, a real iodate depletion was observed in surface waters between winter and summer, suggesting that biological iodate depletion does occur in surface waters, but in relation to winter surface layer concentrations rather than deep water concentrations. Iodate depletion in surface waters relative to deep waters, if used to estimate annual iodate uptake, would probably overestimate this figure several fold, depending on the region studied. Another process that deserves attention is the exchange of iodate in surface waters with that in waters below. For most of the studied region, intermediate and mode waters (in the SAZ) are directly beneath surface waters. So, simplified oceanic iodine cycles, such as the one shown in Figure 1.2, can consider iodate input to surface waters from deep waters, when in reality such exchanges are occurring with intermediate or mode waters, with exception of regions where deep waters sit immediately below surface waters, such as around 63°S latitude along the SR3 transect. Since iodate concentrations in intermediate waters are lower than in deep waters, fluxes considered between different "compartments", such as surface, intermediate, deep and bottom waters, might need to be taken into more detailed consideration.

Iodide showed the opposite trend to iodate, decreasing southwards along the SR3 transect. The decrease of iodide south of the STF was not so abrupt as the observed increase in iodate. Iodide concentration in deep waters was also measured for some stations, and at one station (St.91 at 50°S, Figure 3.20a) it appeared to increase close to the bottom of the profile. Seasonal variation of iodide concentration in surface waters could not be discerned, which was believed to be caused partly by slight deterioration in instrument performance and variability of measurements in the last research cruise. In both winter and summer profiles along the SR3 (Figure 3.7 and 3.20), a sub-surface maximum in iodide concentration was noticed in the Interpolar Frontal Zone, between the Polar Front north (PF-N) and the Polar Front south (PF-S). These features are believed to be related to a chlorophyll maximum observed by Parslow *et al.* (2001) for the same region. An iodate minimum accompanied one of

the observed iodide sub-surface maximum, suggesting that iodide production was likely to be coupled with iodate uptake during new or nitrate-based production, at that particular site. More data in this region are certainly necessary to confirm this observation.

Iodate contoured plots along the SR3 (Figures 3.6, 3.11 and 3.19) presented vertical patches in deep water, which were not related to either nitrate or phosphate distributions, or any known physical parameters, such as salinity or temperature. However, the patches were related to different days of analysis, which confirmed that the long-term precision or reproducibility of the method used was higher than the short term precision measurements calculated for samples analysed in the same day. As the variability of the measurements was not related to a blank or offset, but to the slope of the calibration curves, a multiplicative correction, called analytical correction was applied to all the iodate data along the SR3 in relation to a stable deep water mass (LCDW). Iodate contours of corrected data no longer showed the vertical patches and confirmed that the patches were caused by daily variations during iodate analysis. These results suggest that the automated colorimetric method from Truesdale (1978a) for iodate analysis needs the introduction of a sample of well known concentration to be measured on a daily basis to correct for these variations, as suggested and more recent papers (Truesdale *et al.*, Truesdale and Bailey, 2000).

Seasonal iodate depletion in surface waters was also successfully used to estimate seasonal new production along the SR3 transect. The link between iodine and carbon cycles in the oceans has long been studied (Wong and Brewer, 1974; Elderfield and Truesdale, 1980; Tian *et al.*, 1996; Campos *et al.*, 1996a; Wong and Hung, 2001; Wong, 2001). Here, in this study, the link is again confirmed. Although the excellent correlation of iodate and nitrate in surface waters of subtropical oceanic zones is no longer observed in subantarctic and antarctic waters, the distributions of these species still related well in surface waters from these zones. From the iodate data obtained in this work, the relationship between iodate and nitrate appears to change from subtropical to subantarctic waters, with more iodate being assimilated or reduced per mole of nitrate in the warmer subtropical waters than in the cooler subantarctic waters. South of 63°S, in the proximity of the southern Antarctic Circumpolar Current front (SACCF), this relationship appears to change again, with

more iodate being taking up or reduced per mole of nitrate, concomitant with an increase in phytoplankton productivity in the area. It has been suggested previously (Campos *et al.*, 1999) that the decrease in iron concentration from subtropical to subantarctic surface waters (Sedwick *et al.*, 1999) may restrict the activity of nitrate reductase enzyme (Martin *et al.*, 1990). Because this enzyme is also reputedly responsible for iodate reduction (Wong and Hung, 2001), diminished levels of it may be responsible for the observed increase in iodate concentration in subantarctic waters. As iodate and nitrate concentrations both increased south of the STF, the iodate-to-nitrate uptake ratio also appeared to decrease, suggesting that if nitrate reductase activity was limited south of the STF, so was the ratio to which iodate is preferred to nitrate during nitrate uptake. This was also supported by the findings at the Antarctic zone south of 63°S (AZ-S), with the observed increase in iodate-to-nitrate uptake ratio possibly linked to an observed increase in dissolved iron in the region (Measures and Vink, 2001). In turn, this may have increased nitrate reductase activity and possibly decreased competition between iodate and nitrate during nitrate uptake. Changes in the biological communities between different zones in the Southern Ocean may also be a reason to the observed changes in iodate-to-nitrate uptake ratio. More studies are necessary to confirm both of these possible links. Dissolved iron concentrations in surface waters have not been confirmed to directly limit nitrate reductase activity, but as nitrate reductase extracted from phytoplankton in subtropical regions has been shown to reduce iodate to iodide (Wong and Hung, 2001), it is likely that this enzyme is also responsible for iodate reduction in the Southern Ocean. Dissolved iron concentration measurements coincident with nitrate reductase and iodate measurements in the Southern Ocean are needed to confirm this hypothesis and should be considered for future work. Direct biological uptake of iodate and its relation to iron concentration can also be carried out in phytoplankton cultures and it would possibly be an appropriate complement to the work done in this thesis.

Although the seasonal depletion of iodate in surface waters has been observed before in the Mediterranean Sea (Tian *et al.*, 1996) and in the Bermudan waters (Jickells *et al.*, 1988; Campos *et al.*, 1996a), it had not been used to estimate seasonal new production prior to this work. Iodate depletion from winter (July) to summer (January) was highest in the subtropical zone (STZ), decreasing from the

Subantarctic zone (SAZ) into the Antarctic zone north of 63°S. In the Antarctic zone south of 63°S, a relative increase in iodate depletion was observed, with depletion occurring to greater depths than further north, probably related to higher productivity in that region. Seasonal new production estimates, calculated from depth-integrated iodate depletions, led to values within the ones calculated for the Southern Ocean by other investigations. The observed iodate depletion might have been coupled with iodide production, as suggested by Wong (2001); however, an iodide increase from winter to summer was not observed. This may reflect analytical limitations, which did not allow resolution of small changes in iodide, or perhaps that iodate uptake was not directly coupled with iodide release, contrary to what Wong and Hung (2001) observed in the East China Sea. Perhaps iodate was taken up by phytoplankton and reduced, but not released immediately, being partly exported to intermediate waters as particulate matter. Any small fraction of iodate that might have been reduced and released as iodide in surface waters was likely to fall below the analytical capabilities of the methods used in this work, as considered before. However, the findings from this work support Wong's (2001) findings that iodate (and not total iodine) uptake is directly coupled with nitrate-based or new production, because only iodate (and not total iodine) was depleted in surface waters of the studied region from winter to summer. Here again, the use of phytoplankton cultures would be an appropriate follow up work to confirm iodine cycling in subantarctic and Antarctic waters.

Iodate distribution also proved useful to identify AABW along the southern end of the SR3 transect. The presence of a large number of water masses in the Southern Ocean provided a unique opportunity to observe these changes, especially with the intrusion of freshly formed Adélie Land Bottom Water (ALBW) at the southern end of the SR3 transect. Iodate concentrations were lower in AABW than in LCDW above, and differences were not related to observed salinity changes, because they were also seen for salinity-normalised iodate values. There has been no previous studies of iodine distribution in deep and bottom waters in the Southern Ocean. Results of this study suggested that as AABW is formed partly from waters that have been exposed to the surface in the summer, where biological activity can be intense and nutrient decrease noticeable, the lower iodate concentration in these waters is partly preserved and becomes a signal in freshly formed ALBW. Iodate's good correlation to nitrate and other nutrients also confirmed surface waters characteristics

attribute to ALBW. Contrary to other nutrients, iodate input from remineralised organic matter (or in the case of silica, dissolution of planktonic shells) in the water column and from the bottom, is minimal. Thus the low iodate signature in AABW is perhaps more likely to extend further from its source than nitrate or silicate, as noticed in the southern part of the SR3, where iodate (but not nitrate or silicate) concentrations were lower in AABW than in both LCDW and in MLCDW below. These results also suggested that the distribution of iodate in bottom waters in the Southern Ocean is primarily related to the origins of these water masses, and not to differences in salinity. The results also highlight the close link between iodate and nitrate uptake in surface waters, and consequently the close link between iodate and carbon cycling in these waters, which would still remain and could be traced in freshly formed ALBW. So the suggestion by previous workers that iodate concentration in deep waters is directly proportional to salinity was not confirmed by the results presented here in deep and bottom waters from the Southern Ocean. Further studies of dissolved iodate-to-nitrate ratio in newly formed bottom waters may be of help in tracing productivity levels of the source surface shelf water prior to mixing and bottom water formation.

REFERENCES

Arrigo, K. R., Worthen, D. L., Schnell, A., and Lizotte, M. P. (1998). Primary production in Southern Ocean waters. *J.Geophys.Res., [Oceans]* **103**, 15587-15600.

Barkley, R. A. and Thompson, T. G. (1960a). The total iodine and iodate-iodine content of sea-water. *Deep-Sea Res.*, 7, 24-34.

Barkley, R. A. and Thompson, T. G. (1960b). Determination of chemically combined iodine in sea water by amperometric and catalytic methods. *Anal.Chem.* **32**, 154-158.

Bates, N. R., Hansell, D. A., Carlson, C. A., and Gordon, L. I. (1998). Distribution of CO2 species, estimates of net community production, and air-sea CO2 exchange in the Ross Sea polynya. *J.Geophys.Res., [Oceans]* **103**, 2883-2896.

Belkin, I. M. and Gordon, A. L. (1996). Southern Ocean fronts from the Greenwich meridian to Tasmania. *J.Geophys.Res., [Oceans]* **101**, 3675-3696.

Bindoff, N. L., Rosenberg, M. A., and Warner, M. J. (2000). On the circulation and water masses over the Antarctic continental slope and rise between 80 and 150 degrees E. *Deep-Sea Res., Part II* **47**, 2299-2326.

Boyd, P. W., LaRoche, J., Gall, M., Frew, R., and Mckay, R. M. L. (1999). Role of iron, light, and silicate in controlling algal biomass in subantarctic waters SE of New Zealand. *J.Geophys.Res., [Oceans]* **104**, 13,395-13,408.

Brandão, A. C. M. (1992). Experimento-modelo para estudo da influência de processos fotoquímicos e biológicos na especiação do iodo em água do mar . *M.Sc.Thesis* **PUC-Rio**, 81pp.

Brandão, A. C. M., Wagener, A. d. L., and Wagener, K. (1994). Model experiments on the diurnal cycling of iodine in seawater. *Mar.Chem.* **46**, 25-31.

Brandão, A. C. M., Buchberger, W. W., Butler, E. C. V., Fagan, P. A., and Haddad, P. R. (1995). Matrix-elimination ion chromatography with post-column reaction detection for the determination of iodide in saline waters. *J.Chromatogr., A* **706**, 271-275.

Broecker, W. S. and Peng, T. H. (1982). 'Tracers in the sea.' (Lamont-Doherty Geological Observatory: Columbia University, Palisades, NY.)

Broecker, W. S., Takahashi, T., and Takahashi, T. (1985). Sources and flow patterns of deep-ocean waters as deduced from potential temperature, salinity, and initial phosphate concentration. *J.Geophys.Res., [Oceans]* **90**, 6925-6939.

Buchberger, W. (1988). Determination of iodide and bromide by ion chromatography with post-column reaction detection. *J.Chromatogr.* **439**, 129-135.

Butler, E. C. V. (1981). Studies of iodine in natural waters. *PhD thesis.* **University of Melbourne**, 285pp.

Butler, E. C. V. (1996). The analytical chemist at sea: measurements of iodine and arsenic in marine waters. *TrAC, Trends Anal.Chem.* **15**, 45-52.

Butler, E. C. V. and Gershey, R. M. (1984). Application of ion-exchange chromatography with an ion-selective electrode detector to iodine determination in natural waters. *Anal.Chim.Acta* **164**, 153-161.

Butler, E. C. V. and Plaschke, R. B. (1988). Iodate as a chemical tracer in marine waters. *Proc.Australian Marine Sciences Association Jubilee Conference 1963-1988* 159-163.

Butler, E. C. V. and Smith, J. D. (1980). Iodine speciation in sea waters - the analytical use of ultraviolet photo-oxidation and differential pulse polarography. *Deep-Sea Res., Part A* **27**, 489-493.

Butler, E. C. V., Smith, J. D., and Fisher, N. S. (1981). Influence of phytoplankton on iodine speciation in seawater. *Limnol.Oceanogr.* **26**, 382-386.

Butler, E. C. V., Burton, H. R., and Smith, J. D. (1988). Iodine distribution in an antarctic meromictic saline lake. *Hydrobiologia* **165**, 97-101.

Butler, E. C. V., Butt, J. A., Lindstrom, E. J., Tildesley, P. C., Pickmere, S., and Vincent, W. F. (1992). Oceanography of the Subtropical Convergence Zone around southern New Zealand. *N.Z.J.Mar.Freshwater Res.* **26**, 131-154.

Callahan, J. E. (1972). The structure and circulation of deep water in the Antarctic. *Deep-Sea Res.*, **19**, 563-575.

Campos, M. L. A. M. (1997). New approach to evaluating dissolved iodine speciation in natural waters using cathodic stripping voltammetry and a storage study for preserving iodine species. *Mar.Chem.* **57**, 107-117.

Campos, M. L. A. M., Farrenkopf, A. M., Jickells, T. D., and Luther, G. W., III (1996a). A comparison of dissolved iodine cycling at the Bermuda Atlantic Time-series station and Hawaii Ocean Time-series station. *Deep-Sea Res., Part II* **43**, 455-466.

Campos, M. L. A. M., Nightingale, P. D., and Jickells, T. D. (1996b). A comparison of methyl iodide emissions from seawater and wet depositional fluxes of iodine over the southern North Sea. *Tellus, Ser.B* **48B**, 106-114.

Campos, M. L. A. M., Sanders, R., and Jickells, T. (1999). The dissolved iodate and iodide distribution in the South Atlantic from the Weddell Sea to Brazil. *Mar.Chem.* **65**, 167-175.

Chameides, W. L. and Davis, D. D. (1980). Iodine: its possible role in tropospheric photochemistry. *J.Geophys.Res., [Oceans]* **85**, 7383-7398.

Chapman, P. (1983). Changes in iodine speciation in the Benguela Current upwelling system. *Deep-Sea Res., Part A* **30**, 1247-1259.

Chapman, P. and Liss, P. S. (1977). The effect of nitrite on the spectrophotometric determination of iodate in seawater. *Mar.Chem.* **5**, 243-249.

Cheng, X., Yu, G., and Zhang, P. (1993). Zonal discrepancy of iodine in the West Pacific Ocean and adjacent seas. *Acta Oceanologica Sinica* **12**, 405-415.

Cheng, X., Pan, J., Zhang, H., and Zhang, P. (1994). Biolimitation of iodine distribution in Antarctic Ocean. *Oceanologia et limnologia sinica.Haiyang Yu Huzhao* **25**, 38-47. (in chinese).

Cook, P. L. M., Carpenter, P. D., and Butler, E. C. V. (2000). Speciation of dissolved iodine in the waters of a humic-rich estuary. *Mar.Chem.* **69**, 179-192.

Copin-Montegut, C. and Copin-Montegut, G. (1978). The chemistry of particulate matter from the south Indian and Antarctic oceans. *Deep-Sea Res., Part II* **25**, 911-931.

De Baar, H. J. W., Van Leeuwe, M. A., Scharek, R., Goyens, L., Bakker, K. M. J., and Fritsches, P. (1997). Nutrient anomalies in *Fragilariopsis kerguelensis* blooms, iron deficiency and the nitrate/phosphate ratio (A. C. Redfield) of the Antarctic Ocean. *Deep-Sea Res., Part II* **44**, 229-260.

Deacon, G. E. R. (1984). Oxygen in Antarctic water. *Deep-Sea Res., Part A* **31**, 1369-1371.

Dionex Corporation (2000). IONPAC AS11 Column Care. In 'DIONEX- Manuals and Literature'. CD-rom, Dionex Corporation.

Dubravcic, M. (1955). Determination of iodine in natural waters (sodium chloride as a reagent in the catalytic reduction of ceric ions). *Analyst* **80**, 295-300.

Elderfield, H. and Truesdale, V. W. (1980). On the biophilic nature of iodine in seawater. *Earth Planet.Sci.Lett.* **50**, 105-114.

England, M. H. (1995). Using chlorofluorocarbons to assess ocean climate models. *Geophys.Res.Lett.* **22**, 3051-3054.

England, M. H. and Maier-Reimer, E. (2001). Using chemical tracers to assess ocean models [Review]. *Reviews of Geophysics* **39**, 29-70.

Eppley, R. W. (1989). New production: history, methods, problems. In 'Productivity of the ocean: present and past'. (Eds. W. H. Berger, V. S. Smetacek, and G. Wefer.) pp. 85-97. (John Wiley & Sons: New York.)

Fagan, P. A. and Haddad, P. R. (1991). Determination of free cyanide in gold cyanidation process liquors by ion-interaction chromatography with post-column derivatization. *J.Chromatogr.* **550**, 559-571.

Farrenkopf, A. M. (2000). Iodine speciation at the Hawaii ocean time-series station ALOHA and in the Arabian Sea. *PhD thesis* **University of Delaware**, 213pp.

Farrenkopf, A. M., Luther, G. W., III, Truesdale, V. W., and Van Der Weijden, C. H. (1997a). Sub-surface iodide maxima: evidence for biologically catalyzed redox cycling in Arabian Sea OMZ [oxygen minimum zone] during the SW intermonsoon. *Deep-Sea Res., Part II* **44**, 1391-1409.

Farrenkopf, A. M., Dollhopf, M. E., Chadhain, S. N., George, W., and Nealson, K. H. (1997b). Reduction of iodate in seawater during Arabian Sea shipboard incubations and in laboratory cultures of the marine bacterium Shewanella putrefaciens strain MR-4. *Mar.Chem.* **57**, 347-354.

Franck, V. M., Brzezinski, M. A., Coale, K. H., and Nelson, D. M. (2000). Iron and silicic acid concentrations regulate Si uptake north and south of the Polar Frontal Zone in the Pacific Sector of the Southern Ocean. *Deep-Sea Res., Part II* **47**, 3315-3338.

Fukamachi, Y., Wakatsuchi, M., Taira, K., Kitagawa, S., Ushio, S., Takahashi, A., Oikawa, K., Furukawa, T., Yoritaka, H., Fukuchi, M., and Yamanouchi, T. (2000). Seasonal variability of bottom water properties off Adelie Land, Antarctica. *J.Geophys.Res., [Oceans]* **105**, 6531-6540.

Fuse, H., Takimura, O., and Yamaoka, Y. (1989). Effects of iodide and iodate ions on marine phytoplankton. In 'Red Tides: Biol., Environ.Sci., Toxicol..Proc.1st Int.Symp.'. (Eds. T. Okaishi, D. Anderson, and T. Nemoto.) pp. 229-32. (Elsevier: Amsterdan).

Garland, J. A. and Curtis, H. (1981). Emission of iodine from the sea surface in the presence of ozone. *J.Geophys.Res., [Oceans]* **86C**, 8183-8186.

Giese, B., Laturnus, F., Adams, F. C., and Wiencke, C. (1999). Release of Volatile Iodinated C1-C4 Hydrocarbons by Marine Macroalgae from Various Climate Zones. *Environ.Sci.Technol.* **33**, 2432-2439.

Gordon, A. L. and Tchernia, P. (1972). Waters of the continental margin off Adélie coast, Antarctica. In 'Antarctic Oceanology II: the Australian-New Zealand sector'. (Ed. D. E. Hayes.) pp. 59-69.

Gozlan, R. S. and Margalith, P. (1973). Iodide oxidation by a marine bacterium. *J.Appl.Bacteriol.* **36**, 470-17.

Gozlan, R. S. and Margalith, P. (1974). Iodide oxidation by *Pseudomonas iodooxidans*. *J.Appl.Bacteriol.* **37**, 493-499.

Greenwood, N. N. and Earnshaw, A. (1984). 'Chemistry of the Elements.' (Pergamon Press: Oxford.)

Griffiths, F. B., Bates, T. S., Quinn, P. K., Clementson, L. A., and Parslow, J. S. (1999). Oceanographic context of the first Aerosol Characterization Experiment (ACE 1): a physical, chemical, and biological overview. *J.Geophys.Res., [Atmos.]* **104** (D17), 21649-21671.

Gschwend, P. M., MacFarlane, J. K., and Newman, K. A. (1985). Volatile halogenated organic compounds released to seawater from temperate marine macroalgae. *Science (Washington, D.C.)* **227**, 1033-1035.

Haddad, P. R. and Jackson, P. E. (1990). 'Ion chromatography: principles and applications.' (Elsevier: Amsterdam, Netherlands).

Happell, J. D. and Wallace, D. W. R. (1996). Methyl iodide in the Greenland/Norwegian Seas and the tropical Atlantic Ocean: evidence for photochemical production. *Geophys.Res.Lett.* **23**, 2105-2108.

Herring, J. R. and Liss, P. S. (1974). New method for the determination of iodine species in sea water. *Deep-Sea Res.* **21** , 777-783.

Hoppema, M. and Goeyens, L. (1999). Redfield behavior of carbon, nitrogen, and phosphorus depletions in Antarctic surface water. *Limnol.Oceanogr.* **44**, 220-224.

Hu, W. and Haddad, P. R. (1998). Electrostatic ion chromatography using dilute electrolytes as eluents: a new method for separation of anions. *Anal.Commun.* **35**, 317-320.

Hu, W., Haddad, P. R., Hasebe, K., Tanaka, K., Tong, P., and Khoo, a. C. (1999a). Direct Determination of Bromide, Nitrate, and Iodide in Saline Matrixes Using Electrostatic Ion Chromatography with an Electrolyte as Eluent. *Anal.Chem.* **71**, 1617-1620.

Hu, W., Hasebe, K., Tanaka, K., and Haddad, P. R. (1999b). Electrostatic ion chromatography of polarizable anions in saline waters with N-{2-[acetyl(3-sulfopropyl)amino]ethyl}-N,N-dimethyldodecanaminium hydroxide (ammonium sulfobetaine-1) as the stationary phase and a dilute electrolytic solution as the mobile phase. *J.Chromatogr., A* **850**, 161-166.

Ishii, M., Inoue, H. Y., Matsueda, H., and Tanoue, E. (1998). Close coupling between seasonal biological production and dynamics of dissolved inorganic carbon in the Indian Ocean sector and the western Pacific Ocean sector of the Antarctic Ocean. *Deep-Sea Res., Part I* **45**, 1187-1209.

Ito, K. (2001). Semi-micro ion chromatography of iodide in seawater using ODS column coated with cetyltrimethylammonium. *Journal of Chromatography* **Symposium volume**, submitted.

Ito, K. and Sunahara, H. (1990). Ion chromatography with ultraviolet and amperometric detection for iodide and thiocyanate in concentrated salt solutions. *J.Chromatogr.* **502**, 121-129.

Jennings, J. C., Jr., Gordon, L. I., and Nelson, D. M. (1984). Nutrient depletion indicates high primary productivity in the Weddell Sea. *Nature (London)* **309**, 51-54.

Jickells, T. D., Boyd, S. S., and Knap, A. H. (1988). Iodine cycling in the Sargasso Sea and the Bermuda inshore waters. *Mar.Chem.* **24**, 61-82.

Johannesson, J. K. (1957). Nature of the bactericidal agent in sea water. *Nature* **180** , 285-286.

Johannesson, J. K. (1958). Oxidized iodine in sea water. *Nature* **182**, 251.

Karl, D. M., Tilbrook, B. D., and Tien, G. (1991). Seasonal coupling of organic matter production and particle flux in the western Bransfield Strait, Antarctica. *Deep-Sea Res., Part A* **38**, 1097-1126.

Kennedy, H. A. and Elderfield, H. (1987). Iodine diagenesis in pelagic deep-sea sediments. *Geochim.Cosmochim.Acta* **51**, 2489-2504.

Klick, S. and Abrahamsson, K. (1992). Biogenic volatile iodated hydrocarbons in the ocean. *J.Geophys.Res., [Oceans]* 97, 12683-12687.

Lambert, J. L., Ramasamy, J., and Paukstelis, J. V. (1975). Stable reagents for the colorimetric determination of cyanide by modified Koenig reactions. *Anal.Chem.* **47**, 916-918.

Laturnus, F. (1995). Release of volatile halogenated organic compounds by unialgal cultures of polar macroalgae. *Chemosphere* **31**, 3387-3395.

Laturnus, F. (2001). Marine macroalgae in polar regions as natural sources for volatile organohalogens. *Environ.Sci.Pollut.Res.Int.* **8**, 103-108.

Laturnus, F. and Adams, F. C. (1998). Methyl halides from Antarctic macroalgae. *Geophys.Res.Lett.* **25**, 773-776.

Laturnus, F., Wiencke, C., and Kloeser, H. (1996). Antarctic macroalgae-sources of volatile halogenated organic compounds. *Mar.Environ.Res.* **41**, 169-181.

Longhurst, A., Sathyendranath, S., Platt, T., and Caverhill, C. (1995). An estimate of global primary production in the ocean from satellite radiometer data. *Journal of Plankton Research* **17**, 1245-1271.

Lourey, M. J. and Trull, T. W. (2001). Seasonal Nutrient Depletion and Carbon Export in the Sub-Antarctic and Polar Frontal Zones of the Southern Ocean, south of Australia. *J.Geophys.Res., [Oceans]* **SAZ project special section**, submitted.

Lovelock, J. E. (1975). Natural halocarbons in the air and in the sea. *Nature (London)* **256**, 193-194.

Lovelock, J. E., Maggs, R. J., and Wade, R. J. (1973). Halogenated hydrocarbons in and over the Atlantic. *Nature (London)* **241**, 194-196.

Luther, G. W., III and Cole, H. (1988). Iodine speciation in Chesapeake Bay waters. *Mar.Chem.* **24**, 315-325.

Luther, G. W., III, Swartz, C. B., and Ullman, W. J. (1988). Direct determination of iodide in seawater by cathodic stripping square wave voltammetry. *Anal.Chem.* **60** , 1721-1724.

Luther, G. W., III, Ferdelman, T., Culberson, C. H., Kostka, J., and Wu, J. (1991). Iodine chemistry in the water column of the Chesapeake Bay: evidence for organic iodine forms. *Estuarine, Coastal Shelf Sci.* **32**, 267-279.

Luther, G. W., III, Wu, J., and Cullen, J. B. (1995). Redox chemistry of iodine in seawater: Frontier molecular orbital theory considerations. In 'Aquatic Chemistry: Interfacial and Interspecies Processes'. (Eds. C. P. Huang, C. R. O'Melia, and J. J. Morgan.) pp. 135-55. (American Chemical Society: Washington, DC.)

Manley, S. L. (1994). The possible involvement of methylcobalamin in the production of methyl iodide in the marine environment. *Mar.Chem.* **46**, 361-369.

Manley, S. L. and Dastoor, M. N. (1988). Methyl iodide (CH3I) production by kelp and associated microbes. *Mar.Biol.(Berlin)* **98**, 477-482.

Manley, S. L. and de la Cuesta, J. L. (1997). Methyl iodide production from marine phytoplankton cultures. *Limnol.Oceanogr.* **42**, 142-147.

Manley, S. L., Goodwin, K., and North, W. J. (1992). Laboratory production of bromoform, methylene bromide, and methyl iodide by macroalgae and distribution in nearshore southern California waters. *Limnol.Oceanogr.* **37**, 1652-1659.

Mantyla, A. W. and Reid, J. L. (1983). Abyssal characteristics of the World Ocean waters. *Deep-Sea Res.* **30**, 805-833.

Marheni, Haddad, P. R., and McTaggart, A. R. (1991). On-column matrix elimination of high levels of chloride and sulfate in non-suppressed ion chromatography. *J.Chromatogr.* **546**, 221-228.

Martin, J. H., Fitzwater, S. E., and Gordon, R. M. (1990). Iron deficiency limits phytoplankton growth in Antarctic waters. *Global Biogeochem.Cycles* **4**, 5-12.

Matthews, A. D. and Riley, J. P. (1970). A study of Sugawara's method for the determination of iodine in seawater. *Anal.Chim.Acta* **51**, 295-301.

McTaggart, A. R. (1994). Dimethylsulfide and iodine in Australian waters. *PhD thesis.* **University of New South Wales**, 341pp.

McTaggart, A. R., Butler, E. C. V., Haddad, P. R., and Middleton, J. H. (1994). Iodide and iodate concentrations in eastern Australian subtropical waters, with iodide by ion chromatography. *Mar.Chem.* **47**, 159-172.

Measures, C. I. and Vink, S. (2001). Dissolved iron in the upper waters of the Southern Ocean during the 1997/98 US JGOFS cruises. *Deep-Sea Res., Part II* **JGOFS Southern Ocean special issue**, in press.

Metzl, N., Tilbrook, B., and Poisson, A. (1999). The annual fCO2 cycle and the air-sea CO2 flux in the sub-Antarctic Ocean. *Tellus, Ser.B* **51B**, 849-861.

Minas, H. J. and Minas, M. (1992). Net community production in "High Nutrient-Low Chlorophyll" waters of the tropical and Antarctic Oceans: grazing vs. iron hypothesis. *Oceanologica Acta* **15**, 145-162.

Miyake, Y. and Tsunogai, S. (1963). Evaporation of iodine from the ocean. *J.Geophys.Res.* **68**, 3989-3993.

Miyake, Y. and Tsunogai, S. (1966). Problème de l'iode dans les océan. *La mer, Bull.Soc.franco-japon.océanogr.* **4**, 65-77.

Moeller, A., Lovric, M., and Scholz, F. (1996). Evidence for the occasional appearance of molecular iodine in sea water. *Int.J.Environ.Anal.Chem.* **63**, 99-106.

Moisan, T. A., Dunstan, W. M., Udomkit, A., and Wong, G. T. F. (1994). The uptake of iodate by marine phytoplankton. *J.Phycol.* **30**, 580-587.

Moore, R. M. and Groszko, W. (1999). Methyl iodide distribution in the ocean and fluxes to the atmosphere. *J.Geophys.Res., [Oceans]* **104**, 11163-11171.

Moore, R. M. and Tokarczyk, R. (1992). Chloro-iodomethane in N. Atlantic waters: A potentially significant source of atmospheric iodine. *Geophys.Res.Lett.* **19**, 1779-1782.

Moore, R. M. and Tokarczyk, R. (1993). Volatile biogenic halocarbons in the northwest Atlantic. *Global Biogeochem.Cycles* **7**, 195-210.

Moore, R. M. and Zafiriou, O. C. (1994). Photochemical production of methyl iodide in seawater. *J.Geophys.Res., [Atmos.]* **99**, 16415-16420.

Moore, R. M., Tokarczyk, R., Tait, V. K., Poulin, M., and Geen, C. (1995). Marine phytoplankton as a natural source of volatile organohalogens. *Environ.Chem.(Dordrecht, Neth.)* **1**, 283-294.

Moore, R. M., Webb, M., Tokarczyk, R., and Wever, R. (1996). Bromoperoxidase and iodoperoxidase enzymes and production of halogenated methanes in marine diatom cultures. *J.Geophys.Res., [Oceans]* **101**, 20899-20908.

Murphy, C. D., Moore, R. M., and White, R. L. (2000). Peroxidases from marine microalgae. *J.Appl.Phycol.* **12**, 507-513.

Nakayama, E., Kimoto, T., and Okazaki, S. (1985). Automatic determination of iodine species in natural waters by a new flow-through electrode system. *Anal.Chem.* **57**, 1157-1160.

Nakayama, E., Kimoto, T., Isshiki, K., Sohrin, Y., and Okazaki, S. (1989). Determination and distribution of iodide- and total-iodine in the North Pacific Ocean - by using a new automated electrochemical method. *Mar.Chem.* **27**, 105-116.

Neidleman, S. L. and Geigert, J. (1986). 'Biohalogenation: principles, basic roles, and applications.' (Ellis Horwood: Chichester, West Sussex, England.)

Nightingale, P. D., Malin, G., and Liss, P. S. (1995). Production of chloroform and other low-molecular-weight halocarbons by some species of macroalgae. *Limnol.Oceanogr.* **40**, 680-689.

Oguma, K., Kitada, K., and Kuroda, R. (1993). Microchemical determination of iodate and iodide in sea waters by flow injection analysis. *Mikrochim.Acta* **110**, 71-77.

Orsi, A. H., Whitworth III, T., and Nowlin Jr., W. D. (1995). On the meridional extent and fronts of the Antarctic Circumpolar Current. *Deep-Sea Res., Part I* **42**, 641-673.

Orsi, A. H., Johnson, G. C., and Bullister, J. L. (1999). Circulation, mixing, and production of Antarctic Bottom Water. *Progress in Oceanography* **43**, 55-109.

Parslow, J. S., Boyd, P. W., Rintoul, S. R., and Griffiths, F. B. (2001). A sub-surface chlorophyll maximum in the inter-polar frontal zone south of Australia: seasonal evolution and implications for phytoplankton- light-nutrient interactions. *J.Geophys.Res., [Oceans]* **SAZ project special issue**. Submitted.

Passier, H. F., Luther, G. W. I., and De Lange, G. J. (1997). Early diagenesis and sulfur speciation in sediments of the Oman Margin, northwestern Arabian Sea. *Deep-Sea Res., Part II* **44**, 1361-1380.

Patterson, S. L. and Whitworth III, T. (1990). Physical oceanography. In 'Antarctic sector of the Pacific'. (Ed. G. P. Glasby.) pp. 55-93.

Platt, T., Jauhari, P., and Sathyendranath, S. (1992). The importance and measurement of new production. *Environ.Sci.Res.* **43**, 273-284.

Popp, B. N., Trull, T. W., Kenig, F., Wakeham, S. G., Rust, T. M., Tilbrook, B., Griffiths, F. B., Wright, S. W., Marchant, H. J., Bidigare, R. R., and Laws, E. A. (1999). Controls on the carbon isotopic composition of Southern Ocean phytoplankton. *Global Biogeochem.Cycles* **13**, 827-843.

Priddle, J., Nedwell, D. B., Whitehouse, M. J., Reay, D. S., Savidge, G., Gilpin, L. C., Murphy, E. J., and Ellis-Evans, J. C. (1998a). Re-examining the Antarctic Paradox: speculation on the Southern Ocean as a nutrient-limited system. *Ann.Glaciol.* **27**, 661-668.

Priddle, J., Boyd, I. L., Whitehouse, M. J., Murphy, E. J., and Croxall, J. P. (1998b). Estimates of Southern Ocean primary production- constraints from predator carbon demand and nutrient drawdown. *Journal of Marine Systems* **17**, 275-288.

Redfield, A. C., Ketchum, B.H. and Richards, F.A. (1963). The influence of organisms in the composition of seawater. In: "The sea". (Ed. M.N. Hill). Vol.2, pp.26-77.

Reid, J. L. (1989). On the total geostrophic circulation of the South Atlantic Ocean: flow patterns, tracers, and transports. *Progress in Oceanography* **23**, 149-244.

Rintoul, S. R. (1998). On the origin and influence of Adélie Land bottom water. In 'Ocean, ice, and atmosphere: interactions at the Antarctic continental margin'. (Eds. S. S. Jacobs and R. F. Weiss.) pp. 151-71. (American Geophysical Union: Washington, D.C.)

Rintoul, S. R. and Bullister, J. L. (1999). A late winter hydrographic section from Tasmania to Antarctica. *Deep-Sea Res., Part I* **46**, 1417-1454.

Rintoul, S. R. and Trull, T. W. (2001). Mixed layer properties of the Subantarctic and Polar Frontal Zones south of Australia. *J.Geophys.Res., [Oceans]* **SAZ project special issue**, submitted.

Rintoul, S. R., Donguy, J. R., and Roemmich, D. H. (1997). Seasonal evolution of upper ocean thermal structure between Tasmania and Antarctica. *Deep-Sea Res., Part I* **44**, 1185-1202.

Rintoul, S. R., Wolff, B., Griffiths, F. B., Bindoff, N., Church, J., Tilbrook, B., Parslow, J., Rosenberg, M., and Trull, T. W. (2001). Physical, chemical and biological oceanography of the Southern Ocean: recent progress by ANARE. In 'The silence broken: 50 years of ANARE science'. (Ed. H. Marchant.) in press.

Rosenberg, M., Eriksen, R., Bell, S., Bindoff, N., and Rintoul, S. R. (1995). 'Aurora Australis marine science cruise AU9407- oceanographic field mesurements and analysis.' Antarctic CRC Research Report No. 6 Edn. (Antarctic CRC: Hobart, Tasmania.)

Rosenberg, M., Eriksen, R., Bell, S., and Rintoul, S. R. (1996). 'Aurora Australis marine science cruise AU9404- oceanographic field mesurements and analysis.' Antarctic CRC Research Report No. 8 Edn. (Antarctic CRC: Hobart, Tasmania.)

Rosenberg, M., Bray, S., Bindoff, N., Rintoul, S. R., Johnston, N., Bell, S., and Towler, P. (1997). 'Aurora Australis marine science cruises AU9501, AU9604, AU9601- oceanographic field mesurements and analysis,inter-cruise comparisons and data quality notes.' Antarctic CRC Report No. 12 Edn. (Antarctic CRC: Hobart, Tasmania.)

Rubin, S. I., Takahashi, T., Chipman, D. W., and Goddard, J. G. (1998). Primary productivity and nutrient utilization ratios in the Pacific sector of the Southern Ocean based on seasonal changes in seawater chemistry. *Deep-Sea Res., Part I* **45** , 1211-1234.

Rue, E. L., Smith, G. J., Cutter, G. A., and Bruland, K. W. (1997). The response of trace element redox couples to suboxic conditions in the water column. *Deep-Sea Res., Part I* **44**, 113-134.

Scarratt, M. G. and Moore, R. M. (1996). Production of methyl chloride and methyl bromide in laboratory cultures of marine phytoplankton. *Mar.Chem.* **54**, 263-272.

Scarratt, M. G. and Moore, R. M. (1998). Production of methyl bromide and methyl chloride in laboratory cultures of marine phytoplankton II. *Mar.Chem.* **59**, 311-320.

Scarratt, M. G. and Moore, R. M. (1999). Production of chlorinated hydrocarbons and methyl iodide by the red microalga Porphyridium purpureum. *Limnol.Oceanogr.* **44**, 703-707.

Sedwick, P. N., Edwards, P. R., Mackey, D. J., Griffiths, F. B., and Parslow, J. S. (1997). Iron and manganese in surface waters of the Australian sub-Antarctic region. *Deep-Sea Res., Part I* **44**, 1239-1253.

Sedwick, P. N., DiTullio, G. R., Hutchins, D. A., Boyd, P. W., Griffiths, F. B., Crossley, A. C., Trull, T. W., and Queguiner, B. (1999). Limitation of algal growth by iron deficiency in the Australian Subantarctic region. *Geophys.Res.Lett.* **26**, 2865-2868.

Shaw, T. I. (1962). Halogens. In 'Physiology and biochemistry of algae'. (Ed. R. A. Lewin.) pp. 247-53. (Academic Press: New York.)

Shaw, T. I. and Cooper, L. H. N. (1957). State of iodine in sea water. *Nature* **180**, 250.

Shaw, T. I. and Cooper, L. H. N. (1958). Oxidized iodine in sea water. *Nature* **182**, 251-252.

Sillen, L. G. (1961). The physical chemistry of seawater. In 'Oceanography'. (Ed. M. Sears.) pp. 549-81. (AAAS: Washington, D.C.)

Sivaraman, C. P. and Rajeswari, S. (1983). Determination of iodide and iodate in seawater. *Indian J.Mar.Sci.* **12**, 177-180.

Smith, J. D. and Butler, E. C. V. (1979). Speciation of dissolved iodine in estuarine waters. *Nature (London)* **277**, 468-469.

Sohrin, Y., Iwamoto, S., Matsui, M., Obata, H., Nakayama, E., Suzuki, K., Handa, N., and Ishii, M. (1999). The distribution of Fe in the Australian sector of the Southern Ocean. *Deep-Sea Res., Part I* **47**, 55-84.

Spokes, L. J. and Liss, P. S. (1996). Photochemically induced redox reactions in seawater, II. Nitrogen and iodine. *Mar.Chem.* **54**, 1-10.

Strutton, P. G., Griffiths, F. B., Waters, R. L., Wright, S. W., and Bindoff, N. L. (2000). Primary productivity off the coast of East Antarctica (80-150 degrees E): January to March 1996. *Deep-Sea Res., Part II* **47**, 2327-2362.

Sugawara, K. and Terada, K. (1957). Iodine distribution in the Western Pacific Ocean. *J.Earth Sci., Univ.Nagoya* **5**, 81-102.

Sugawara, K. and Terada, K. (1958). Oxidized iodine in sea water. *Nature* **182**, 250-251.

Sugawara, K. and Terada, K. (1967). Iodine assimilation by a marine *Navicula sp.* and the production of iodate accompanied by the growth of the algae. *Information Bulletin on Planktology in Japan* **Commemoration number of Dr. Y. Matsue**, 213-218.

Sugawara, K., Koyama, T., and Terada, K. (1955). A new method of spectrophotometric determination of iodine in natural waters. *Bull.Chem.Soc.Japan* **28**, 494-497.

Sugawara, K., Terada, K., Kanamori, S., Kanamori, N., and Okabe, S. (1962). Different distribution of calcium, strontium, iodine, arsenic, and molybdenum in the northwestern Pacific, Indian, and Antarctic oceans. *J.Earth Sci., Nagoya Univ.* **10**, 34-50.

Tait, V. K. and Moore, R. M. (1995). Methyl chloride (CH3Cl) production in phytoplankton cultures. *Limnol.Oceanogr.* **40**, 189-195.

Takayanagi, K. and Wong, G. T. F. (1986). The oxidation of iodide to iodate for the polarographic determination of total iodine in natural waters. *Talanta* **33**, 451-454.

Thompson, A. M. and Zafiriou, O. C. (1983). Air-sea fluxes of transient atmospheric species. *J.Geophys.Res., [Oceans]* **88**, 6696-6708.

Tian, R. C. and Nicolas, E. (1995). Iodine speciation in the northwestern Mediterranean Sea: method and vertical profile. *Mar.Chem.* **48**, 151-156.

Tian, R. C., Marty, J. C., Nicolas, E., Chiaverini, J., Ruiz-Pino, D., and Pizay, M. D. (1996). Iodine speciation: A potential indicator to evaluate new production versus regenerated production. *Deep-Sea Res., Part I* **43**, 723-738.

Tokarczyk, R. and Moore, R. M. (1994). Production of volatile organohalogens by phytoplankton cultures. *Geophys.Res.Lett.* **21**, 285-288.

Truesdale, V. W. (1974). Chemical reduction of molecular iodine in sea water. *Deep-Sea Res.* **21**, 761-766.

Truesdale, V. W. (1975). Reactive and unreactive iodine in sea water. Possible indication of an organically bound iodine fraction. *Mar.Chem.* **3**, 111-119.

Truesdale, V. W. (1978a). The automatic determination of iodate and total iodine in seawater. *Mar.Chem.* **6**, 253-273.

Truesdale, V. W. (1978b). Iodine in inshore and off-shore marine waters. *Mar.Chem.* **6**, 1-13.

Truesdale, V. W. (1994). A re-assessment of Redfield correlations between dissolved iodine and nutrients in oceanic waters and a strategy for further investigations of iodine. *Mar.Chem.* **48**, 43-56.

Truesdale, V. W. and Bailey, G. W. (2000). Dissolved Iodate and Total Iodine During an Extreme Hypoxic Event in the Southern Benguela System. *Estuarine, Coastal Shelf Sci.* **50**, 751-760.

Truesdale, V. W. and Chapman, P. (1976). Optimisation of a catalytic procedure for the determination of total iodine in sea water. *Mar.Chem.* **4**, 29-42.

Truesdale, V. W. and Moore, R. M. (1992). Further studies on the chemical reduction of molecular iodine added to seawater. *Mar.Chem.* **40**, 199-213.

Truesdale, V. W. and Smith, C. J. (1979). A comparative study of three methods for the determination of iodate in seawater. *Mar.Chem.* **7**, 133-139.

Truesdale, V. W. and Spencer, C. P. (1974). Studies on the determination of inorganic iodine in sea water. *Mar.Chem.* **2**, 33-47.

Truesdale, V. W., Bale, A. J., and Woodward, E. M. S. (2000). The meridional distribution of dissolved iodine in near-surface waters of the Atlantic Ocean [Review]. *Progress in Oceanography* **45**, 387-400.

Trull, T., Rintoul, S. R., Hadfield, M., and Abraham, E. R. (2001). Circulation and seasonal evolution of polar waters south of Australia: implications for iron fertilization of the Southern Ocean. *Deep-Sea Res., Part II* **48**, 2439-2466.

Tsunogai, S. (1971a). Iodine in the deep water of the ocean. *Deep-Sea Res.* **18**, 913-919.

Tsunogai, S. (1971b). Determination of iodine in seawater by an improved Sugawara method. *Anal.Chim.Acta* **55**, 444-447.

Tsunogai, S. and Henmi, T. (1971). Iodine in the surface water of the ocean. *J.Oceanogr.Soc.Jpn.(Nippon Kaiyo Gakkai-Shi)* **27**, 67-72.

Tsunogai, S. and Sase, T. (1969). Formation of iodide-iodine in the ocean. *Deep-Sea Res.* **16**, 489-496.

Udomkit, A. (1994). Iodate transformation by marine phytoplankton. *PhD thesis.* **Old Dominion University**, 160pp.

Verma, K. K., Jain, A., and Verma, A. (1992). Determination of iodide by high-performance liquid chromatography after precolumn derivatization. *Anal.Chem.* **64**, 1484-1489.

Vinall, G. (1991). '42344 Fieldwork 3.' (Faculty of Aquatic Science, Deakin University: Warrnambool.)

Wang, X., Matear, R. J., and Trull, T. W. (2001). Modeling the seasonal phosphate export and resupply in the Subantarctic and Polar Frontal Zones in the Australian sector of the Southern Ocean. *J.Geophys.Res., [Oceans]* **SAZ project special issue** , submitted.

Weiss, R. F., Oestlund, H. G., and Craig, H. (1979). Geochemical studies of the Weddell Sea. *Deep-Sea Res., Part A* **26**, 1093-1120.

Whitworth III, T., Orsi, A. H., Nowlin Jr., W. D., and Locarnini, R. A. (1998). Water masses and mixing near the Antarctic slope front. In 'Ocean, ice, and atmosphere: interactions at the Antarctic continental margin'. (Eds. S. S. Jacobs and R. F. Weiss.) pp. 1-27. (American Geophysical Union: Washington, D.C.)

Woittiez, J. R. W., Van der Sloot, H. A., Wals, G. D., Nieuwendijk, B. J. T., and Zonderhuis, J. (1991). The determination of iodide, iodate, total inorganic iodine and charcoal-adsorbable iodine in seawater. *Mar.Chem.* **34**, 247-259.

Wong, A. P. S., Bindoff, N. L., and Forbes, A. (1998). Ocean-ice interaction and possible bottom water formation in Prydz Bay, Antarctica. In 'Ocean, ice, and atmosphere: interactions at the Antarctic continental margin'. (Eds. S. S. Jacobs and R. F. Weiss.) pp. 173-87. (American Geophysical Union: Washington, D.C.)

Wong, G. T. F. (1976). Dissolved inorganic and particulate iodine in the oceans. *PhD thesis* **Woods Hole Oceanographic Institution**, 272pp.

Wong, G. T. F. (1980). The stability of dissolved inorganic species of iodine in sea water. *Mar.Chem.* **9**, 13-24.

Wong, G. T. F. (1991). The marine geochemistry of iodine. *Rev.Aquat.Sci.* **4**, 45-73.

Wong, G. T. F. (1995). Dissolved iodine across the Gulf Stream Front and in the South Atlantic Bight. *Deep-Sea Res., Part I* **42**, 2005-2023.

Wong, G. T. F. (2001). Coupling iodine speciation to primary, regenerated or "new" production: a re-evaluation. *Deep-Sea Res., Part I* **48**, 1459-1476.

Wong, G. T. F. and Brewer, P. G. (1974). Determination and distribution of iodate in South Atlantic waters. *J.Mar.Res.* **32**, 25-36.

Wong, G. T. F. and Brewer, P. G. (1976). The determination of iodide in sea water by neutron activation analysis. *Anal.Chim.Acta* **81**, 81-90.

Wong, G. T. F. and Brewer, P. G. (1977). The marine chemistry of iodine in anoxic basins. *Geochim.Cosmochim.Acta* **41**, 151-159.

Wong, G. T. F. and Cheng, X. H. (1998). Dissolved organic iodine in marine waters: Determination, occurrence and analytical implications. *Mar.Chem.* **59**, 271-281.

Wong, G. T. F. and Cheng, X. H. (2001). The formation of iodide in inshore waters from the photochemical decomposition of dissolved organic iodine. *Mar.Chem.* **74**, 53-64.

Wong, G. T. F. and Hung, C. C. (2001). Speciation of dissolved iodine: integrating nitrate uptake over time in the oceans. *Continental Shelf Research* **21**, 113-128.

Wong, G. T. F. and Zhang, L. S. (1992a). Chemical removal of oxygen with sulfite for the polarographic or voltammetric determination of iodate or iodide in seawater. *Mar.Chem.* **38**, 109-116.

Wong, G. T. F. and Zhang, L. S. (1992b). Determination of total inorganic iodine in seawater by cathodic stripping square wave voltammetry. *Talanta* **39**, 355-360.

Wong, G. T. F., Brewer, P. G., and Spencer, D. W. (1976). The distribution of particulate iodine in the Atlantic Ocean. *Earth Planet.Sci.Lett.* **32**, 441-450.

Wong, G. T. F., Takayanagi, K., and Todd, J. F. (1985). Dissolved iodine in waters overlying and in the Orca Basin, Gulf of Mexico. *Mar.Chem.* **17**, 177-183.

Woolery, M. L. and Lewin, R. A. (1973). Influence of iodine on growth and development of the brown alga Ectocarpus siliculosus in axenic cultures. *Phycologia* **12**, 131-138.

Wright, S. W. and van den Enden, R. L. (2000). Phytoplankton community structure and stocks in the East Antarctic marginal ice zone (BROKE survey, January-March 1996) determined by CHEMTAX analysis of HPLC pigment signatures. *Deep-Sea Res., Part II* **47**, 2363-2400.

Zafiriou, O. C. (1977). Marine organic photochemistry previewed. *Mar.Chem.* **5**, 497-522.

Zafiriou, O. C. (1983). Natural water photochemistry. In 'Chemical Oceanography', Volume 8. pp. 339-79. (Academic Press; New York.)

Zafiriou, O. C., Joussot-Dubien, J., Zepp, R. G., and Zika, R. G. (1984). Photochemistry of natural waters. *Environ.Sci.Technol.* **18**, 358A-371A.

Appendix I

Iodide results obtained by cathodic stripping square wave voltammetry (CSSWV) and by ion chromatography (IC) as plotted in Figure 2.8.

Station number	Sample number	Depth (dbar)	CSWV (nM)	IC (nM)
093-au9404	24	9.54	26.71	22.62
093-au9404	23	50.9	28.61	19.46
093-au9404	22	85.9	18.52	18.12
093-au9404	21	162	15.92	14.18
093-au9404	20	251	16.23	13.40
093-au9404	19	352	15.21	12.37
093-au9404	18	452	13.32	14.66
093-au9404	16	703	8.35	8.43
093-au9404	6	2902	1.26	4.65
093-au9404	1	4347	1.53	3.78
106-au9404	22	9.16	46.65	38.93
106-au9404	19	23.1	44.52	39.87
106-au9404	16	47.5	32.70	32.07
106-au9404	13	80.1	24.98	26.32

Appendix II

Detailed list of stations sampled during the three cruises: au9407 starting in January 1994 (V7); au9404 starting in December 1994 (V4) and au9501 starting July 1995 (V1).

Station number and transect	Latitude and Longitude (start point)	Date	Depth (m)	Iodate Samples Analysed	Iodide Samples analysed
V7 003 SR3	43:59.97S 146:19.04E	02/01/94	248	9	Nil
V7 006 SR3	44:43.08S 146:02.64E	02/01/94	3211	24	Nil
V7 008 SR3	45:12.82S 145:51.28E	03/01/94	2859	21	Nil
V7 010 SR3	46:10.33S 145:27.67E	03/01/94	2776	23	Nil
V7 013 SR3	47:08.67S 145:03.06E	04/01/94	4610	20	Nil
V7 015 SR3	47:48.25S 144:44.48E	04/01/94	3957	22	Nil
V7 020 SR3	49:16.17S 144:05.64E	05/01/94	4237	24	Nil
V7 023 SR3	50:14.06S 143:38.95E	06/01/94	3729	23	Nil
V7 025 SR3	51:01.99S 143:14.29E	07/01/94	3729	24	Nil
V7 028 SR3	51:51.07S 142:49.83E	07/01/94	3729	24	Nil
V7 030 SR3	52:38.34S 142:23.24E	08/01/94	3522	5	Nil
V7 031 SR3	52:39.41S 142:22.88E	08/01/94	3522	24	Nil
V7 033 SR3	53:34.86S 141:51.95E	08/01/94	2382	24	Nil
V7 036 SR3	54:31.79S 141:19.31E	09/01/94	2797	24	Nil
V7 038 SR3	55:29.83S 140:43.65E	09/01/94	3988	23	Nil
V7 043 SR3	57:23.02S 139:50.86E	10/01/94	4143	6	Nil
V7 044 SR3	57:22.42S 139:51.08E	10/01/94	4143	24	Nil
V7 048 SR3	59:20.87S 139:50.81E	12/01/94	4221	24	Nil
V7 052 SR3	60:51.05S 139:50.83E	12/01/94	4408	6	Nil
V7 053 SR3	60:51.14S 139:50.63E	12/01/94	4408	24	Nil
V7 058 SR3	62:50.69S 139:50.24E	14/01/94	3211	24	Nil
V7 060 SR3	63:52.03S 139:51.10E	14/01/94	3739	24	Nil
V7 063 SR3	64:49.16S 139:50.91E	15/01/94	2610	24	Nil
V7 065 SR3	65:24.14S 139:50.91E	15/01/94	2455	23	Nil
V7 067 SR3	65:31.84S 139:51.13E	16/01/94	1274	18	Nil
V7 069 SR3	65:42.49S 139:51.13E	16/01/94	307	10	Nil
V7 070 SR3	65:48.39S 139:51.04E	16/01/94	220	9	Nil
Total: 27				Total: 530	
V7 076 PET	66:19.31S 84:43.02E	26/01/94	569	12	Nil
V7 078 PET	65:59.22S 85:25.88E	26/01/94	258	9	Nil
V7 079 PET	65:53.61S 85:24.69E	26/01/94	1253	17	Nil
V7 081 PET	65:44.83S 85:24.48E	26/01/94	2517	24	Nil
V7 085 PET	64:37.05S 84:59.92E	27/01/94	3612	23	Nil
V7 088 PET	63:43.22S 84:08.56E	27/01/94	3729	24	Nil
V7 092 PET	62:09.89S 83:16.70E	28/01/94	2672	24	Nil
V7 095 PET	60:56.51S 82:46.17E	29/01/94	2517	24	Nil
V7 097 PET	59:58.36S 82:22.28E	29/01/94	1647	18	Nil
V7 099 PET	58:57.72S 82:01.64E	30/01/94	1310	18	Nil
Total: 10				Total: 193	
V7 Total: 37				V7 total: 723	

Station number and transect	Latitude and Longitude (start point)	Date	Depth (m)	Iodate Samples Analysed	Iodide Samples analysed
V4 001 Test	57:30.52S 127:47.81E	20/12/94	4690	6	Nil
V4 003 S4	62:00.30S 119:00.65E	21/12/94	4215	24	7
V4 004 S4	61:59.97S 118:00.14E	22/12/94	4260	18	nil
V4 006 S4	65:59.05S 109:54.21E	02/01/95	255	9	nil
V4 007 S4	65:23.42S 112:33.55E	03/01/95	482	13	9
V4 010 S4	64:44.42S 111:55.21E	04/01/95	2250	24	6
V4 013 S4	63:41.02S 112:36.06E	04/01/95	3358	24	7
V4 017 S4	62:00.05S 114:59.98E	05/01/95	4286	23	nil
V4 020 S4	62:00.02S 121:24.93E	07/01/95	4153	24	nil
V4 023 S4	61:59.92S 125:39.57E	07/01/95	4338	24	nil
V4 025 S4	62:00.04S 128:29.96E	08/01/95	4400	5	nil
V4 026 S4	61:59.83S 129:54.96E	08/01/95	4490	24	nil
V4 030 S4	62:00.19S 135:35.04E	09/01/95	4335	24	nil
V4 033 S4	62:21.05S 139:51.96E	10/01/95	3950	24	7
V4 036 S4	62:45.08S 143:36.91E	11/01/95	4110	14	8
V4 039 S4	63:11.17S 147:50.05E	12/01/95	3915	24	nil
V4 043 S4	63:26.11S 153:41.67E	13/01/95	3125	24	nil
V4 047 S4	63:25.74S 159:26.55E	14/01/95	2710	21	8
V4 050 S4	65:17.95S 161:24.01E	15/01/95	3100	24	8
V4 052 S4	66:06.84S 162:03.08E	16/01/95	1510	16	8
V4 053 S4	66:09.13S 162:15.49E	16/01/95	567	11	nil
Total: 21				Total: 400	Total: 68
V4 057 SR3	65:50.53S 141:25.71E	19/01/95	332	9	Nil
V4 058 SR3	65:34.98S 139:51.24E	19/01/95	595	12	Nil
V4 060 SR3	65:25.93S 139:50.77E	20/01/95	1875	24	Nil
V4 062 SR3	64:49.03S 139:50.94E	20/01/95	2600	24	Nil
V4 063 SR3	64:16.92S 139:52.08E	20/01/95	3470	24	Nil
V4 066 SR3	62:51.09S 139:50.70E	21/01/95	3220	24	Nil
V4 067 SR3	62:20.78S 139:50.44E	21/01/95	3970	24	Nil
V4 070 SR3	60:35.99S 139:50.67E	22/01/95	4440	24	Nil
V4 071 SR3	59:50.90S 139:50.94E	22/01/95	4485	24	Nil
V4 074 SR3	57:38.75S 139:51.77E	23/01/95	4250	24	Nil
V4 076 SR3	56:12.73S 140:17.60E	24/01/95	3620	24	Nil
V4 077 SR3	55:30.06S 140:44.00E	24/01/95	3915	23	9
V4 079 SR3	54:32.38S 141:19.09E	25/01/95	2850	24	nil
V4 081 SR3	53:35.18S 141:52.10E	25/01/95	2590	24	10
V4 083 SR3	52:40.06S 142:23.46E	26/01/95	3400	24	10
V4 085 SR3	51:51.13S 142:50.05E	26/01/95	3620	24	nil
V4 088 SR3	51:01.97S 143:13.93E	28/01/95	3800	23	9
V4 090 SR3	50:24.88S 143:32.04E	28/01/95	3588	18	11
V4 091 SR3	50:05.08S 143:43.24E	28/01/95	4060	24	12
V4 093 SR3	49:16.03S 144:06.03E	29/01/95	4225	24	10
V4 094 SR3	48:47.02S 144:19.01E	29/01/95	4150	24	9
V4 095 SR3	48:18.66S 144:32.00E	30/01/95	4005	24	nil
V4 097 SR3	47:27.94S 144:53.89E	30/01/95	4270	22	nil

V4 098 SR3	47:09.06S 145:02.97E	30/01/95	4000	24	9
V4 100 SR3	46:09.92S 145:28.08E	31/01/95	2730	24	9
V4 102 SR3	45:13.01S 145:51.10E	31/01/95	2860	24	nil
V4 103 SR3	44:42.98S 146:03.06E	31/01/95	3200	23	9
V4 104 SR3	44:22.95S 146:10.85E	01/02/95	2345	24	nil
V4 105 SR3	44:06.89S 146:12.99E	01/02/95	1000	14	9
V4 106 SR3	44:00.00S 146:19.01E	01/02/95	254	10	6
Total: 30				Total:	Total:
V4 total: 51				658	122
				V4 total:	V4 total:
				1058	190
V1 002 SR3	43:59.89S 146:19.05E	18/07/95	235	8	8
V1 003 SR3	44:07.30S 146:13.55E	18/07/95	1051	14	8
V1 004 SR3	44:22.70S 146:10.63E	18/07/95	2351	24	nil
V1 005 SR3	44:43.08S 146:02.76E	18/07/95	3150	24	9
V1 006 SR3	45:12.82S 145:51.21E	19/07/95	2800	24	8
V1 008 SR3	46:10.37S 145:27.58E	20/07/95	2680	23	8
V1 009 SR3	46:39.07S 145:15.33E	20/07/95	3270	23	nil
V1 010 SR3	47:08.73S 145:03.11E	20/07/95	3510	24	nil
V1 011 SR3	47:28.20S 144:54.37E	20/07/95	4200	22	nil
V1 012 SR3	47:59.91S 144:40.56E	21/07/95	3970	23	nil
V1 013 SR3	48:18.67S 144:31.80E	21/07/95	3910	24	nil
V1 014 SR3	48:46.60S 144:18.93E	21/07/95	4080	24	nil
V1 015 SR3	49:16.21S 144:05.64E	21/07/95	4120	24	10
V1 018 SR3	50:09.62S 143:40.73E	22/07/95	3625	24	nil
V1 019 SR3	50:23.92S 143:33.68E	22/07/95	3530	20	nil
V1 021 SR3	51:00.05S 143:17.82E	23/07/95	3720	24	11
V1 024 SR3	51:48.56S 142:50.72E	23/07/95	3670	24	nil
V1 026 SR3	52:39.46S 142:22.96E	24/07/95	3270	24	nil
V1 028 SR3	53:34.88S 141:51.83E	24/07/95	2450	24	10
V1 030 SR3	54:31.72S 141:19.43E	25/07/95	2750	24	nil
V1 032 SR3	55:29.82S 140:43.48E	25/07/95	3900	24	nil
V1 034 SR3	56:26.28S 140:06.02E	26/07/95	3800	24	nil
V1 036 SR3	57:22.29S 139:50.95E	27/07/95	3980	24	9
V1 039 SR3	58:51.44S 139:50.48E	27/07/95	3850	24	nil
V1 041 SR3	59:51.44S 139:50.96E	28/07/95	4390	24	nil
V1 042 SR3	60:21.31S 139:50.28E	28/07/95	4340	24	9
V1 046 SR3	62:15.68S 140:00.46E	30/07/95	3960	24	nil
V1 048 SR3	63:17.16S 139:50.38E	30/07/95	3730	24	11
V1 051 SR3	64:46.54S 140:20.44E	01/08/95	3250	24	nil
V1 101 SR3	65:21.79S 139:56.55E	09/08/95	2490	12	nil
V1 103 SR3	65:30.65S 139:44.86E	09/08/95	1715	12	nil
V1 total: 31				V1	V1 total:
				total:685	101

Appendix III

Average seasonal depth-integrated iodate depletion values for both summer cruises along the SR3 transect for different zones.

Zone	9407		9404		Total Average (mmol $IO_3^-.m^{-2}$)
	Average (mmol $IO_3^-.m^{-2}$)	Standard deviation	Average (mmol $IO_3^-.m^{-2}$)	Standard deviation	
STZ	1.367	0.663	2.492	0.928	1.930
SAZ	1.081	1.690	0.515	1.416	0.799
PFZ	0.210	0.449	0.189	0.621	0.199
AZ-N	0.108	0.613	0.085	0.501	0.187
AZ-S	1.116	0.151	0.821	0.821	0.968

Appendix IV

Average seasonal production estimated from iodate depletion values for both summer cruises along the SR3 transect for different zones.

Zone	9407		9404			
	Average (mmol $C.m^{-2}$)	Standard deviation (mmol $C.m^{-2}$)	Average (mmol $C.m^{-2}$)	Standard deviation (mmol $C.m^{-2}$)	Total Average (mmol $C.m^{-2}$)	Standard deviation (mmol $C.m^{-2}$)
STZ	3625	1983	5904	2317	4765	3049
SAZ	4504	7161	2860	8025	3684	10755
PFZ	870	1900	521	1725	696	2566
AZ-N	276	1565	252	1510	264	2175
AZ-S	2846	3369	2471	2487	2658	4188